

Cover Page



Universiteit Leiden



The handle <http://hdl.handle.net/1887/67534> holds various files of this Leiden University dissertation.

Author: Roushan, M.R.

Title: Visualization of effector protein translocation from *Agrobacterium tumefaciens* into host cells

Issue Date: 2018-11-27

**Visualization of effector protein translocation from
Agrobacterium into host cells**

Mohammad Reza Roushan

Cover image: "The iceberg". A little you are aware of, is like the small ice part above the surface. But the gigantic bulk of self is invisible to view; beneath awareness.

Photo taken by: Ralph A. Clevenger

Printed by: Gildeprint, Enschede, the Netherlands

Visualization of effector protein translocation from *Agrobacterium tumefaciens* into host cells

PROEFSCHRIFT

Ter verkrijging van
de graad van Doctor aan de Universiteit Leiden,
op gezag van de Rector Magnificus Prof. mr. C.J.J.M. Stolker,
volgens besluit van het College voor Promoties
te verdedigen op dinsdag 27 november 2018
klokke 10.00 uur

door

Mohammad Reza Roushan

Geboren te Teheran, Iran

24 maart 1983

Promotiecommissie

Promotor: Prof. dr. P.J.J. Hooykaas

Co-promotor: Dr. G.P.H. van Heusden

Overige leden: Prof. dr. G.P. van Wezel

Prof. dr. J. Memelink

Prof. dr. A. Briegel

Dr. P. Fransz

Dr. J. van Kan

To my beloved wife Sally and my son Arsha

Table of Contents

Chapter 1	9
General introduction	
Chapter 2	37
<u>Visualization of virulence protein translocation from <i>Agrobacterium</i> to yeast and plant cells using the split GFP approach</u>	
Chapter 3	79
<u>Application of phiLOV2.1 as a fluorescent marker for visualization of <i>Agrobacterium</i> effector protein translocation</u>	
Chapter 4	129
<u>Application of <i>Agrobacterium</i> – mediated protein translocation to induce mating type switching in the yeast <i>Saccharomyces cerevisiae</i></u>	
Chapter 5	151
<u>Targeting <i>Agrobacterium tumefaciens</i> virulence proteins into the organelles of plant and yeast cells</u>	
Chapter 6	199
Summary	
Chapter 7	209
Samenvatting	
Chapter 8	219
Curriculum Vitae	

Chapter 1

General introduction

M.Reza Roushan

Molecular and Developmental Genetics, Institute of Biology, Leiden University, Leiden, The Netherlands.

General introduction

Agrobacterium

Agrobacterium tumefaciens is a soil-borne, Gram-negative, rod shaped bacterium, which is the causative agent of crown gall disease in plants (Smith and Townsend, 1907). The bacterium transfers a part of its DNA (T-DNA) located on a tumor-inducing plasmid (Ti-Plasmid) simultaneously with virulence proteins expressed from the *vir* region, which is also located on the Ti-plasmid, into host cells resulting in tumor formation in plants (for reviews see: Tzfira and Citovsky, 2006; Gelvin, 2010). Because of its unique interkingdom gene transfer capability this bacterium was developed as a natural genetic engineer. *A. tumefaciens* has both a linear (2.1 Mbp) and a circular chromosome (2.8Mbp) and virulent strains also have a Ti-plasmid (Vaudequin-Dransart *et al.*, 1998; Goodner *et al.*, 2001; Wood *et al.*, 2001). One of the important features of *Agrobacterium* is its broad host range. *Agrobacterium* can transfer T-DNA not only into dicot and monocot plants (Hooykaas-van Slogteren *et al.*, 1984), but also into yeast (Bundock *et al.*, 1995; Piers *et al.*, 1996), fungi (de Groot *et al.*, 1998), algae (Kumar *et al.*, 2004), sea urchin embryos (Bulgakov *et al.*, 2006) and possibly human cells (Kunik *et al.*, 2001) under laboratory conditions. Therefore *A. tumefaciens* is used as a genetic tool to modify the genome of more and more different eukaryotic organisms for molecular biological studies and for biotechnological purposes. Even though *A. tumefaciens* has such a broad host range, the efficiency with which certain species or even cultivars within a species are transformed may differ tremendously. Also different *Agrobacterium* strains may differ in their host range for tumor induction. This is mostly due to difference in the constitution of the virulence genes on the Ti plasmid (Melchers *et al.*, 1990). The host range also relies on unknown properties of the recipient plant cells.

Induction of the virulence genes

The genes in the *A. tumefaciens* virulence region (*vir* region) are induced when the bacterium senses various plant-secreted compounds at the infected wound site on the plant (Stachel *et al.*, 1986). These signals include phenolic compounds and monosaccharides. The phenolic compounds also serve as chemo-attractants for *A. tumefaciens* (Brencic *et al.*, 2005; Palmer *et al.*, 2004). The phenolic compound acetosyringone was the first identified inducer of *A. tumefaciens* virulence (Stachel *et al.*, 1985). This compound is used in the laboratory for *Agrobacterium* mediated transformation (AMT) of non-plant hosts (Bundock *et al.*, 1995; de Groot *et al.*, 1998). The *Agrobacterium* sensory system consists of Ti-plasmid encoded proteins VirA and VirG and the chromosomally encoded sugar binding protein ChvE. VirA

and VirG are parts of a two component regulatory system (for review see McCullen and Binns, 2006). The constitutively expressed membrane receptor VirA functions as a sensor for the plant-derived signals. VirA forms a dimer with four domains: the periplasmic, cytoplasmic linker, kinase, and receiver domains. Upon the presence of a sugar and phenolic signals, VirA phosphorylates VirG. Phosphorylated VirG binds to a 12 bp *vir*-box located upstream of the transcription initiation sites in the *vir*-region. VirG is thereby activating the transcription of the *vir B, C, D, E, F, G* and *H* operons. Phosphorylated VirG initiates its own expression by activating VirG transcription at the distal promoter (reviewed by Brencic and Winans *et al.*, 2005).

T-DNA processing

After induction of the virulence genes, the relaxase VirD2 in cooperation with VirD1, VirC1 and VirC2 nicks one of two imperfect direct repeats (left and right borders; LB and RB, respectively) surrounding the T-DNA (Atmakuri *et al.*, 2007). These borders determine the T-region (van Haaren *et al.*, 1987) and nicking is thought to promote DNA synthesis leading to the release of a piece of single stranded DNA (T-strand) (Atmakuri *et al.*, 2007). VirD1 is facilitating in the nicking process by enhancing the binding of VirD2 and nicking of supercoiled DNA, while VirC1 and VirC2 act as specific binding proteins (Toro *et al.*, 1988; Lu *et al.*, 2009). The VirD2 protein remains covalently attached to the 5' end of the T-strand forming a nucleo-protein complex (Ward *et al.*, 1988; Pansegrau *et al.*, 1993). This complex is recognized by the type IV secretion system (T4SS) and is translocated into the host cell (van Kregten *et al.*, 2009).

The type IV secretion system (T4SS) of *Agrobacterium*

T4SSs are widely found in gram negative bacteria and serve as a conjugation system to exchange genetic information between bacteria or to deliver proteins to fungal, plant or mammalian cells. Conjugation enables bacteria to adapt to changes in the environment through acquisition of beneficial traits (reviewed by Rego *et al.*, 2010). During AMT the T-complex is translocated to the host cell through a specialized T4SS. In addition, a number of effector proteins, i.e. VirE2, VirE3, VirF and VirD5, is translocated through the T4SS independently from the T-complex (Vergunst *et al.*, 2000; Schrammeijer *et al.*, 2003). A translocation sequence at the C-terminus of the effector proteins is recognized resulting in translocation (Vergunst *et al.*, 2005). In *A. tumefaciens* the T4SS is composed of VirB1-11

and VirD4. Together they form a *trans*-envelope secretion channel, which on top has an outward extension, the T-pilus, which is mainly composed of VirB2 subunits. The process of T-DNA transfer through the T4SS consists of a series of temporally and spatially ordered close contacts of the T-complex with the T4SS forming proteins. In the T4SS, VirD4 functions as a substrate receptor; VirB11, VirD4 and VirB4 are ATPases and provide the energy for the transfer through the inner membrane. Contacts with the VirB6 and VirB8 inner membrane subunits as well as the periplasmic- and outer-membrane-associated subunits VirB2 and VirB9 also participate in the protein translocation. VirD4 and VirB11 energize a structural transition in VirB10 that is required for a late-stage assembly or gating activity for DNA passage to the cell surface (extensively reviewed by Christie *et al.*, 2014).

Virulence proteins translocated into the host cell

As mentioned above, during AMT independently from the T-strand – VirD2 complex a number of virulence proteins (VirD5, VirE2, VirE3, VirF) are translocated in the host cell. The VirE2 protein is able to bind single-stranded DNA in a sequence-independent way. Inside *Agrobacterium* the VirE2 protein is stabilized by its chaperone VirE1, which also protects its self-association and aggregation (Deng *et al.*, 1999; McBride and Knauf, 1988). VirE1 is therefore also required for VirE2 translocation from *A. tumefaciens* into the plant cells (Sundberg *et al.*, 1996), but otherwise VirE2 the translocation peptide suffices for the translocation of heterologous cargo (Vergunst *et al.*, 2003). In the plant cell VirE2 binds to the T-strand and protects it from host cell nucleases (Gietl *et al.*, 1987; Citovsky *et al.*, 1989; Sen *et al.*, 1989) and may help the T-strand passing the lipid bilayers of membranes (Dumass *et al.*, 2001). VirE2 may also hijack clathrin mediated endocytosis as recently reported by Li and Pan (2017). Furthermore, VirE2 helps in facilitating the nuclear uptake of the T-complex by converting it in a long thin thread and by guiding to the nucleus through binding of the VirE2 binding protein (VIP1) (Citovsky *et al.*, 1989; Ziemienowicz *et al.*, 2001). VIP1 is a transcription factor that responds to biotic and abiotic stresses by MPK3-mediated phosphorylation. Phosphorylated-VIP1 localizes to the plant nucleus leading to the expression of many defense-related genes. Therefore, VirE2-VIP1 interaction may direct the T-complex into the nucleus (Djamei *et al.*, 2007; Pitzschke *et al.*, 2009). However, recently such a role of VIP1 was disputed (Shi *et al.*, 2014). Besides, it has been reported that VirE2 facilitates the chromatin targeting of the T-complex through an association with VIP2 (Anand *et al.*, 2007).

The VirD2 protein with a strong nuclear localization sequence (NLS) at its C-terminus is prime to guide the T-complex into the nucleus (Ziemienowicz *et al.*, 2001). Recently interaction between VirD2 and histones in *S. cerevisiae* has been reported and it may help direct the T-DNA to the chromatin prior to integration into one of the chromosomes (Wolterink-van Loo *et al.*, 2015). The virulence protein VirF is a host range factor of *Agrobacterium* (Hooykaas *et al.*, 1984; Melchers *et al.*, 1990). VirF contains a putative F-box and it has been shown that it associates with plant homologs of the yeast Skp1 protein suggesting a role of VirF in targeted protein degradation (Schrammeijer *et al.*, 2001). Tzfira *et al.* reported that VirF is involved in destabilization and degradation of VirE2 and VIP1; this would lead to the uncoating of the T-DNA enabling its integration into the host's chromosomal DNA (Tzfira and Citovsky, 2001). Certain plants including *Arabidopsis thaliana* express an F-box protein called VBP which obviates the need for the VirF protein in transformation (Zaltsman *et al.*, 2010). VirE3 interacts with pBrp, a plant-specific transcription factor (García-Rodríguez *et al.*, 2006). pBrp localizes at the outside of plastids; however, when the cell is stressed or when VirE3 is present, pBrp translocates to the nucleus to stimulate transcription. Niu *et al.* (2015) showed that in *Arabidopsis thaliana* VirE3 activates the *VBF* promoter and thus possibly by inducing the VBF F-box protein indirectly regulates the levels of VirE2 and VIP1. This clarifies why the transformation is only slightly decreased with a mutation in either *virF* or *virE3*, while the inactivation of both genes leads to low transformation efficiency (García-Rodríguez *et al.*, 2006). The VirD5 protein binds to the VIP1-VirE2 complex, hence inhibiting the degradation of this complex (Wang *et al.*, 2014). VirD5 also interacts with another VirE2 binding protein, VIP2 (Wang *et al.*, 2018). Zhang *et al.* (2017) showed that VirD5 binds to the kinetochores in host cells, resulting in chromosome mis-segregation during mitosis and inhibition of yeast and plant growth.

T-DNA integration

After nuclear uptake, the T-strand is converted in a double-stranded form and integrates into the host genome. In plants the T-DNA integrates by a process of non-homologous recombination (for review see: Gelvin, 2000); even when large segments of homology are present in the T-DNA integration by homologous recombination (HR) only occurs with a very low efficiency (Offringa *et al.*, 1990). However, in the yeast *S. cerevisiae* the T-DNA is preferentially integrated via homologous recombination (HR) showing that T-DNA integration is largely determined by the host (Bundock *et al.*, 1995). In the absence of

homologous sequences in yeast and in many fungi the T-DNA is integrated via non homologous end-joining (NHEJ) that relies on Ku70, Ku80 and DNA ligase 4 proteins (van Attikum *et al.*, 2001; van Attikum *et al.*, 2003). Inactivation of one of the NHEJ factors prevented non-homologous integration in yeast and fungi (Kooistra *et al.*, 2004), but in plants such mutation of host had as most a minor negative effect on integration (Park *et al.*, 2015). Recently, van Kregten *et al.* (2016) showed that in *Arabidopsis thaliana* polymerase theta plays critical role in T-DNA integration. They have reported that POLQ mutant (*teb1*) plants are resistant to T-DNA integration, revealing that TMEJ (Theta-Mediated End Joining) is the prime pathway for T-DNA integration in plants.

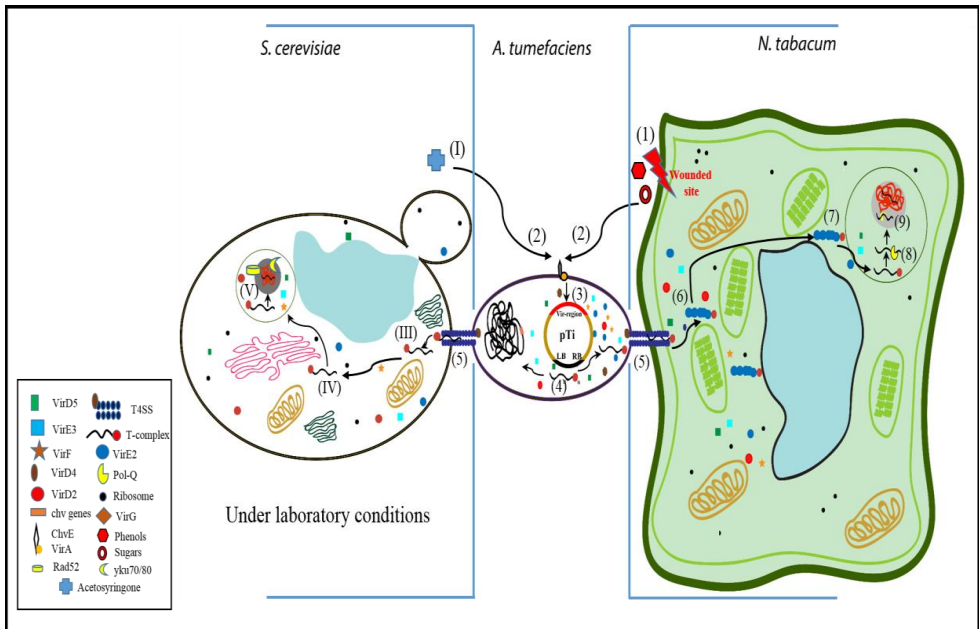


Figure 1. Schematic overview of the main processes during *Agrobacterium*-mediated transformation of plant and yeast cells. (1) Wounded plant cells (e.g. *N. tabacum*) excrete sugars and phenolic compounds (1), or under laboratory condition presence of acetosyringone (I) are recognized by the ChvE and VirA proteins of the sensory system at the bacterial membrane (2). VirG is phosphorylated by VirA and induces expression of *vir* genes located on the Ti plasmid (3). *A. tumefaciens* forms a strong specific bond to the plant cell through interaction of bacterial and plant receptors (not shown in this picture). Virulence protein VirD2 forms a relaxosome and is involved in the generation of a T-strand that stays covalently bound to VirD2 (4). The nucleoprotein complex and the virulence proteins VirD5, VirE2, VirE3 and VirF are directed to a Type IV Secretion System (T4SS) (5). Inside the plant cell the VirE2, no longer bound to VirE1, coats the nucleoprotein complex and a mature T-complex is formed (5) which moves to the nucleus (6 and III); VirE2 protein is not necessary for yeast transformation. Interaction between host factors and virulence proteins assist in the nuclear uptake of the T-complex (7 and IV). Upon nuclear uptake, the T-strand is uncoated (8) and the Pol-Q polymerase facilitates T-DNA integration into random positions of the host genome via micro-homology-mediated recombination (9). The T-DNA integration into the yeast genome occurs via Rad52- mediated homologous recombination or via yKu70/80-mediated non-homologous end joining (V).

Other bacterial secretion systems

The most conserved protein transport systems involved in protein translocation through the cytoplasmic membrane into either the periplasmic space or the inner membrane are the general secretion (Sec) system and the twin arginine translocation (Tat) system which have been identified in all bacteria (Natale *et al.*, 2008; Papanikou *et al.*, 2007; Lenz *et al.*, 2003). Proteins are translocated in their unfolded state through the Sec system that is composed of a protein targeting part, a motor protein and a membrane integrated conducting channel (Papanikou *et al.*, 2007). The Tat pathway, which consists of 2-3 subunits namely TatA, TatB and TatC, is used for secretion of folded proteins such as cytoplasmic synthesized redox factors (Natale *et al.*, 2008; Robinson and Bolhuis, 2004; Berks *et al.*, 2005). Pathogenic bacteria exploit various methods to infect mammalian and plant host cells and to prevent the host immune defense response. Effector protein secretion is one of the crucial factors of the pathogenicity of these bacteria. Therefore, several different secretion systems are employed by the pathogenic bacteria to secrete their specific effector proteins from the bacteria into the host cells or the host environment to facilitate the infection processes (Deng *et al.*, 2017; O'Boyle and Boyd, 2014). In general, bacterial protein secretion systems can be divided into five major classes, based on their structures, functions, and specificity namely the Type III Secretion System (T3SS), T4SS, T5SS, T6SS, and T7SS. The T3SS is a molecular machine similar evolutionary derived from the bacterial flagellar apparatus. Its capability to secrete effector proteins into the extrabacterial environment and into host cells was first proposed in *Yersinia pestis* (Rosqvist *et al.*, 1994). Since then T3SSs have been found in many gram-negative bacterial species, including pathogens and commensals of mammals, plants, and insects (see review, Troisfontaines and Cornelis *et al.*, 2005). The T3SS is a complex structure composed of approximately 20 bacterial proteins (Coburn *et al.*, 2007). For a description of the other system see the review by Green and Mecsas (2016).

Detection of Type III and IV effector protein translocation

To study protein translocation from bacteria into host cells, several different methods have been used over the past decades which are described here briefly (for review see O'Boyle *et al.*, 2017). **Effector-CyaA fusion.** In this method the desired effector protein is fused to the calmodulin-dependent adenylate-cyclase domain of adenylate cyclase (CyaA). After successful CyaA-tagged protein translocation through the T3SS into the host cell, calmodulin

activates the CyaA and it converts adenosine triphosphate into cyclic adenosine monophosphate (cAMP). The cAMP concentration can be measured using an enzyme-linked antibody, which is commercially available. This method has been used for detection of the translocation of translocated YopE and YopH proteins by *Yersinia* (Sory *et al.*, 1995).

Glycogen synthase kinase (GSK) tag is a 13-residue peptide derived from the human GSK-3beta kinase. The GSK-tagged effector protein will be phosphorylated after protein translocation into a host cell which can be detected with antibodies. This technique has been used to detect translocation of *Yersinia enterocolitica* Yops proteins for instance (Sory and Cornelis, 1994).

Direct tetracysteine-fluorescein biarsenical hairpin binder (4Cys-FIAsh) labelling. To visualize translocation of desired effector proteins they can be fused with a 12-18 residues amino acid tag including a 4Cys hairpin. 4Cys-tagged effector protein become fluorescent and detectable by binding of the FIAsh dye (Hoffmann *et al.*, 2010). This has been applied for instance in *Shigella* and *Salmonella* to visualize translocation of IpaB, IpaC and SopE2 and SptP effector proteins into host cells (Enninga *et al.*, 2005; Van Engelenburg and Palmer, 2008). More recently two new techniques using split-GFP and phiLOV2.1 were described. These have been used in this thesis and will be described in more detail below.

Split GFP complementation system

Green fluorescent protein (GFP) is well known and widely used to visualize the location of proteins in living cells. It was discovered by Osamu Shimomura to be the agent responsible for fluorescence in jellyfish *Aequorea victoria* (Shimomura *et al.*, 1962). GFP can be excited at 470 nm and shows emission at 508 nm and requires no substrate and coenzyme (Tsien, 1998; Morise *et al.*, 1974). In 1992, the GFP gene was cloned and expressed in non-jellyfish organisms making those fluorescent (Prasher *et al.*, 1992; Chalfie *et al.*, 1994). Fusions to other proteins did not have a negative effect on its functionality. Thus, proteins fused with GFP can be followed inside the cells, with minimum light exposure and low photobleaching effects (Lippincott-Schwartz *et al.*, 2000). Variants of GFP with different emission and excitation spectra were obtained by mutagenesis including cyan (CFP), blue fluorescent protein (BFP) (Heim *et al.*, 1994; Rizzuto *et al.*, 1996) and red-shifted yellow fluorescent protein (YFP) (Ormö *et al.*, 1996). GFP was successfully used to visualize the translocation of effector proteins from the pathogenic fungus *Magnaporthe oryzae* into rice (Khang *et al.*, 2010). However, only one report of successful measurement of protein translocation in

bacteria using GFP is available, in contrast with all other negative results which were obtained. This is suggesting that GFP-tagged proteins do not pass through T3SS and T4SS. In addition, the large size of GFP (27 k Da) and loss of activity of some effector proteins after tagging with GFP make tagging with GFP less useful (Akeda and Galán, 2005; Chang *et al.*, 2014; Tanaka *et al.*, 2015).

The bimolecular fluorescence complementation (BiFC) assay can be used for visualization of protein-protein interactions in cells (Hu *et al.*, 2002) or even in visualization of effector protein translocation from bacteria to its recipient cells (Sakalis *et al.*, 2014). This technique is based on reassembly of two split fragments of a fluorescent protein such as EYFP, Venus, GFP, Cerulean and mRFP1 by fusion of each fragment to proteins that interact in the cell (Hu and Kerppola, 2006; Shyu *et al.*, 2006; Huu and Kerppola, 2003; Jach *et al.*, 2006). In addition, simultaneous detection of multiple binding partners of a desired protein can be accomplished using BiFC. However, physical constraints due to the properties of these large fusion proteins may prevent reconstitution of the fluorescent protein. Alternatively, split GFP fluorescent protein complementation system has been developed (Cabantous *et al.*, 2005). In the split GFP system, the first 10 β -strands of GFP containing amino acids 1-214 (GFP₁₋₁₀) is expressed in host cells and the effector protein to be studied is tagged to the eleventh β -strand of GFP containing amino acids 214-230 (GFP₁₁) (Cabantous *et al.*, 2005). After successful translocation of the GFP₁₁-tagged effector protein into their recipient cells, the two non-fluorescent parts reconstitute to form the complete GFP structure which is fluorescent and can be detected by confocal or fluorescent microscopy (Figure 2). The split-GFP system was used to visualize translocation of *Salmonella* effector proteins PipB2 and SteA into human host cells (Van Engelenburg and Palmer). Recently Henry *et al.* (2017) used the split GFP system to directly visualize the translocation of bacterial effector proteins via T3SS in *A. thaliana*. They have shown the translocation of GFP₁₁-tagged effector proteins AvrPto, AvrPtoB, AvrB from *Pseudomonas syringae* and effector protein PopP2 from *Ralstonia solanacearum* into leaf cells of *A. thaliana* expressing GFP₁₋₁₀ during natural infection. Translocation of virulence protein VirE2 from *A. tumefaciens* through the T4SS was successfully visualized using the split GFP system in yeast, Arabidopsis, and *Nicotiana tabacum* (Sakalis *et al.*, 2014; Li *et al.*, 2014; Li and Pan, 2017). Despite all of the benefits of the split GFP technique, it still has also some disadvantages. For instance, it can only be used for recipient cells that have been transformed to enable expression of GFP₁₋₁₀. Another

disadvantage is that the translocated proteins will only be detectable in cellular compartments where GFP₁₋₁₀ is present (Park *et al.*, 2017).

Direct labelling of effectors with phiLOV2.1

A wide range of LOV domain-containing photoreceptors proteins have been found in bacteria, fungi and plants (Christie, 2007). The fluorescent properties of these plant blue-light receptor kinases are regulated either by Light, Oxygen or Voltage (Huala *et al.*, 1997; Buckley *et al.*, 2015). LOV domains can bind to the chromophore flavin mononucleotide (FMN) and subsequently emit green fluorescence upon blue/UV light irradiation. By protein production from pET-based vectors, it has been shown that the LOV-domain variant iLOV (improved LOV) is more effective as a fluorescent reporter (Chapman *et al.*, 2008). Moreover, tagging EspG with iLOV did not impede functionality of this effector protein upon microinjection into Normal Rat Kidney (NRK) cells which resulted in Golgi apparatus disruption (Gawthorne *et al.*, 2012) as previously observed with GFP-tagged EspG (Selyunin *et al.*, 2011). The structure of iLOV was further manipulated to generate novel, photostable variants that could readily be detected in bacterial and mammalian model systems. Subsequent structural analysis of a representative fraction of the resulting photostable iLOV variants revealed several additional possibilities to both improve the photochemical properties of iLOV, and also to generate alternative, photostable variants (phiLOV2.1), thus providing new LOV scaffold proteins as oxygen-independent fluorescence reporters (Christie *et al.*, 2012a, b). The smaller size of LOV (12.1 kDa) in comparison with GFP (27 kDa) is an advantage and also the fact that no specific genetically modified recipient cells are required for the detection of protein translocation into host cells (Chapman *et al.*, 2009). PhiLOV2.1 was used to observe Tir-phiLOV2.1 and IpaB-phiLOV2.1 expression inside *E.coli* O157H7 and *Shigella flexneri*, respectively, and also the phiLOV2.1-tagged SipA effector protein of *Salmonella* was detected in macrophages and intestinal epithelial cells after translocation (Gawthorne *et al.*, 2016; McIntosh *et al.*, 2017).

Each of the mentioned techniques have their strengths and drawbacks. Not all techniques are generally applicable. Some of these techniques give only information on the fact that protein translocation does occur, but give no information on the location of the translocated protein in the host cell. In this thesis I was focused on two methods that are summarized in figure 2.

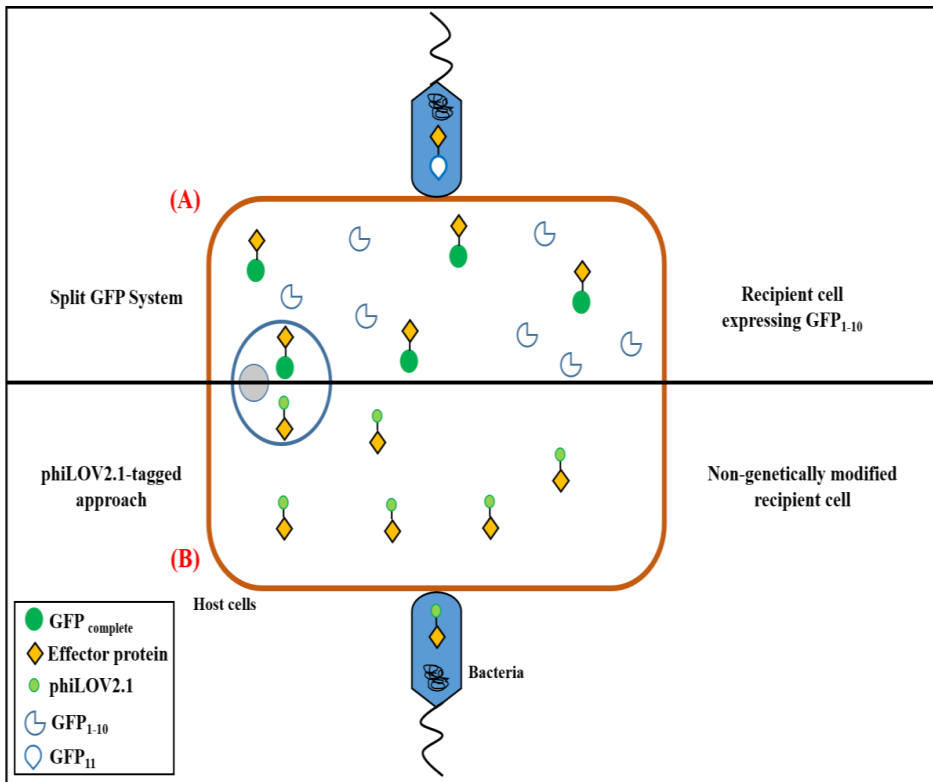


Figure 2. Two techniques to visualize protein translocation from bacteria into living host cells. (A) The split GFP system. The effector protein is tagged with the non-fluorescent GFP₁₁; the non-fluorescent GFP₁₋₁₀ is expressed in the host cell; upon successful translocation of the GFP₁₁-tagged effector protein is will bind to GFP₁₋₁₀ and thus reassemble into a complete GFP fluorescent protein which can be detected. (B) The phiLOV2.1 tagging approach. The effector protein is tagged with the fluorescent protein phiLOV2.1. The effector protein can be detected upon expression inside the bacteria and after translocation into the recipient cell.

Visualization of effector protein translocation from *Agrobacterium* into plant and yeast host cells.

Vergunst *et al.* (2000 and 2005) used the Cre-Recombinase Reporter Assay For Translocation (CRAFT) to demonstrate for the first time that the VirF, VirD5, VirE3 and VirE2 virulence proteins are translocated from *Agrobacterium* into plant cells through the T4SS directed by C-terminal translocational sequences. To this end, the effector proteins were tagged with the Cre-recombinase and host cells were used that contain a reporter gene disrupted by a segment of DNA flanked by two *lox*-sites. Upon translocation of the tagged effector protein, the floxed segment was excised and either a kanamycin resistance selection marker or a GFP reporter gene becomes active. By the same technique translocation of these virulence proteins into yeast host cells was demonstrated (Schrammeijer *et al.*, 2003). Translocation of the effector proteins from *Agrobacterium* into their host cells is independent of the translocation of T-DNA (Vergunst *et al.*, 2005). However, reversely translocation of the T-DNA is dependent on the translocation of the relaxase VirD2, which has a more complex bipartite translocation signal (van Kregten *et al.*, 2009). To directly monitor the translocation of virulence proteins from *Agrobacterium* into host cells and the trafficking of these virulence proteins inside the host cell we (Sakalis *et al.*, 2014) and another research group (Li *et al.*, 2014) have visualized the translocation of VirE2 from *Agrobacterium* into yeast and plant cells using BiFC and the split GFP system.

➤ **Thesis outline**

In this thesis protein translocation from *Agrobacterium* into yeast and plant cells is studied to obtain fundamental insights in the translocation process and in the fate of the translocated proteins in the host cells and the potential biotechnological applications of *Agrobacterium* mediated protein translocation were explored.

In this thesis we studied the *Agrobacterium* virulence protein expression, translocation and localization via direct visualization and also potential biotechnological applications of protein translocation from *Agrobacterium* into the recipient cells.

In **Chapter 2**, we used the split-GFP system to visualize translocation and localization of VirE2 and VirD2 in plant and yeast cells. We tagged the VirE2 protein with GFP₁₁ internally instead of N-terminally and the quality of signal observation, biological activities and expression timing were greatly improved compared to our previous studies. Besides, we were able to capture the movement of internally tagged VirE2. By using the split-GFP system, we could observe translocation of VirD2 which accumulated in the nucleus and cytoplasm of plant and yeast cells, whether or not T-DNA was co-delivered from the *Agrobacterium* donor into the host.

In **Chapter 3**, we made use of the novel phiLOV2.1 fluorescent peptide to directly visualize effector protein translocation to host cells. In contrast to previous GFP based methodologies, the new method does not rely on special transgenic host cells, thus we successfully visualized protein translocation into *Arabidopsis thaliana* root, tobacco leaf and yeast cells.

In **Chapter 4**, we engineered *Agrobacterium* so that it can translocate the HO endonuclease into the host cells. In this chapter, we show that the mating type of *S. cerevisiae* cells can be switched after the introduction of the HO endonuclease by protein translocation from *Agrobacterium* into yeast. This chapter is a good example of using *Agrobacterium* to deliver foreign proteins into eukaryotic cells as an epigenetic inducer or as a tool for protein therapy.

In **Chapter 5**, it was investigated whether AMT can be adapted in a way that transformation of organellar DNA may become possible. It was shown that VirE2 and VirD2 tagged with a mitochondrial or chloroplast targeting sequence can be directed into yeast mitochondria and plant chloroplasts, respectively. This result may be exploited in future research to target T-DNA into organelles and may ultimately lead to organellar genome modification.

REFERENCES

- Abu-Arish, A., Frenkiel-Krispin, D., Fricke, T., Tzfira, T., Citovsky, V., Wolf, S.G. and Elbaum, M. (2004).** Three-dimensional reconstruction of *Agrobacterium* VirE2 protein with single-stranded DNA. *J. Biol. Chem.*, 279, 25359–25363.
- Akeda, Y. and Galán, J. E. (2005).** Chaperone release and unfolding of substrates in type III secretion. *Nature*, 437, 911.
- Anand, A., Krichevsky, A., Schornack, S., Lahaye, T., Tzfira, T., Tang, Y., Citovsky, V. and Mysore, K. S. (2007).** Arabidopsis VirE2 interacting protein2 is required for *Agrobacterium* T-DNA integration in plants. *The Plant Cell*, 19, 1695–1708.
- Atmakuri, K., Cascales, E., Burton, O. T., Banta, L. M. and Christie, P. J. (2007).** *Agrobacterium* ParA/MinD-like VirC1 spatially coordinates early conjugative DNA transfer reactions. *EMBO J.*, 26, 2540–2551.
- Bansal, K. C. and Sharma, R. K. (2003).** Chloroplast transformation as a tool for prevention of gene flow from GM crops to weedy or wild relatives. *Current Science*, 84, 1286–1287.
- Brawn, L. C., Hayward, R. D. and Koronakis, V. (2007).** Salmonella SPI1 effector SipA persists after entry and cooperates with a SPI2 effector to regulate phagosome maturation and intracellular replication. *Cell Host Microbe*, 1, 63–75.
- Brencic, A., Angert, E.R. and Winans, S.C. (2005).** Unwounded plants elicit *Agrobacterium vir* gene induction and T-DNA transfer: Transformed plant cells produce opines yet are tumor free. *Mol. Microbiol.* 57, 1522–31.
- Brencic, A. and Winans, S. (2005).** Detection and response to signals involved in host-microbe interactions by plant-associated bacteria. *Microbiol. Mol. Biol. Rev.*, 69, 155–94.
- Briones, G., Hofreuter, D. and Galán, J. E. (2006).** Cre reporter system to monitor the translocation of type III secreted proteins into host cells. *Infect. Immun*, 74, 1084–1090.
- Buckley, A.M., Petersen, J., Roe, A.J., Douce, G.R. and Christie, J.M. (2015)** LOV-based reporters for fluorescence imaging. *Curr. Opin. Chem. Biol.* 27, 39–45.
- Bulgakov V.P., Kisselev, K.V., Yakovlev, K.V., Zhuravlev, Y.N., Gontcharov A.A. and Odintsova, N.A. (2006).** *Agrobacterium* -mediated transformation of sea urchin embryos. *Biotechnol J*, 1, 454–461.
- Bundock, P., den Dulk-Ras, A., Beijersbergen, A. and Hooykaas, P.J.J. (1995).** Transkingdom T-DNA transfer from *Agrobacterium tumefaciens* to *Saccharomyces cerevisiae*. *EMBO J.*, 14, 3206–3214.

- Cabantous, S., Terwilliger, T. C. and Waldo, G. S.** (2005). Protein tagging and detection with engineered self-assembling fragments of green fluorescent protein. *Nat. Biotechnol.*, 23, 102–107.
- Cain, R. J., Hayward, R. D., and Koronakis, V.** (2004). The target cell plasma membrane is a critical interface for Salmonella cell entry effector–host interplay. *Mol Microbiol.*, 54, 887–904.
- Cerutti, H., Johnson, A.M., Boynton, J.E. and Gilham, N.W.** (1995) Inhibition of chloroplast DNA recombination and repair by dominant negative mutants of Escherichia coli RecA. *Mol Cell Biol.*, 15, 3003-3011.
- Chalfie, M., Tu, Y., Euskirchen, G., Ward, W.W. and Prasher, D.C.** (1994). Green fluorescent protein as a marker for gene expression. *Science*, 263,802–805.
- Chapman, S., Faulkner, C., Kaiserli, E., Garcia-Mata, C., Savenkov, E.I., Roberts, A.G., Oparka, K.J. and Christie, J.M.** (2008). The photoreversible fluorescent protein iLOV outperforms GFP as a reporter of plant virus infection. *Proc. Natl. Acad. Sci. USA*, 105, 20038 –20043.
- Chang, J.H., Desveaux, D., and Creason, A.L.** (2014). The ABCs and 123s of bacterial secretion systems in plant pathogenesis. *Annu. Rev. Phytopathol.*, 52, 317–345.
- Christie, J.M., Corchnoy, S.B., Swartz, T.E., Hokensn, M., Han, I.S., Briggs, W.R. and Bogomolni, R.A.** (2007). Steric interactions stabilize the signaling state of the LOV2 domain of phototropin 1. *Biochem.*, 46, 9310–19.
- Christie, J.M., Gawthorne, J.A., Young, G., Fraser, N.J. and Roe, A.J.** (2012a). LOV to BLUF: Flavoprotein contributions to the optogenetic toolkit. *Mol. Plant.*, 5, 533–544.
- Christie, J.M., Hitomi, K., Arvai, A.S., Hartfield, K.A., Mettlen, M., Pratt, A.J., Tainer, J.A. and Getzoff, E.D.** (2012b). Structural tuning of the fluorescent protein iLOV for improved photostability. *J. Biol. Chem.* 287, 22295–22304.
- Christie, P.J., Whitaker, N. and González-Rivera, C.** (2014). Mechanism and structure of the bacterial type IV 732 secretion systems. *Biochim. Biophys. Acta.* 1843, 1578–1591.
- Coburn, B., Sekirov, I. and Finlay, B.B.,** (2007). Type III secretion systems and disease. *Clin. Microbiol. Rev.*, 20, 535–549.
- Cormack, B.P, Valdivia, R.H, Falkow, S.** (1996). FACS-optimized mutants of the green fluorescent protein (GFP). *Gene*, 173, 33–38.
- Citovsky, V., Wong, M. L. and Zambryski, P.** (1989). Cooperative interaction of *Agrobacterium* VirE2 protein with single-stranded DNA: implications for the T-DNA transfer process. *Proc. Nat. Acad. Sci. U. S. A.*, 86, 1193–7.

- de Groot, M. J., Bundock, P., Hooykaas, P. J.J. and Beijersbergen, A. G.** (1998). *Agrobacterium tumefaciens*-mediated transformation of filamentous fungi. *Nat. Biotechnol.*, *16*, 839–842.
- Deng, W., Chen, L., Peng, W. T., Liang, X., Sekiguchi, S., Gordon, M. P., Comai, L. and Nester, E. W.** (1999). VirE1 is a specific molecular chaperone for the exported single-stranded-DNA-binding protein VirE2 in *Agrobacterium*. *Mol Microbiol*, *31*, 1795–1807.
- Deng, W., Marshall, N. C., Rowland, J. L., McCoy, J. M., Worrall, L. J., Santos, A. S., Strynadka, N.C.J. and Finlay, B. B.** (2017). Assembly, structure, function and regulation of type III secretion systems. *Nat. Rev. Microbiol.*, *15*, 323–337.
- Djamei, A., Pitzschke, A., Nakagami, H., Rajh, I. and Hirt, H.** (2007). Trojan horse strategy in *Agrobacterium* transformation: abusing MAPK defense signaling. *Science* *318*, 453–456
- Dumas, F., Duckely, M., Pelczar, P., Van Gelder, P. and Hohn, B.** (2001). An *Agrobacterium* VirE2 channel for transferred-DNA transport into plant cells. *Proc. Natl. Acad. Sci. USA*, *98*, 485–490.
- Enninga, J., Mounier, J., Sansonetti, P. and Van Nhieu, G. T.** (2005). Secretion of type III effectors into host cells in real time. *Nature Methods*, *2*, 959.
- García-Rodríguez, F. M., Schrammeijer, B., Hooykaas, P. J. J. and Garci, F. M.** (2006). The *Agrobacterium* VirE3 effector protein: a potential plant transcriptional activator. *Nucleic Acids Res.*, *34*, 6496–504.
- Gawthorne, J. A., Reddick, L. E., Akpunarlieva, S. N., Beckham, K. S., Christie, J. M., Alto, N. M., Gabrielsen, M. and Roe, A.J.** (2012). Express your LOV: an engineered flavoprotein as a reporter for protein expression and purification. *PLoS ONE*, *7*, e52962.
- Gawthorne, J. A., Audry, L., McQuitty, C., Dean, P., Christie, J. M., Enninga, J., and Roe, A. J.** (2016). Visualizing the translocation and localization of bacterial Type III effector proteins by using a genetically encoded reporter system. *Appl. Environ. Microbiol.*, *82*, 2700–2708.
- Gelvin, S.B** (2000). *Agrobacterium* and plant genes involved in T-DNA transfer and integration. *Annu. Rev. Plant Biol.*, *51*, 223-256.
- Gelvin, S.B.** (2010). Plant proteins involved in *Agrobacterium* -mediated genetic transformation. *Annu. Rev. Phytopathol.* *48*, 45-68.
- Gietl, C., Koukoulíková-Nicola, Z. and Hohn, B.** (1987). Mobilization of T-DNA from *Agrobacterium* to plant cells involves a protein that binds single-stranded DNA. *Proc. Nat. Aca. Sci. USA.*, 9006–9010.
- Goedhart, J., van Weeren, L., Hink, M.,A, Vischer, N.O., Jalink, K. and Gadella, T.W.J.** (2010). Bright cyan fluorescent protein variants identified by fluorescence lifetime screening. *Nat Methods*, *7*, 137–139.

Gordon, J. E. and Christie, P. J. (2014). The *Agrobacterium* Ti Plasmids. *Microbiology Spectrum*, 2(6).

Goodner, B. W., B. P. Markelz, M. C. Flanagan, C. B. Crowell, J. L. Racette, A. Schilling, L. M. Halfon, J. S. Mellors, and G. Grabowski. (1999). Combined genetic and physical map of the complex genome of *Agrobacterium tumefaciens*. *J. Bacteriol*, 181, 5160–5166.

Goodner, B., G. Hinkle, S. Gattung, N. Miller, M. Blanchard, B. Quorollo, B. S. Goldman, Y. Cao, M. Askenazi, C. Halling, L. Mullin, K. Houmiel, J. Gordon, M. Vaudin, O. Iartchouk, A. Epp, F. Liu, C. Wollam, M. Allinger, D. Doughty, C. Scott, C. Lappas, B. Markelz, C. Flanagan, C. Crowell, J. Gurson, C. Lomo, C. Sear, G. Strub, C. Cielo, and S. Slater. (2001). Genome sequence of the plant pathogen and biotechnology agent *Agrobacterium tumefaciens* C58. *Science*, 294, 2323–2328.

Green, E.R. and Mecsas, J. (2016) Bacterial secretion systems: an overview. *Microbiol. Spectr.* 4, VMBF.0012-2015.

Haraga, A., Ohlson, M. B. and Miller, S. I. (2008). Salmonellae interplay with host cells. *Nat. Rev. Microbiol*, 6, 53–66.

Heim, R. and Tsien, R. Y. (1996). Engineering green fluorescent protein for improved brightness, longer wavelengths and fluorescence energy transfer. *Curr. Biol*, 6, 178–182.

Henry, E., Toruño, T.Y., Jauneau, A., Deslandes, L. and Coaker, G.L. (2017) Direct and indirect visualization of bacterial effector delivery into diverse plant cell types during infection. *Plant Cell*, 29, 1555.

Hoffmann, C., Gaietta, G., Zurn, A., Adams, S. R., Terrillon, S., Ellisman, M.H., Tsien, R.Y. and Lohse, M. J. (2010). Fluorescent labeling of tetracysteine-tagged proteins in intact cells. *Nat Protoc*, 5, 1666–1677.

Hooykaas, P. J. J., Hofker, M., den Dulk-Ras, A. and Schilperoort, R. A. (1984). A comparison of virulence determinants in an octopine Ti plasmid, a nopaline Ti plasmid, and an Ri plasmid by complementation analysis of *Agrobacterium tumefaciens* mutants. *Plasmid*, 11, 195–205.

Hooykaas-VanSlogteren, G. M. S., Hooykaas, P. J. J. and Schilperoort, R. A. (1984). Expression of Ti plasmid genes in monocotyledonous plants infected with *Agrobacterium tumefaciens*. *Nature*, 311, 763-64.

Hu, C.D., Chinenov, Y. and Kerppola, T.K. (2002). Visualization of interactions among bZIP and Rel family proteins in living cells using bimolecular fluorescence complementation. *Mol. Cell*, 9, 789–98.

Hu, C.D. and Kerppola, T.K. (2003). Simultaneous visualization of multiple protein interactions in living cells using multicolor fluorescence complementation analysis. *Nat. Biotechnol*, 21, 539–45.

- Huala, E., Oeller, P.W., Liscum, E., Han, I.S., Larsen, E. and Briggs, W.R.** (1997). *Arabidopsis* NPH1: a protein kinase with a putative redox-sensing domain. *Science*, 278, 2120–2123.
- Inouye, S. and Tsuji, F.I.** (1994). *Aequorea* green fluorescent protein. Expression of the gene and fluorescence characteristics of the recombinant protein. *FEBS Lett*, 1994, 34, 277–80.
- Jach, G., Pesch, M., Richter, K., Frings, S. and Uhrig, J.F.** (2006). An improved mRFP1 adds red to bimolecular fluorescence complementation. *Nature Methods*, 3, 597–600.
- Jarchow, E., Grimsley, N. H. and Hohn, B.** (1991). VirF, the host-range determining virulence gene of *Agrobacterium tumefaciens*, affects T-DNA transfer to *Zea mays*. *Proc. Natl. Acad. Sci. USA*, 88, 10426–10430.
- Jin, S., T. Komari, Gordon, M. P. and Nester, E. W.** (1987). Genes responsible for the supervirulence phenotype of *Agrobacterium tumefaciens* A281. *J. Bacteriol.* 169, 4417–4425.
- Kamiyama, D., Sekine, S., Barsi-Rhyne, B., Hu, J., Chen, B., Gilbert, L. A., Ishikawa, H., Leonetti, M.D., Marshall, W.F. and Weissman, J.S.** (2016). Versatile protein tagging in cells with split fluorescent protein. *Nat. Commun.*, 7, 11046.
- Kenny, B., DeVinney, R., Stein, M., Reinscheid, D. J., Frey, E. A. and Finlay, B. B.** (1997). Enteropathogenic *E. coli* (EPEC) transfers its receptor for intimate adherence into mammalian cells. *Cell*, 91, 511–520.
- Khan, M.** (2017). Molecular engineering of plant development using *Agrobacterium* - mediated protein translocation. PhD thesis, Leiden University, Leiden, the Netherlands.
- Khang, C.H., Berruyer, R., Giraldo, M.C., Kankanala, P., Park, S.Y., Czymbek, K., Kang, S. and Valent, B.** (2010). Translocation of *Magnaporthe oryzae* effectors into rice cells and their subsequent cell-to-cell movement. *Plant Cell*, 22, 1388–1403.
- Kooistra, R., Hooykaas, P.J.J. and Steensma, H.Y.** (2004). Efficient gene targeting in *Kluyveromyces lactis*. *Yeast*, 21, 781–792.
- Kumar, S. V., Misquitta, R. W., Reddy, V. S., Rao, B. J. and Rajam, M. V.** (2004). Genetic transformation of the green alga--*Chlamydomonas reinhardtii* by *Agrobacterium tumefaciens*. *Plant Sci.*, 166(3), 731–738.
- Kunik, T., T. Tzfira, Y. Kapulnik, Y. Gafni, C. Dingwall, and V. Citovsky.** (2001). Genetic transformation of HeLa cells by *Agrobacterium*. *Proc. Natl. Acad. Sci. USA.*, 98, 1871–1876.

Krenek, P., Samajova, O., Luptovciak, I., Duskocilova, A., Komis, G. and Samaj, J. Transient plant transformation mediated by *Agrobacterium tumefaciens*: Principles, methods and applications. *Biotechnol. Adv.* 33, 1024–42.

Lee K, Dudley MW, Hess KM, Lynn DG, Joerger RD, Binns AN. (1992). Mechanism of activation of *Agrobacterium* virulence genes: identification of phenol-binding proteins. *Proc. Natl. Acad. Sci. USA.*, 89, 8666–8670.

Lenz, L.L, Mohammadi, S., Geissler, A., Portnoy, D.A. (2003). SecA2-dependent secretion of autolytic enzymes promotes *Listeria monocytogenes* pathogenesis. *Proc. Nat. Aca. Sci. USA*, 100, 12432–12437.

Li, X., Yang, Q., Tu, H., Lim, Z. and Pan, S. Q. (2014). Direct visualization of *Agrobacterium* -delivered VirE2 in recipient cells. *Plant J.* 77(3), 487–495.

Li, X. and Pan, S.Q. (2017). *Agrobacterium* delivers VirE2 protein into host cells via clathrin-mediated endocytosis. *Sci. Adv.* 3. e1601528.

Lippincott-Schwartz, J., Roberts, T. H. and Hirschberg, K. (2000). Secretory protein trafficking and organelle dynamics in living cells. *Annu. Rev. Cell Dev. Biol.*, 16, 557–589.

Lu, J., den Dulk-Ras, A., Hooykaas, P.J.J. and Glover, J.N.M. (2009). *Agrobacterium tumefaciens* VirC2 enhances T-DNA transfer and virulence through its C-terminal ribbon-helix-helix DNA-binding fold. *Proc. Natl. Acad. Sci. USA.*, 106, 9643–8.

Ma, L., Yang, F. and Zheng, J. (2014). Application of fluorescence resonance energy transfer in protein studies. *J. Mol. Struct.*, 1077, 87 – 100.

Maliga, P., Staub, J., Carrer, H., Kanevski, I. and Svab, Z. (1994). Homologous recombination and integration of foreign DNA in plastids of higher plants. Homologous Recombination and Gene Silencing in Plants, Kluwer Academic Publishers, the Netherlands 83–93.

McBride, K. E. and Knauf, V. C. (1988). Genetic analysis of the virE operon of the *Agrobacterium* Ti plasmid pTiA6. *J. Bacteriol.*, 170, 1430–1437.

McCullen, C. A. and Binns, A. N. (2006). *Agrobacterium tumefaciens* and plant cell interactions and activities required for interkingdom macromolecular transfer. *Annu. Rev. Cell Dev. Biol.*, 22, 101–127.

McIntosh, A., Meikle, L. M., Ormsby, M. J., McCormick, B. A., Christie, J. M., Brewer, J. M., Roberts, M. and Wall, D. M. (2017). SipA activation of caspase-3 is a decisive mediator of host cell survival at early stages of *Salmonella enterica* serovar typhimurium infection. *Infect. Immun.*, 85(9). e00393-17.

Melchers, L. S., Maroney, M. J., den Dulk-Ras, A., Thompson, D. V., van Vuuren, H. A. J., Schilperoort, R. A. and Hooykaas, P. J. J. (1990). Octopine and nopaline strains of

Agrobacterium tumefaciens differ in virulence: molecular characterization of the virF locus. *Plant Mol. Biol.*, 14, 249–259.

Meyers, B., Zaltsman, A., Lacroix, B., Kozlovsky, S.V. and Krichevsky, A. (2010). Nuclear and plastid genetic engineering of plants: comparison of opportunities and challenges. *Biotechnol Adv*, 28, 747–756.

Morise, H., Shimomura, O., Johnson, F.H. and Winant, J. (1974). Intermolecular energy transfer in the bioluminescent system of *Aequorea*. *Biochemistry*, 13,2656–62

Nagai, T., Iбата, K., Park, E.S., Kubota, M., Mikoshiba, K. and Miyawaki, A. (2002). A variant of yellow fluorescent protein with fast and efficient maturation for cell-biological applications. *Nat. Biotechnol.* 20, 87–90.

Natale, P., Bruser, T. and Driessen, A.J. (2008). Sec- and Tat-mediated protein secretion across the bacterial cytoplasmic membrane--distinct translocases and mechanisms. *Biochim Biophys Acta*, 1778, 1735–56.

Ninomiya, Y., Suzuki, K., Ishii, C. and Inoue, H. (2004). Highly efficient gene replacements in *Neurospora* strains deficient for nonhomologous end-joining. *Proc Natl. Acad. Sci. USA.*, 101, 12248–12253.

Niu, X., Zhou, M., Henkel, C. V., van Heusden, G. P. H., and Hooykaas, P. J. J. (2015). The *Agrobacterium tumefaciens* virulence protein VirE3 is a transcriptional activator of the F-box gene VBF. *Plant J.*, 914–924.

O'Boyle, N. and Boyd, A. (2014). Manipulation of intestinal epithelial cell function by the cell contact-dependent type III secretion systems of *Vibrio parahaemolyticus*. *Front. Cell. Infect. Microbiol.*, 3, 114.

Offringa, R., M. J. A. de Groot, H. J. Haagsman, M. P. Does, P. J. M. van den Elzen, and P. J. J. Hooykaas. (1990). Extrachromosomal homologous recombination and gene targeting in plant cells after *Agrobacterium* mediated transformation. *EMBO J.*, 9, 3077–3084.

Ormo M, Cubitt AB, Kallio K, Gross LA, Tsien RY, Remington SJ. (1996). Crystal structure of the *Aequorea victoria* green fluorescent protein. *Science* 273, 1392–1395.

Otten, L., DeGreve, H., Leemans, J., Hain, R., Hooykaas, P.J.J. and Schell, J. (1984). Restoration of virulence of vir region mutants of *Agrobacterium tumefaciens* strain B6S3 by coinfection with normal and mutant *Agrobacterium* strains. *Mol. Gen. Genet*, 195, 159–163.

Palmer, A.G., Gao, R., Maresh, J., Erbiol, W.K. and Lynn, D.G. (2004). Chemical biology of multi host/pathogen interactions: chemical perception and metabolic complementation. *Annu Rev Phytopathol*, 42,439–464.

- Pansegrau, W., Schoumacher, F., Hohn, B. and Lanka, E. (1993).** Site-specific cleavage and joining of single-stranded DNA by VirD2 protein of *Agrobacterium tumefaciens* Ti plasmids: analogy to bacterial conjugation. *Proc. Natl. Acad. Sci. USA.*, 90, 11538–11542.
- Papanikou, E., Karamanou, S. and Economou, A. (2007).** Bacterial protein secretion through the translocase nanomachine. *Nat Rev Microbiol*, 5, 839–851.
- Park, S.Y., Vaghchhipawala, Z., Vasudevan, B., Lee, L.-Y., Shen, Y., Singer, K., Waterworth, W.M., Zhang, Z.J., West, C.E., Mysore, K.S., Kirankumar, S. and Gelvin, S.B. (2015).** *Agrobacterium* T-DNA integration into the plant genome can occur without the activity of key non-homologous end-joining proteins. *Plant J.*, 81, 934–946.
- Park, E., Lee, H.-Y., Woo, J., Choi, D. and Dinesh-Kumar, S.P. (2017).** Spatiotemporal monitoring of *Pseudomonas syringae* effectors via type III secretion using split fluorescent protein fragments. *Plant Cell*, 29, 1571–1584.
- Piers, K. L., Heath, J. D., Liang, X., Stephens, K. M. and Nester, E. W. (1996).** *Agrobacterium tumefaciens*-mediated transformation of yeast. *Proc. Nat. Aca. Sci.USA.*, 93(4), 1613–1618.
- Pitzschke, A., Djamei, A., Teige, M. and Hirt, H. (2009).** VIP1 response elements mediate mitogen-activated protein kinase 3-induced stress gene expression. *Proc. Nat. Aca. Sci.USA.*, 106, 18414–18419.
- Plano, L. R. Fischer, W. and Plano, G. V. (2006).** Measurement of effector protein injection by type III and type IV secretion systems by using a 13-residue phosphorylatable glycogen synthase kinase tag. *Infect. Immun*, 74, 5645–5657.
- Prasher, D.C, Eckenrode, V.K, Ward, W.W., Prendergast, F.G., Cormier, M.J., Bokman, S.H. (1992).** Primary structure of the *Aequorea victoria* green-fluorescent protein. *Gene*, 111, 229–33.
- Rego, A. T., Chandran, V. and Waksman, G. (2010).** Two-step and one-step secretion mechanisms in Gram-negative bacteria: contrasting the type IV secretion system and the chaperone–usher pathway of pilus biogenesis. *Biochem. J.*, 425, 475–488.
- Rizzo, M. A., Springer, G. H., Granada, B. and Piston, D. W. (2004).** An improved cyan fluorescent protein variant useful for FRET. *Nature Biotechnol*, 22, 445–449.
- Rizzuto, R., Brini, M., De Giorgi, F., Rossi, R., Heim, R., Tsien, R. Y. and Pozzan, T. (1996).** Double labelling of subcellular structures with organelle-targeted GFP mutants in vivo. *Curr. Biol.*, 6, 183–188.
- Rolloos ,M., Hooykaas, P.J.J. and van der Zaal, B.J. (2015).** Enhanced targeted integration mediated by translocated I-SceI during the *Agrobacterium* mediated transformation of yeast. *Sci. Rep.* 5, 8345.

Rosqvist, R., Magnusson, K. E. and Wolf-Watz, H. (1994). Target cell contact triggers expression and polarized transfer of Yersinia YopE cytotoxin into mammalian cells. *EMBO J.* 13, 964–972.

Roushan, M.R., de Zeeuw, A. M., Hooykaas, Paul J.J. and van Heusden, G. P. H. (2018). Application of phiLOV2.1 as a fluorescent marker for visualization of *Agrobacterium* effector protein translocation. *Plant Journal*.

Sakalis, P.A., van Heusden, G.P.H. and Hooykaas, P.J.J. (2014). Visualization of VirE2 protein translocation by the *Agrobacterium* type IV secretion system into host cells. *MicrobiologyOpen*, 3, 104–117.

Schmitz, D. (2018). CRISPR/Cas-induced targeted mutagenesis with *Agrobacterium* mediated protein delivery. PhD thesis, Leiden University, Leiden, the Netherlands.

Schrammeijer, B., den Dulk-Ras, A., Vergunst, A., C., Jurado Jacome, E. and Hooykaas, P.J. J. (2003). Analysis of Vir protein translocation from *Agrobacterium tumefaciens* using *Saccharomyces cerevisiae* as a model: evidence for transport of a novel effector protein VirE3. *Nucl. Acids Res*, 31, 860–868.

Schrammeijer, B., Risseeuw, E., Pansegrau, W., Regensburg-Tuink, T. J. G., Crosby, W. L. and Hooykaas, P. J. J. (2001). Interaction of the virulence protein VirF of *Agrobacterium tumefaciens* with plant homologs of the yeast Skp1 protein. *Curr. Biol*, 11, 258–262.

Selyunin, A.S., Sutton, S.E., Weigle, B.A., Reddick, L.E., Orchard, R.C., Bresson, S.M., Tomchick, D.R. and Alto, N.M. (2011) The assembly of a GTPase-kinase signalling complex by a bacterial catalytic scaffold. *Nature*, 469, 107–111.

Sen, P., Pazour, G. J., Anderson, D. and Das, A. (1989). Cooperative binding of *Agrobacterium tumefaciens* VirE2 protein to single-stranded DNA. *J. Bacteriol.*, 171, 2573–2580.

Sharma, K.K., Bhatnagar-Mathur, P. and Thorpe, T.A. (2005). Genetic transformation technology: status and problems. *In Vitro Cell Dev Biol Plant*, 41, 102–112.

Shi, Y., Lee, L.-Y. and Gelvin, S. B. (2014). Is VIP1 important for *Agrobacterium* - mediated transformation? *Plant J.* 79, 848–860.

Shimomura, O., Johnson, F.H. and Saiga Y. (1962). Extraction, purification and properties of aequorin, a bioluminescent protein from the luminous hydromedusan, *Aequorea*. *J Cell Comp Physiol*, 59, 223–239.

Shyu, J., Liu, H., Deng, X. and Hu, C.D. (2006). Identification of new fluorescent protein fragments for bimolecular fluorescence complementation analysis under physiological conditions. *Bio-Techniques*, 40, 61–66.

- Smith, E.F. and Townsend, C.O.** (1907). A plant-tumor of bacterial origin. *Science*, 25, 671–673.
- Sory, M.P. and Cornelis, G. R.** (1994). Translocation of a hybrid YopE-adenylate cyclase from *Yersinia enterocolitica* into HeLa cells. *Mol Microbiol*, 14, 583–594.
- Sory, M.P., Boland, A., Lambermont, I. and Cornelis, G.R.** (1995). Identification of the YopE and YopH domains required for secretion and internalization into the cytosol of macrophages, using the *cyaA* gene fusion approach. *Proc. Natl. Acad. Sci. USA.*, 92, 11998–12002.
- Stachel, S. E., Messens, M., Van Montagu, A. and Zambryski, P.** (1985). Identification of the signal molecules produced by wounded plant cells that activate T-DNA transfer in *Agrobacterium tumefaciens*. *Nature*, 318, 624–629.
- Stachel, S. E., and Nester, E. W.** (1986). The genetic and transcriptional organization of the *vir* region of the A6 Ti plasmid of *Agrobacterium tumefaciens*. *EMBO J*, 5, 1445–1454.
- Subramoni, S., Nathoo, N., Klimov, E., and Yuan, Z. C.** (2014). *Agrobacterium* responses to plant-derived signaling molecules. *Frontiers in plant science*, 5, 322.
- Sundberg, S., Meek, L., Carroll, K., Das, A. and Ream, W.** (1996). VirE1 protein mediates export of the single-stranded DNA-binding protein virE2 from *Agrobacterium tumefaciens* into plant cells. *J. Bacteriol.*, 178, 1207–1212.
- Tanaka, S., Djamei, A., Presti, L.L., Schipper, K., Winterberg, S., Amati, S., Becker, D., Büchner, H., Kumlehn, J., Reissmann, S. and Kahmann, R.** (2015). Experimental approaches to investigate effector translocation into host cells in the *Ustilago maydis*/maize pathosystem. *Eur. J. Cell Biol.* 94, 349–358.
- Thomashow, M. F., Nutter, R., Montoya, A. L., Gordon, M. P. and Nester, E. W.** (1980). Integration and organization of Ti plasmid sequences in crown gall tumors. *Cell*, 19, 729–739.
- Toro, N., Datta, A., Carmi, O.A., Young, C., Prusti, R.K. and Nester, E.W.** (1989). The *Agrobacterium tumefaciens* *virC1* gene product binds to overdrive, a T-DNA transfer enhancer. *J. Bacteriol*, 171, 6845–6849.
- Troisfontaines, P. and Cornelis, G. R.** (2005) Type III secretion: more systems than you think. *Physiology*, 20, 326–339.
- Tsien, R.Y.** (1998). The green fluorescent protein. *Annu. Rev. Biochem.* 67, 509–544.
- Tzfira, T. and Citovsky, V.** (2001). Comparison between nuclear localization of nopaline- and octopine-specific *Agrobacterium* VirE2 proteins in plant, yeast and mammalian cells. *Mol. Plant Pathol.* 2, 171–176.

- Tzfira, T. and Citovsky, V.** (2006). *Agrobacterium*-mediated genetic transformation of plants: biology and biotechnology. *Curr. Opin. Biotechnol.*, 17, 147–54.
- van Attikum, H., Bundock, P., Hooykaas, P.J.J.** (2001). Non-homologous end-joining proteins are required for *Agrobacterium* T-DNA integration. *EMBO J*, 20, 6550–8.
- van Attikum, H. and Hooykaas, P.J.J.** (2003). Genetic requirements for the targeted integration of *Agrobacterium* T-DNA in *Saccharomyces cerevisiae*. *Nucleic Acids Res*, 31, 826–832.
- van Engelenburg, S. B. and Palmer, A. E.** (2008). Quantification of real time *Salmonella* effector type III secretion kinetics reveals differential secretion rates for SopE2 and SptP. *Chem. Biol*, 15, 619–628.
- van Engelenburg, S. B. and Palmer, A. E.** (2010). Imaging type-III secretion reveals dynamics and spatial segregation of *Salmonella* effectors. *Nat. Methods*, 7, 325–330.
- van Haaren, M. J. J., Sedee, N. J. A., Schilperoort, R. A. and Hooykaas, P. J. J.** (1987). Overdrive is a T-region enhancer which stimulates T-strand production in *Agrobacterium tumefaciens*. *Nucleic Acids Res*, 15, 8983–8997.
- van Kregten, M., Lindhout, B.I., Hooykaas, P.J.J. and van der Zaal, B.J.** (2009). *Agrobacterium* -mediated T-DNA transfer and integration by minimal VirD2 consisting of the relaxase domain and a type IV secretion 730 system translocation signal. *Mol. Plant-Microbe Interact*, 22, 1356–1365.
- van Kregten, M.** (2011). *Agrobacterium* -mediated delivery of a meganuclease into target plant cells. PhD thesis, Leiden University, Leiden, the Netherlands.
- van Kregten, M., de Pater, S., Romeijn, R., van Schendel, R., Hooykaas, P.J.J. and Tijsterman, M.** (2016). T-DNA 2499 integration in plants results from polymerase- θ -mediated DNA repair. *Nat. Plants*, 2, 16164.
- van Larebeke, N., Engler, G., Holsters, M., van den Elsacker, S., Zaenen, I., Schilperoort, R.A. and Schell, J.** (1974). Large plasmid in *Agrobacterium tumefaciens* essential for crown gall-inducing ability. *Nature*, 252, 169–170.
- Vaudequin-Dransart, V., Petit, A., Chilton, W. S. and Dessaux, Y.** (1998). The cryptic plasmid of *Agrobacterium tumefaciens* cointegrates with the Ti plasmid and cooperates for opine degradation. *Mol. Plant-Microbe Interact*, 11, 583–591.
- Vergunst, A. C., Schrammeijer, B., den Dulk-Ras, A., de Vlaam, C. M. T., Regensburg-Tuink, T. J. G. and Hooykaas, P. J. J.** (2000). VirB/D4-dependent protein translocation from *Agrobacterium* into plant cells. *Science*, 290, 979–982.

Vergunst, A. C., M. C. Van Lier, A. Den Dulk-Ras. and P. J. Hooykaas. (2003). Recognition of the *Agrobacterium tumefaciens* VirE2 translocation signal by the VirB/D4 transport system does not require VirE1. *Plant Physiol*, 133, 978–988.

Vergunst, A.C., van Lier, M.C., den Dulk-Ras, A., Grosse Stuve, T.A., Ouwehand, A. and Hooykaas, P.J.J. (2005). Positive charge is an important feature of the C-terminal transport signal of the VirB/D4-translocated proteins of *Agrobacterium*. *Proc. Natl. Acad. Sci. USA*, 102,832–837.

Wang, H.-H., Yin, W.-B., and Hu, Z.-M. (2009). Advances in chloroplast engineering. *Genet. Genomics*, 36, 387–398.

Wang, Y., Peng, W., Zhou, X., Huang, F., Shao, L. and Luo, M. (2014). The putative *Agrobacterium* transcriptional activator-like virulence protein VirD5 may target T-complex to prevent the degradation of coat proteins in the plant cell nucleus. *New Phytol.* 203, 1266–1281.

Wang, Y., Zhang, S., Huang, F., Zhou, X., Chen, Z., Peng, W. and Luo, M. (2018). VirD5 is required for efficient *Agrobacterium* infection and interacts with Arabidopsis VIP2. *New Phytol.* 217, 726–738.

Ward, E. R. and Barnes, W. M. (1988). VirD2 protein of *Agrobacterium tumefaciens* very tightly linked to the 5' end of T-strand DNA. *Science*, 242, 927–930.

Wolterink-van Loo, S., Escamilla Ayala, A. A., Hooykaas, P. J. J. and van Heusden, G. P. H. (2015). Interaction of the *Agrobacterium tumefaciens* virulence protein VirD2 with histones. *Microbiology*, 161, 401–410.

Wood, D.W., Setubal, J.C., Kaul, R., Monks, D.E., Kitajima, J.P., Okura, V.K. Zhou, Y., Chen, L., Wood, G.E., Almeida, N.F., Woo, L., Chen, Y., Paulsen, I.T., Eisen, J.A., Karp, P.D., Bovee, D., Chapman, P., Clendenning, J., Deatherage, G., Gillet, W., Grant, C., Kutuyavin, T., Levy, R., Li, M.J., McClelland, E., Palmieri, A., Raymond, C., Rouse, G., Saenphimmachak, C., Wu, Z., Romero, P., Gordon, D., Zhang, S., Yoo, H., Tao, Y., Biddle, P., Jung, M., Krespan, W., Perry, M., Gordon-Kamm, B., Liao, L., Kim, S., Hendrick, C., Zhao, Z.Y., Dolan, M., Chumley, F., Tingey, S.V., Tomb, J.F., Gordon, M.P., Olson, M.V. and Nester, E.W. (2001) The genome of the natural genetic engineer *Agrobacterium tumefaciens* C58. *Science*, 294, 2237–2416

Yanofsky, M. F. and Nester, E. W. (1986). Molecular characterization of a host-range-determining locus from *Agrobacterium tumefaciens*. *J. Bacteriol.*, 168, 244–250.

Zaltsman, A., Krichevsky, A., Loyte, A. and Citovsky, V. (2010). *Agrobacterium* induces expression of a host F-box protein required for tumorigenicity. *Cell Host Microbe* 7, 197–209.

Zhang, X., van Heusden, G.P.H. and Hooykaas, P.J.J.(2017). Virulence protein VirD5 of *Agrobacterium tumefaciens* binds to kinetochores in host cells via an interaction with Spt4. *Proc. Natl. Acad. Sci. USA*, *38*, 10238–10243.

Ziemienowicz, A., Merkle, T., Schoumacher, F., Hohn, B. and Rossi, L. (2001). Import of *Agrobacterium* T-DNA into plant nuclei: two distinct functions of VirD2 and VirE2 proteins. *The Plant Cell*, *13*, 369–383.

Visualization of virulence protein translocation
from *Agrobacterium* to yeast and plant cells
using the split GFP approach

M.Reza Roushan, G. Paul H. van Heusden and Paul J.J. Hooykaas

Molecular and Developmental Genetics, Institute of Biology, Leiden University, Leiden, The Netherlands.

ABSTRACT

During *Agrobacterium* -mediated transformation of eukaryotic organisms a number of effector proteins (VirD2, VirD5, VirE2, VirE3 and VirF) are translocated from the bacterium into the host cell. The VirE2 protein is an essential effector protein for the transformation of plant cells. It is thought that after translocation, it binds to the T-strand to protect it from host nucleases and assist in its delivery into the nuclei of plant cells. However, the translocation process itself and the fate of translocated VirE2 inside the recipient cell are poorly understood. In this study, we used the split-GFP strategy for visualization of the translocation of VirE2 to both plant and yeast cells. To this end, we co-cultivated *Agrobacterium* strains expressing VirE2 internally tagged with GFP₁₁ with host cells expressing the complementary part of GFP, GFP₁₋₁₀. Already after 8 hours of co-cultivation fluorescent filamentous and dot-like structures became visible in *Saccharomyces cerevisiae*, *Arabidopsis thaliana* and *Nicotiana tabacum* cells. Similar results were obtained when *Agrobacterium* strains lacking T-DNA were used. The filamentous VirE2 structures translocated showed a random movement inside these plant cells, but not in yeast cells. Using a similar approach we could observe translocation of the VirD2 virulence protein, which accumulated in the nucleus and cytoplasm of plant leaves and yeast cells, whether or not T-DNA was co-delivered from the *Agrobacterium* donor or host.

INTRODUCTION

Agrobacterium tumefaciens is a gram-negative soil-borne bacterium, which causes tumor formation in root crowns and stems of plants (Smith and Townsend, 1907) by transferring part of its tumor-inducing plasmid (T-DNA) (Chilton *et al.*, 1977). The host range of *Agrobacterium* comprises a large number of dicotyledonous plant species as host cell (De Cleese and De Ley, 1976). The T-DNA is integrated in one of the plant chromosomes and expressed in plant cells. Transformed plant cells overproduce the plant growth regulators indole acetic acid (IAA; auxin) and cytokinin which initiates uncontrolled cell proliferations (Hooykaas and Schilperoort, 1992). In addition, crown gall cells secrete tumor-specific compounds called opines, which can be used as carbon and nitrogen source by *A. tumefaciens* (Petit *et al.*, 1978). The bacterium uses a type IV secretion system (T4SS) to deliver single stranded copies of the T-DNA (T-strands) and the effector proteins VirE2, VirE3, VirD2, VirD5 and VirF into the host cells (Vergunst *et al.*, 2000). *A. tumefaciens* not only transforms plants, but also is able to transform yeast (Bundock *et al.*, 1995; Piers *et al.*, 1996), algae (Kumar *et al.*, 2004) and fungi (de Groot *et al.*, 1998) under laboratory conditions.

Formation of the T-strand initiates with the nicking of the Ti plasmid at the 24bp left and right border repeats surrounding the T-region by the VirD2 endonuclease assisted by VirD1. Hereby VirD2 remains covalently attached to the 5'-end of the T-DNA. The liberated T-strand with VirD2 still attached is then transferred into the host cells via T4SS (Mysore *et al.*, 1998; Porter *et al.*, 1987; Herrera-Estrella *et al.*, 1988; Ghai and Das, 1989).

The *virE* operon consists of the *virE1*, *virE2* and *virE3* genes. The VirE2 protein is able to bind single-stranded DNA in a sequence-independent way (Gietl *et al.*, 1987; Citovsky *et al.*, 1989; Sen *et al.*, 1989). Inside *Agrobacterium* the VirE2 protein is stabilized by its chaperone VirE1, which prevents its self-association and aggregates formation (Deng *et al.*, 1999; McBride and Knauf, 1988). Therefore, VirE1 is also required for VirE2 translocation from *A. tumefaciens* into plant cells (Sundberg *et al.*, 1996). In the plant cell VirE2 is thought to bind to the T-strand, protect it from host cell nucleases (Citovsky *et al.*, 1989; Sen *et al.*, 1989) and may help the T-strand in passing the lipid bilayers of membranes (Dumass *et al.*, 2001; Volokhina *et al.*, 2012). Furthermore, VirE2 helps in facilitating the nuclear uptake of the T-strand in cooperation with VirD2 and VirE2-Interacting Protein 1 (VIP1) (Ziemienowicz *et al.*, 2001). VIP1 is a transcription factor that responds to biotic and abiotic stresses after its MPK3-mediated phosphorylation (Pitzschke *et al.*, 2009; Wu *et al.*, 2010;

Tsugama *et al.*, 2012, 2013). Phosphorylated-VIP1 localizes in the plant nucleus leading to the expression of many stress-related genes (Djamei *et al.*, 2007). Therefore, it is thought that the VirE2-VIP1 interaction may help to direct the T-complex into the plant cell nucleus (Gietl *et al.*, 1987; Pitzschke *et al.*, 2009). However, recently such a role of VIP1 was disputed (Shi *et al.*, 2014). Besides, it has been reported that VirE2 facilitates the chromatin targeting of the T-complex through an association with VIP2 (Anand *et al.*, 2007). The nuclear localization sequence (NLS) in the C-terminus of VirD2 was found to be essential for guidance of the T-complex to the nucleus (Ziemienowicz *et al.*, 2001). Recently interaction between VirD2 and histones in *S. cerevisiae* has been reported and it may help direct the T-DNA to the chromatin prior to integration into one of the chromosomes (Wolterink-van Loo *et al.*, 2015).

VirE2 also binds to the effector protein VirE3, which has a nuclear localization (Lacroix *et al.*, 2005). In this way VirE3 may facilitate trafficking and nuclear import of the T-complex inside the recipient cells by mimicking the function of VIP1 (Lacroix *et al.*, 2005). Using a yeast two-hybrid screen interactions of VirE3 were found with *A. thaliana* importins, the Csn5 component of the host signalosome complex, and with pBrp, a plant-specific general transcription factor of the TFIIB family (García-Rodríguez *et al.*, 2006). The interaction with pBrp suggests a role in transcriptional activation and recently we showed that VirE3 may indeed have such a function. Upon expression of VirE3 in *A. thaliana* the expression levels of numerous genes are affected. This suggests that VirE3 affects the transcriptional machinery of the host cell to facilitate the transformation process (Niu *et al.*, 2015).

The *virF* gene identified on octopine type Ti plasmids (Hooykaas *et al.*, 1984) is a host range determinant. For example, nopaline *A. tumefaciens* strains, which lack VirF, are not able to infect *Nicotiana glauca*, in contrast to octopine strains (Melchers *et al.*, 1990). However, transgenic *N. glauca*, expressing the *Agrobacterium* VirF protein showed tumor formation by VirF lacking strains and VirF mutants indicating that VirF functions within plant cells (Regensburg-Tuink and Hooykaas, 1993). VirF contains a putative F-box and it has been shown that it associates with plant homologs of the yeast Skp1 protein suggesting a role of VirF in targeted protein degradation (Schrammeijer *et al.*, 2001). Tzfira *et al.* (2004) reported that VirF is involved in destabilization and degradation of VirE2 and VIP1 in the host nucleus leading to the uncoating of T-DNA enabling its integration into the host's chromosomal DNA. VirD5 is not essential for *A. tumefaciens* tumorigenicity, but in its absence tumors are attenuated (Wang *et al.*, 2018). It has been reported that VirD5 may

function as VirF stabilizer (Magori and Citovsky, 2011). Recently Zhang *et al.* (2017) showed that VirD5 binds to the kinetochores resulting in chromosome mis-segregation during mitosis and inhibition of yeast and plant growth.

Although it is well documented that during AMT virulence proteins are translocated into eukaryotic host cells (Vergunst *et al.*, 2001), the mechanisms of their translocation and of their trafficking inside the host cell are only poorly understood. To further elucidate these mechanisms we (Sakalis *et al.*, 2014) and others (Li *et al.*, 2014) visualized the translocation of VirE2 into yeast and plant cells using the Split GFP system. This system makes use of the observation that GFP can be split into two non-fluorescent fragments: GFP₁₋₁₀, consisting of β -strands 1-10 containing 215 amino acids residues and GFP₁₁, consisting of β -strand 11, containing 16 amino acids residues (Cabantous *et al.*, 2005). The two parts can bind to each other and re-associate spontaneously and restore fluorescence. To visualize protein translocation, GFP₁₋₁₀ is expressed in the host cells and the effector protein to be studied is tagged with GFP₁₁. Following translocation of the GFP₁₁-tagged effector protein, GFP fluorescence is restored (Cabantous *et al.*, 2005) (Figure 2C). The yeast *Saccharomyces cerevisiae* is a good eukaryotic model system to study *Agrobacterium* mediated transformation (Bundock *et al.*, 1995; Bundock and Hooykaas, 1996; Van Attikum *et al.*, 2001). Also for studies on protein translocation this yeast has several advantages over plant cells, especially its lack of fluorescent chlorophyll. In this study, we used the split GFP system to visualize the translocation of the effector proteins VirE2 and VirD2 from *Agrobacterium* into cells of the yeast *S. cerevisiae* and of the plants *Arabidopsis thaliana* and *Nicotiana tabacum*. Instead of biologically inactive N-terminally tagged GFP₁₁-VirE2, we used internally tagged GFP₁₁-VirE2 for visualization of VirE2 translocation, which greatly improved detection.

MATERIALS AND METHODS

Yeast strains and media. Yeast strains used in this study are listed in Table 1. All yeast strains were grown in YPD medium or selective MY medium supplemented, if required, with histidine, leucine, tryptophan and/or uracil to the final concentration of 20 mg/ml (Zonneveld, 1986). Yeast transformation was performed using Lithium Acetate method (Gietz *et al.*, 1995). Yeast strains carrying plasmids were obtained by transforming parental

strains with the appropriate plasmids followed by selection for histidine, leucine and/or uracil prototrophy.

Agrobacterium strains and media. *A. tumefaciens* strains used in this study are listed in Table 2. All *A. tumefaciens* strains were grown in LC medium containing, if required, the appropriate antibiotics at the following concentrations: rifampicin, 20 µg/ml; gentamicin, 40 µg/ml; kanamycin, 100 µg/ml. *A. tumefaciens* carrying plasmids were obtained by electroporation as described by Den Dulk-Ras and Hooykaas (1995).

Plasmid constructions. All plasmids used and constructed in this study are listed in Table 3. Cloning steps were performed in *E. coli* strain XL1-Blue. PCR amplifications were done with Phusion™ High-Fidelity DNA Polymerase and Table 4 lists all primers used for PCR amplification.

A permissive site for internal insertion in VirE2 protein without any effect on its functionality has been reported (Zhou and Christie, 1999) and to tag VirE2 internally with GFP₁₁ at proline39 a 628 bp DNA fragment (Figure 1) was synthesized and cloned into pEX-A2 by Eurofins (Germany).

```

5'ACTAGTCATATGGATCTTTCTGGCAATGAGAAATCCAGGCCTTGAAGAAGGCGAATGTCAG
TTCCAGCACCATCTCCGATATTCAGATGACGAATGGCGAAAACCTTGAATCAGGGAGCCCTCG
GGACCACATGGTGTGTCACGAGTACGTGAACGCCGCCGCATCAACCCGAACGGAAGTTTT
AAGCCCACGTCTGGATGATGGATCGGTGATTCCTCCTCCAGCCTTATTCTGGCAGCGAGCAC
GGAAATCAAGCTGAGATTCAAAAAGAGCTGTCCGCCTTGTCTCGAACATGTCTTTGCCAGGC
AACGATCGGCGCCCGGACGAATACATTCTCGTGCCTCAAACGGGACAAGATGCTTTACTGGT
ATTGCCAAAGGCAACCTCGACCACATGCCACCAAGGCGGAATTTAACGCGTGTCTGCCGTCTC
TACAGGGACGGAGCCGGTAATTACTATCCGCCACCTCTCGCGTTCGACAAGATTAGCGTTCCA
GCCCAACTGGAGGAAACATGGGGGATGATGGAGGCGAAGGAACGTAACAAACTACGGTTTCA
GTACAAGTTGGACGTATGGAATCATGCGCACGCTGATATGGGGATCACTGGCAGAGAGATCT
3'

```

Figure 1. The synthetic DNA fragment used to internally tag VirE2 with GFP₁₁. The 48 bp GFP₁₁-coding sequence (underlined) was inserted into *virE2* at the CCT codon of Proline39 (bold). *SpeI* (red), *NdeI* (green) and *BgIII* (blue) restriction sites were added at the end of the fragment.

This DNA fragment containing the 5'-end of the *virE2* gene, was cloned into pUG36YFP[VirE2] using *SpeI* and *BgIII* to generate pUG36YFP-39GFP₁₁[VirE2]. For expression in yeast an *XbaI*-*XhoI* fragment containing tagged *virE2*, was ligated into pUG34 digested with *XbaI* and *XhoI* yielding pUG34[39GFP₁₁-VirE2]. For expression in *Agrobacterium* pSDM3163[39GFP₁₁-VirE2] was constructed by replacing the *NdeI* –

*Hind*III fragment with N-terminally tagged *virE2* of pSDM3163[GFP₁₁-VirE2] by the *Nde*I-*Hind*III fragment of pUG34[39GFP₁₁-VirE2] with internally tagged *virE2* and the constructed plasmid was checked by sequencing using primers VirE2-seq-FW, VirE2-seq-Rev and VirE2-seq-int (Table 4). The pURedStar2NLS was prepared by removing yEGFP3 from the plasmid pUG36 by digestion with *Xba*I and *Bam*HI. The RedStar2 gene was obtained by PCR on the vector pYM43 with the primers P1Redstar2-*Xba*I-Fw and P2Redstar2-*Bam*HI-Rev (Table 4). After digestion with *Bam*HI and *Xba*I, the fragment was ligated into *Bam*HI- and *Xho*I-digested vector pUG36 yielding pURedstar36. Plasmid pURedstar2NLS allowing the expression of the RedStar2-NLS was obtained by ligation of an NLS fragment into the *Bam*HI- and *Xho*I-digested pURedStar36. The NLS fragment was obtained as follows. The oligonucleotides O1RedStar2-NLS and O2 Redstar2-NLS (Table 4) were mixed, boiled for 5 minutes and then cooled overnight in the water bath (Rodrigues *et al.*, 2001). pURedStar2NLS(CYC1) was created by inserting a *Sac*I-*Xba*I fragment with the *CYC1* promoter from p416CYC1 into pURedStar2NLS digested with *Sac*I and *Xba*I.

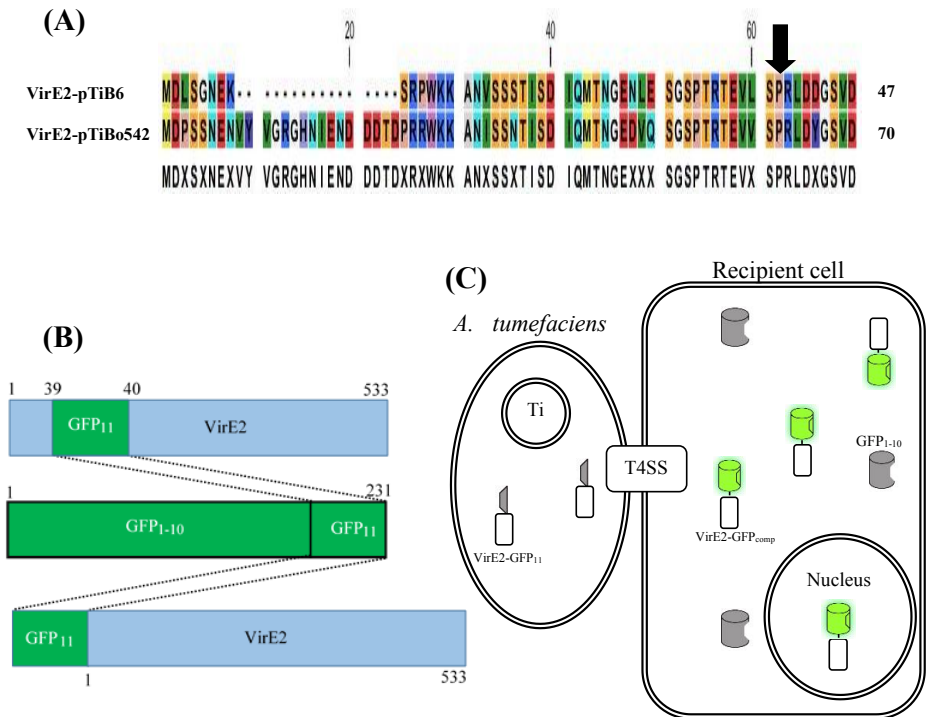


Figure 2. Strategy used to study VirE2 translocation from *Agrobacterium* into host cells. A, comparison of the N-terminal sequence of VirE2 from pTiB6 used in this study with that of VirE2 from pTiBo542 (Li *et al.*, 2014). The permissive site is indicated with an arrow. B, illustration of N-terminal and internal-tagging of VirE2 with GFP₁₁. C, the strategy used for the visualization of VirE2 translocation from *A. tumefaciens* into the host cells.

Plant lines and media. *Nicotiana tabacum* SR1 expressing GFP₁₋₁₀ (Sakalis *et al.*, 2014) was grown on soil to full plants and after three weeks young leaves were selected for agroinfiltration. *A. thaliana* Columbia-0 seeds expressing GFP₁₋₁₀ (M. Kahn, unpublished) were grown on MS-0 medium supplemented with hygromycin (50 µg/ml) for two weeks and then transferred to soil and grown for a week. The largest leaves were selected for agroinfiltration. The *efr-1* (SALK_044334) T-DNA insertion mutant line, ecotype Col-0, was obtained from Nottingham *Arabidopsis* stock center.

Transformation of *A. tumefaciens* by electroporation.

Agrobacterium competent cells preparation:

Agrobacterium was grown on LC agar medium for 3 days at 29°C. A loopful of bacteria was transferred into 2 ml of liquid LC medium and incubated at 29°C for 6 hours with agitation. One hundred µl of this preculture was used to inoculate 100 ml of LC medium and the culture was grown till early log phase ($A_{660}=1.0-1.5$). Then, cells were collected by centrifugation (4000g) at 4 °C for 20 minutes. Prior to electroporation, cells were washed three times with ice-cold HEPES (pH 7.0) followed by washing once with ice-cold 10% glycerol. The cell pellet was then re-suspended in 500-750 µl of ice-cold 10% glycerol and suspension distributed in 40 µl aliquots, freezed in liquid Nitrogen and stored at -80 °C (den Dulk-Ras and Hooykaas, 1995).

Electroporation of *Agrobacterium* :

Competent cells were gently thawed on ice and transferred into a pre-chilled 50*2mm Pulsestar electroporation cuvette (Westburg). The Gene Pulser II Electroporation System (Bio-Rad) was used for electroporation (Capacitance 25 µF, Voltage 2.5 kV, Pulse controller set to 200 Ω). After electroporation, 1 ml of SOC-medium was quickly added into the cuvette and the cell suspension was transferred into a culture tube. After cultivation for 1-1.5 hours at 29 °C, 100 µl of cells were plated onto LC agar plates with appropriate antibiotics for selection (den Dulk-Ras and Hooykaas, 1995).

Co-cultivation of *Agrobacterium* and yeast. Cocultivation of *Agrobacterium* and yeast was performed using an adapted version of the published protocol (Bundock *et al.*, 1995). *Agrobacterium* strains were grown overnight in 15 ml of LC medium with appropriate antibiotics (Table 2) at 28°C. Subsequently, *Agrobacterium* cells were centrifuged and re-suspended in IM supplemented with 0.2 mM acetosyringone and grown at 28°C for 6 hours. After overnight incubation of yeast strain 426::GFP₁₋₁₀ in 10 ml of YPD medium at 30°C, 100 µl of cells were inoculated in 20 ml of fresh YPD medium and incubated for 6 hours more at 28°C. Then, 1 ml of yeast culture was washed with 500 µl of IM and re-suspended in 1 ml of IM. Sixty microliters of *Agrobacterium* suspension were mixed with 60 µl of yeast suspension and 100 µl of the mixture were spotted on cellulose nitrate filters (Sartorius). Filters were dried at room temperature and were laid onto IM plates supplemented with histidine (2 mg/ml), uracil (2 mg/ml), tryptophan (2 mg/ml) and incubated at 21°C. For

microscopy, cells were eluted from the filters by transferring the filters to a 2 ml Eppendorf tube, adding 0.5 ml of MY medium and vigorously vortexing, followed by two more washes with 0.5 ml MY medium. Cells were centrifuged and were re-suspended into 200 μ l of MY medium and an aliquot (5 μ l) was used for microscopy.

Determination of AMT efficiency with LBA1100(pRAL7100):

After 6 to 9 days co-cultivation of *Agrobacterium* strain LBA1100 (pRAL7100) with yeast strain 426::GFP₁₋₁₀ at 21°C, filters were transferred to 2 ml Eppendorf tubes, 1 ml minimal medium (MY) was added and tubes were vortexed vigorously to wash all the cells off the filters. Aliquots of 100 μ l and 200 μ l of the cell suspensions were applied on MY selection plates supplemented with tryptophan (2 mg/ml), histidine (2 mg/ml) and cefotaxime (200 μ g/ml) to quantify transformed yeast cells. The total number of survived yeast cells was quantified by plating 200 μ l aliquots of 10⁻² and 10⁻⁴ dilutions of the cell suspensions on MY plates contain tryptophan (2 mg/ml), histidine (2 mg/ml), uracil (2 mg/ml) and cefotaxime (200 μ g/ml). To obtain the transformation efficiency, the number of colonies on the selective plates was divided by the number of colonies on the non-selective plates .

Agroinfiltration of plants. After overnight growth of *A. tumefaciens* strains at 28°C in LC medium, cultures were diluted to the OD₆₀₀≈0.8 in 10 ml of induction medium with 200 μ mol/L acetosyringone (AS) and incubated for three hours at 28°C. A blunt-tipped 10 ml plastic syringe (Nissho NIPRO Europe N.V) was used to inject smoothly and with gentle pressure the lower surface of the leaves of *A. thaliana* Columbia.0 and *N. tabacum* SR1 lines expressing GFP₁₋₁₀. After 18 hours, the lower side of injected leaves was used for confocal microscopy (Wroblewski *et al.*, 2005).

Agroinfiltration sample preparation for microscopy: Eighteen hours after agroinfiltration a small piece of the lower side of the injected leaf was cut, transferred to a slide, one drop of immersion oil applied and images were captured by confocal microscopy.

Tumor formation assay. *A. tumefaciens* cells were grown for overnight at 28°C in LC medium with the appropriate antibiotics. Then, cells were washed three times with 0.9% (w/v) NaCl solution and diluted to OD₆₆₀≈ 1.0 in 0.9% (w/v) NaCl. One month old *N. glauca* plants were wounded at three sites on the stem with sterile toothpick. Subsequently, 20 μ l of *A. tumefaciens* suspension was inoculated at each wounded site. Tumors were photographed one month after inoculation.

AGROBEST infection and GUS assay. AGROBEST infection procedure was performed as described by Wu *et al.*, 2014 with some minor modifications. *A. thaliana efr-1* seeds were sterilized and grown on plates containing MA medium. Seeds were grown for 4 days before AGROBEST infection.

A. tumefaciens was freshly streaked out from the -80°C glycerol stock onto a LC agar plate containing appropriate antibiotics and incubated for 2 days at 28°C. A fresh single colony from the plate was used to inoculate 5 ml of LC liquid medium containing appropriate antibiotics at 28°C overnight with shaking. For pre-induction of *A. tumefaciens vir* gene expression, *A. tumefaciens* cells were pelleted and re-suspended to OD₆₀₀ 0.2 in 3ml of IM with 200 µM Acetosyringone with appropriate antibiotics and incubated at 20°C overnight. Before co-cultivation, *A. tumefaciens* cells were pelleted and re-suspended in IM to OD₆₀₀ 0.02. The 4 days grown *efr-1* seedlings were transferred into plates containing MA with 200 µM Acetosyringone and 200 µl *A. tumefaciens* cells freshly prepared before was added to the 6-wells plates and incubated in growth chamber (16hr light/8hr darkness) at 21°C for 4 days before GUS staining (Wu *et al.*, 2014).

For GUS staining, seedlings were stained with 5-bromo-4-chloro-3-indolyl glucuronide (X-Gluc) at 37°C for 24 hrs in dark with gentle shaking. After overnight staining, seedlings were destained with 70% ethanol for 24 hrs. Then, pictures were taken with stereo microscope.

Root Protein Translocation. In this study we used root transformation approach as described by Vergunst *et al* (2000). Root segments of *A.thaliana* Col-0 lines expressing GFP₁₋₁₀ were co-cultivated with *Agrobacterium* strains LBA2572(3163-39GFP₁₁-VirE2), LBA2573(3163-39GFP₁₁-VirE2) and LBA1010 as a negative control on callus induction medium with 200 µM Acetosyringone for 3 days in growth room (8hr light/24hr darkness) at 24°C. After 3 days of co-cultivation, root segments were analyzed by confocal microscopy for protein translocation visualization.

Confocal microscopy. To observe leaf epidermis, agro-infiltrated leaf tissues were detached from *N. tabacum* SR1 and *A. thaliana* Col-0 plants and put in 1.5% low-melting agarose gel on a glass slide with a coverslip. For yeast images, the cells were grown in MY medium supplemented with appropriate nutrients and then put on a slide with a coverslip. Plant and yeast cells were analyzed using a Zeiss LSM5 Exciter confocal microscope using a 20X and 63X magnifying objective, respectively. GFP signal was detected using an argon 488 nm laser and a 505-600 nm band pass emission filter. RedStar2 was excited at 543 nm and emitted

light collected at 580-640 nm. Chlorophyll fluorescence was determined using a long pass 650 nm emission filter after excitation at 488 nm. All images were processed using ImageJ 1.48F software (Abràmoff *et al.*, 2004).

Table 1: Yeast strains used in this study

Yeast strain	Genotype	Source/reference
426::GFP ₁₋₁₀ (GG3388)	<i>MATa ura3-52 leu2-112 trp1-289 his3-delta1 leu2::pRS305[P_{MET25}-GFP₁₋₁₀-T_{CYC1}] (LEU2)</i>	(Sakalis <i>et al.</i> , 2014)
426::GFP ₁₋₁₀ [RedStar2NLS]	<i>MATa ura3-52 leu2-112 trp1-289 his3-delta1 leu2::pRS305[P_{MET25}-GFP₁₋₁₀-T_{CYC1}] (LEU2), pURedStar2NLS(pRUL1352) (URA3).</i>	This study.

Table 2: *Agrobacterium* strains used in this study

<i>Agrobacterium</i> strain	Specifications ^a	Source/reference
LBA1010	C58 containing pTiB6, Rif	(Koekman <i>et al.</i> , 1982)
LBA1100	C58 containing pTiB6Δ (ΔT-DNA, Δocc, Δtra), Rif, Spc	Beijersbergen <i>et al.</i> , 1992)
LBA1100 (pRAL7100)	LBA1100 with binary vector pRAL7100, Rif, Km	(Bundock <i>et al.</i> , 1995)
LBA2572 (LBA1010ΔE2)	<i>virE2</i> deletion in LBA1010, Rif	den Dulk-Ras, unpublished
LBA2573 (LBA1100 ΔE2)	<i>virE2</i> deletion in LBA1100, Rif, Spc	(Hodges <i>et al.</i> , 2006)
LBA2572 (3163GFP ₁₁ -E2)	LBA2572 with pSDM3163[GFP ₁₁ -VirE2]. Expression of the GFP ₁₁ -VirE2 fusion protein under control of the <i>virE</i> promoter, Rif, Gm	(Sakalis <i>et al.</i> , 2014)
LBA2573 (3163GFP ₁₁ -E2)	LBA2573 with pSDM3163[GFP ₁₁ -VirE2]. Expression of the GFP ₁₁ -VirE2 fusion protein under control of the <i>virE</i> promoter, Rif, Spc, Gm	(Sakalis <i>et al.</i> , 2014)
LBA2560 (3163GFP ₁₁ -F)	LBA2560 (ΔirF in LBA1010) with pSDM3163[GFP ₁₁ -F]. Expression of the GFP ₁₁ -VirF fusion protein under control of the <i>virF</i> promoter, Rif, Spc, Gm	(Sakalis <i>et al.</i> , 2014)
LBA2561 (3163GFP ₁₁ -F)	LBA2561 (ΔvirF in LBA1100) with pSDM3163[GFP ₁₁ -F]. Expression of the GFP ₁₁ -VirF fusion protein under control of the <i>virF</i> promoter, Rif, Spc, Gm	(Sakalis <i>et al.</i> , 2014)
LBA2569 (3163GFP ₁₁ -D2)	LBA2569 (ΔvirD2 in LBA1010) with pSDM3163[GFP ₁₁ -VirD2], expressing the GFP ₁₁ -VirD2 fusion protein under control of the <i>virD</i> promoter, Rif, Gm	(Sakalis <i>et al.</i> , 2014)

LBA2556 (3163GFP ₁₁ -D2)	LBA2556 (Δ virD2 in LBA1100) with pSDM3163[GFP ₁₁ -VirD2], expressing the GFP 11-VirD2 fusion protein under control of the <i>virD</i> promoter, Rif, Spc,Gm	(Sakalis <i>et al.</i> , 2014)
LBA2573 (3163-39GFP ₁₁ -VirE2)	LBA2573 with pSDM3163[39-GFP ₁₁ -VirE2]. Expression of the internal-tagged GFP 11-VirE2 fusion protein under control of the <i>virE</i> promoter, Rif, Spc,Gm	This study.
LBA2572 (3163-39GFP ₁₁ -VirE2)	LBA2572 with pSDM3163[39-GFP ₁₁ -VirE2]. Expression of the internal-tagged GFP 11-VirE2 fusion protein under control of the <i>virE</i> promoter, Rif, Spc,Gm	This study.

^a tra: transfer region, occ: octopine catabolism, Rif: rifampicin, Spc: spectinomycin, Km: kanamycin, Gm: gentamicin, Δ : deletion

Table 3. Plasmids used in this study

Name	Properties	Source/reference
pCAMBIA3301	High copy vector with <i>GUS</i> gene under control of the 35S promoter and the <i>NOS</i> terminator. (bacterial kanamycin resistance and plant bialophos/phosphinothricin selection)	Cambia, Australia®
pRS305-GFP1-10 (pRUL1278)	pRS305 containing <i>GFP 1-10</i> under control of <i>MET25</i> promoter and <i>CYC1</i> terminator. <i>LEU2</i> marker, integration plasmid.	P. A. Sakalis thesis
pUG36YFP[VirE2] (pRUL1244)	Centromeric plasmid with YFP-VirE2 under control of <i>MET25</i> promoter and <i>CYC1</i> terminator. <i>URA3</i> marker.	P. A. Sakalis thesis
pUG36YFP-39GFP ₁₁ [VirE2] (pSDM3765)	pUG36YFP[VirE2] backbone with the coding sequence of proline39GFP ₁₁ -VirE2 under control of <i>MET25</i> promoter.	This study.
pURedStar2NLS (pRUL1352)	pURedStar36 backbone with NLS fragment under control of <i>CYC1</i> promoter.	Asmae Bakane ,MSc research project report
pUG36YFP (pRUL1004)	Centromeric plasmid to make N-terminal YFP fusions under control of the <i>MET25</i> promoter and <i>CYC1</i> terminator. <i>URA3</i> marker.	M. Miedema and G.P.H. van Heusden, unpublished
pUG34	Centromeric plasmid to make N-terminal GFP fusions under control of the <i>MET25</i> promoter and <i>CYC1</i> terminator. <i>HIS3</i> marker.	U. Güldener and J.H. Hegemann, unpublished

pUG34[39GFP ₁₁ -VirE2] (pSDM3766)	pUG34 backbone with the coding sequence of proline39 GFP ₁₁ -VirE2 under control of <i>MET25</i> promoter.	This study.
pUG34GFP ₁₁ [VirD2] (pRUL1280)	Centromeric plasmid with <i>GFP₁₁-virD2</i> under control of the <i>MET25</i> promoter and <i>CYC1</i> terminator. <i>HIS3</i> marker.	(Sakalis, 2013)
pUG36GFP ₁₁ [VirE3] (pRUL1291)	Centromeric plasmid with <i>GFP 11-VirE3</i> under control of the <i>MET25</i> promoter and <i>CYC1</i> terminator. <i>URA3</i> marker.	(Sakalis, 2013)
pUG34GFP ₁₁ [VirF] (pRUL1295)	Centromeric plasmid with <i>GFP 11-VirF</i> under control of <i>MET25</i> promoter and <i>CYC1</i> terminator. <i>HIS3</i> marker.	(Sakalis, 2013)
pSDM3163[GFP ₁₁ -VirE2] (pSDM3756)	pSDM3163 backbone with the coding sequence of GFP ₁₁ -VirE2 under control of the <i>virE</i> promoter.	P. A. Sakalis thesis
pSDM3163[39GFP ₁₁ -VirE2] (pSDM3767)	pSDM3163 backbone with the coding sequence of proline39 GFP ₁₁ -VirE2 under control of the <i>virE</i> promoter.	This study.
pSDM3163[GFP ₁₁ -VirE2] (pSDM3756)	pBBR6 backbone with the coding sequence of GFP ₁₁ -VirE2 under control of the <i>virE</i> promoter.	(Sakalis <i>et al.</i> , 2014)
pSDM3163[GFP ₁₁ -VirD2] (pSDM3755)	pSDM3163 backbone with the coding sequence of GFP ₁₁ -VirD2 under control of the <i>virD</i> promote	(Sakalis, 2013)
pYM43	Plasmid; Redstar2 natNT2	(Janke <i>et al.</i> , 2004)

Table 4. Primers used in this study

Primer name	Sequence (5' → 3') ^a
VirE2-seq-FW	AAGTGCGACATCATCATCGG
VirE2-seq-Rev	GAGATGGTGCACGATGCACA
VirE2-seq-int	TCCAGGCTGGTTCGCTGCT
VirE2-SmaI-Fw	A <u>ACCCGGG</u> ATGGATCTTTCTGGCAA
VirE2-PstI-Rev	GG <u>CTGCAG</u> TCAAAAGCTGTTGACGC
VirE2-BamHI-Fw	AA <u>AGGATCC</u> ATGGATCTTTCTGGCAATGA
VirE2-XhoI-Rev	GGGG <u>CTCGAG</u> TCAAAAGCTGTTGACGCTTT
P1Redstar2-Fw-XbaI	AA <u>TCTAGAG</u> GAGCTGGAGCTGGTGCA
P2Redstar2-Rev-BamHI	AA <u>GGATCCC</u> AAGAACAAGTGGTGTCTAC
O1RedStar2-NLS	GATCGCCAAAAAAGAAGAGAAAGGTCGTTGTTAAATAG
O2Redstar2-NLS	TCGACTATTTAACAACGACCTTTCTCTCTTTTTTGGC

a, restriction sites are underlined.

RESULTS

Biological functionality of 39-GFP₁₁-VirE2

To further elucidate the translocation of virulence proteins from *Agrobacterium* into host cells and the trafficking of these virulence proteins inside the host cell we (Sakalis *et al.*, 2014) and another research group (Li *et al.*, 2014) have visualized the translocation of VirE2 from *Agrobacterium* into yeast and plant cells using the split GFP system. Li *et al.* (2014) showed that VirE2 from the hypervirulent pTiBo542 plasmid internally tagged with GFP₁₁ gave a stronger signal than VirE2 from octopine pTiB6 plasmid N-terminally tagged with GFP₁₁ as we used and preserved its virulence function. Therefore, in the present study, we internally tagged our octopine pTiB6 VirE2 with GFP₁₁ and compared with our N-terminally tagged VirE2. As shown in figure 2A, the N-terminus of the two proteins is different. Li *et al.* introduced the GFP₁₁ -tag next to proline54 (Li *et al.*, 2014). The corresponding amino acid residue in our VirE2 is proline39, a site where small insertions are possible without interfering with the biological function (Christie *et al.*, 1999) (Figure 2A). Therefore, we tagged VirE2 at proline39, with GFP₁₁. Indeed as shown in figure 3C expression of 39-GFP₁₁ [VirE2] in *Agrobacterium* strains lacking *virE2* resulted in restoration of virulence of the *virE2* mutant *Agrobacterium* strains, indicating that the internally tagged VirE2 had retained its biological activity. The N-terminally tagged VirE2 had lost its biological activity (Figure 3D) and could not complement the *virE2* mutant. When we tagged another virulence protein, VirD2 at the N-terminus with GFP₁₁, this kept its virulence properties and could complement a *virD2* mutant (Figure 3E). This was further confirmed in a transformation experiment with strains carrying the binary vector pCAMBIA 3301, where we used β -Glucuronidase (*gus*) activity as a read out of transformation. As can be seen in figure 3G, (β -Glucuronidase) blue positive spots were observed in *A. thaliana* (*efr-1* mutant) leaves transformed with *A. tumefaciens* LBA2573 Δ virE2 mutant complemented by carrying (3163-39GFP₁₁-VirE2) and carrying pCAMBIA3301. This confirmed that the internally tagged VirE2 is still biologically active and mediates transformation as seen by transient gene expression. However, blue positive spots were not observed in *A. thaliana* (*efr-1*mutant) leaves inoculated with the *virE2* deletion mutant LBA2573 harboring pCAMBIA3301 as a negative control (Figure 3F).



Figure 3. Biological activity assessments. Tumor formation on *Nicotiana glauca* plants inoculated with different *A. tumefaciens* strains (A) Negative control, LBA2572 (LBA1010ΔE2). (B) Positive control, LBA1010. (C) LBA2572 (3163-39GFP₁₁-VirE2). (D) LBA2572 (3163-GFP₁₁-VirE2). (E) LBA2569 (LBA1010ΔD2+3163-GFP₁₁-VirD2). Transient expression (GUS assay) in *A.thaliana efr-1* mutant transformed with *A. tumefaciens* strains (F) Negative control, LBA2573 (LBA1100ΔVirE2) carrying pCAMBIA3301 and (G) LBA2573 (3163-39GFP₁₁-VirE2) carrying pCAMBIA3301.

Comparison of N-terminally and internally tagged GFP₁₁-VirE2

To compare our new internally tagged VirE2 (39-GFP₁₁-VirE2) with the N-terminally tagged GFP₁₁-VirE2 (N-GFP₁₁-VirE2) used previously (Sakalis *et al.*, 2014) both proteins were expressed in yeast strain 426::GFP₁₋₁₀. As shown in figure 4A, expression of N-GFP₁₁-VirE2 resulted in fluorescent dot-shaped structures as observed before (Sakalis *et al.*, 2014, Li and Pan, 2014). Expression of 39-GFP₁₁-VirE2 resulted also in fluorescent dot-shaped and filamentous structures in the majority of yeast cells (Figure 4 B).

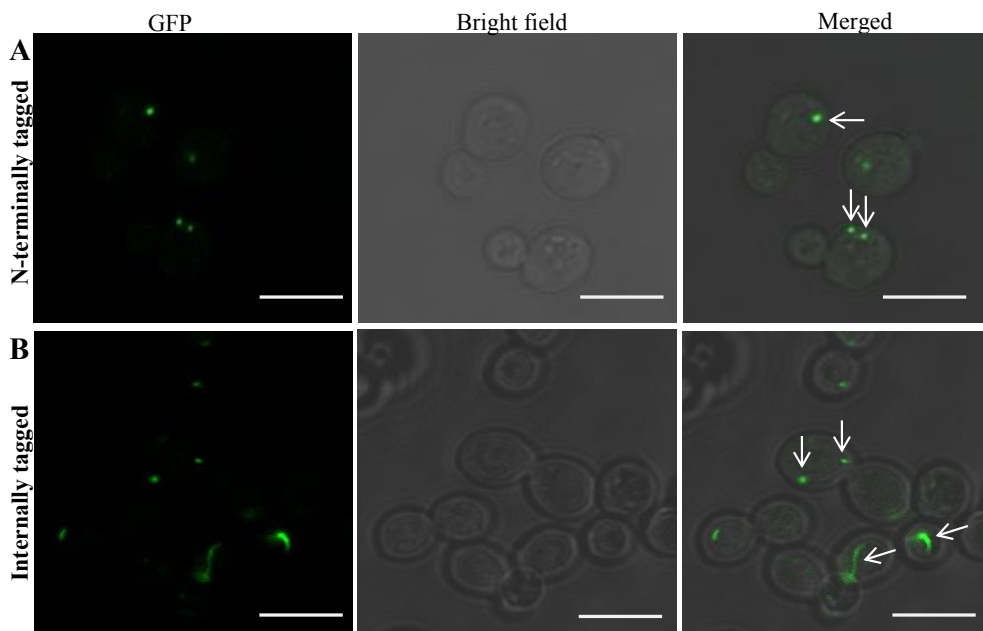


Figure 4. Confocal microscopy of yeast strain 426::GFP₁₋₁₀ expressing N-terminally GFP₁₁-tagged VirE2 (A) or 39-GFP₁₁[VirE2] (B). Arrows indicate GFP-VirE2 localization as filamentous and dot-like (perinuclear-like aggregates) structures in yeast. Scale bars: 5µm.

Localization of 39-GFP₁₁[VirE2] in yeast

One of the proposed roles of VirE2 in the transformation process is targeting of the T-complex into the nucleus of the host cell. After ectopic expression in plants VirE2 was initially reported to be localized in the nucleus (Citovsky *et al.*, 1990), but later other groups reported a cytoplasmic localization (Bhattacharjee *et al.*, 2008). On the other hand no evidence of nuclear import of VirE2 in yeast or mammalian cells was found (Tzfira *et al.*, 2001) but in these cells VirE2 remained in the cytoplasm. We found that N-terminally tagged VirE2 ectopically expressed in yeast co-localized and physically interacted with microtubules in the cytoplasm. Similarly, in plants addition of oryzalin, which disrupt microtubules, led to the dissociation of VirE2 filaments (Sakalis *et al.*, 2014). Now we studied the localization of biologically active 39-GFP₁₁[VirE2] protein in yeast. To this end 39-GFP₁₁[VirE2] was expressed in yeast strain 426::GFP₁₋₁₀ containing plasmid pURedStar2NLS expressing the nuclear marker Redstar2NLS. As shown in figure 5, the fluorescence contributed by the 39-GFP₁₁[VirE2] protein was present in filamentous and dot-like structures that occasionally overlapped or were present inside the nucleus in 4 out of 26 counted cells.

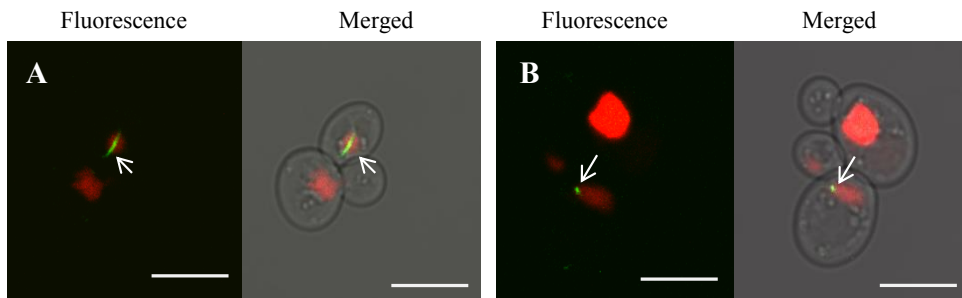


Figure 5. Localization of 39-GFP₁₁[VirE2] in yeast strain 426::GFP₁₋₁₀ containing plasmid pURedStar2NLS encoding the nuclear marker Redstar2NLS. VirE2 filamentous (A) and dot-like structures (B) (displayed in green) localized in or near the nucleus (red). Scale bars: 5μm.

Visualization of 39GFP₁₁[VirE2] in yeast after *Agrobacterium*-mediated transformation

To visualize VirE2 delivery from *Agrobacterium* into the yeast cells, *A. tumefaciens* strains expressing 39-GFP₁₁ [VirE2] and yeast strain 426::GFP₁₋₁₀ were co-cultivated for various times (2-4-6-8-10-12-16-20-24 hours) and the cells were analyzed by confocal microscopy. A GFP signal was not observed during the first 6 hrs of co-cultivation and after 8 hrs. fluorescent dot-shaped structures started to appear inside the yeast cells (Figure 6A). After 24 hours of co-cultivation, longer and intense fluorescent structures were seen in the cells receiving 39-GFP₁₁[VirE2] (Figure 6C). Sakalis *et al.* (2014) started to observe translocation of N-terminus tagged GFP₁₁-VirE2 only after 25 hrs. To investigate whether the presence of T-DNA influenced the translocation of 39-GFP₁₁[VirE2] similar co-cultivations were done using *Agrobacterium* strains lacking T-DNA. As shown in figures 6B and 6D, the translocation of VirE2 was not affected by the presence of T-DNA. To further analyze the other *Agrobacterium* effector proteins VirF and VirE3, yeast strain 426::GFP₁₋₁₀ was chemically transformed with pUG34-GFP₁₁[VirF] and pUG36-GFP₁₁[VirE3]. As shown in figure 15, we were not able to obtain reliable signals after expression of GFP₁₁-VirF and GFP₁₁-VirE3.

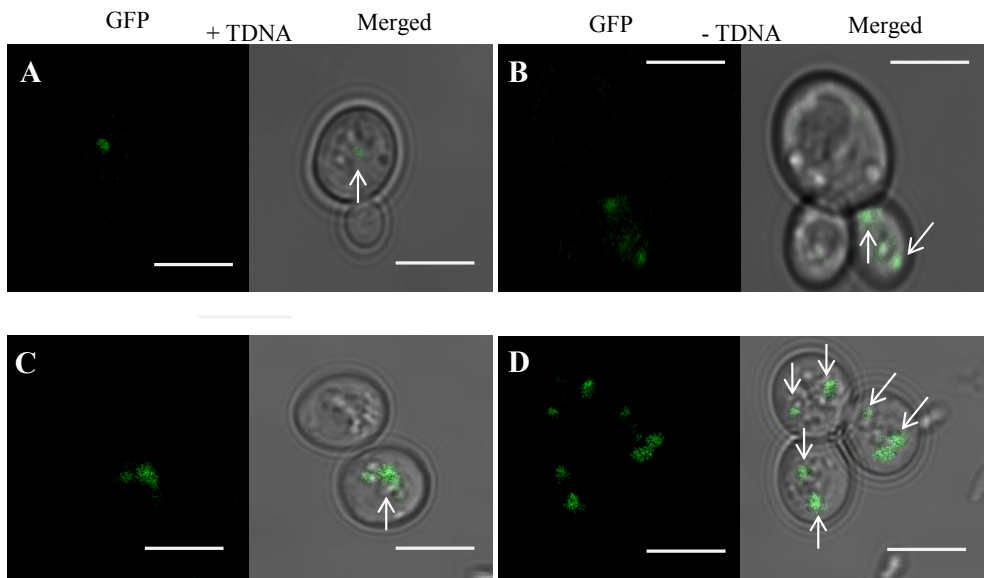


Figure 6. Confocal microscopy of 426::GFP₁₋₁₀ cells after co-cultivation with *Agrobacterium* strains expressing 39-GFP₁₁[VirE2] for 8 (A and B) or 24 hours (C and D). (A and C) Co-cultivation of *A. tumefaciens* strain LBA2572-39GFP₁₁[VirE2] (+ T-DNA) and yeast strain 426::GFP₁₋₁₀. (B and D) Co-cultivation of *A. tumefaciens* strain LBA2573-39GFP₁₁[VirE2] (- T-DNA) and yeast strain 426::GFP₁₋₁₀. Scale bars: 5μm.

Visualization of 39-GFP₁₁[VirE2] translocation from *A. tumefaciens* to *N. tabacum* SR1 leaves and *A. thaliana* Col.0 leaves and roots expressing GFP₁₋₁₀

To visualize translocated VirE2 inside plant leaf cells, *A. tumefaciens* strains LBA2572-39GFP₁₁[VirE2] containing T-DNA and LBA2573-39GFP₁₁[VirE2] lacking T-DNA were infiltrated into transgenic *N. tabacum* SR1 and *A. thaliana* Col.0 leaves expressing GFP₁₋₁₀. As shown in figures 7B-C and 8B-C in all cases both filamentous and dot-like structures were detected in the cytosol of plant cells 18 hours after agroinfiltration indicating that the presence of T-DNA does neither influence the delivery of VirE2 into the plant cells nor the formation of thread-like structures which is consistent with the observations in yeast cells (Figure 6). After co-cultivation with the negative control strain LBA1100 that does not encode GFP₁₁-VirE2, no GFP signals were observed in the plant tissues (Figure 7A and 8A).

To analyze VirE2 protein translocation into a different plant tissue, *A. tumefaciens* strains LBA2572-39GFP₁₁[VirE2], LBA2573-39GFP₁₁[VirE2], and LBA1010 were similarly co-cultivated with transgenic *A. thaliana* Col.0 root explants expressing GFP₁₋₁₀. As shown in figures 9B, C and D, again cord-like and dot-like structures were observed at the periphery of cells and in the cytosolic regions of root cells after 3 days of co-cultivation. In contrast with cells in plant leaves, movements of VirE2 were not observed in root cells (see next paragraph).

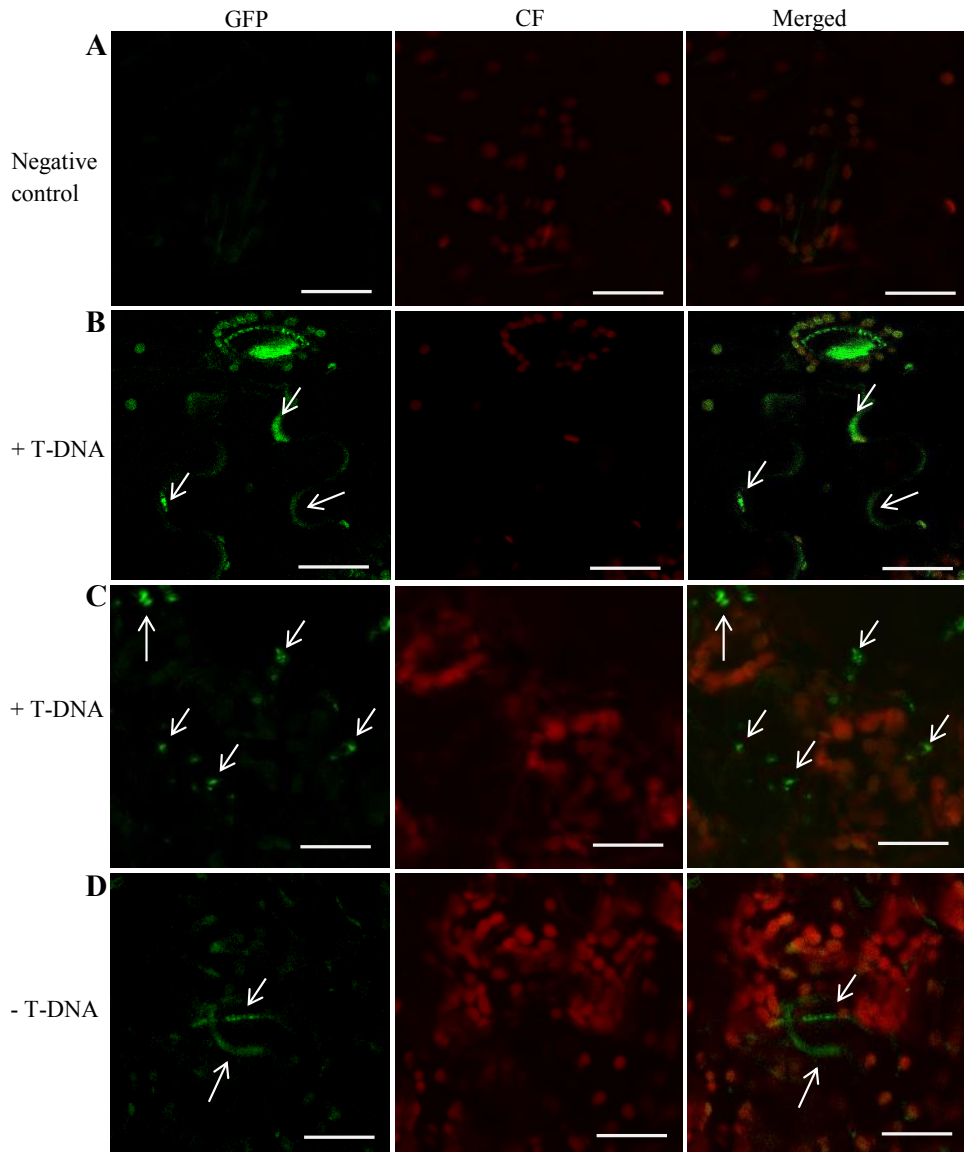


Figure 7. Visualization of 39-GFP₁₁[VirE2] translocation into leaf cells of *N. tabacum* SR1, 18 hours after agroinfiltration. (A) Co-cultivation of *N. tabacum* SR1 expressing GFP₁₋₁₀, with *A. tumefaciens* strains LBA1100(pRAL7100) used as negative control. (B and C) Formation of VirE2 filamentous and dot-like structures after co-cultivation of *N. tabacum* SR1 expressing GFP₁₋₁₀, with *A. tumefaciens* strains LBA2572-39GFP₁₁-VirE2 (+T-DNA) and (D) with LBA2573-39GFP₁₁-VirE2 (-T-DNA). Scale bars: 15 μ m. Arrows indicate reconstituted GFP signal in plant cells. CF, chlorophyll fluorescence.

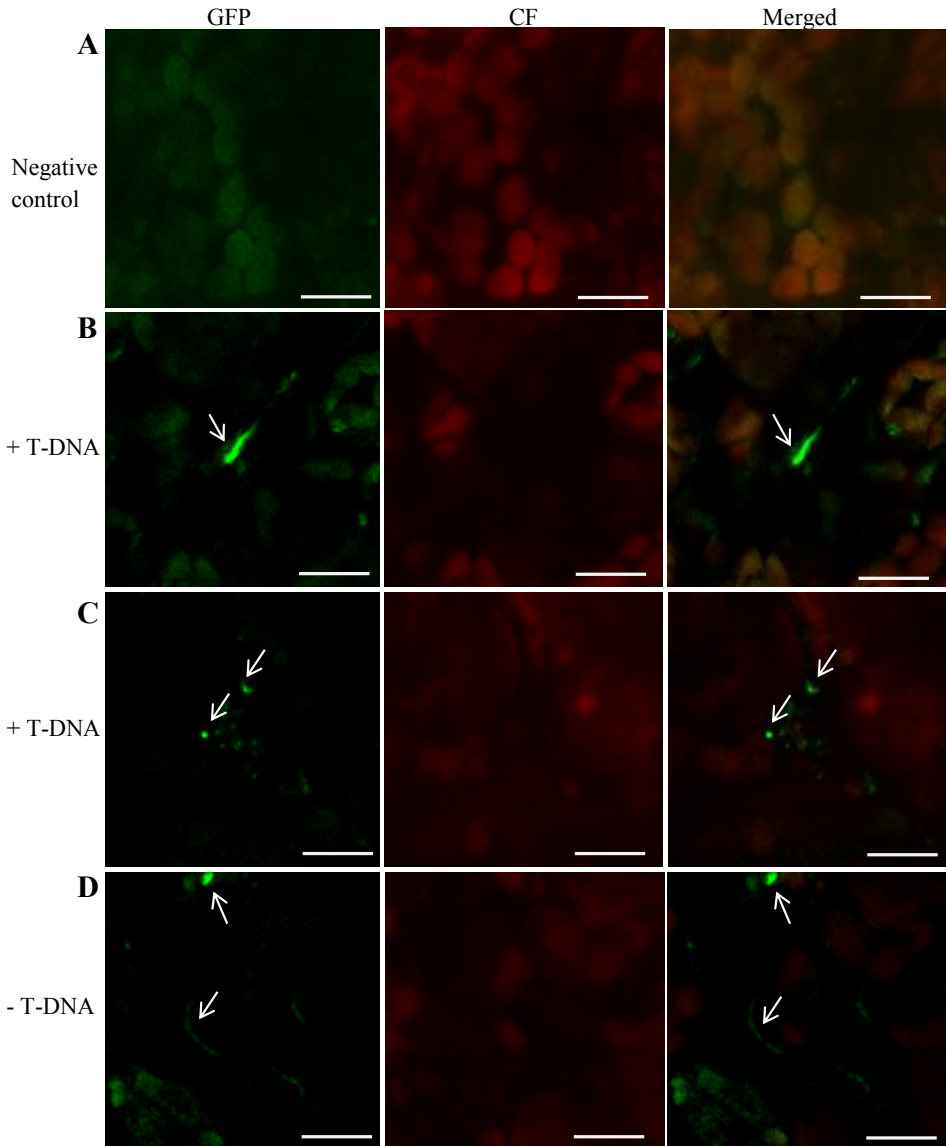


Figure 8. Visualization of 39-GFP₁₁[VirE2] translocation into leaf cells of *A. thaliana* Col-0 18 hours after agroinfiltration. Co-cultivation of *A. thaliana* Col-0 expressing GFP₁₋₁₀ with *A. tumefaciens* strain LBA1100 (pRAL7100) used as negative control (A). Formation of filamentous and dot-like structures by VirE2 translocated from *A. tumefaciens* strains LBA2572-39GFP₁₁ (B,C; +T-DNA) and LBA2573-39GFP₁₁ (D; -T-DNA) into *A. thaliana* Col-0 expressing GFP₁₋₁₀. Scale bars: 15µm. Arrows indicate reconstituted GFP signal in plant cells. CF, Chlorophyll florescence.

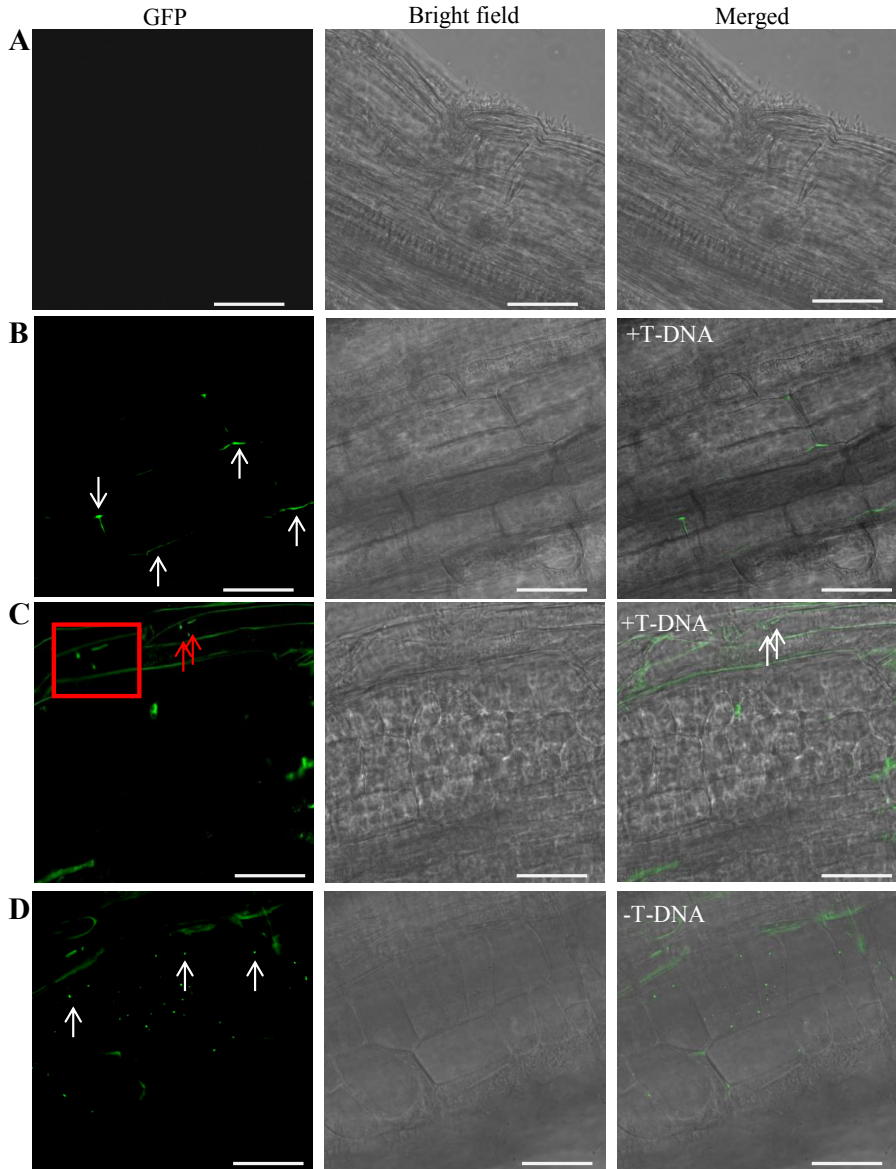


Figure 9. Visualization of 39-GFP₁₁[VirE2] translocation into *A. thaliana* Col-0 72 hours after root infection. *A. tumefaciens* strain LBA1010 used as negative control (A). Formation of filamentous and dot-like structures by VirE2 translocated form *A. tumefaciens* strains LBA2572-39GFP₁₁ (B,C; +TDNA) and LBA2573-39GFP₁₁ (D; -TDNA) into *A. thaliana* Col-0 roots expressing GFP₁₋₁₀. Red square is enlargement of part of the picture which indicated with red arrows. zoom in Scale bars: 15µm. Arrows indicate reconstituted GFP signal in plant root cells.

Visualization of the transformation of VirE2 protein movement inside *N. tabacum* SR1 and *A. thaliana* Col-0 cells

VirE2 may play an important role in T-complex trafficking inside the plant cells, for example by hijacking the MAPK-targeted VIP1 defense signaling pathway (Pitzschke *et al.*, 2009). Furthermore, the localization of VirE2 at the cytoplasmic microtubules in yeast and plant cells suggested a possible movement along the cytoskeleton (Sakalis *et al.*, 2014). To investigate whether movement of the translocated VirE2 can be visualized, time-lapse experiments were performed in both *N. tabacum* SR1 and *A. thaliana* Col-0. As shown in figures 10 and 11 in leaf cells of both plants movement of translocated 39-GFP₁₁[VirE2] was observed. This movement was random and not directed towards the nucleus.

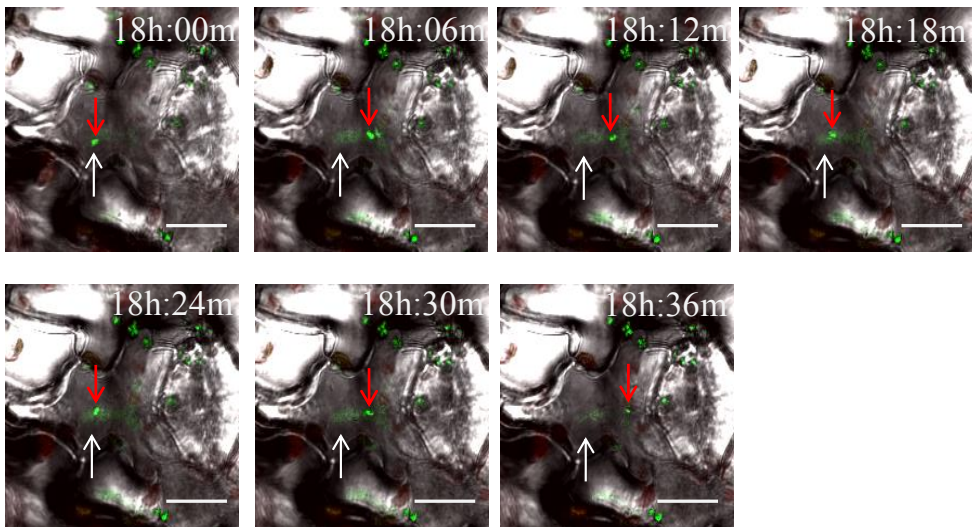


Figure 10. Analysis by confocal laser-scanning microscopy of 39-GFP₁₁[VirE2] trafficking inside *N. tabacum* SR1 expressing GFP₁₋₁₀ 18 hours after agroinfiltration. The initial position of the fluorescent signal is indicated by a white arrow and the observed position with a red arrow. Cells were photographed in 30s intervals at 20X magnification. Scale bars: 15µm. The time after agroinfiltration is shown above each image; h: hours and m: minutes.

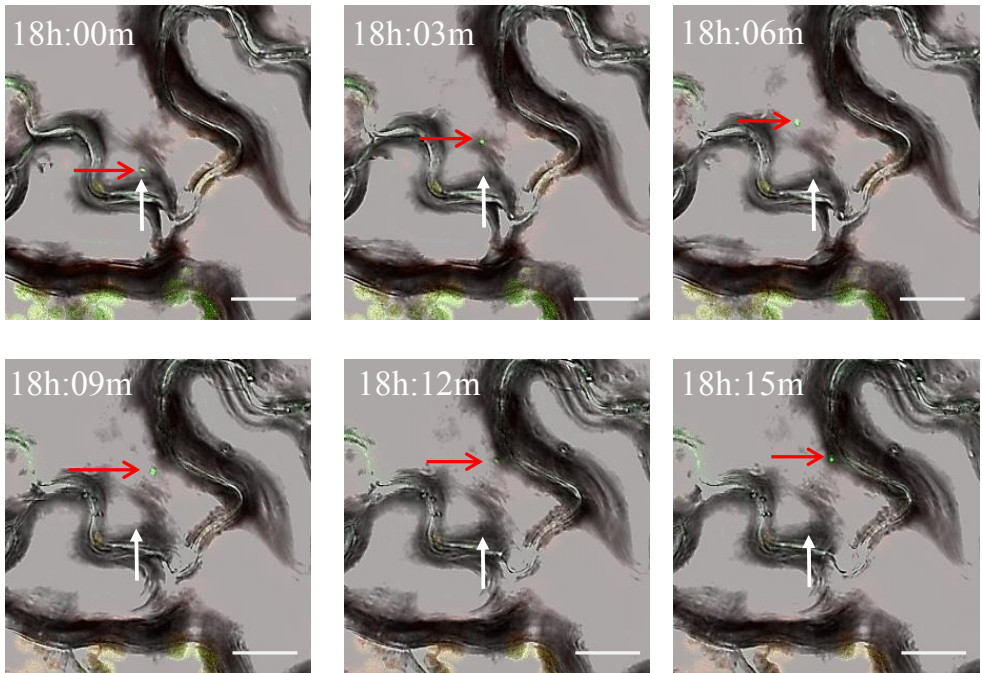


Figure 11. Analysis by confocal laser-scanning microscopy of 39-GFP₁₁[VirE2] trafficking in *A. thaliana Col-0* expressing GFP₁₋₁₀ 18 hours after agroinfiltration. The initial position of the fluorescent signal is indicated by a white arrow and the observed position with a red arrow. Cells were photographed in 30s intervals at 20X magnification. Scale bars: 15 μ m. The time after agroinfiltration is shown above each image; h: hours and m: minutes.

Visualization of the translocation of the VirD2 virulence proteins into Yeast from *Agrobacterium*

We tested whether translocation of any of the other effector proteins could be detected after fusion of GFP₁₁ to the N-terminus. Clear signals were obtained only in case of VirD2. Previously, nuclear localization of VirD2 was reported (Ziemienowicz *et al.*, 2001; Wolterink-van Loo *et al.*, 2015). The VirD2 protein had been visualized by Sakalis (2013) and these initial experiments suggested that the presence of T-DNA may influence where the VirD2 accumulates in the cell. To further analyze the influence of T-DNA on the localization of translocated VirD2, yeast strain 426::GFP₁₋₁₀ expressing Redstar2NLS was co-cultivated with *A. tumefaciens* strains LBA2569(3163GFP₁₁-D2) and LBA2556(3163GFP₁₁-D2). As shown in figure 12, translocated GFP₁₁-VirD2 accumulated both in the nucleus and in the cytoplasm. This localization was similar, irrespective of whether or not T-DNA was present.

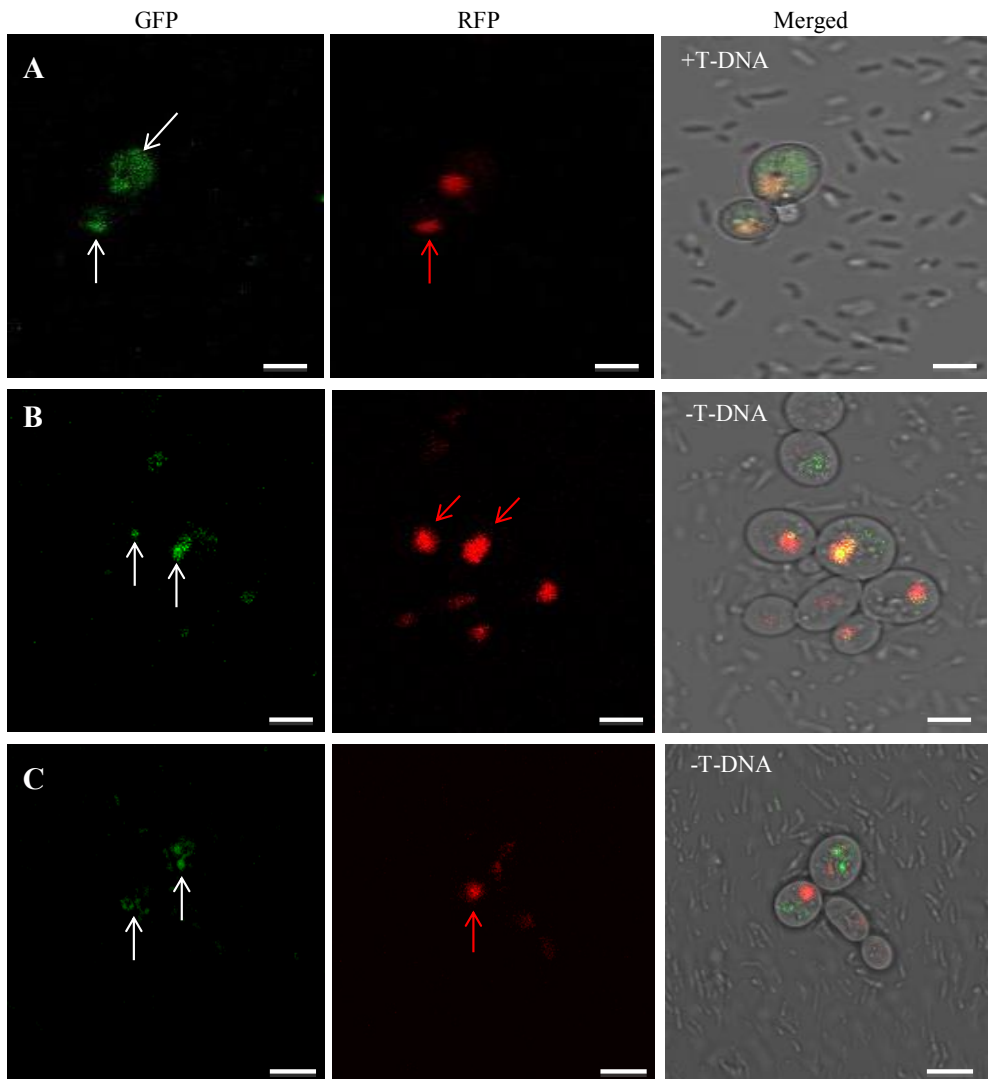


Figure 12. Presence of VirD2 in yeast after translocation from *Agrobacterium* after 48 hours of co-cultivation. Co-cultivation of *A. tumefaciens* strains LBA2569(LBA1010 Δ VirD2)(3163GFP₁₁-D2) (A) or LBA2556(LBA1100 Δ VirD2)(3163GFP₁₁-D2) (B and C) with yeast strain 426::GFP₁₋₁₀ expressing Redstar2NLS. GFP₁₁-VirD2 was found both in the nucleus and elsewhere in cells whether T-DNA was cotransferred or not. The white arrows indicate GFP₁₁-VirD2 and red arrows indicate Redstar2NLS marking the nucleus. Scale bars: 5 μ m.

Visualization of GFP₁₁[VirD2] translocation from *A. tumefaciens* to *N. tabacum* SR1 and *A. thaliana* Col-0 plants expressing GFP₁₋₁₀

We applied the split GFP system to visualise translocation of virulence protein VirD2 into *N. tabacum* SR1 and *A. thaliana* Col-0 leaf cells as recipients. *N. tabacum* SR1 cells and *A. thaliana* Col-0 cells were expressing GFP₁₋₁₀. The pictures were taken by CSL microscopy 20 hours after agroinfiltration of the 5 weeks old *N. tabacum* SR1 and *A. thaliana* Col-0 plants. Due to fluorescence originating from the chlorophyll, even in untransformed plants, fluorescence was detected in the GFP channel, irrespective of protein translocation. The CF channel shows the chlorophyll fluorescence and autofluorescence. Figure 13 shows translocation of the virulence proteins from *Agrobacterium* LBA2569(3163GFP₁₁-D2), LBA2556(3163GFP₁₁-D2) and negative control strain LBA1100 (pRAL7100) to *A. thaliana* Col-0 cells. Figure 14 shows translocation of the virulence proteins from *Agrobacterium* LBA2569(3163GFP₁₁-D2), LBA2556(3163GFP₁₁-D2) and LBA1100(pRAL7100) to *N. tabacum* SR1 cells. The virulence protein translocation from *A. tumefaciens* to 5 week old *N. tabacum* plants and *A. thaliana* plants expressing GFP₁₋₁₀ was observed 20 hours after agroinfiltration with GFP₁₁-tagged virulence proteins VirD2. Similar results were obtained with the *Agrobacterium* strain LBA2556 (3163GFP₁₁-D2) lacking T-DNA and LBA2569 (3163GFP₁₁-D2) with T-DNA. Due to fluorescence originating from the chlorophyll, even in the negative control LBA1100 without the GFP₁₁ construct, background fluorescence was detected (Figure 13A and Figure 14A). As indicated in figure 13 (B and C) and Figure 14 (B and C) by arrowheads, additional signals of reconstructed GFP were seen in *A. thaliana* and *N. tabacum* leaves, infiltrated with *A. tumefaciens* strains delivering GFP₁₁-tagged VirD2. Protein translocation was observed into the epidermal cells of the leaves.

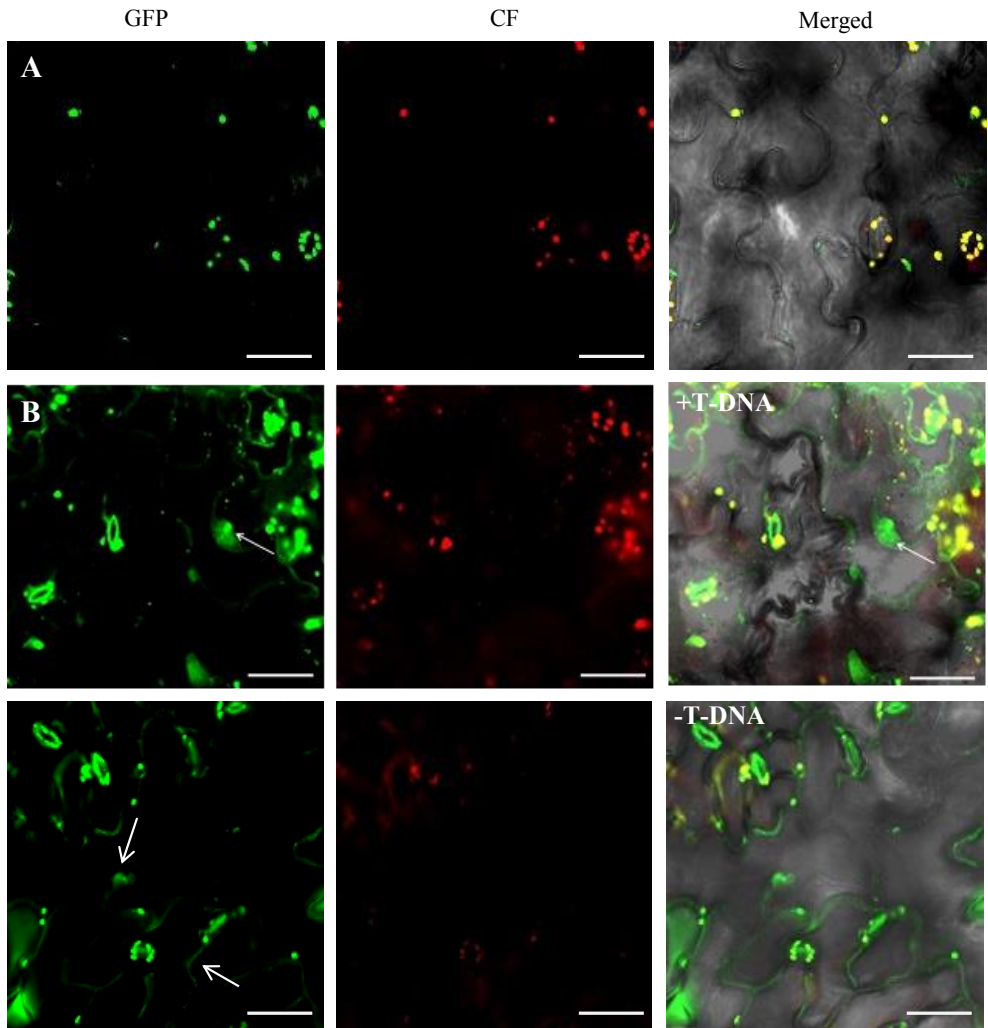


Figure 13. Visualization of GFP₁₁-VirD2 translocation from *Agrobacterium* to *A. thaliana* leaves. (A) The negative control LBA1100 without any GFP₁₁ construct. (B) Translocation of GFP₁₁-VirD2 (+T-DNA), (c) translocation of GFP₁₁-VirD2 (-T-DNA) (C), from *A. tumefaciens* to *A. thaliana Col-0* leaf cells expressing GFP₁₁₋₁₀, 20 hours after agroinfiltration. Analysis of CF chloroplast fluorescence (CF) and reconstituted GFP were performed with the Zeiss Imager. Scale bar, 15 μ m. Arrows indicate reconstituted GFP signals in the plant cells.

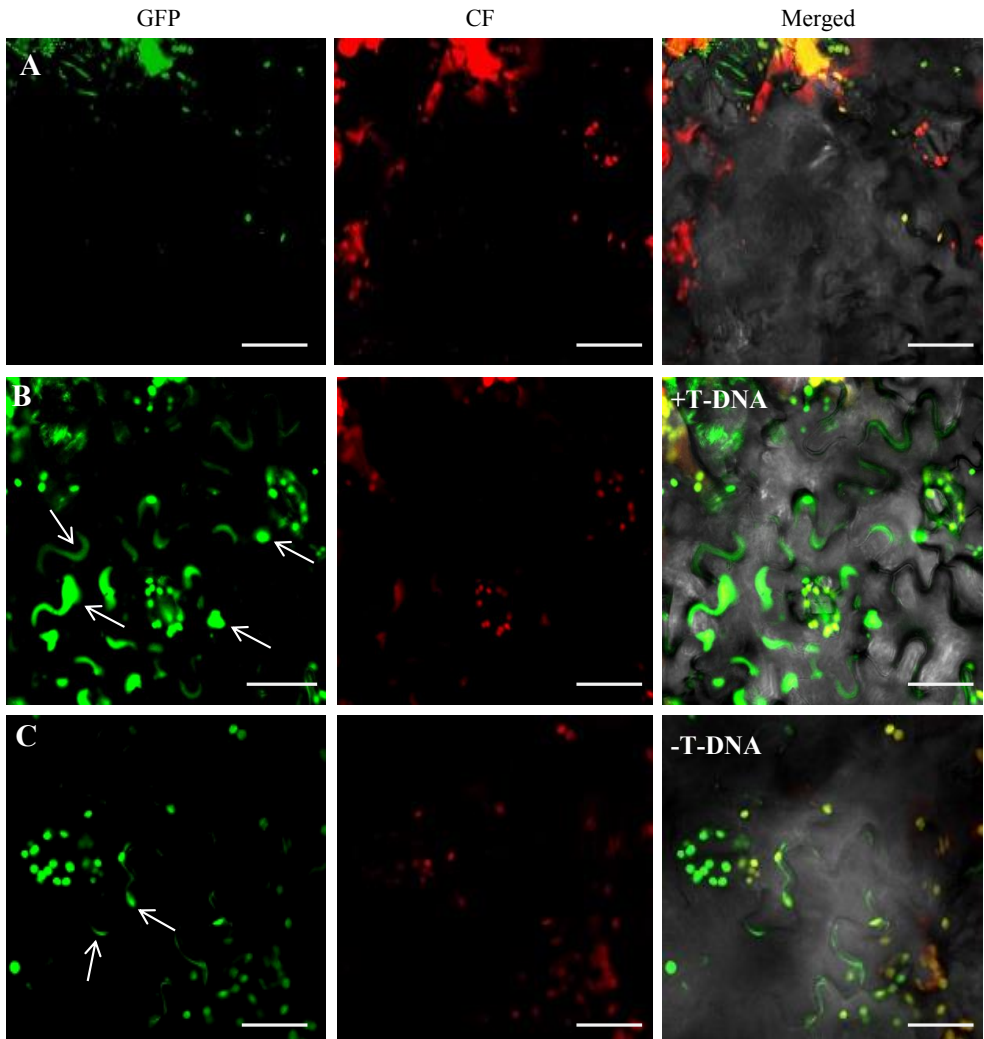


Figure 14. Visualization of GFP₁₁-VirD2 translocation from *Agrobacterium* to *N. tabacum* leaves. (A) The negative control LBA1100 without any GFP₁₁ construct. (B) translocation of GFP₁₁-VirD2 (+T-DNA), (C) translocation of GFP₁₁-VirD2 (-T-DNA), from *A. tumefaciens* to *N. tabacum* *SRI* leaf cells expressing GFP1-10, 20 hours after agroinfiltration. Analysis of CF chloroplast autofluorescence (CF) and reconstituted GFP were performed with the Zeiss Imager. Scale bar, 15 μ m. Arrows indicate reconstituted GFP signals in the plant cells.

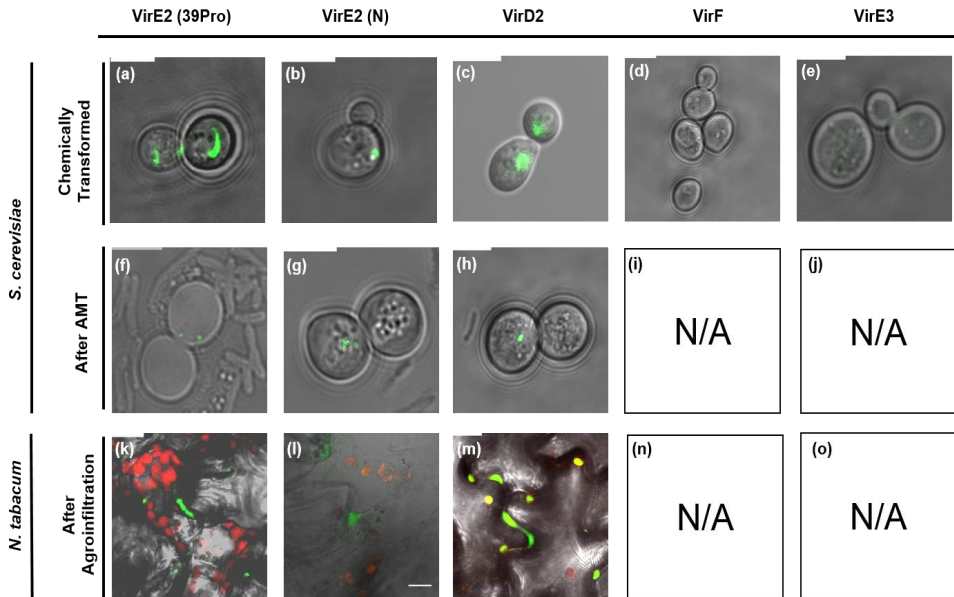


Figure 15. Summary of the results of this chapter.

Upper panel, confocal microscopy of yeast strain 426::GFP₁₋₁₀ chemically transformed with pUG36-39GFP₁₁[VirE2] (internally tagged) (A), with pUG36-GFP₁₁[VirE2] (N-terminally tagged) (B), with pUG36-GFP₁₁[VirD2] (C), with pUG34-GFP₁₁[VirF] (D), with pUG36-GFP₁₁-VirE3 (E). Scale bars: 5 μ m. Middle panel, confocal microscopy of 426::GFP₁₋₁₀ yeast cells after co-cultivation with *Agrobacterium* strains LBA2572-39GFP₁₁-[VirE2] (F), with LBA2572-GFP₁₁-VirE2 (G) or with LBA2556-GFP₁₁-[VirD2] (H).

Lower panel, visualization of VirE2 and VirD2 virulence proteins translocation into leaf cells of *N. tabacum* SR1, approximately 20 hours after agroinfiltration. VirE2 translocated from *A. tumefaciens* strains LBA2572-39GFP₁₁[VirE2] (K), LBA2572-GFP₁₁[VirE2] (L), and VirD2 translocated from *A. tumefaciens* strain LBA2556-GFP₁₁[VirD2] into leaf cells of *N. tabacum* SR1. Scale bars: 15 μ m.

DISCUSSION

Agrobacterium is known as a natural genetic engineer that can deliver DNA into dicotyledonous plant cells (Hooykaas and Schilperoort, 1992) and into many different types of host cells under laboratory conditions (Bundock *et al.*, 1995; Piers *et al.*, 1996; Kumar *et al.*, 2004; de Groot *et al.*, 1998). In addition to T-DNA, virulence proteins, VirE2, VirF, VirD2, VirE3 and VirD5, can translocate via the T4SS into the host cells during AMT (Vergunst *et al.*, 2000; Schrammeijer *et al.*, 2003). Translocation of these virulence proteins was detected initially by the development of the CRAFT system, in which co-delivery of the Cre-recombinase fused N-terminally to these virulence proteins resulted in a DNA recombination event that could be detected (Vergunst *et al.*, 2000, 2005). However, the translocation process itself, its timing and the fate of the translocated effector proteins inside the recipient cell are still only partly understood. In order to get more information on the translocation of effector proteins we made use of the split-GFP system. This system was originally used to study effector protein translocation from *Salmonella* (PipB2, SteA and SteC) to host cells through a type 3 secretion system (Van Engelenburg and Palmer, 2010). Later, we (Sakalis *et al.*, 2014), and others (Li *et al.*, 2014) used the split GFP system to visualize the translocation of the *Agrobacterium* VirE2 protein into yeast and plant cells. In our previous study we used N-terminally tagged GFP₁₁-VirE2 from the octopine Ti plasmid pTiB6 (Sakalis *et al.* 2014) whereas Li *et al.*, (2014) used internally tagged GFP₁₁-VirE2 from the hypervirulent pTiBo542. The VirE2 amino acid sequences from these two different *Agrobacteria* are somewhat different (Figure 2A). In our experiments GFP₁₁-VirE2 translocation to yeast was observed after more than 24 hours of co-cultivation (Sakalis *et al.*, 2014), whereas Li *et al.*, (2014) found protein translocation already after 4 hours of co-cultivation. In our new study we found that translocation of the VirE2 isoform used in our laboratory internally tagged GFP₁₁ (39-GFP₁₁[VirE2]) became visible after 8 hours of co-cultivation indicating that the position of the GFP₁₁-tag strongly affected the time when translocation can be observed. The GFP₁₁-tag at the N-terminus may hinder proper functioning of VirE2 possibly by blocking its self-association. The biological activity of internally tagged-VirE2 was confirmed by tumor formation and GUS assays as shown in figure 3. The internally-tagged VirE2 signals were detected more clearly and were observed earlier after cell infection in comparison with N-terminus tagged VirE2 signals. Translocation of 39-GFP₁₁[VirE2] to *N. tabacum* cells was observed 18 hrs. after agroinfiltration, similarly as was previously observed for N-terminally tagged-GFP₁₁[VirE2] (Sakalis *et al.*, 2014).

Translocated 39-GFP₁₁ [VirE2] was rapidly moving inside the host plant cells (Figures 10 and 11), which was not observed previously for N-terminally tagged-GFP₁₁ [VirE2]. Previously, Sakalis *et al* (2014) showed that VirE2 formed cord-like structures that colocalized with the microtubules. Hence, it will be interesting to investigate whether the movement is along microtubules or not. VirE2 protein translocation could also be observed into root cells when *A. tumefaciens* strains were co-cultivated with transgenic *A. thaliana* Col-0 root explants expressing GFP₁₋₁₀. A reconstituted GFP signal, resulting from 39GFP₁₁-VirE2 translocation into root cells from *Agrobacterium* was first detected only after 3 days of co-cultivation. This delay in comparison to leaf cells, where a signal was observed already after 18 hrs, might be due to slow translocation or slow aggregation and thread and dot formation of VirE2 in root cells. In this study the split GFP system was also used to visualize the translocation of N-terminally GFP₁₁-tagged virulence protein VirD2 into yeast and plant cells. The reconstituted GFP signal, resulting from GFP₁₁-VirD2 translocation into yeast and plant cells from *Agrobacterium* was first detected after 20 and 48 hours of co-cultivation in plant and yeast cells respectively. The translocation of VirE3 and VirF could not be studied as the GFP₁₁-fusions did not lead to GFP reconstitution with GFP₁₋₁₀. This is possibly due to steric hindrance by the virulence proteins parts preventing GFP reconstitution. The lack of data in case of VirF and VirE3 promoted us to look for an alternation system. The split-GFP system has the disadvantage that transgenic lines expressing GFP₁₋₁₀ need to be developed first before the system can be used. Therefore, in Chapter 4 we analyzed whether the LOV fluorescent protein may be a better alternative to study protein translocation.

ACKNOWLEDGEMENTS

We would like to thank Philippe Sakalis for providing *N. tabacum* GFP₁₋₁₀ seeds and also plasmids indicated in tables 2 and 3, Amke den Dulk-Ras for help with tumor formation experiment, Dr. Majid Khan for providing *A. thaliana* GFP₁₋₁₀ seeds, his technical assistance for agroinfiltration of plants, Gerda Lamers for help with microscopy, Joyce van der Meer for doing agroinfiltration and confocal microscopy of VirD2 protein translocation in planta and Esmae Bakane for the RedStarII NLS plasmid. Also we would like to appreciate P.A. Sakalis for providing us the picture of VirE2 translocation used in figure 15 (L).

REFERENCES

- Abràmoff, M. D., Magalhães, P. J. and Ram, S. J.** (2004). Image processing with imageJ. *Biophotonics Int.*, 11, 36–41.
- Anand, A., Krichevsky, A., Schornack, S., Lahaye, T., Tzfira, T., Tang, Y., Citovsky V. and Mysore, K. S.** (2007). Arabidopsis VirE2 interacting protein2 is required for *Agrobacterium* T-DNA integration in plants. *The Plant Cell*, 19, 1695–1708.
- Beijersbergen A., Dulk-Ras A D., Schilperoort R A. and Hooykaas, P.J.J.**(1992). Conjugative transfer by the virulence system of *Agrobacterium tumefaciens*. *Science*, 256,1324–7.
- Bundock, P., den Dulk-Ras, A., Beijersbergen, A. and Hooykaas, P. J. J.** (1995). Trans-kingdom T-DNA transfer from *Agrobacterium tumefaciens* to *Saccharomyces cerevisiae*. *The EMBO J.*, 14, 3206–14.
- Bundock, P. and Hooykaas, P. J. J.** (1996). Integration of *Agrobacterium tumefaciens* T-DNA in the *Saccharomyces cerevisiae* genome by illegitimate recombination. *Proc. Nat. Aca. Sci.U. S. A.*, 93, 15272–15275.
- Cabantous, S., Terwilliger, T. C. and Waldo, G. S.** (2005). Protein tagging and detection with engineered self-assembling fragments of green fluorescent protein. *Nat. Biotechnol.*, 23, 102–107.
- Chilton, M.-D., Drummond, M. H., Gordon, M. P., Merlo, D. J., Montoya, A. L., Sciaky, D., Nutter, R. and Nester, E. W.** (1977). Stable incorporation of plasmid DNA into higher plant cells: The molecular basis of tumorigenesis. *Cell* 11, 263-271.
- Citovsky, V., Wong, M. L. and Zambryski, P.** (1989). Cooperative interaction of *Agrobacterium* VirE2 protein with single-stranded DNA: implications for the T-DNA transfer process. *Proc. Nat. Aca. Sci.U. S. A.*, 86, 1193–7.
- Citovsky, V., Zupan, J., Warnick, D. and Zambryski, P.** (1990). Nuclear Localization of *Agrobacterium* VirE2 Protein in Plant Cells. *Science*, 256, 1802–1805.
- De Cleene, M. and De Ley, J.** (1976). The host range of crown gall. *Bot Rev*, 42, 389-466.
- de Groot, M. J., Bundock, P., Hooykaas, P. J. and Beijersbergen, A. G.** (1998). *Agrobacterium tumefaciens*-mediated transformation of filamentous fungi. *Nat. Biotechnol.*, 16, 839–842.
- den Dulk-Ras, A. and Hooykaas, P. J. J.** (1995). Electroporation of *Agrobacterium tumefaciens*. *Methods Mol. Biol.*, 55, 63–72.
- Deng, W., Chen, L., Peng, W. T., Liang, X., Sekiguchi, S., Gordon, M. P., Comai, L. and Nester, E. W.** (1999). VirE1 is a specific molecular chaperone for the exported single-stranded-DNA-binding protein VirE2 in *Agrobacterium* . *Mol Microbiol*, 31, 1795–1807.

- Djamei, A., Pitzschke, A., Nakagami, H., Rajh, I. and Hirt, H.** (2007). Trojan horse strategy in *Agrobacterium* transformation: abusing MAPK defense signaling. *Science*, 318, 453–456.
- García-Rodríguez, F. M., Schrammeijer, B., Hooykaas, P. J. J. and Garci, F. M.** (2006). The *Agrobacterium* VirE3 effector protein: a potential plant transcriptional activator. *Nucleic Acids Res.*, 34, 6496–504.
- Gelvin, S. B.** (2010). Finding a way to the nucleus. *Curr. Opin. Microbiol.*, 13, 53–58.
- Ghai, J. and Das, A.** (1989). The virD operon of *Agrobacterium tumefaciens* Ti plasmid encodes a DNA-relaxing enzyme. *Proc. Nat. Aca. Sci.U. S. A.*, 86(9), 3109–13.
- Gietl, C., Koukoulíková-Nicola, Z. and Hohn, B.** (1987). Mobilization of T-DNA from *Agrobacterium* to plant cells involves a protein that binds single-stranded DNA. *Proc. Nat. Aca. Sci.U. S. A.*, 84, 9006–9010.
- Gietz, R. D., Schiestl, R. H., Willems, A. R. and Woods, R. A.** (1995). Studies on the transformation of intact yeast-cells by the LiAc/ssDNA/PEG procedure. *Yeast*, 11, 355–360.
- Herrera-Estrella, A., Chen, Z. M., Van Montagu, M. and Wang, K.** (1988). VirD proteins of *Agrobacterium tumefaciens* are required for the formation of a covalent DNA–protein complex at the 5' terminus of T-strand molecules. *The EMBO J.*, 7, 4055–4062.
- Hodges, L. D., Vergunst, A. C., Neal-McKinney, J., Den Dulk-Ras, A., Moyer, D. M., Hooykaas, P. J. J. and Ream, W.** (2006). *Agrobacterium rhizogenes* GALLS protein contains domains for ATP binding, nuclear localization, and type IV secretion. *J. Bacteriol.*, 188, 8222–8230.
- Hooykaas, P. J. and Schilperoort, R. A.** (1992). *Agrobacterium* and plant genetic engineering. *Plant Mol. Biol.*, 19, 15–38.
- Janke, C., Magiera, M. M., Rathfelder, N., Taxis, C., Reber, S., Maekawa, H., Moreno-Borchart, A., Doenges, G., Schwob, E., Schiebel, E. and Knop, M.** (2004). A versatile toolbox for PCR-based tagging of yeast genes: New fluorescent proteins, more markers and promoter substitution cassettes. *Yeast*, 21, 947–962.
- Jarchow, E., Grimsley, N. H. and Hohn, B.** (1991). *virF*, the host-range-determining virulence gene of *Agrobacterium tumefaciens*, affects T-DNA transfer to *Zea mays*. *Proc. Nat. Aca. Sci.U. S. A.*, 88, 10426–30.
- Kalogeraki, V. S., Zhu, J., Stryker, J. L. and Winans, S. C.** (2000). The right end of the vir region of an octopine-type Ti plasmid contains four new members of the vir regulon that are not essential for pathogenesis. *J. Bacteriol.*, 182, 1774–1778.
- Koekman, B. P., Hooykaas, P. J. J. and Schilperoort, R. A.** (1982). A functional map of the replicator region of the octopine Ti plasmid. *Plasmid*, 7, 119–132.
- Kumar, S. V., Misquitta, R. W., Reddy, V. S., Rao, B. J. and Rajam, M. V.** (2004).

Genetic transformation of the green alga--*Chlamydomonas reinhardtii* by *Agrobacterium tumefaciens*. *Plant Sci.*, 166, 731–738.

Lacroix, B., Vaidya, M., Tzfira, T. and Citovsky, V. (2005). The VirE3 protein of *Agrobacterium* mimics a host cell function required for plant genetic transformation. *Embo J.*, 24, 428–437.

Li, X., Yang, Q., Tu, H., Lim, Z. and Pan, S. Q. (2014). Direct visualization of *Agrobacterium* -delivered VirE2 in recipient cells. *Plant J.*, 77, 487–495.

Magori, S. and Citovsky, V. (2011). *Agrobacterium* Counteracts Host-Induced Degradation of Its Effector F-Box Protein. *Sci. Signal.*, 4, ra69–ra69.

McBride, K. E. and Knauf, V. C. (1988). Genetic analysis of the virE operon of the *Agrobacterium* Ti plasmid pTiA6. *J. Bacteriol.*, 170, 1430–1437.

Melchers, L. S., Maroney, M. J., den Dulk-Ras, A., Thompson, D. V., van Vuuren, H. A. J., Schilperoort, R. A. and Hooykaas, P. J. J. (1990). Octopine and nopaline strains of *Agrobacterium tumefaciens* differ in virulence; molecular characterization of the virF locus. *Plant Mol. Biol.*, 14, 249–259.

Moore, L. W., Chilton, W. S. and Canfield, M. L. (1997). Diversity of opines and opine-catabolizing bacteria isolated from naturally occurring crown gall tumors. *Appl. Environ. Microbiol.*, 63, 201–207.

Mysore, K. S., Bassuner, B., Deng, X. B., Darbinian, N. S., Motchoulski, A., Ream, W. and Gelvin, S. B. (1998). Role of the *Agrobacterium tumefaciens* VirD2 protein in T-DNA transfer and integration. *Mol Plant Microbe Interact.*, 11, 668–683.

Niu, X., Zhou, M., Henkel, C. V., van Heusden, G. P. H. and Hooykaas, P. J. J. (2015). The *Agrobacterium tumefaciens* virulence protein VirE3 is a transcriptional activator of the F-box gene VBF. *Plant J.*, 84, 914–924.

Piers, K. L., Heath, J. D., Liang, X., Stephens, K. M. and Nester, E. W. (1996). *Agrobacterium tumefaciens*-mediated transformation of yeast. *Proc. Nat. Aca. Sci. U. S. A.*, 93, 1613–1618.

Pitzschke, A., Djamei, A., Teige, M. and Hirt, H. (2009). VIP1 response elements mediate mitogen-activated protein kinase 3-induced stress gene expression. *Proc. Nat. Aca. Sci. U. S. A.*, 106, 18414–18419.

Porter, S. G., Yanofsky, M. F. and Nester, E. W. (1987). Nucleic Acids Research Molecular characterization of the virD operon from *Agrobacterium tumefaciens*. *Nucleic Acids Res.*, 15, 7503–7517.

Regensburg-Tuink, A. J. G. and Hooykaas, P. J. J. (1993). Transgenic *N. glauca* plants expressing bacterial virulence gene virF are converted into hosts for nopaline strains of *A. tumefaciens*. *Nature*, 362, 69–71.

Rodrigues, F., van Hermet, M., Steensma, H.Y., Corte-Real, M. and Leao, C. (2001).

Red Fluorescent Protein (DsRed) as a Reporter in *Saccharomyces cerevisiae*. *J. Bacteriol.*, 183, 3791–3794.

Sakalis, P. A., van Heusden, G. P. H. and Hooykaas, P. J. J. (2014). Visualization of VirE2 protein translocation by the *Agrobacterium* type IV secretion system into host cells. *MicrobiologyOpen*, 3, 104–117.

Schrammeijer, B., Beijersbergen, a, Idler, K. B., Melchers, L. S., Thompson, D. V. and Hooykaas, P. J. (2000). Sequence analysis of the vir-region from *Agrobacterium tumefaciens* octopine Ti plasmid pTi15955. *J. Exp. Bot.*, 51, 1167–1169.

Schrammeijer, B., Risseuw, E., Pansegrau, W., Regensburg-Tuïnk, T. J. G., Crosby, W. L. and Hooykaas, P. J. J. (2001). Interaction of the virulence protein VirF of *Agrobacterium tumefaciens* with plant homologs of the yeast Skp1 protein. *Curr. Biol.*, 11, 258–262.

Sen, P., Pazour, G. J., Anderson, D. and Das, A. (1989). Cooperative binding of *Agrobacterium tumefaciens* VirE2 protein to single-stranded DNA. *J. Bacteriol.*, 171, 2573–2580.

Sundberg, S., Meek, L., Carroll, K., Das, A. and Ream, W. (1996). VirE1 protein mediates export of the single-stranded DNA-binding protein virE2 from *Agrobacterium tumefaciens* into plant cells. *J. Bacteriol.*, 178, 1207–1212.

Smith, E. F. and Townsend, C. O. (1907) A plant tumor of bacterial origin. *Science*, 25, 671–673.

Petit, A., Tempe, J., Kerr, A., Holsters, M., Van Montagu, M. and Schell, J. (1978). Substrate induction of conjugative activity of *Agrobacterium tumefaciens* Ti plasmids. *Nature*, 271, 570–572.

Tsugama, D., Liu, S. and Takano, T. (2012). A bZIP protein, VIP1, is a regulator of osmosensory signaling in Arabidopsis. *Plant Physiol*, 159, 144–155.

Tsugama, D., Liu, S. and Takano, T. (2013). A bZIP protein, VIP1, interacts with Arabidopsis heterotrimeric G protein b subunit, AGB1. *Plant Physiol. Biochem*, 71, 240–246.

Tzfira, T. and Citovsky, V. (2001). Comparison between nuclear localization of nopaline- and octopine-specific *Agrobacterium* VirE2 proteins in plant, yeast and mammalian cells. *Mol. Plant Pathol.*, 2, 171–176.

Tzfira, T., Vaidya, M. and Citovsky, V. (2001). VIP1, an Arabidopsis protein that interacts with *Agrobacterium* VirE2, is involved in VirE2 nuclear import and *Agrobacterium* infectivity. *EMBO J.*, 20, 3596–3607.

Tzfira, T., Vaidya, M. and Citovsky, V. (2004). Involvement of targeted proteolysis in plant genetic transformation by *Agrobacterium*. *Nature*, 431, 87–92.

Van Attikum, H., Bundock, P. & Hooykaas, P. J. J. (2001). Non-homologous end-joining proteins are required for *Agrobacterium* T-DNA integration. *EMBO J.*, 20, 6550–6558.

van Engelenburg, S. B. and Palmer, A. E. (2010). Segregation of Salmonella effectors, 7, 325–330.

Vergunst, A. C., Schrammeijer, B., den Dulk-Ras, A., de Vlaam, C. M. T., Regensburg-Tuink, T. J. G. and Hooykaas, P. J. J. (2000). VirB / D4-Dependent Protein Translocation from *Agrobacterium* into Plant Cells. *Science*, 290, 979–982.

Vergunst, A. C., van Lier, M. C. M., den Dulk-Ras, A., Stüve, T. A. G., Ouwehand, A. and Hooykaas, P. J. J. (2005). Positive charge is an important feature of the C-terminal transport signal of the VirB/D4-translocated proteins of *Agrobacterium*. *Proc. Nat. Aca. Sci. U. S. A.*, 102, 832–7.

Wang, Y., Zhang, S., Huang, F., Zhou, X., Chen, Z., Peng, W. and Luo, M. (2018). VirD5 is required for efficient *Agrobacterium* infection and interacts with Arabidopsis VIP2. *New Phytol*, 2, 726-738.

Wolterink-van Loo, S., Escamilla Ayala, A. A., Hooykaas, P. J. J. and van Heusden, G. P. H. (2015). Interaction of the *Agrobacterium tumefaciens* virulence protein VirD2 with histones. *Microbiology*, 161, 401–410.

Wroblewski, T., Tomczak, A. and Micheltore, R. (2005). Optimization of *Agrobacterium*-mediated transient assays of gene expression in lettuce, tomato and Arabidopsis. *Plant Biotech. J.*, 3, 259–273.

Wu, Y., Zhao, Q., Gao, L., Yu, X. M., Fang, P., Oliver, D. J. and Xiang, C. B. (2010). Isolation and characterization of low-sulphur-tolerant mutants of Arabidopsis. *J. Exp. Bot.*, 61, 3407–3422.

Wu, H., Liu, K., Wang, Y., Wu, J., Chiu, W. and Chen, C. (2014). AGROBEST: an efficient *Agrobacterium*-mediated transient expression method for versatile gene function analyses in Arabidopsis seedlings. *Plant Methods*, 10, 1–16.

Zhang, X., van Heusden, G.P.H. and Hooykaas, P.J.J.(2017). Virulence protein VirD5 of *Agrobacterium tumefaciens* binds to kinetochores in host cells via an interaction with Spt4. *Proc. Natl. Acad. Sci. USA*, 38, 10238–10243.

Zhou, X. R. and Christie, P. J. (1999). Mutagenesis of the *Agrobacterium* VirE2 single-stranded DNA-binding protein identifies regions required for self-association and interaction with VirE1 and a permissive site for hybrid protein construction. *J. Bacteriol.*, 181, 4342–4352.

Ziemienowicz, A, Merkle, T., Schoumacher, F., Hohn, B. and Rossi, L. (2001). Import of *Agrobacterium* T-DNA into plant nuclei: two distinct functions of VirD2 and VirE2 proteins. *Plant Cell*, 13, 369–383.

Zonneveld, B. J. M. (1986). Cheap and simple yeast media. *J. Microbiol.Methods*, 4, 287–291.

Chapter 3

Application of phiLOV2.1 as a fluorescent marker for visualization of *Agrobacterium* effector protein translocation

Reprinted from

Roushan, M. R., de Zeeuw, M. A., Hooykaas, P. J. J. and van Heusden, G. P. H. (2018).
Application of phiLOV2.1 as a fluorescent marker for visualization of *Agrobacterium*
effector protein translocation. *Plant J*, doi:10.1111/tpj.14060.

With permission from Willey

Molecular and Developmental Genetics, Institute of Biology, Leiden University, Leiden, The
Netherlands.

ABSTRACT

Agrobacterium tumefaciens can genetically transform plants by translocating a piece of oncogenic DNA, called T-DNA, into host cells. Transfer is mediated by a type IV secretion system (T4SS). Besides the T-DNA which is transferred in a single stranded form and at its 5' end covalently bound to VirD2, several other effector proteins (VirE2, VirE3, VirD5 and VirF) are translocated into the host cells. The fate and function of the translocated proteins inside the host cell is only partly known. Therefore, several studies were conducted to visualize the translocation of the VirE2 protein. As GFP-tagged effector proteins are unable to pass the T4SS, other approaches like the split GFP system were used, but these require specific transgenic recipient cells expressing the complementary part of GFP. Here, we investigated whether use can be made of the photostable variant of LOV, phiLOV2.1, to visualize effector protein translocation from *Agrobacterium* to non-transgenic yeast and plant cells. We were able to visualize the translocation of all five effector proteins, both to yeast cells, and to cells in *Nicotiana tabacum* leaves and *Arabidopsis thaliana* roots. Clear signals were obtained that are easily distinguishable from the background, even in cases where by comparison the split GFP system did not generate a signal.

INTRODUCTION

Dicotyledonous plants are susceptible to infection by *Agrobacterium tumefaciens* resulting in the formation of crown gall tumors (De Cleene and De Ley, 1976; Nester *et al.*, 1984). During infection a segment of oncogenic DNA, called T-DNA, is translocated to the nucleus of host cells, where it is integrated into the genome (Tinland *et al.*, 1994). The T-DNA and other genes that are involved in virulence are located on a tumor inducing (Ti) plasmid (van Larebeke *et al.*, 1974; Nester *et al.*, 1975). The *virulence* (*vir*) region on this plasmid consists of several operons: *virA-R* (Zhu *et al.*, 2000). Wounded plant cells excrete several compounds, including phenolic compounds and sugars. These compounds activate VirA and VirG, resulting in expression of the other *vir* genes (Lee *et al.*, 1996). It has been shown that the effector proteins VirD2, VirD5, VirE2, VirE3 and VirF are translocated into the host cell through a type 4 secretion system (T4SS) formed by VirB1 to 11 and VirD4 (Vergunst *et al.*, 2000). This translocation is mediated by C-terminal signal sequences and can occur independently of T-DNA transfer (Vergunst *et al.*, 2000; Vergunst *et al.*, 2005). The T-DNA is translocated into host cells in a single strand form, the T-strand (Stachel and Nester, 1986). The VirD2 protein is covalently linked to the 5' end of the T-strand when acting as a relaxase and is responsible for the transport of the T-DNA into host cells (van Kregten *et al.*, 2009). However, even in absence of T-DNA, VirD2 can be transported through the T4SS (Vergunst *et al.*, 2005). VirD2 contains nuclear localization signals (NLS) that may guide the T-DNA to the nucleus of the host cell (Ziemienowicz *et al.*, 2001). VirE2 binds cooperatively to single-stranded DNA without any sequence specificity (Gietl *et al.*, 1987). Inside the host cell, the T-strand may be coated by VirE2 proteins and thereby VirE2 may protect the T-strand against host nucleases (Citovsky *et al.*, 1989; Rossi *et al.*, 1996). VirE2 has two putative NLSs, but their activity is weak and they may be hidden when the protein is bound to the T-strand (Citovsky *et al.*, 1992). Also whether these NLSs are involved in nuclear import of VirE2 is still unclear. Ziemienowicz *et al.* (2001) suggested that VirD2 is essential and sufficient for import of short single-stranded DNA into the plant nucleus, whereas for import of longer DNA VirE2 is also required. Djamei *et al.* (2007) were unable to obtain evidence that VirE2 by itself is imported into the nucleus of *Arabidopsis thaliana* cells. Instead, the VirE2 Interacting Protein 1 (VIP1) may guide VirE2 and the associated T-complex into the nucleus. VIP1 may also be important for the association of the T-complex with the host chromatin (Tzfira *et al.*, 2001) However, recently the role of VIP1 in the transformation process was questioned (Shi *et al.*, 2014). The virulence protein VirF is a host range factor of

Agrobacterium (Hooykaas *et al.*, 1984; Melchers *et al.*, 1990). This protein contains an F-box domain, and may form a Skp-Cullin-F-box protein (SCF) complex by interacting with the plant proteins ASK1 and ASK2 (Schrammeijer *et al.*, 2001; Magori and Citovsky, 2011). This complex may enable T-DNA integration by proteasomal degradation of VIP1 and VirE2 (Tzfira *et al.*, 2004). In addition, it may destabilize VFP4, a transcriptional activator of defense response genes (García-Cano *et al.*, 2018). VBF, a plant F-box protein, might functionally replace VirF in plant species that do not require VirF for successful transformation (Zaltsman *et al.*, 2010). VirE3 interacts with pBrp, a plant-specific transcription factor (García-Rodríguez *et al.*, 2006). pBrp localizes at the outside of plastids; however, when the cell is stressed or when VirE3 is present, pBrp translocates to the nucleus to stimulate transcription. Niu *et al.* (2015) showed that VirE3 activates the *VBF* promoter and thus possibly indirectly regulates the levels of VirE2 and VIP1. This clarifies why the transformation is only slightly decreased with a mutation in either *virF* or *virE3*, while the inactivation of both genes leads to low transformation efficiency (García-Rodríguez *et al.*, 2006). VirD5 has two bipartite NLSs, but is not essential for tumor formation. Wang *et al.* (2014) demonstrated that VirD5 can interact directly with the VIP1. They showed that VirD5 competes with VBF to bind to the VIP1-VirE2 complex, thereby inhibiting the degradation of this complex. In addition, VirD5 interacts with another VirE2 binding protein, VIP2 (Wang *et al.*, 2018). On the other hand, Zhang *et al.* (2017) showed that VirD5 can inhibit yeast and plant growth by binding to the kinetochores and thus provoking spindle checkpoint and chromosome mis-segregation during mitosis.

Several studies were initiated to visualize protein translocation into the host cell. Such studies are hampered by the inability of GFP-tagged proteins to translocate through the T4SS probably due to the rigidity of the GFP protein. By using the split GFP technique developed by van Engelenburg and Palmer (2010), translocation of the *Agrobacterium* effector protein VirE2 could, however, successfully be visualized (Sakalis, 2013; Sakalis *et al.*, 2014; Li *et al.*, 2014). *Saccharomyces cerevisiae* and plants expressing the first ten helices of GFP (GFP₁₋₁₀) were infected with *Agrobacterium* strains expressing VirE2 tagged with the remaining helix of GFP (GFP₁₁). After translocation of the GFP₁₁-tagged effector protein into the host cell, GFP is reconstituted and the translocated protein can be visualized. GFP₁₁-VirE2 formed dot-shaped and filamentous structures of different lengths after translocation to yeast and plant cells (Sakalis *et al.*, 2014; Li *et al.*, 2014). Unfortunately, the split GFP technique has some drawbacks. First of all, it can only be used with a genetically modified host expressing

GFP₁₋₁₀. Another disadvantage is that translocated proteins will only be visible in those cellular compartments where also GFP₁₋₁₀ is available (Park *et al.* , 2017). Recently, protein translocation into mammalian cells through the type 3 secretion system of *Shigella flexneri* was visualized using phiLOV2.1, an improved version of LOV (Gawthorne *et al.* , 2016). The LOV domain is responsible for the fluorescent properties of the plant blue-light receptor kinases called phototropins, regulated either by Light, Oxygen or Voltage (Huala *et al.*, 1997; Buckley *et al.*, 2015). Compared to LOV phiLOV2.1 has increased fluorescence and photostability (Christie *et al.* , 2012a, b). phiLOV2.1 is much smaller than GFP, 12.1 kDa vs. 27 kDa, which may be compatible with protein translocation through the T4SS. In this study, we used phiLOV2.1 to tag virulence proteins VirD2, VirD5, VirE2, VirE3 and VirF to visualize their translocation and localization in cells of the yeast *S. cerevisiae*, in *Nicotiana tabacum* leaves and in *A. thaliana* roots.

MATERIAL AND METHOD

Yeast strains and media. Yeast strains used in this study are listed in supplementary Table S1. All yeast strains were grown in YPD medium or selective MY medium supplemented, if required, with histidine, tryptophan, methionine and/or uracil to the final concentration of 20 mg/ml (Zonneveld, 1986). Yeast transformation was performed using the Lithium Acetate method (Gietz *et al.*, 1995). Yeast strains carrying plasmids were obtained by transforming parental strains with the appropriate plasmids followed by selection for histidine and/or uracil prototrophy.

Agrobacterium strains and media. The *Agrobacterium* strains used are listed in supplementary Table S2. *Agrobacterium* was grown in LC supplemented with the appropriate antibiotics (40 µg/ml gentamicin, 20 µg/ml rifampicin) at 28°C and 175 rpm. *Agrobacterium* strains carrying plasmids were obtained by electroporation as described by den Dulk-Ras and Hooykaas, (1995).

Plant lines. The plant lines used in this study were: *Nicotiana tabacum* (SR1), *N. tabacum* (SR1) expressing GFP₁₋₁₀ (Sakalis *et al.*, 2014), *Nicotiana glauca*, *A. thaliana* Columbia-0 (Col-0) and *A. thaliana* Col-0 mRFP-NLS (At2051) (obtained from Prof. Dr. S. B. Gelvin , Purdue University).

Agroinfiltration. *N. tabacum* was grown on soil at 25°C, 50% relative humidity and 16 hours photoperiod, to full plants and after one month young leaves were selected for agroinfiltration. After overnight growth of *Agrobacterium* strains at 28°C in LC medium, cultures were resuspended to the OD₆₀₀≈0.8 in 10 ml of induction medium with 200 μM acetosyringone (AS) and incubated for three hours at 28°C. The lower surface of the leaves of one-month-old *N. tabacum* SR1 was injected with this culture with a blunt-tipped 10 ml syringe using gentle pressure. After 10-48 hours the lower side of the leaves was analyzed using confocal microscopy.

Tumor formation assay. To assess whether the tagged virulence proteins are still biologically active, a tumor formation assay was performed. The plasmids with the genes for the tagged effector proteins were introduced in *Agrobacterium* strains with a deletion for that particular *vir* gene. An overnight culture of *Agrobacterium* was washed and resuspended with 0.9% (w/v) NaCl solution to an OD₆₀₀ of 1.0. After growing the *N. glauca* plants for six to seven weeks at 25°C, 75% relative humidity and 16 hours photoperiod, their stem was damaged with a sterile toothpick, followed by the inoculation of 20 μl of the *Agrobacterium* culture. After four weeks the tumor formation was scored and photographed.

Arabidopsis root transformation assay. *A. thaliana* Col-0 seeds were surface-sterilized and incubated at 4°C for 4 days. They were placed into liquid B5 medium supplemented with 3% sucrose and 0.5 g 2-(*N*-morpholino) ethanesulfonic acid (MES), pH 5.7 (Vergunst *et al.*, 1998). The flasks were incubated under a 16 hours photoperiod at 21°C for 10 days with gentle shaking. Roots from individual seedlings were cut into 0.3-0.5 cm long segments and re-suspended in 20 ml of fresh B5 medium containing *A. tumefaciens* cells at a concentration of 10⁹ cells/ml. The mixtures were spread onto B5 plates containing 200 μM acetosyringone and subsequently incubated at 24°C for 2 days. The root segments were washed three times with liquid B5 and then aligned onto B5 medium plates containing 100 mg/ml Timentin and kept at 24°C for 4 weeks.

Root protein translocation assay. *A. thaliana* Col-0 wild type and *A. thaliana* Col-0 mRFP-NLS (At2051) were used for the root protein translocation assays. Approximately 3 mg of sterilized seeds were grown in 50 ml of B5 medium while shaking 90 rpm at 21°C with 16 hours of light per day and 50% relative humidity. After at least eight days the roots were separated from the hypocotyls and placed on callus induction medium (CIM) for three days.

Subsequently, the roots were placed in a clean sterile petri dish containing 20 ml of the *Agrobacterium* overnight culture with a OD₆₀₀ of 0.3 and incubated for at least 20 min at room temperature. The roots were then dried on a sterile paper towel and placed on CIM containing 100 µM acetosyringone. The cocultivation plates were placed underneath a piece of aluminum foil in the growth chamber with a temperature of 24°C and 50% relative humidity. After 20 to 48 hours, root protein translocation was analyzed using confocal laser scanning microscopy. LBA1010 was used as a negative control. B5 and CIM are described by Vergunst *et al.* (1998) as liquid growth medium (LGM) and callus induction medium (CIM), respectively.

Protoplast transformation. Protoplasts were derived from a five days old *A. thaliana* Col-0 cell suspension as described by Schirawski *et al.* (2000) and were transformed with 10 µg of plasmid DNA per 10⁶ protoplasts using Polyethyleneglycol (PEG) (Schirawski *et al.* , 2000). The transformed protoplasts were incubated at 27°C in the dark for 24 hours before treatments and microscopy.

Microscopic analysis. The localization of fluorescent proteins in yeast and plants was analyzed using the Zeiss Imager M1 confocal microscope equipped with a LSM5 Exciter, using a 40x (aperture 1.30) or a 63x (aperture 1.40) magnifying objective. phiLOV2.1 and reconstituted GFP were detected using an argon laser of 488 nm and a band-pass emission filter of 505-600 nm. The nuclear marker NLS::RFP was captured with an excitation wavelength of 543 nm and a 650 nm long-pass emission filter. CFP signals were detected after excitation at 458 nm using a 475-515 nm emission filter. Microscopy of *Agrobacterium* expressing phiLOV2.1-tagged effector proteins was done with an Axioplan2 imaging microscope equipped with DIC and fluorescent filters to detect phiLOV2.1 signals at excitation wavelength of 488 and emission of 505-600 nm. The ImageJ (Abràmoff *et al.* , 2004) software was used to process and analyze the pictures.

Plasmid constructions. All plasmids used and constructed in this study are listed in supplementary Table S3. *E. coli* strain XL1-Blue was used for cloning of the plasmids and the cultures were grown in LC medium containing 10 µg/ml gentamycin or 100 µg/ml carbenicillin while shaking 175 rpm at 37°C. PCR amplifications were done with Phusion™ High-Fidelity DNA Polymerase. Supplementary Table S4 lists all primers used for PCR amplification and sequencing.

DNA fragments with phiLOV2.1 including or lacking its stop codon, were amplified by PCR on pGEX-6p1[phiLOV2.1] using primer pairs *XbaI*-phiLOV2.1-Fw and *BamHI*-phiLOV2.1-Rev or *XbaI*-phiLOv2.1-Fw and *BamHI*-phiLOv2.1ΔTAA-Rev, respectively. Then, they were used to replace GFP in pUG36 after digesting with *XbaI* and *BamHI*, yielding pUG36phiLOV2.1 and pUG36phiLOV2.1ΔTAA, respectively.

Li et al , 2014 showed that VirE2 (from *Agrobacterium* strain EHA105) can be tagged internally at proline-54 with GFP₁₁ without loss of function, as originally found by (Zhou and Christie, 1999). The corresponding site in VirE2 from the octopine Ti-plasmid used in our studies, is proline-39. To insert GFP₁₁ at this position, a DNA fragment was synthesized containing the 5' -end of *virE2* and GFP₁₁ adjacent to the codon for proline-39, with *SpeI* and *BgIII* restriction sites at the ends by Eurofins (Germany):

5'ACTAGTCATATGGATCTTTCTGGCAATGAGAAATCCAGGCCTTGGAAGAAGGCG
AATGTCAGTTCAGCACCATCTCCGATATTCAGATGACGAATGGCGAAAACCTTG
AATCAGGGAGCCCTCGGGACCACATGGTGCTGCACGAGTACGTGAACGCCGCCG
GCATCACAACCCGAACGGAAGTTTTAAGCCACGTCTGGATGATGGATCGGTCG
ATTCCCTCCTCCAGCCTTTATTCTGGCAGCGAGCACGGAAATCAAGCTGAGATTCA
AAAAGAGCTGTCCGCTTGTCTCGAACATGTCTTTGCCAGGCAACGATCGGCGC
CCGGACGAATACATTCTCGTGCGTCAAACGGGACAAGATGCTTTTACTGGTATTG
CCAAAGGCAACCTCGACCACATGCCACCAAGGCGGAATTTAACGCGTGCTGCC
GTCTCTACAGGGACGGAGCCGGTAATTACTATCCGCCACCTCTCGCGTTCGACAA
GATTAGCGTTCAGCCCAACTGGAGGAAACATGGGGGATGATGGAGGCGAAGG
AACGTAACAAACTACGGTTTCAGTACAAGTTGGACGTATGGAATCATGCGCACG
CTGATATGGGGATCACTGGCACAGAGATCT-3' (underlined: 48 bp GFP₁₁-coding
sequence; bold: the CCT codon of Proline39; double underlined: *SpeI* restriction site; italics:

NdeI restriction site; dots: *BgIII* restriction site). To insert the phiLOV2.1 coding sequence adjacent to the codon for proline-39, a similar DNA fragment was synthesized in which the GFP₁₁ coding sequence was replaced by the 339 bp phiLOV2.1 coding sequence:

5'ATGATAGAGAAGAGTTTCGTCATCACTGATCCTAGGCTTCCCAGCTATCCCATT
ATCTTTGCATCAGACGGCTTTCTTGAATTGACAGAGTATTCGCGCGAGGAAATAA
TGGGGAGAAATGCCCGGTTTCTTCAGGGGCCAGAGACAGATCAAGCGACTGTCC
AGAAGATAAGGGACGCAATTAGAGATCAGAGGGAGACTACTGTGCAGTTGATAA
ACTACACTAAAAGCGGAAAGAAATTCTGGAACCTACTCCACCTGCAACCTGTGC

GTGATCGGAAGGGGAGGGCTTCAATACTTCATCGGTGTGCAGCTCGTTGGAAGTG ATCATGTACCCTAA-3'. To obtain full length *VirE2* internally tagged with GFP₁₁ or phiLOV2.1 the synthetic DNAs were used to replace the *SpeI* - *BglII* fragment with the 5'-end of *virE2* of pUG36YFP::VirE2 to generate pUG36YFP::39GFP₁₁-VirE2 and pUG36YFP::39phiLOV2.1-VirE2, respectively. For expression in yeast an *XbaI*-*XhoI* fragment containing tagged *virE2*, was ligated into pUG34 digested with *XbaI* and *XhoI* yielding pUG34::39GFP₁₁-VirE2 and pUG34::39phiLOV2.1-VirE2. For expression in *Agrobacterium* pBBR6::39GFP₁₁[VirE2] and pBBR6::39phiLOV2.1[VirE2] (pBBR6-derived plasmids) were constructed by replacing the *NdeI* - *HindIII* fragment with N-terminally tagged *virE2* of pSDM3163::GFP₁₁[VirE2] (Sakalis *et al.*, 2014) by the *NdeI*-*HindIII* fragment of pUG34-39GFP₁₁[VirE2] and pUG34-39phiLOV2.1[VirE2]. The constructed plasmids were checked by sequencing using primers VirE2-seq-FW, VirE2-seq-Rev and VirE2-seq-int (Table S4).

To express phiLOV2.1-tagged VirD2, VirD5, VirF and VirE3 in protoplasts under control of 35S promoter (not used in this study), the *EcoRI*-phiLOV2.1VirD2-*XbaI*, *KpnI*-phiLOV2.1VirD5-*XbaI*, *EcoRI*- phiLOV2.1VirF-*HindIII* and *EcoRI*-phiLOV2.1VirE3-*HindIII* PCR fragments were generated using the primer pairs of *EcoRI*- phiLOVD2-Fw & *XbaI*-phiLOVD2-Rev, *KpnI*-phiLOVD5-Fw & *XbaI*-phiLOVD5-Rev, *EcoRI*-phiLOVF-Fw & *HindIII*-phiLOVF-Rev or *EcoRI*-phiLOVE3-FW & *HindIII*-phiLOVE3 and pSDM3777, pSDM3780, pSDM3778 and pSDM3779 respectively, as templates. These PCR fragments were cloned into pART7 digested via either *EcoRI* and *XbaI* (VirD2), *KpnI* and *XbaI* (VirD5) or *EcoRI* and *HindIII* (VirF and VirE3), to obtain pART7[phiLOV2.1-VirD2], pART7[phiLOV2.1-VirD5], pART7[phiLOV2.1-VirF] and pART7[phiLOV2.1-VirE3].

For expression of other phiLOV2.1-tagged effector proteins in yeast, plasmid pUG36 was used. A *XbaI*-phiLOV2.1VirD2-*EcoRI* PCR fragment, amplified using the primers *XbaI*-phiLOVD2-Fw and *EcoRI*-phiLOVD2-Rev and pART7[phiLOV2.1-VirD2] as template, was cloned into the pUG36 digested with *XbaI* and *EcoRI* creating pUG36[phiLOV2.1-VirD2]. To produce pUG36[phiLOV2.1-VirD5], the *XbaI*-phiLOV2.1VirD5-*SalI* DNA fragment amplified by PCR using the *XbaI*-phiLOVD5-Fw and *SalI*-phiLOVD5-Rev primers and pART7[phiLOV2.1-VirD5] as a template, was inserted into *XbaI* and *SalI* digested pUG36. A *XbaI*-phiLOV2.1VirF-*HindIII* and *XbaI*-phiLOV2.1VirE3-*HindIII* PCR fragments were produced by PCR using *XbaI*-phiLOV-Fw and *HindIII*-phiLOVF-Rev or *HindIII*-phiLOVE3-

Rev primers and pART7[phiLOV2.1-VirF] and pART7[phiLOV2.1-VirE3], respectively as template, ligated into digested (with *XbaI* and *HindIII*) pUG36, to obtain pUG36[phiLOV2.1-VirF] and pUG36[phiLOV2.1-VirE3] respectively.

For expression of phiLOV2.1-tagged effector proteins in *Agrobacterium*, plasmid pBBR6 was used. To construct pBBR6[phiLOV2.1-VirD2], first a DNA fragment with the *virD* promoter was amplified from pSDM3076 by PCR using the primers *EcoRI*-pVirD2-Fw and *PstI*-pVirD2-Rev. This fragment was ligated into pBBR6 after digestion with *EcoRI* and *PstI*. Subsequently, a DNA fragment with phiLOV2.1 was amplified from pUG36phiLOV2.1 using the primers *PstI*-phiLOV2.1-Fw and *SpeI*-phiLOV2.1ΔTAA –Rev and ligated into pBBR6-pVirD2 digested with *PstI* and *SpeI*. *SpeI*-VirD2-Fw and *XbaI*-VirD2-Rev were used to get the fragment *SpeI*-VirD2-*XbaI* using pSDM3149 as a PCR template, which was then cloned in pBBR6-phiLOV2.1 digested with *SpeI* and *XbaI*. pBBR6[phiLOV2.1-VirD5] was constructed by ligation of the fragment *EcoRI*-*virD* promoter-*PstI*, obtained by PCR from pSDM3759 with the primers *EcoRI*-pVirD-Fw and *PstI*-pVirD-Rev, into pBBR6 using *EcoRI* and *PstI*. The primers *PstI*-phiLOV2.1-Fw and *XmaI*-phiLOV2.1-Rev were used to generate *PstI*-phiLOV2.1-*XmaI* from pUG36 phiLOV2.1 and followed by ligation into pBBR6-p*virD* plasmid digested by *PstI* and *XmaI*. The primers, *XmaI*-VirD5-Fw and *XbaI*-VirD5-Rev were used to generate *XmaI*-VirD5-*XbaI* from pSDM3759. Subsequently, *XmaI*-VirD5-*XbaI* fragment was ligated into pBBR6 containing the *virD* promoter and phiLOV2.1 using *XmaI* and *XbaI*. The plasmids pBBR6[phiLOV2.1-VirE2] and pBBR6[phiLOV2.1-VirE3] were made by ligating first the *EcoRI*-*virE* promoter-*PstI* fragment into the vector pBBR6. This promoter was obtained by PCR using *EcoRI*-pVirE-Fw and *PstI*-pVirE-Rev on pBBR6::39phiLOV2.1[VirE2]. A *PstI*-*BamHI* fragment containing phiLOV2.1ΔTAA was obtained by PCR from pUG36phiLOV2.1 with the primers *PstI*-phiLOV2.1-Fw and *BamHI*-phiLOV2.1ΔTAA-Rev and subsequently ligated into pBBR6-VirE promoter backbone digested with *PstI* and *BamHI* to generate pBBR6-pVirE-PhiLOV2.1. To create pBBR6[phiLOV2.1-VirE2], the *BamHI*-VirE2-*XbaI* fragment, obtained with *BamHI*-VirE2-Fw and *XbaI*-VirE2-Rev from pJET[VirE2], was ligated into pBBR6[pVirE- phiLOV2.1] digested with *BamHI* and *XbaI*. pBBR6[phiLOV2.1-VirE3] was constructed in the same way, using pUG36[GFP₁₁-VirE3] as a template for the PCR, using primers *BamHI*-VirE3-Fw and *XbaI*-VirE3-Rev. To express phiLOV2.1-tagged VirE2 under control of 35S promoter in protoplasts, we constructed pART7[39phiLOV2.1-VirE2]. To this end, first phiLOV2.1-

tagged *virE2*, was amplified by PCR on pBBR6[39phiLOV2.1-VirE2] using the primers *KpnI*-39phiLOVE2-Fw and *XbaI*-39phiLOVE2-Rev. Then, pART7[39phiLOV2.1-VirE2] was created by ligation of *XbaI*-*KpnI* 39phiLOV2.1-VirE2 fragment into *XbaI* and *KpnI* digested pART7.

Table1.Yeast strains used in this study

Yeast strain	Genotype	Source/reference
BY4741	<i>MATa his3Δ1 leu2Δ0 met15Δ0 ura3Δ0</i>	(Brachmann <i>et al.</i> , 1998)
CEN.PK2-1C	<i>MATa ura3-52 leu2-112 trp1-289 his3-Δ1</i>	P. Kötter, Göttingen, Germany.
426::GFP ₁₋₁₀ (GG3388)	CEN.PK2-1C <i>leu2::pRS306[P_{MET25}-GFP₁₋₁₀-T_{CYC1}] (LEU2)</i>	(Sakalis <i>et al.</i> , 2014)
426::GFP ₁₋₁₀ -34GFP ₁₁ (GG3389)	CEN.PK2-1C <i>leu2::pRS306[P_{MET25}-GFP₁₋₁₀-T_{CYC1}] (LEU2)</i> pUG34[P _{MET25} -GFP ₁₁ -T _{CYC1}] (<i>HIS3</i>)	(Sakalis, 2013)
426::GFP ₁₋₁₀ -34GFP ₁₁ [VirE2] (GG3390)	CEN.PK2-1C <i>leu2::pRS306[P_{MET25}-GFP₁₋₁₀-T_{CYC1}] (LEU2)</i> pUG34[P _{MET25} -GFP ₁₁ -VirE2-T _{CYC1}] (<i>HIS3</i>)	(Sakalis, 2013)
426::GFP ₁₋₁₀ -34GFP ₁₁ [VirD2] (GG3392)	CEN.PK2-1C <i>leu2::pRS306[P_{MET25}-GFP₁₋₁₀-T_{CYC1}] (LEU2)</i> pUG34[P _{MET25} -GFP ₁₁ -VirD2-T _{CYC1}] (<i>HIS3</i>)	(Sakalis, 2013)
426::GFP ₁₋₁₀ -34GFP ₁₁ [VirD5] (GG3393)	CEN.PK2-1C <i>leu2::pRS306[P_{MET25}-GFP₁₋₁₀-T_{CYC1}] (LEU2)</i> pUG34[P _{MET25} -GFP ₁₁ -VirD5-T _{CYC1}] (<i>HIS3</i>)	(Sakalis, 2013)
BY4741 – CFP-TUB1 (GG3456)	BY4741 <i>leu2::pRS306[TUB1] (LEU2)</i>	This study.
BY4741 – CFP-TUB1 +pUG34[39phiLOV2.1] (GG3457)	BY4741 <i>leu2::pRS306[TUB1] (LEU2)</i> pUG34[P _{MET25} -39phiLOV2.1-VirE2-T _{CYC1}] (<i>HIS3</i>)	This study.

Table 2. *Agrobacterium* strains used in this study

<i>Agrobacterium</i> strain	Specifications	Source/reference
LBA1010	C58 containing pTiB6, Rif	(Koekman <i>et al.</i> , 1982)
LBA1100	C58 containing pTiB6Δ (Δ T-DNA, Δ occ, Δ tra), Rif, Spc [†]	(Beijersbergen <i>et al.</i> , 1992)
LBA1100 (pRAL7100)	LBA1100 with binary vector pRAL7100, Rif, Km [†]	(Bundock <i>et al.</i> , 1995)
AGL1 (pCambia1302-GFP ₁₋₁₀)	AGL1 with pCambia1302-GFP1-10 (pSDM3764);pCambia1302 with <i>GFP</i> ₁₋₁₀ under control of the <i>35S</i> promoter and the <i>CaMV</i> terminator).	(Sakalis <i>et al.</i> , 2014)
LBA1143 (LBA1100ΔB4)	<i>virB4</i> deletion in LBA1100,Rif, Spc, T4SS deficient	(Beijersbergen <i>et al.</i> , 1992)
LBA2572 (LBA1010ΔE2)	<i>virE2</i> deletion in LBA1010, Rif	den Dulk-Ras, unpublished
LBA2573 (LBA1100 ΔE2)	<i>virE2</i> deletion in LBA1100, Rif, Spc	(Hodges <i>et al.</i> , 2006)
LBA2556 (LBA1100ΔD2)	<i>virD2</i> deletion in LBA1100, Rif, Spc	Jurado-Jácome, den Dulk-Ras, Vergunst, and Hooykaas, unpublished
LBA2560 (LBA1010ΔF)	<i>virF</i> deletion in LBA1010, Rif	(Schrammeijer <i>et al.</i> , 1998)
LBA2561 (LBA1100ΔF)	<i>virF</i> deletion in LBA1100, Rif, Spc	(Schrammeijer <i>et al.</i> , 1998)
LBA2564 (LBA1010ΔE3)	<i>virE3</i> deletion in LBA1010, Rif	(García-Rodríguez <i>et al.</i> , 2006)
LBA2565 (LBA1100ΔE3)	<i>virE3</i> deletion in LBA1100, Rif, Spc	(Schrammeijer <i>et al.</i> , 1998)
LBA2566 (LBA1010ΔE3/F)	<i>virE3</i> and <i>virF</i> deletion in LBA1010	(García-Rodríguez <i>et al.</i> , 2006)
LBA2569 (LBA1010ΔD2)	<i>virD2</i> deletion in LBA1010, Rif	Vergunst, den Dulk-Ras and Hooykaas, unpublished
LBA3550 (LBA1010ΔD5)	<i>virD5</i> deletion in LBA1010, Rif	Ouwehand, Vergunst and Hooykaas, unpublished

LBA3551 (LBA1100ΔD5)	<i>virD5</i> deletion in LBA1100, Rif, Spc	den Dulk-Ras, unpublished
LBA2573 (3163-GFP ₁₁ -VirE2)	LBA2573 with pSDM3163[GFP ₁₁ -VirE2]. Expression of the GFP ₁₁ -VirE2 under control of the <i>virE</i> promoter, Rif, Spc, Gm	(Sakalis <i>et al.</i> , 2014)
LBA2572 (3163-GFP ₁₁ -VirE2)	LBA2573 with pSDM3163[GFP ₁₁ -VirE2]. Expression of the GFP ₁₁ -VirE2 under control of the <i>virE</i> promoter, Rif, Spc, Gm	(Sakalis <i>et al.</i> , 2014)
LBA2569(3163GFP ₁₁ - D2)	LBA2569 with pSDM3163[GFP ₁₁ - VirD2],expressing the GFP ₁₁ -VirD2 under control of the <i>virD</i> promoter, Rif, Gm	(Sakalis, 2013)
LBA2556(3163GFP ₁₁ - D2)	LBA2556 with pSDM3163[GFP ₁₁ -VirD2], expressing the GFP ₁₁ -VirD2 under control of the <i>virD</i> promoter, Rif, Spc, Gm	(Sakalis, 2013)
LBA3567 (placZ-GFP)	LBA1100 with pSDM1761 expressing EGFP.	(Wolterink-van Loo <i>et al.</i> , 2015)
LBA3551(3076GFP ₁₁ - D5)	LBA3551 with pSDM3076[GFP ₁₁ -VirD5]. Expression of the GFP ₁₁ -VirD5 under control of the <i>virD</i> promoter, Rif, Spc, Gm	(Sakalis, 2013)
LBA3550(3076GFP ₁₁ - D5)	LBA3550 with pSDM3076[GFP ₁₁ -VirD5]. Expression of the GFP ₁₁ -VirD5 under control of the <i>virD</i> promoter, Rif, Spc, Gm	(Sakalis, 2013)
LBA2573 (pBBR6-39GFP ₁₁ - VirE2)	LBA2573 with pBBR6[39-GFP ₁₁ -VirE2]. Expression of the internally-tagged GFP ₁₁ - VirE2 fusion protein under control of the <i>virE</i> promoter, Rif, Spc,Gm	This study.
LBA2572 (pBBR6-39GFP ₁₁ - VirE2)	LBA2572 with pBBR6[39-GFP ₁₁ -VirE2]. Expression of the internally-tagged GFP ₁₁ - VirE2 fusion protein under control of the <i>virE</i> promoter, Rif, Spc,Gm	This study.
LBA2573 (pBBR6-39phiLOV2.1- VirE2)	LBA2573 with pBBR6[39phiLOV2.1-VirE2]. Expression of the internal-tagged phiLOV2.1- VirE2 fusion protein under control of the <i>virE</i> promoter, Rif, Spc, Gm	This study.

LBA2572 (pBBR6-39phiLOV2.1-VirE2)	LBA2572 with pBBR6-39phiLOV2.1-VirE2. Expression of the internal-tagged phiLOV2.1-VirE2 fusion protein under control of the <i>virE</i> promoter, Rif, Spc, Gm	This study.
LBA2573 (pBBR6-phiLOV2.1-VirE2)	LBA2573 with pBBR6[phiLOV2.1-VirE2]. Expression of the N-terminally-tagged phiLOV2.1-VirE2 fusion protein under control of the <i>virE</i> promoter, Rif, Spc, Gm	This study.
LBA2572 (pBBR6-phiLOV2.1-VirE2)	LBA2572 with pBBR6[phiLOV2.1-VirE2]. Expression of the N-terminally-tagged phiLOV2.1-VirE2 fusion protein under control of the <i>virE</i> promoter, Rif, Spc, Gm	This study.
LBA2572 (pSDSM3163)	LBA2572 with pBBR6[VirE1-VirE2] Expression of the VirE1-VirE2 under control of the <i>virE</i> promoter, Rif, Spc, Gm	This study.
LBA2556 (pBBR6-phiLOV2.1-VirD2)	LBA2556 with pBBR6[phiLOV2.1-VirD2]. Expression of the N-terminally-tagged phiLOV2.1-VirD2 fusion protein under control of the <i>virD2</i> promoter, Rif, Spc, Gm	This study.
LBA2560 (pBBR6-phiLOV2.1-VirF)	LBA2560 with pBBR6 [phiLOV2.1-VirF]. Expression of the N-terminally-tagged phiLOV2.1-VirF fusion protein under control of the <i>virF</i> promoter, Rif, Gm	This study.
LBA2561 (pBBR6-phiLOV2.1-VirF)	LBA2561 with pBBR6 [phiLOV2.1-VirF]. Expression of the N-terminally-tagged phiLOV2.1-VirF fusion protein under control of the <i>virF</i> promoter, Rif, Spc, Gm	This study.
LBA2564 (pBBR6-phiLOV2.1-VirE3)	LBA2564 with pBBR6 [phiLOV2.1-VirE3]. Expression of the N-terminally-tagged phiLOV2.1-VirE3 fusion protein under control of the <i>virE</i> promoter, Rif, Gm	This study.
LBA2565 (pBBR6-phiLOV2.1-VirE3)	LBA2565 with pBBR6 [phiLOV2.1-VirE3]. Expression of the N-terminally-tagged phiLOV2.1-VirE3 fusion protein under control of the <i>virE</i> promoter, Rif, Spc, Gm	This study.
LBA2569 (pBBR6-phiLOV2.1-VirD2)	LBA2569 with pBBR6 [phiLOV2.1-VirD2]. Expression of the N-terminally-tagged phiLOV2.1-VirD2 fusion protein under control of the <i>virD2</i> promoter, Rif, Gm	This study.

LBA3550 (pBBR6-phiLOV2.1-VirD5)	LBA3550 with pBBR6 [phiLOV2.1-VirD5]. Expression of the N-terminally-tagged phiLOV2.1-VirD5 fusion protein under control of the <i>virD</i> promoter, Rif, Gm	This study.
LBA3551 (pBBR6-phiLOV2.1-VirD5)	LBA3551 with pBBR6 [phiLOV2.1-VirD5]. Expression of the N-terminally-tagged phiLOV2.1-VirD5 fusion protein under control of the <i>virD</i> promoter, Rif, Spc,Gm	This study.

†, Rif: rifampicin;; Spc: spectinomycin; Km: kanamycin; Gm: gentamicin

Table 3. Plasmids used in this study

Name	Properties	Source/reference
pART7	Plant cloning vector with 35S promoter, octopine synthase (<i>OCS</i>) terminator and ampicillin resistance marker.	(Gleave, 1999)
pART7-39phiLOv2.1-VirE2 (pSDM3774)	pART7 based vector with 39phiLOV2.1- <i>virE2</i> under control of 35S promoter and octopine synthase (<i>OCS</i>) terminator.	This study.
pBBR6	Broad host range, non-mobilizable plasmid with Gentamycin resistance marker derived from pBBR1-MS2.	(Kovach <i>et al.</i> ,1994)
pBBR6-phiLOV2.1-VirE2 (pSDM3775)	pBBR6 backbone with the coding sequence of phiLOV2.1- <i>virE2</i> (N-terminally tagged) under control of the <i>virE</i> promoter.	This study.
pBBR6-39phiLOV2.1-VirE2 (pSDM3776)	pBBR6 backbone with the coding sequence of 39phiLOV2.1- <i>virE2</i> under control of the <i>virE</i> promoter.	This study.
pBBR6-phiLOV2.1-VirD2 (pSDM3777)	pBBR6 backbone with the coding sequence of phiLOV2.1- <i>virD2</i> under control of the <i>virD2</i> promoter.	This study.
pBBR6-phiLOV2.1-VirF (pSDM3778)	pBBR6 backbone with the coding sequence of phiLOV2.1- <i>virF</i> under control of the <i>virF</i> promoter.	This study.
pBBR6-phiLOV2.1-VirE3 (pSDM3779)	pBBR6 backbone with the coding sequence of phiLOV2.1- <i>virE3</i> under control of the <i>virE</i> promoter.	This study.

pBBR6-phiLOV2.1-VirD5 (pSDM3780)	pBBR6 backbone with the coding sequence of phiLOV2.1- <i>virE2</i> under control of the <i>virD</i> promoter.	This study.
pCambia1302	High copy vector with <i>mGFP</i> under control of the <i>35S</i> promoter and the <i>CaMV</i> terminator. (Bacterial kanamycin resistance, plant hygromycin selection)	Cambia®, Australia
pCambia1302-GFP ₁₋₁₀ (pSDM3764)	pCambia1302 with <i>mGFP</i> replaced by <i>GFP₁₋₁₀</i> under control of the <i>35S</i> promoter and the <i>CaMV</i> terminator.	(Sakalis <i>et al.</i> , 2014)
pGEX-6p1[phiLOV2.1]	Bacterial vector for expressing GST in frame fusion with phiLOV2.1 protein under <i>tac</i> promoter.	(Christie <i>et al.</i> , 2012)
pJET1.2[VirE2] (pRUL1236)	pJET1.2 with <i>virE2</i> flanked by <i>SpeI</i> and <i>XmaI</i> restriction sites.	(Sakalis <i>et al.</i> , 2014)
pRS306[CFP-Tub1]	Yeast integrative vector with CFP-TUB1 under control of the HIS promoter and terminator. URA3 marker.	(Jensen <i>et al.</i> , 2001)
pSDM3149	<i>virD2</i> under control of the <i>virD</i> promoter, located on plasmid pBBR6 (pVD43 was cloned as <i>EcoRV</i> - <i>EcoRI</i> fragment in pIC2OH by Amke den Dulk).	(Rossi <i>et al.</i> , 1993)
pSDM1761	Plasmid that confers tetracycline resistance in <i>E. coli</i> and <i>rhizobia</i> , carrying EGFP from pME2444.	(Bloemberg <i>et al.</i> , 2000)
pSDM3163	pBBR6 with coding sequence of <i>virE1</i> and <i>virE2</i> under control of the <i>virE</i> promoter.	Dennis Schneider, unpublished.
pSDM3076	pBIN19 backbone with coding sequence of <i>virD5</i> under control of the <i>virD</i> promoter	Amke den Dulk, unpublished
pSDM3163[GFP ₁₁ -VirE2] (pSDM3756)	pBBR6 backbone with the coding sequence of GFP ₁₁ -VirE2 under control of the <i>virE</i> promoter.	(Sakalis <i>et al.</i> , 2014)
pBBR6[39GFP ₁₁ -VirE2] (pSDM3767)	pBBR6 backbone with the coding sequence of 39phiLOV2.1- <i>virE2</i> under control of the <i>virE</i> promoter.	This study.

pSDM3163[GFP ₁₁ -D5] (pSDM3759)	pSDM3076 backbone with coding sequence of GFP ₁₁ -VirD5 under control of the <i>virD</i> promoter.	(Sakalis, 2013)
pSDM3163[GFP ₁₁ -VirD2] (pSDM3755)	pSDM3163 backbone with the coding sequence of GFP ₁₁ -VirD2 under control of the <i>virD</i> promoter	(Sakalis, 2013)
pUG34	Centromeric plasmid to express N-terminal GFP fusions in yeast under control of the <i>MET17</i> (alias <i>MET25</i>) promoter and <i>CYC1</i> terminator. <i>HIS3</i> marker.	U. Güldener and J.H. Hegemann, unpublished.
pUG34GFP ₁₁ [VirD2] (pRUL1280)	Centromeric plasmid with <i>GFP₁₁-virD2</i> under control of the <i>MET25</i> promoter and <i>CYC1</i> terminator. <i>HIS3</i> marker.	(Sakalis, 2013)
pUG34GFP ₁₁ [VirE2] (pRUL1282)	Centromeric plasmid with GFP ₁₁ -VirE2 under control of <i>MET25</i> promoter and <i>CYC1</i> terminator. <i>HIS3</i> marker.	(Sakalis, 2013)
pUG34GFP ₁₁ [VirD5] (pRUL1294)	Centromeric plasmid with <i>GFP₁₁-VirD5</i> under control of <i>MET25</i> promoter and <i>CYC1</i> terminator. <i>HIS3</i> marker.	(Sakalis, 2013)
pUG34[39GFP ₁₁ -VirE2] (pSDM3766)	Centromeric plasmid for expression of proline39 GFP ₁₁ -VirE2 in yeast under control of the <i>MET25</i> promoter and <i>CYC1</i> terminator. <i>HIS3</i> marker.	This study.
pUG34-phiLOV2.1-VirE2 (pSDM3781)	Centromeric plasmid for expression of phiLOV2.1-VirE2 in yeast under control of <i>MET17</i> promoter and <i>CYC1</i> terminator. <i>HIS3</i> marker.	This study.
pUG34-39phiLOV2.1-VirE2 (pSDM3782)	Centromeric plasmid for expression of 39phiLOV2.1-VirE2 in yeast under control of <i>MET17</i> promoter and <i>CYC1</i> terminator. <i>HIS3</i> marker.	This study.
pUG36	Centromeric plasmid to express N-terminal GFP fusions in yeast under control of the <i>MET25</i> promoter and <i>CYC1</i> terminator. <i>URA3</i> marker.	U. Güldener and J.H. Hegemann, unpublished.

pUG36phiLOV2.1 (pSDM3783)	Centromeric plasmid for expression of free phiLOV2.1 under control of <i>MET25</i> promoter and <i>CYC1</i> terminator. <i>URA3</i> marker.	This study.
pUG36phiLOV2.1ΔTAA (pSDM3784)	Centromeric plasmid containing phiLOV2.1 without stop codon under control of <i>MET25</i> promoter and <i>CYC1</i> terminator. <i>URA3</i> marker.	This study.
pUG36-phiLOV2.1-VirE2 (pSDM3785)	Centromeric plasmid for expression of phiLOV2.1-VirE2 (N-terminal) under control of <i>MET25</i> promoter and <i>CYC1</i> terminator. <i>URA3</i> marker.	This study.
pUG36-39phiLOV2.1-VirE2 (pSDM3786)	Centromeric plasmid for expression of 39phiLOV2.1-VirE2 under control of <i>MET25</i> promoter and <i>CYC1</i> terminator. <i>URA3</i> marker.	This study.
pUG36-phiLOV2.1-VirD2 (pSDM3787)	Centromeric plasmid for expression of phiLOV2.1-VirD2 under control of <i>MET25</i> promoter and <i>CYC1</i> terminator. <i>URA3</i> marker.	This study.
pUG36-phiLOV2.1-VirE3 (pSDM3788)	Centromeric plasmid for expression of phiLOV2.1-VirE3 under control of <i>MET25</i> promoter and <i>CYC1</i> terminator. <i>URA3</i> marker.	This study.
pUG36-phiLOV2.1-VirF (pSDM3789)	Centromeric plasmid for expression of phiLOV2.1-VirF under control of <i>MET25</i> promoter and <i>CYC1</i> terminator. <i>URA3</i> marker.	This study.
pUG36-phiLOV2.1-VirD5 (pSDM3790)	Centromeric plasmid for expression of phiLOV2.1-VirD5 under control of <i>MET25</i> promoter and <i>CYC1</i> terminator. <i>URA3</i> marker.	This study.
pUG36YFP[VirE2] (pRUL1244)	Centromeric plasmid for expression of YFP-VirE2 under control of <i>MET25</i> promoter and <i>CYC1</i> terminator. <i>URA3</i> marker.	(Sakalis <i>et al.</i> , 2014)
pUG36YFP-39GFP ₁₁ [VirE2] (pSDM3791)	pUG36YFP[VirE2] backbone with the coding sequence of proline39phiLOV2.1-VirE2 under control of <i>MET25</i> promoter.	This study.

Table 4. Primers used in this study

Primer name	Sequence (5' → 3')
<i>EcoRI</i> -pVirD-Fw	AAAGAATTCCTGATCCCGCCTGTCCTGTG
<i>PstI</i> -pVirD-Rev	AAACTGCAGCCTCCAAAAAAGCGGAAGG
<i>EcoRI</i> -pVirD2-Fw	AAAGAATTCAAACGGAGTGCATTTGTATTTTG
<i>PstI</i> -pVirD2-Rev	AAACTGCAGAGCTTCTCCAAAAAAGCG
<i>EcoRI</i> -pVirE-Fw	AAAGAATTCGGCTGCTCGTACCAAC
<i>PstI</i> -pVirE-Rev	AAACTGCAGTGTTCTCTCCTGCAAAATTGCG
<i>EcoRI</i> -pVirF-Fw	GGGGAATTCTACCGAGCTCCTATGATAGTCG
<i>PstI</i> -pVirF-Rev	GGGCTGCAGGCTCCTGTGCTTTTGAAAGG
<i>PstI</i> -phiLOV2.1-Fw	GGCTGCAGATGATAGAGAAGAGTTTC
<i>SpeI</i> -phiLOV2.1ΔTAA-Rev	GGACTAGTTACATGATCACTTCCAAC
<i>PstI</i> - phiLOV2.1-Fw	GGCTGCAGATGATAGAGAAGAGTTTC
<i>XmaI</i> - phiLOV2.1ΔTAA-Rev	GGCCCGGGTACATGATCACTTCCAAC
<i>PstI</i> -phiLOV2.1-Fw	GGCTGCAGATGATAGAGAAGAGTTTC
<i>BamHI</i> -phiLOV2.1ΔTAA-Rev	AAAGGATCCTACATGATCACTTCCAACGAG
<i>XmaI</i> -VirD5-Fw	GGCCCGGGATGACAGGAAAGTCGAAAG
<i>XbaI</i> -VirD5-Rev	GGTCTAGATTATCAGCGTTTAAACGC
<i>SpeI</i> -VirD2-Fw	GGACTAGTATGCCCCGATCGCG
<i>XbaI</i> -VirD2-Rev	GGTCTAGATAGGTCCCCCG
<i>BamHI</i> -VirE2-Fw	GGGGGATCCATGGATCTTTCTGGCAATG
<i>XbaI</i> -VirE2-Rev	GGTCTAGATCAAAAGCTGTTGACGCTTTG
<i>BamHI</i> -VirE3-Fw	GGGGGATCCATGGTGAGCACTACGAAGAAAAG
<i>XbaI</i> -VirE3-Rev	GGTCTAGATTAGAAACCTCTGGAGGTGG
<i>BamHI</i> -VirF-Fw	GGGGGATCCATGAGAAATTCG
<i>XbaI</i> -VirF-Rev	GGTCTAGATCATAGACCGCGC
<i>KpnI</i> -39phiLOVE2-Fw	CCCGGTACCATGGATCTTTCTGGCAATGAG
<i>XbaI</i> -39phiLOVE2-Rev	GGTCTAGATCAAAAGCTGTTGACGC
<i>EcoRI</i> -phiLOVE3-Fw	CCCCGAATTCATGATAGAGAAGAGTTTCGTC
<i>HindIII</i> -phiLOVE3-Rev	GGGAAGCTTTTAGAAACCTCTGGAGGTG
<i>EcoRI</i> -phiLOVD2-Fw	CCCCGAATTCATGATAGAGAAGAGTTTCGTC

<i>XbaI</i> -phiLOVD2-Rev	GGTCTAGACTAGGTCCCCCGC
<i>XhoI</i> -phiLOVE2-Fw	GGGGCTCGAGATGATAGAGAAGAGTTTCGTC
<i>XbaI</i> -phiLOVE2-Rev	GGTCTAGATCAAAAGCTGTTGACGC
<i>EcoRI</i> -phiLOVF-Fw	CCCCGAATTCATGATAGAGAAGAGTTTCGTC
<i>HindIII</i> -phiLOVF-Rev	GGGAAGCTTTCATAGACCGCGC
<i>KpnI</i> -phiLOVD5-Fw	CCCGGTACCATGATAGAGAAGAGTTTCGTC
<i>XbaI</i> -phiLOVD5-Rev	GGTCTAGATCAGCGTTTAAACGC
<i>XbaI</i> -phiLOVD2-Fw	GGTCTAGAATGATAGAGAAGAGTTTCGTC
<i>EcoRI</i> -phiLOVD2-Rev	CCCCGAATTCCTAGGTCCCCCGC
<i>XbaI</i> -phiLOVD5-Fw	GGTCTAGAATGATAGAGAAGAGTTTCGTC
<i>Sall</i> -phiLOVD5-Rev	AAAGTCGACTCAGCGTTTAAACGC
<i>NcoI</i> -GFP ₁₋₁₀ -Fw	GCCCATGGTTTCGAAAGGCGAGGA
<i>BstEII</i> -GFP ₁₋₁₀ -Rev	GGGTCACCTTATTTCTCGTTTGGGTCTT
<i>XbaI</i> -GFP1-10-Fw	GCTCTAGAATGGTTTCGAAAGGCGA
<i>XhoI</i> -GFP1-10-Rev	CCCTCGAGTTATTTCTCGTTTGGGT

a, restriction sites are underlined.

RESULTS

Ectopic expression of phiLOV2.1-tagged virulence proteins in yeast

First we investigated whether *Agrobacterium* effector proteins can be visualized by confocal microscopy when tagged with phiLOV2.1. To this end, we ectopically expressed N-terminally phiLOV2.1-tagged effector proteins in yeast under control of the *MET17* (alias *MET25*) promoter. In addition, a plasmid was constructed expressing VirE2 internally tagged with phiLOV2.1 at proline-39 (39phiLOV2.1-VirE2). Tagging with GFP₁₁ or insertion of a peptide at this position was shown not to affect the biological activity of VirE2 (Zhou and Christie, 1999; Li *et al.*, 2014). As shown in Figure 1 (A-F) a fluorescent signal was found for all five phiLOV2.1-tagged effector proteins. However, no fluorescent signals were detected in yeast cells containing plasmid pUG36ΔGFP which lacks genes encoding phiLOV2.1 or GFP (Figure 1G). To study whether the subcellular localization of the phiLOV2.1-tagged effector proteins is similar to that found using other fluorescent tags, we expressed GFP₁₁-tagged effector proteins in a yeast strain expressing GFP₁₋₁₀. This resulted in a fluorescent signal, except for GFP₁₁-tagged VirE3 and VirF (Figure 1, H-M). As shown in Figure 1(N), fluorescent signals were not detected in yeast cells containing plasmid pUG36ΔGFP. The localizations of the effector proteins observed after using the different tags are highly similar for all the effector proteins. We observed filamentous structures and dots inside cells expressing either internally or N-terminally tagged phiLOV2.1-VirE2 and also in cells expressing VirE2 internally-tagged with GFP₁₁ (Figure 1A, B and H). In contrast, only sporadically a dot-like structure was found in cells expressing N-terminally tagged GFP₁₁-VirE2 (Figure 1I), similarly as we reported previously (Sakalis *et al.*, 2014). VirD2 and VirD5 were found concentrated in the nucleus, independently of the tag used (Figure 1, C, E, J, L). This nuclear localization was confirmed by 4',6-diamidino-2-phenylindole (DAPI) staining (Figure S1). phiLOV2.1-VirF was observed all over the yeast cell (Figure 1D), but we were not able to obtain reliable signals after expression of GFP₁₁-VirF. phiLOV2.1-VirE3 was located inside the nucleus (Figure 1F). Also this nuclear localization was confirmed by DAPI staining (Figure S1). No fluorescence could be detected after expression of GFP₁₁-VirE3. Expression of free phiLOV2.1 in yeast resulted in a fluorescent signal all over the yeast cell (supplementary Figure S2A), indicating that phiLOV2.1 itself is not targeted to a specific cellular location.

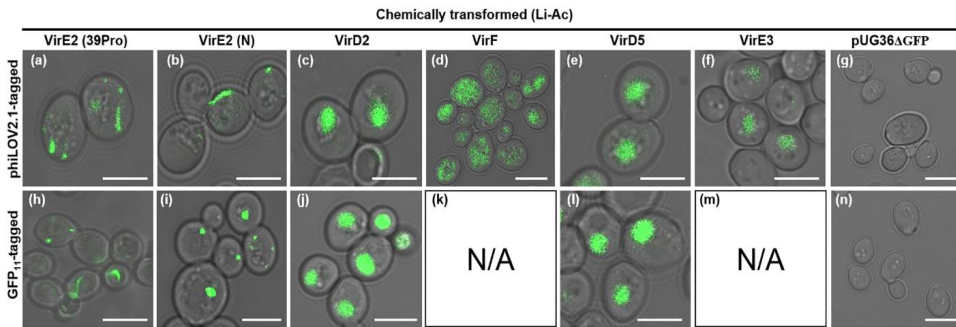


Figure 1. Visualization of ectopically expressed phiLOV2.1- and GFP₁₁-tagged *Agrobacterium* effector proteins in yeast. Upper panel, confocal microscopy of yeast strain BY4741 transformed with pUG36-39phiLOV2.1-VirE2 (A), with pUG36-phiLOV2.1-VirE2 (N-terminally tagged) (B), with pUG36-phiLOV2.1-VirD2 (C), with pUG36-phiLOV2.1-VirF (D), with pUG36-phiLOV2.1-VirD5 (E), with pUG36-phiLOV2.1-VirE3 (F) and with pUG36ΔGFP as a negative control (G). Lower panel, confocal microscopy of yeast strain 426::GFP₁₋₁₀ transformed with pUG34[39GFP₁₁-VirE2] (H), with pUG34GFP₁₁[VirE2] (N-terminally tagged) (I), with pUG34GFP₁₁[VirD2] (J), with pUG34GFP₁₁[VirD5] (I) or with pUG36ΔGFP as a negative control (N). Scale bars: 5 μm.

Expression of phiLOV2.1-tagged virulence proteins in *Agrobacterium*

To study the expression of virulence proteins in *Agrobacterium* and their translocation to yeast and plant cells, we created phiLOV2.1 fusions in the pBBR6 plasmid backbone under control of the endogenous promoters. These constructs were introduced into *Agrobacterium* strains lacking the corresponding endogenous *vir* gene. The expression of the *vir* genes was induced by addition of acetosyringone to a final concentration 200μM. After 6 and 24 hours expression was analyzed by fluorescence microscopy. As shown in figure 2A, in the *Agrobacterium* strain LBA2572(pBBR6-39phiLOV2.1-VirE2) after 6 hours expression of 39phiLOV2.1-VirE2 was observed in about half of the *Agrobacterium* cells. In many cells signals were more concentrated at cellular poles. After 24 hours, 39phiLOV2.1-VirE2 was localized in horseshoe-like structures in the majority of cells (Figure 2B). Very weak fluorescent signals were found in cells expressing the other phiLOV2.1-tagged virulence proteins (not shown). As expected, no fluorescence was seen in an *Agrobacterium* strain harboring the empty plasmid pBBR6 after induction for 12 and 24 hours with acetosyringone (supplementary Figure S2, C and D).

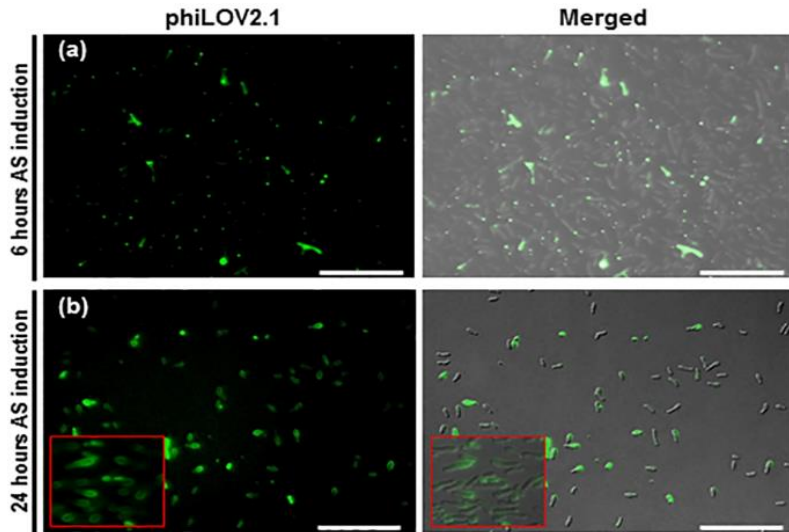


Figure 2. Analysis of 39phiLOV2.1-VirE2 expression in *Agrobacterium* by fluorescent microscopy. LBA2572(pBBR6-39phiLOV2.1-VirE2) was induced with acetosyringone for 6 (A) or 24 (B) hours. Scale bars: 2 μ m.

Biological activity of phiLOV2.1-tagged virulence proteins

To check whether the virulence proteins had retained their biological activity after tagging with phiLOV2.1 we performed tumor formation assays in *N. glauca* shoots and *A. thaliana* Col-0 roots. To this end, *N. glauca* shoots were injected with the different *Agrobacterium* strains and after 4 weeks tumor formation was scored. Tumors were easily visible after injection of the positive control strain LBA1010, whereas no tumors were formed after injection of the control strain lacking T-DNA (LBA1100) (supplementary Figure S3 A and B, respectively). Injection of LBA2572 (the *virE2* mutant) or LBA2572(pBBRR6-phiLOV2.1-VirE2) expressing N-terminally tagged phiLOV2.1-VirE2, did not result in tumor formation, confirming the important role of VirE2 in tumorigenesis and that N-terminal tagging of VirE2 results in loss of activity (Figure S3 C and D). In contrast, injection of LBA2572(pBBR6-39phiLOV2.1-VirE2), which expresses 39phiLOV2.1-VirE2, resulted in tumor formation, although the tumors were somewhat smaller in size (Figure S3E). This indicates that VirE2 internally-tagged with phiLOV2.1 at proline-39 kept, albeit somewhat reduced, biological activity. Injection of LBA2572(pBBR6-39GFP₁₁-VirE2) resulted in slightly larger tumors compared to injection of LBA2572(pBBR6-39phiLOV2.1-VirE2)

indicating that tagging with GFP₁₁ has less negative effect on VirE2 than tagging with phiLOV2.1 (Figure S3F). After injection of LBA2569, a *virD2* mutant, no tumors were found, in agreement with the essential role of VirD2 in *Agrobacterium*-mediated transformation (AMT) (Figure S3G). However, infection with LBA2569(pBBR6-phiLOV2.1-VirD2) expressing phiLOV2.1-VirD2, resulted in tumor formation, indicating that phiLOV2.1-VirD2 is at least partially functional (Figure S3H). As VirD5, VirE3 and VirF are not essential for tumor formation on *N. glauca*, the activity of the phiLOV2.1-tagged versions of these proteins could not easily be tested. García-Rodríguez *et al.* (2006) showed that deletion of both *virE3* and *virF* resulted in a decreased tumor size. As shown in Figure S3I, the *virE3 virF* double mutant LBA2566 generated none or very small tumors. Complementation with phiLOV2.1-VirF generated a strain that was clearly more tumorigenic (Figure S3J), while complementation with phiLOV2.1-VirE3 had less clear effect (Figure S3K).

To further investigate to what extent the phiLOV2.1-tag affects the biological activity of the effector proteins, we performed Arabidopsis root transformation assays. In these assays segments of Arabidopsis roots were co-cultivated with *Agrobacteria* and after 4 weeks tumor formation was observed. While the *virE2* mutant LBA2572 harboring the empty plasmid pBBR6 was not able to induce tumor formation in this assay (supplementary Figure S4A), tumors were seen after complementation with either pBBR6-VirE2 (Figure S4B) or pBBR6-39phiLOV2.1-VirE2 (Figure S4C) confirming that 39phiLOV2.1-tagged VirE2 is still at least partly active. Similarly, whereas no tumors were found after infection with the *Agrobacterium virD2* mutant LBA2569 (Figure S4D), comparable tumors were observed in root segments infected with *Agrobacterium* strains LBA2569(pBBR6-phiLOV2.1-VirD2) and LBA2569(pBBR6-VirD2), expressing phiLOV2.1-tagged and untagged VirD2, respectively (Figure S4F and E) revealing the biological activity of phiLOV2.1-tagged VirD2. Infection of the *virE3 virF* double mutant resulted in small tumors (Figure S4 G). Complementation of this double mutant with phiLOV2.1-tagged-VirE3 or phiLOV2.1-VirF resulted in the formation of larger tumors (Figure S4 H and I, respectively), indicating that tagging VirE3 and VirF with phiLOV2.1 did not inactivate these proteins.

Visualization of translocation of phiLOV2.1- or GFP₁₁-tagged effector proteins into yeast after AMT.

To visualize the translocation of effector proteins into yeast during AMT we employed *Agrobacterium* strains expressing phiLOV2.1- and GFP₁₁-tagged effector proteins in co-cultivation experiments. *Agrobacterium* strains expressing phiLOV2.1-tagged effector proteins were co-cultivated for 24-48 hours with BY4741, whereafter clear fluorescent signals became visible inside the yeast cells for all five effector proteins (Figure 3 A-F). Using an *Agrobacterium* strain lacking phiLOV2.1 such fluorescence signals could not be detected (supplementary Figure S2 B). Also fluorescent signals could not be detected in the yeast cells after co-cultivation with an *Agrobacterium virB4* mutant expressing the same phiLOV2.1-tagged effector proteins (Figure 3, G-L). As the *virB4* mutant is unable to assemble the VirB T4SS, this indicates that the observed fluorescent signals are the result of T4SS-dependent protein translocation. For comparison, similar co-cultivations were done with the *Agrobacterium* strains expressing the GFP₁₁-tagged effector proteins with a yeast strain expressing GFP₁₋₁₀ as recipient. As shown in Figure 3 M-R, a clear fluorescent signal was observed in the yeast cells after co-cultivation for 42 hours with *Agrobacterium* strains expressing GFP₁₁-tagged VirE2, -VirD2 and -VirD5. No signals were found upon co-cultivation with *Agrobacterium* strains expressing GFP₁₁-tagged *virF* and *virE3*, which was not unexpected as these proteins in yeast also did not lead for visualization of expression. The number of yeast cells in which a fluorescent signal is seen after co-cultivation is rather low, less than one percent for all virulence proteins which is line with even lower frequencies of transformation (Bundock *et al*, 1995; Sakalis *et al.*, 2014; Li *et al*, 2014). For most virulence proteins dot-shaped fluorescent structures were observed, irrespective of the tag used. Because of weak signals, it was difficult to perform additional staining to identify subcellular organelles. Although fluorescence could be seen in *Agrobacteria* cultured in induction medium, *Agrobacteria* recovered from the co-cultivation mixture had hardly detectable phiLOV2.1-fluorescence, corroborating that the fluorescent signals detected were the result of protein translocation.

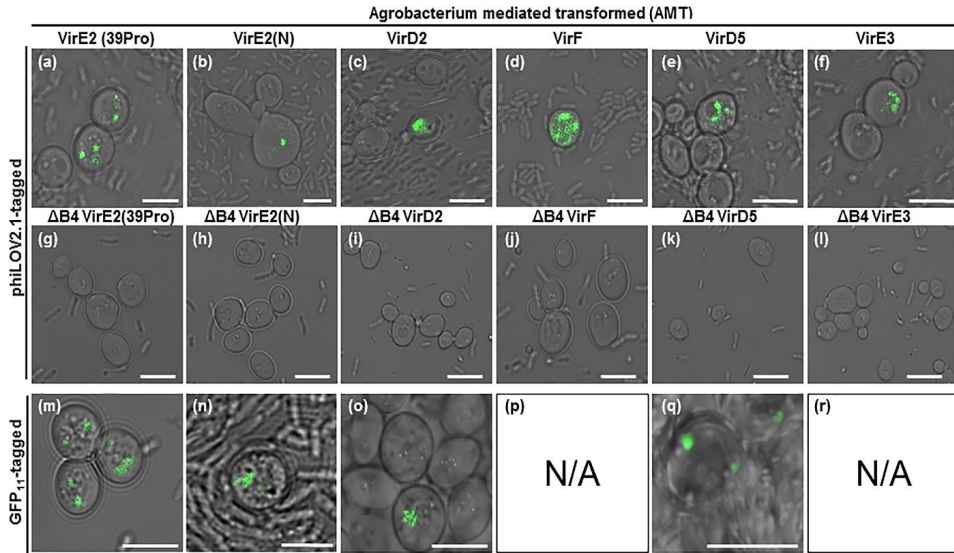


Figure 3. Visualization of translocated phiLOV2.1- and GFP₁₁-tagged effector proteins in yeast by confocal microscopy. Confocal microscopy of BY4741 (A-L) and 426::GFP₁₋₁₀ (M-R) yeast cells after co-cultivation with *Agrobacterium* strains LBA2573(pBBR6-39phiLOV2.1-VirE2)(A), with LBA2573(pBBR6-phiLOV2.1-VirE2) (B), with LBA2556(pBBR6-phiLOV2.1-VirD2) (C), with LBA2561(pBBR6-phiLOV2.1-VirF) (D), with LBA3551(pBBR6-phiLOV2.1-VirD5) (E), with LBA2565(pBBR6-phiLOV2.1-VirE3) (F), with virB4 mutant LBA1143(pBBR6-39phiLOV2.1-VirE2)(G), with LBA1143(pBBR6-phiLOV2.1-VirE2) (H), with LBA1143(pBBR6-phiLOV2.1-VirD2) (I), with LBA1143(pBBR6-phiLOV2.1-VirF) (J), with LBA1143(pBBR6-phiLOV2.1-VirD5) (K), with LBA1143(pBBR6-phiLOV2.1-VirE3) (L) with LBA2573(pBBR6-39GFP₁₁-VirE2) (M), with LBA2573(3163-GFP₁₁-VirE2) (N), with LBA2556(3163-GFP₁₁-D2) (O), or with LBA3551(3076GFP₁₁-D5) (Q). Scale bars: 5 μm.

Translocation of phiLOV2.1-tagged effector proteins from *Agrobacterium* into cells in *A. thaliana* roots

To visualize 39phiLOV2.1-VirE2 translocation to plant cells, *A. thaliana* root explants were co-cultivated with *Agrobacterium* strain LBA2573(pBBR6-39phiLOV2.1-VirE2) for 15 hours. Confocal microscopy revealed many fluorescent dot-shaped structures inside the root cells (supplementary Figure S5). To also investigate a possible nuclear localization of the translocated virulence proteins, we further used *A. thaliana* Col-0 (NLS-RFP) root explants expressing nuclear RFP. As shown in Figure 4A translocated 39phiLOV2.1-VirE2 formed fluorescent dot-shaped structures with cytoplasmic or perinuclear localizations. A minority (5 out of 37) of these dot shaped structures may co-localize with the nuclear marker (Figure 4A,

insert). However, whether these structures have a genuine nuclear localization still has to be established.

To visualize the translocation of the other effector proteins, *A. thaliana* Col-0 (NLS-RFP) root explants were co-cultivated with *Agrobacterium* strains LBA2569(pBBR6-phiLOV2.1-VirD2), LBA3550(pBBR6-phiLOV2.1-VirD5) and LBA2560(pBBR6-phiLOV2.1-VirF). As shown in Figure 4, translocation of these effector proteins was detected. Nuclear localization of translocated VirD2 and VirD5 was observed after co-cultivation for 42 hours (Figure 4B and C). Only few phiLOV2.1-VirF fluorescent signals reflecting VirF translocation events could be detected, and these localized outside the nucleus. After co-cultivations with wild-type strain LBA1010 lacking any phiLOV2.1 protein or the *virB4* mutant LBA1143 containing pBBR6-39phiLOV2.1-VirE2, pBBR6-phiLOV2.1-VirD2, pBBR6-phiLOV2.1-VirF or pBBR6-phiLOV2.1-VirD5 with *A. thaliana* Col-0 (NLS-RFP) root explants for 42 hours, no phiLOV2.1 fluorescence could be detected as expected (supplementary Figure S6A, Figure 4B, D, F and H, respectively). Therefore, detected signals reflected translocation of virulence proteins from *Agrobacterium* into the plant cells via T4SS rather than virulence protein expression in *Agrobacterium*. As mentioned above, *Agrobacteria* recovered from the co-cultivation mixture, had very weak fluorescent signals suggesting low levels of the phiLOV2.1-tagged effector proteins. Also we found that after co-cultivation of *A. thaliana* roots with *Agrobacterium* strain LBA3567(placZ-GFP) constitutively expressing GFP, no GFP fluorescence signals inside cells could be detected, even after inspection of more than 20 root explants in two separate experiments. This shows that *Agrobacteria* are not taken up by plant cells. Instead, only fluorescent *Agrobacterium* cells attached to the outside of the roots were observed (supplementary Figure S6B).

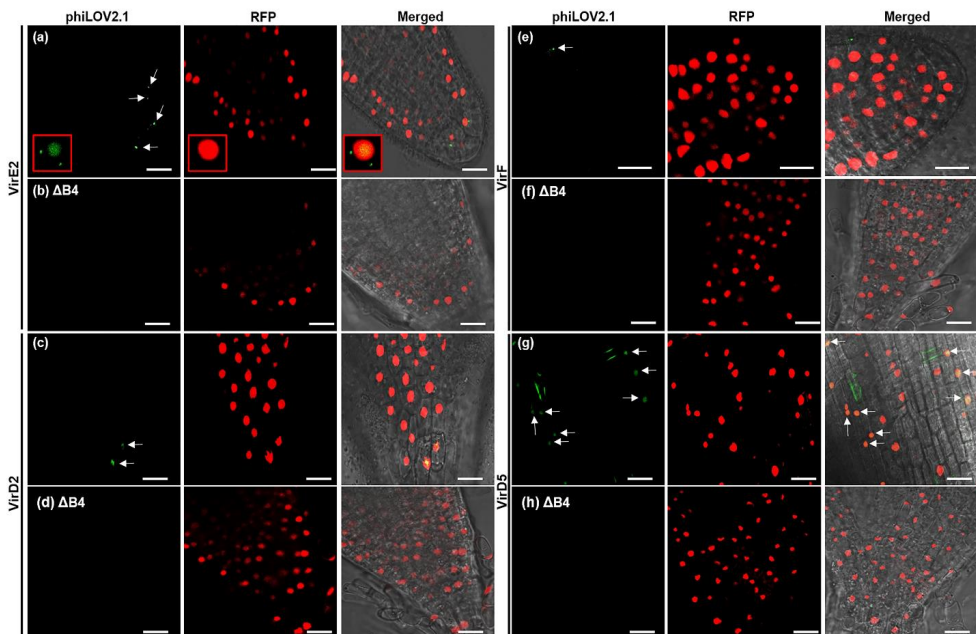


Figure 4. Translocation of phiLOV2.1-tagged effector proteins from *Agrobacterium* to *A. thaliana* Col-0 (NLS-RFP) roots. Roots were agroinfiltrated with *Agrobacterium* strains LBA2573(pBBR6-39phiLOV2.1-VirE2) (A), with LBA2569(pBBR6-phiLOV2.1-D2) (C), with LBA3550(pBBR6-phiLOV2.1-D5) (E), with LBA2560(pBBR6-phiLOV2.1-F) (G) LBA1143(pBBR6-39phiLOV2.1-VirE2) (B), with LBA1143(pBBR6-phiLOV2.1-D2) (D), with LBA1143(pBBR6-phiLOV2.1-D5) (F), or with LBA1143(pBBR6-phiLOV2.1-F) (H). Images were captured 15 hours (A), 42 hours (C), 44 hours (E) and 23 hours (G) after agroinfiltration. Images for negative controls (B, D, F and H) were captured 48 hours after co-cultivations. White arrows indicate perinuclear and nuclear signals. Scale bars: 15 μ m.

Translocation of phiLOV2.1-tagged effector proteins from *Agrobacterium* into cells in *N. tabacum* leaves

In previous studies the split GFP approach was used to visualize VirE2 translocation from *A. tumefaciens* into *N. benthamiana* and *N. tabacum* cells in leaf tissues (Sakalis *et al.*, 2014; Li *et al.*, 2014). Translocated VirE2 was mostly found in dot-shaped and filamentous structures. Li and Pan (2017) showed data which suggested that in *N. benthamiana* *Agrobacterium* -delivered GFP₁₁-VirE2 initially accumulated on plant cytoplasmic membranes that subsequently were internalized through clathrin-mediated endocytosis to form endomembrane compartments. To investigate translocation of 39phiLOV2.1-VirE2 into tobacco cells four weeks old *N. tabacum* SR1 leaves were infiltrated with *Agrobacterium*

strains LBA2572 (containing T-DNA) or LBA2573 (lacking T-DNA) harboring pBBR6-39phiLOV2.1-VirE2. Both after 21 and 48 hours filamentous and dot-like structures of VirE2 were found in the cytoplasm and near the plasma membrane of leaf epidermal cells (Figure 5 A-B and D-E, respectively). No fluorescent signals could be detected after *N. tabacum* leaf agroinfiltration with the *Agrobacterium virB4* mutant (T4SS deficient) harboring pBBR6-39phiLOV2.1-VirE2 (Figure 5C), not even after 48 hours co-cultivation (Figure 5F).

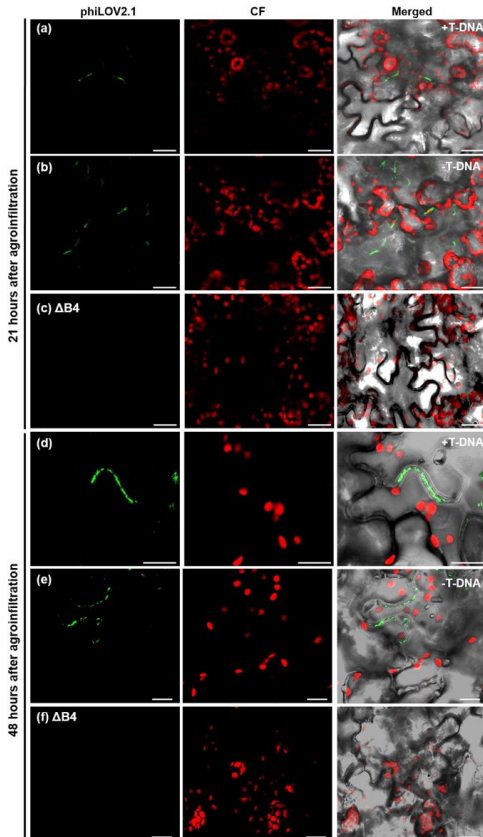


Figure 5. Visualization of 39phiLOV2.1-VirE2 translocation from *Agrobacterium* to *N. tabacum* leaves. Leaves of *N. tabacum* SR1 wild type plants were agroinfiltrated with LBA2572(pBBR6-39phiLOV2.1-VirE2) (containing T-DNA)(A and D) or with LBA2573(pBBR6-39phiLOV2.1-VirE2) (lacking T-DNA)(B and E) and images were captured after 21 hrs (A and B) or after 48 hrs (D and E). Both cytoplasmic localizations (A and B) and membrane localizations (D and E) of translocated 39phiLOV2.1-VirE2 were observed. *Agrobacterium* strain LBA1143(Δ virB4) harboring pBBR6-39phiLOV2.1-VirE2 was infiltrated into *N. tabacum* SR1 leaves and images were captured after 21 hours (C) or 48 hours (F) (negative controls). CF, chlorophyll fluorescence. Scale bars: 30 μ m.

After infiltration of *N. tabacum* SR1 with *Agrobacterium* strains LBA2564(pBBR6-phiLOV2.1-VirE3), LBA2569(pBBR6-phiLOV2.1-VirD2), LBA2560(pBBR6-phiLOV2.1-VirF) or LBA3551(pBBR6-phiLOV2.1-VirD5), sometimes fluorescent signals near the plasma membrane (possibly the endomembrane) were observed for phiLOV2.1-tagged VirE3, VirD2, VirF and VirD5 (Figure 6). Agroinfiltration of *N. tabacum* SR1 leaves with the *Agrobacterium virB4* mutant containing either pBBR6-phiLOV2.1-VirE3 (Figure 6B), pBBR6-phiLOV2.1-VirD2 (Figure 6D), pBBR6-phiLOV2.1-VirF (Figure 6F) or pBBR6-

phiLOV2.1-VirD2 (Figure 6H) did not yield any phiLOV2.1 fluorescent signals inside the plant cells. These results show that the observed signals are representing proteins that are translocated through the T4SS inside plant cells rather than proteins that are present in bacterial cells.

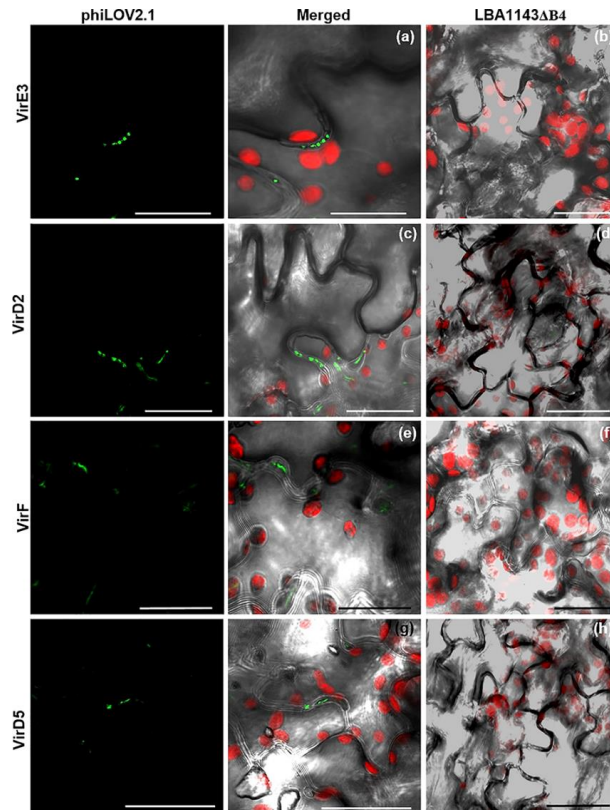


Figure 6. Translocated phiLOV2.1-tagged VirE3, -VirD2, -VirF and -VirD5 localized near the plasma membrane in *N. tabacum* SR1 leaves. *N. tabacum* SR1 wild type plants were agroinfiltrated with LBA2564(pBBR6-phiLOV2.1-VirE3) (A), with LBA2569(pBBR6-phiLOV2.1-VirD2) (C), with LBA2560(pBBR6-phiLOV2.1-F) (E) or with LBA3551(pBBR6-phiLOV2.1-VirD5) (G), with LBA1143(Δ virB4)(pBBR6-VirE3) (B), LBA1143(pBBR6-VirD2) (D), LBA1143(pBBR6-VirF) (F) or LBA1143(pBBR6-VirD5) (H). Images were captured by confocal microscopy after 42 hours. Red signals, chlorophyll fluorescence. Scale bars: 25 μ m. Representative images are shown; similar localizations were found in the majority of cells containing fluorescent structures.

VirE2 interactions with microtubules in yeast and *A. thaliana* protoplasts

Salman *et al.* (2005) showed that VirE2 can bind *in vitro* to microtubules. In addition, we obtained evidence that filaments formed by VirE2 in yeast cells are associated with the microtubules (Sakalis *et al.*, 2014). As shown in Figure 1B ectopic expression of 39-phiLOV2.1-VirE2 in yeast resulted in the formation of fluorescent filamentous structures. Expression of 39-phiLOV2.1-VirE2 or CFP-Tub1 in yeast resulted in fluorescent filamentous structures (Figures 7 A and B). Co-expression of the two fluorescent proteins in the same yeast cell showed colocalization of the VirE2 filaments with the tubulin structures (Figure 7C). To investigate the effect of tubulin disruption on these filamentous structures we treated cells expressing 39phiLOV2.1-VirE2 and CFP-Tub1 for various times with benomyl, a component known to disrupt microtubules (Thomas *et al.*, 1985). As shown in Figure 7 (D-I) this treatment resulted in a decreased length of the filaments over time and finally in a total disruption of the VirE2 filaments along with the tubulins. Determination of the length of the filaments observed in control cells treated for 90 min with DMSO showed an average length of $2.8 \pm 0.4 \mu\text{m}$ (mean \pm SD; n=25). After treatment with benomyl for 45 or 90 min the average length decreased significantly ($P < 0.01$) to $1.8 \pm 0.3 \mu\text{m}$ (n=28) or $1.4 \pm 0.3 \mu\text{m}$ (n=20), respectively. To investigate the effect of tubulin disruption on VirE2 filaments in a plant background, we expressed 39phiLOV2.1-VirE2 in *A. thaliana* protoplasts and disrupted the microtubulins by oryzalin treatment (Baskin *et al.*, 1994). As shown in figure 7 (J-K), 39phiLOV2.1-VirE2 formed dot-shaped structures in protoplasts and these structures are spread all over the cells. Upon treatment with oryzalin these structures are located more closely to the cell membrane (Figure 7, L-M).

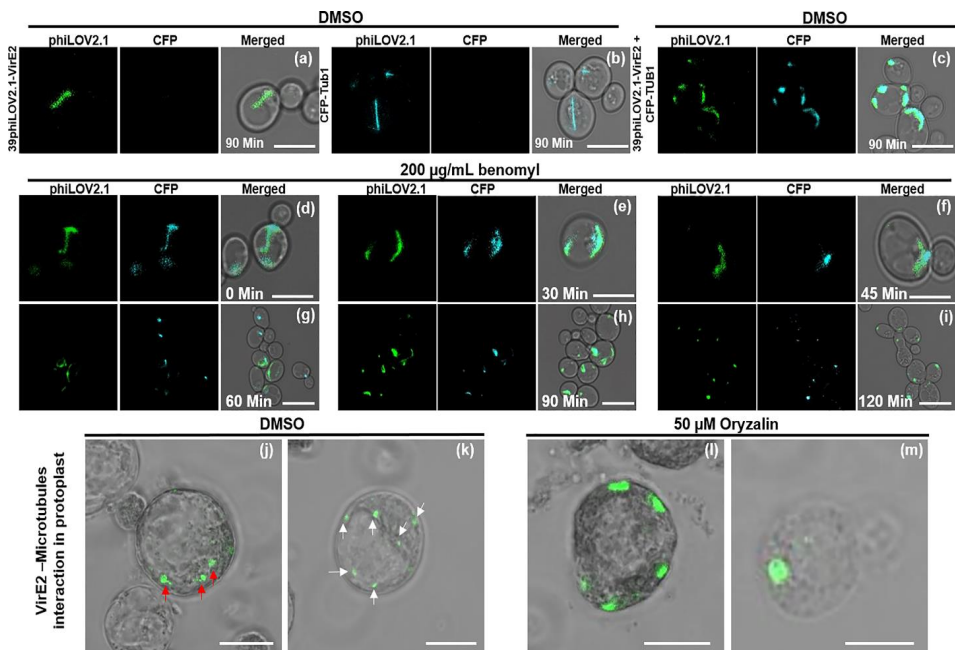


Figure 7. Effect of the microtubule-disturbing drugs benomyl and oryzalin on the 39phiLOV2.1-VirE2 filamentous structures in yeast and *A. thaliana* protoplasts. Cells of yeast strain BY4741 harboring pUG34-39phiLOV2.1-VirE2 (A), of yeast strain BY4741—CFP-TUB1 (B) or of yeast strain BY4741—CFP-TUB1 harboring pUG34-39phiLOv2.1-VirE2 (C-I) were exposed to benomyl or DMSO for the indicated times and the fluorescent structures were analyzed by confocal microscopy (A-I). Scale bars: 5 µm. *A. thaliana* protoplasts harboring pART7[39phiLOV2.1-VirE2] were exposed to oryzalin (L-M) or DMSO (J-K) for 60 min and the localization of 39phiLOv2.1-VirE2 was analyzed by confocal microscopy. Scale bars: 25µm.

DISCUSSION

Effector protein translocation is essential for the trans-kingdom transfer of T-DNA from *Agrobacterium* into eukaryotic host cells. Despite its importance many aspects of the translocation process and the fate of the translocated proteins in the host cell have not yet been clarified. Visualization *in vivo* may provide more detailed information on the translocation process. GFP-tagging of effector proteins was not successful, because of the inability of GFP-tagged proteins to translocate through the T4SS, probably due to the rigidity of the GFP protein. On the other hand, we applied successfully Bimolecular Fluorescence Complementation (BiFC) to visualize translocation of VirE2 into yeast cells (Sakalis *et al.*, 2014). To this end, yeast cells expressing VirE2 tagged with one half of the YFP analog Venus were co-cultivated with *Agrobacterium* expressing VirE2 tagged with the remaining half of Venus. As VirE2 binds to itself, protein translocation brings the two parts of Venus close together, resulting in a fluorescent protein. Alternatively, the split GFP system (Van Engelenburg and Palmer, 2010) was used for the same purpose. Yeast and plants expressing the first ten helices of GFP (GFP₁₋₁₀) were infected with *Agrobacterium* strains expressing VirE2 tagged with the remaining helix of GFP (GFP₁₁). After translocation of the GFP₁₁-tagged effector protein into the host cell, GFP was reconstituted and the translocated protein could be visualized. With this approach translocation of VirE2 was visualized (Sakalis *et al.*, 2014; Li *et al.*, 2014). Although versatile, the split GFP technique has some shortcomings. It may require several hours before GFP₁₋₁₀ is matured and reconstituted with GFP₁₁ (Van Engelenburg and Palmer, 2010). Furthermore, a genetically modified host expressing GFP₁₋₁₀, is needed. Another disadvantage is that the translocated proteins will only be visible in those cellular compartments where also GFP₁₋₁₀ is available (Park *et al.*, 2017). Therefore, in this study we explored whether the LOV-derived fluorophore phiLOV2.1 can be employed to study protein translocation from *Agrobacterium* to yeast and plant cells. The key advantages of using phiLOV2.1 as a reporter are its stability over a wide range of pH values, its molecular oxygen independency and its small size (12.1 kDa). On the other hand, photo bleaching and weaker signals are disadvantages (Buckley *et al.*, 2015). Recently, protein translocation into mammalian cells through the type 3 secretion system of *Shigella flexneri* was successfully visualized using phiLOV2.1 (Gawthorne *et al.*, 2016).

Translocation of VirE2 has been studied before by using the BiFC and split GFP approaches (Sakalis, 2013; Sakalis *et al.*, 2014; Li *et al.*, 2014). Translocated VirE2 was found in dot-

shaped and filamentous structures in both yeast cells as well as in *N. tabacum* and *N. benthamiana* leaves. In this study, translocated 39phiLOV2.1-VirE2 was found in similar dot-shaped and filamentous structures inside *N. tabacum* leaf cells (Figures 5 and 6). In yeast and *A. thaliana* root cells translocated 39phiLOV2.1-VirE2 was mainly present in dot-shaped structures (Figures 3 and 4, respectively). In 5 out of 37 of *A. thaliana* root cells which showed phiLOV2.1-VirE2 signals, we found translocated 39phiLOV2.1-VirE2 colocalizing with the nuclear marker (Figure 4A, insert). However, further studies are needed to show whether this small fraction of translocated VirE2 entered the nucleus or was perinuclear. Li *et al.*, (2014) observed trafficking of GFP₁₁-tagged VirE2 inside plant cells but not in yeast. We were able to observe similar movement of 39GFP₁₁-VirE2 translocated to *N. tabacum* cells (Movie S1). Our attempts to record movement of translocated 39phiLOV2.1-VirE2 in plant cells were unsuccessful mainly because of the fast bleaching of the phiLOV2.1 fluorescence. Previously, we showed that ectopically expressed GFP/YFP/CFP-tagged VirE2 formed filamentous structures associated with the microtubules in both yeast and *A. thaliana* protoplasts (Sakalis *et al.*, 2014). Similar filamentous structures were found in the present study for ectopically expressed 39phiLOV2.1-VirE2 (Figures 1 and 7). These structures were strongly affected by treatments disrupting microtubules (Figure 7). Inside *Agrobacterium* 39-phiLOV2.1-VirE2 was localized at the bacterial membrane visible as horseshoe-like structures in approx. 80% of the cells in which fluorescent signals were observed (Figure 2B). This localization is in line with the detection of VirE2 in the membrane fraction of *Agrobacterium* (Christie *et al.*, 1988; Dumas *et al.*, 2001) and with the observation that VirE2 acts as a channel to transfer ss-DNA *in vitro* (Duckely and Hohn, 2003).

VirD2 contains nuclear localization signals that guide the T-complex to the nucleus of the host cell (Ziemienowicz *et al.*, 2001). Ectopically expressed GFP-VirD2 has a nuclear localization in both yeast and plant cells (Citovsky *et al.*, 1994; Wolterink-van Loo *et al.*, 2015). In this study we found a similar localization for both GFP₁₁- and phiLOV2.1-tagged VirD2 ectopically expressed in yeast (Figures 1 and S1). VirD2 translocation from *Agrobacterium* to yeast could be shown for both GFP₁₁- and phiLOV2.1-tagged VirD2. The translocated VirD2 is most likely located in the nucleus, but because of the low amount of translocated VirD2 we were unable to determine the exact subcellular localization. Using the BiFC approach translocated VirD2 was shown to interact with yeast nuclear histone proteins (Wolterink-van Loo *et al.*, 2015). phiLOV2.1-VirD2 translocated to *A. thaliana* root cells

was found in the nucleus (Figure 4), whereas in *N. tabacum* leaves it was found in dot-shaped structures close to or at the cell membrane (Figures 6).

Localization of the other effector proteins after translocation from *Agrobacterium* has not been studied before. VirE3-RFP expressed in *A. thaliana* protoplasts has a nuclear localization (Niu et al., 2015). As shown in Figure 3 in yeast translocated phiLOV2.1-VirE3 localizes in dot-shaped structures, inside the nucleus. In *A. thaliana* roots translocated phiLOV2.1-VirE3 also localizes in dot-shaped structures, some of them close to the cell membrane (Figure 6). Recently, Zhang *et al* showed ectopically expressed GFP-VirD5 was clustered in bright dots in the nucleus in yeast (Zhang *et al* , 2017). Translocated phiLOV2.1-VirD5 was found both inside and outside the nucleus in *A. thaliana* root cells (Figure 4). Reconstituted GFP signals were not detected in yeast cells expressing GFP₁₁-tagged VirE3 and VirF, possibly due to inaccessibility of the GFP₁₁-tag for GFP₁₋₁₀. Translocation of phiLOV2.1-VirE3 and of phiLOV2.1-VirF from *Agrobacterium* to both yeast and plant cells could be shown (Figures 3, 4 and 6). This indicates that when the split GFP approach does not provide signals the phiLOV2.1 tag may sometimes come to the rescue.

Li and Pan, (2017) provided evidence that *Agrobacterium* VirE2 delivery into host cells was facilitated by the clathrin endocytosis pathway mediated by interaction of dileucine motifs of VirE2 with the AP2M clathrin adaptor. Initially, translocated VirE2 was at the plasma membrane and subsequently entered the cell by trapping inside endocytosis vesicles. We observed a similar localization near the plasma membrane not only for VirE2 (Figure 5 C and D) but also for VirD2, VirF, VirD5 and VirE3 (Figure 6). Analysis of the amino acid sequences of these effector proteins for putative endocytic motifs by the Eukaryotic Linear Motif resource for functional sites in proteins (www.elm.eu.org) revealed the presence of tyrosine-based, dileucine and DPF/W motifs in VirD2, VirF, VirE2, VirD5 and VirE3 which may interact with the AP adaptor (supplemental Figure S7). Therefore, these proteins may enter the host cell by the endocytosis pathway as well. However, further studies are required to establish whether the clathrin-mediated endocytosis pathway is indeed involved in the uptake of the effector proteins.

In summary, we can conclude from this study that phiLOV2.1 can successfully be used to study protein translocation from *Agrobacterium* to yeast and plant cells. A great advantage over the split GFP approach is that it can be used with non-transgenic host cells because

expression of GFP₁₋₁₀ in the host is not needed. On the other hand fluorescence signals were weaker than seen with split GFP. Despite we used the improved phiLOV2.1 form of LOV, photobleaching is still considerable. Translocated effector proteins were often found in dot-shaped and filamentous structures. It remains to be established whether the effector proteins are functional while in such structures. It is expected that host cells respond to the presence of unwanted proteins by degradation or transport to sites where these are shielded from the rest of the cell. So, it is possible that the majority of the translocated proteins are not involved in the transformation process and only a minor fraction can escape the degradation process and can fulfill their role in the transformation process.

ACKNOWLEDGEMENTS

We would like to thank Lan-Ying Lee and Stanton Gelvin (Purdue University) for providing the *A. thaliana* Col-0 mRFP-NLS seeds (At2051), John M. Christie (University of Glasgow, UK) for the plasmid containing the phiLOV2.1 coding sequence, and Gerda Lamers (our institute) for her help with microscopy. We acknowledge Philippe Sakalis for construction of plasmids encoding GFP₁₁-tagged effector proteins and images used in Figure 3 (O and Q) and Jennifer Leentjes for construction of pUG36 plasmids expressing phiLOV2.1-tagged VirD2, VirD5, VirF and VirD5 effector proteins. This study was partly supported by a grant from the Royal Academy of Sciences of The Netherlands to PJJH associated with his appointed as academy professor.

REFERENCES

- Abràmoff, M. D., Magalhães, P. J. and Ram, S. J.** (2004). Image processing with imageJ. *Biophotonics Int.* 11, 36–41.
- Albright, L.M., Yanofsky, M.F., Leroux, B., Ma, D.Q. and Nester, E.W.** (1987). Processing of the T-DNA of *Agrobacterium tumefaciens* generates border nicks and linear, single-stranded T-DNA. *J. Bacteriol.* 169, 1046–1055.
- Baskin T, I., Wilson J.E., Cork, A. and Williamson R.E.** (1994). Morphology and microtubule organization in *Arabidopsis* roots exposed to oryzalin or taxol. *Plant cell physiology*, 35, 935–942.
- Buckley, A.M., Petersen, J., Roe, A.J., Douce, G.R. and Christie, J.M.** (2015) LOV-based reporters for fluorescence imaging. *Curr. Opin. Chem. Biol.* 27, 39–45.
- Bundock, P., den Dulk-Ras, A, Beijersbergen, A. and Hooykaas, P. J. J.** (1995) Trans-kingdom T-DNA transfer from *Agrobacterium tumefaciens* to *Saccharomyces cerevisiae*. *EMBO J.*, 14(13), 3206–14.
- Christie, P.J., Ward, J.E., Winans, S.C. and Nester, E.W.** (1988). The *Agrobacterium tumefaciens virE2* gene product is a single-stranded-DNA-binding protein that associates with T-DNA. *J. Bacteriol.* 170, 2659–2667.
- Christie, P.J., Atmakuri, K., Krishnamoorthy, V., Jakubowski, S. and Cascales, E.** (2005). Biogenesis, Architecture, and Function of Bacterial Type IV Secretion Systems. *Annu. Rev. Microbiol.* 59, 451–485.
- Christie, J.M., Gawthorne, J.A., Young, G., Fraser, N.J. and Roe, A.J.** (2012a). LOV to BLUF: Flavoprotein contributions to the optogenetic toolkit. *Mol. Plant*, 5, 533–544.
- Christie, J.M., Hitomi, K., Arvai, A.S., Hartfield, K.A., Mettlen, M., Pratt, A.J., Tainer, J.A. and Getzoff, E.D.** (2012b). Structural tuning of the fluorescent protein iLOV for improved photostability. *J. Biol. Chem.* 287, 22295–22304.
- Citovsky, V., Wong, M.L. and Zambryski, P.** (1989). Cooperative interaction of *Agrobacterium* VirE2 protein with single-stranded DNA: Implications for the T-DNA transfer process. *Proc. Natl. Acad. Sci. USA.* 86, 1193–1197.
- Citovsky, V., Zupan, J., Warnick, D. and Zambryski, P.** (1992). Nuclear localization of *Agrobacterium* VirE2 protein in plant cells. *Science*, 256, 1802–1805.
- Citovsky, V., Warnick, D. and Zambryski, P.** (1994). Nuclear import of *Agrobacterium* VirD2 and VirE2 proteins in maize and tobacco. *Proc. Natl. Acad. Sci. USA*, 91, 3210–3214.
- De Cleene, M. and De Ley, J.** (1976). The host range of crown gall. *Bot. Rev.* 42, 389–466.

- den Dulk-Ras, A. and Hooykaas, P.J.J.** (1995). Electroporation of *Agrobacterium tumefaciens*. *Methods Mol. Biol.* 55, 63–72.
- Djamei, A., Pitzschke A., Nakagami, H., Rajh, I. and Hirt, H.** (2007). Trojan horse strategy in *Agrobacterium* transformation: abusing MAPK defense signaling. *Science*, 318, 453–456.
- Duckely., M. and Hohn., B.** (2003) The VirE2 protein of *Agrobacterium tumefaciens*: the Yin and Yang of T-DNA transfer. *FEMS Microbiol Lett*, 223, 1–6.
- Dumas, F., Duckely, M., Pelczar, P., Van Gelder, P. and Hohn, B.** (2001). An *Agrobacterium* VirE2 channel for transferred-DNA transport into plant cells. *Proc. Natl. Acad. Sci. USA*, 98, 485–490.
- García-Rodríguez, F.M., Schrammeijer, B. and Hooykaas, P.J.J.** (2006). The *Agrobacterium* VirE3 effector protein: a potential plant transcriptional activator. *Nucleic Acids Res.* 34, 6496–6504.
- García-Cano, E., Hak, H., Magori, S., Lazarowitz, S. and Citovsky, V.** (2018). The *Agrobacterium* F-box protein effector VirF destabilizes the Arabidopsis GLABROUS1 enhancer/binding protein-like transcription factor VFP4, a transcriptional activator of defense response genes. *Mol Plant Microbe Interact*, 31, 576-586.
- Gawthorne, J.A., Audry, L., McQuitty, C., Dean, P., Christie, J.M., Enninga, J. and Roe, A.J.** (2016). Visualizing the translocation and localization of bacterial type III effector proteins by using a genetically encoded reporter system. *Appl. Environ. Microbiol.* 82, 2700–2708.
- Gietl, C., Koukolfkova-Nicola, Z. and Hohn, B.** (1987). Mobilization of T-DNA from *Agrobacterium* to plant cells involves a protein that binds single-stranded DNA. *Cell Biol.* 84, 9006–9010.
- Gietz, R. D., Schiestl, R. H., Willems, A. R. and Woods, R. A.** (1995). Studies on the transformation of intact yeast-cells by the LiAc/ssDNA/PEG procedure . *Yeast*, 11, 355–360.
- Herrera-Estrella, A., Van Montagu, M. and Wang, K.**(1990).A bacterial peptide acting as a plant nuclear targeting signal: the amino-terminal portion of *Agrobacterium* VirD2 protein directs a β -galactosidase fusion protein in to tobacco nuclei. *Proc. Natl. Acad. Sci. USA*, 87, 9534–9537.
- Hooykaas, P. J. J., Hofker, M., den Dulk-Ras, A. and Schilperoort, R. A.**(1984). A comparison of virulence determinants in an octopine Ti plasmid, a nopaline Ti plasmid, and an Ri plasmid by complementation analysis of *Agrobacterium tumefaciens* mutants. *Plasmid*, 11, 195–205.

Howard, E.A., Zupan, J.R., Citovsky, V. and Zambryski, P.C. (1992). The VirD2 protein of *A. tumefaciens* contains a C-terminal bipartite nuclear localization signal: Implications for nuclear uptake of DNA in plant cells. *Cell*, 68, 109–118.

Huala, E., Oeller, P.W., Liscum, E., Han, I.S., Larsen, E. and Briggs, W.R. (1997). *Arabidopsis* NPH1: a protein kinase with a putative redox-sensing domain. *Science*, 278, 2120–2123.

Lee, Y.W., Jin, S., Sim, W.S. and Nester, E.W. (1996). The sensing of plant signal molecules by *Agrobacterium* : Genetic evidence for direct recognition of phenolic inducers by the VirA protein. *Gene*, 179, 83–88.

Li, X., Yang, Q., Tu, H., Lim, Z. and Pan, S. Q. (2014). Direct visualization of *Agrobacterium* -delivered VirE2 in recipient cells. *Plant J.* 77(3), 487–495.

Li, X. and Pan, S.Q. (2017). *Agrobacterium* delivers VirE2 protein into host cells via clathrin-mediated endocytosis. *Sci. Adv.* 3.

Magori, S. and Citovsky, V. (2011). Hijacking of the host SCF ubiquitin ligase machinery by plant pathogens. *Front. Plant. Sci.* 2, 87.

Melchers, L.S., Maroney, M.J., den Dulk-Ras, A., Thompson, D.V., Vuuren, H.A.J., Schilperoort, R.A. and Hooykaas, P.J.J. (1990). Octopine and nopaline strains of *Agrobacterium tumefaciens* differ in virulence; molecular characterization of the virF locus. *Plant Mol Biol.* 14, 249–259.

Mysore, K.S., Bassuner, B., Deng, X. B., Darbinian, N.S., Motchoulski, A., Ream, W. and Gelvin, S. B. (1998). Role of the *Agrobacterium tumefaciens* VirD2 protein in T-DNA transfer and integration. *Mol. Plant. Microbe. Interact.* 11, 668–683.

Nester, E.W., Watson, B., Currier, T.C., Gordon, M.P. and Chilton, M. (1975). Plasmid required for virulence of *Agrobacterium* Plasmid Required for Virulence of *Agrobacterium tumefaciens*. *J. Bacteriol.* 123, 255.

Nester, E.W., Gordon, M.P., Amasino, R.M. and Yanofsky, M.F. (1984). Crown gall: A molecular and physiological analysis. *Annu Rev Plant Physiol.* 35, 387–413.

Niu, X., Zhou, M., Henkel, C. V., van Heusden, G.P.H. and Hooykaas, P.J.J. (2015). The *Agrobacterium tumefaciens* virulence protein VirE3 is a transcriptional activator of the F-box gene VBF. *Plant J.* 84, 914–924.

Pansegrau, W., Schoumacher, F., Hohn, B. and Lanka, E. (1993). Site-specific cleavage and joining of single-stranded DNA by VirD2 protein of *Agrobacterium tumefaciens* Ti plasmids: analogy to bacterial conjugation. *Proc. Natl. Acad. Sci. USA*, 90, 11538–42.

- Park, E., Lee, H.-Y., Woo, J., Choi, D. and Dinesh-Kumar, S.P.** (2017). Spatiotemporal monitoring of *Pseudomonas syringae* effectors via type III secretion using split fluorescent protein fragments. *Plant Cell*, 29, 1571–1584.
- Rossi, L., Hohn, B. and Tinland, B.** (1993). The VirD2 protein of *Agrobacterium tumefaciens* carries nuclear localization signals important for transfer of T-DNA to plant. *Mol. Gen. Genet.*, 239, 345–353.
- Rossi, L., Hohn, B. and Tinland, B.** (1996). Integration of complete transferred DNA units is dependent on the activity of virulence E2 protein of *Agrobacterium tumefaciens*. *Proc. Natl. Acad. Sci. USA*, 93, 126–30.
- Sakalis, P.A.** (2013). Visualizing virulence proteins and their translocation into the host during *Agrobacterium* -mediated transformation. PhD.-thesis. Leiden University.
- Sakalis, P.A., van Heusden, G.P.H. and Hooykaas, P.J.J.** (2014). Visualization of VirE2 protein translocation by the *Agrobacterium* type IV secretion system into host cells. *MicrobiologyOpen*, 3, 104–117.
- Salman, H., Abu-Arish, A., Oliel, S., Loyter, A., Klafner, J., Granel, R. and Elbaum, M.** (2005). Nuclear localization signal peptides induce molecular delivery along microtubules. *Biophys J.* 89,2134-2145.
- Shi, Y., Lee, L.-Y. and Gelvin, S. B.** (2014). Is VIP1 important for *Agrobacterium* -mediated transformation? *Plant J.* 79, 848–860.
- Schirawski, J., Planchais, S. and Haenni, A.L.** (2000) An improved protocol for the preparation of protoplasts from an established *Arabidopsis thaliana* cell suspension culture and infection with RNA of turnip yellow mosaic tymovirus: a simple and reliable method. *J. Virol. Methods.* 86, 85–94.
- Schrammeijer, B., Risseuw, E., Pansegrau, W., Regensburg-Tuink, A.J.G., Crosby, W.L. and Hooykaas, P.J.J.** (2001). Interaction of the virulence protein VirF of *Agrobacterium tumefaciens* with plant homologs of the yeast Skp1 protein. *Curr. Biol.* 11, 258–262.
- Shurvinton, C.E., Hodges, L. and Ream, W.**(1992). A nuclear localization signal and the C- terminal omega sequence in the *Agrobacterium tumefaciens* VirD2 endonuclease are important for tumor formation. *Proc. Natl. Acad. Sci. USA*, 89, 11837–11841.
- Stachel, S.E. and Nester, E.W.** (1986). The genetic and transcriptional organization of the vir region of the A6 Ti plasmid of *Agrobacterium tumefaciens*. *EMBO J.* 5, 1445–1454.
- Thomas, J.H., Neff, N.F. and Botstein, D.** (1985). Isolation and characterization of mutants in the β -tubulin gene of *Saccharomyces cerevisiae*. *Genetics*, 112, 715–734.

Tinland, B., Koukolikova-Nicola, Z., Hall, M.N. and Hohn, B. (1992). The T-DNA-linked VirD2 protein contains two distinct functional nuclear localization signals. *Proc. Natl. Acad. Sci. USA*, 89, 7442–7446.

Tinland, B., Hohn, B. and Puchta, H. (1994). *Agrobacterium tumefaciens* transfers single-stranded transferred DNA (T-DNA) into the plant cell nucleus. *Proc. Natl. Acad. Sci. USA*, 91, 8000–4.

Tzfira, T., Vaidya, M. and Citovsky, V. (2001). VIP1, an *Arabidopsis* protein that interacts with *Agrobacterium* VirE2, is involved in VirE2 nuclear import and *Agrobacterium* infectivity. *EMBO J.* 20, 3596–3607.

Tzfira, T., Vaidya, M. and Citovsky, V. (2004). Involvement of targeted proteolysis in plant genetic transformation by *Agrobacterium*. *Nature*, 431, 87–92.

van Engelenburg, S. B. and Palmer, A. E. (2010). Imaging type-III secretion reveals dynamics and spatial segregation of *Salmonella* effectors. *Nat. Methods*, 7, 325–330.

van Kregten, M., Lindhout, B.I., Hooykaas P.J.J. and van der Zaal, B.J. (2009) *Agrobacterium* -mediated T-DNA transfer and integration by minimal VirD2 consisting of the relaxase domain and a type IV secretion system translocation signal. *Mol Plant-Microbe Inter*, 22, 1356–1365.

van Larebeke, N., Engler, G., Holsters, M., van den Elsacker, S., Zaenen, I., Schilperoort, R.A. and Schell, J. (1974). Large plasmid in *Agrobacterium tumefaciens* essential for crown gall-inducing ability. *Nature*, 252, 169–170.

Vergunst, A.C., de Waal, E.C. and Hooykaas, P.J. (1998). Root transformation by *Agrobacterium tumefaciens*. In J. M. Martinez-Zapater and J. Salinas, eds. *Methods in Molecular Biology*, 227–44.

Vergunst, B., den Dulk-Ras, A., Vlaam, C.M.T., Regensburg-Tuink, T.J.G. and Hooykaas, P.J.J., (2000). VirB/D4 dependent protein translocation from *Agrobacterium* into plant cells. *Science*, 290, 979–981.

Vergunst, A.C., Lier, M.C.M., den Dulk-Ras, A., Grosse Stüve, T.A., Ouwehand, A. and Hooykaas, P.J.J. (2005). Positive charge is an important feature of the C-terminal transport signal of the VirB/D4-translocated proteins of *Agrobacterium*. *Proc. Natl. Acad. Sci. USA*, 102, 832–837.

Vogel, A.M. and Das, A. (1992). Mutational analysis of *Agrobacterium tumefaciens* virD2:tyrosine29 is essential for endonuclease activity. *J. Bacteriol.* 174, 303–308.

Wang, Y., Peng, W., Zhou, X., Huang, F., Shao, L. and Luo, M. (2014). The putative *Agrobacterium* transcriptional activator-like virulence protein VirD5 may target T-complex to prevent the degradation of coat proteins in the plant cell nucleus. *New Phytol.* 203, 1266–1281.

- Wang, Y., Zhang, S., Huang, F., Zhou, X., Chen, Z., Peng, W. and Luo, M.** (2018). VirD5 is required for efficient *Agrobacterium* infection and interacts with Arabidopsis VIP2. *New Phytol.* 217, 726–738.
- Wolterink-van Loo, S., Escamilla Ayala, A. A., Hooykaas, P. J.J. and van Heusden, G. P. H.** (2015). Interaction of the *Agrobacterium tumefaciens* virulence protein VirD2 with histones. *Microbiology*, 161:401–410.
- Yang, Q., Li, X., Tu, H. and Pan, S.Q.** (2017). *Agrobacterium* -delivered virulence protein VirE2 is trafficked inside host cells via a myosin XI-K-powered ER/actin network. *Proc. Natl. Acad. Sci. USA*, 114, 2982–2987.
- Zaltsman, A., Krichevsky, A., Loyter, A. and Citovsky, V.** (2010). *Agrobacterium* Induces Expression of a Host F-Box Protein Required for Tumorigenicity. *Cell Host Microbe*, 7, 197–209.
- Zhang, X., van Heusden, G.P.H. and Hooykaas, P.J.J.**(2017). Virulence protein VirD5 of *Agrobacterium tumefaciens* binds to kinetochores in host cells via an interaction with Spt4. *Proc. Natl. Acad. Sci. USA*, 38, 10238–10243.
- Zhou, X. R. and P. J. Christie.** (1999). Mutagenesis of the *Agrobacterium* VirE2 single-stranded DNA-binding protein identifies regions required for self-association and interaction with VirE1 and a permissive site for hybrid protein construction. *J. Bacteriol.* 181, 4342–4352.
- Zhu, J., Oger, P.M., Schrammeijer, B., Hooykaas, P.J.J., Farrand, S.K. and Winans, S.C.** (2000) The bases of crown gall tumorigenesis. *J Bacteriol*, 182, 3885– 3895.
- Ziemienowicz, A., Merkle, T., Schoumacher, F., Hohn, B. and Rossi, L.** (2001). Import of *Agrobacterium* T-DNA into plant nuclei: two distinct functions of VirD2 and VirE2 proteins. *Plant Cell*, 2001., 13, 369–83.
- Zonneveld, B.J.M.** (1986). Cheap and simple yeast media. *J Microbiol Methods*, 4, 287–291.

SUPPLEMENTARY FIGURES

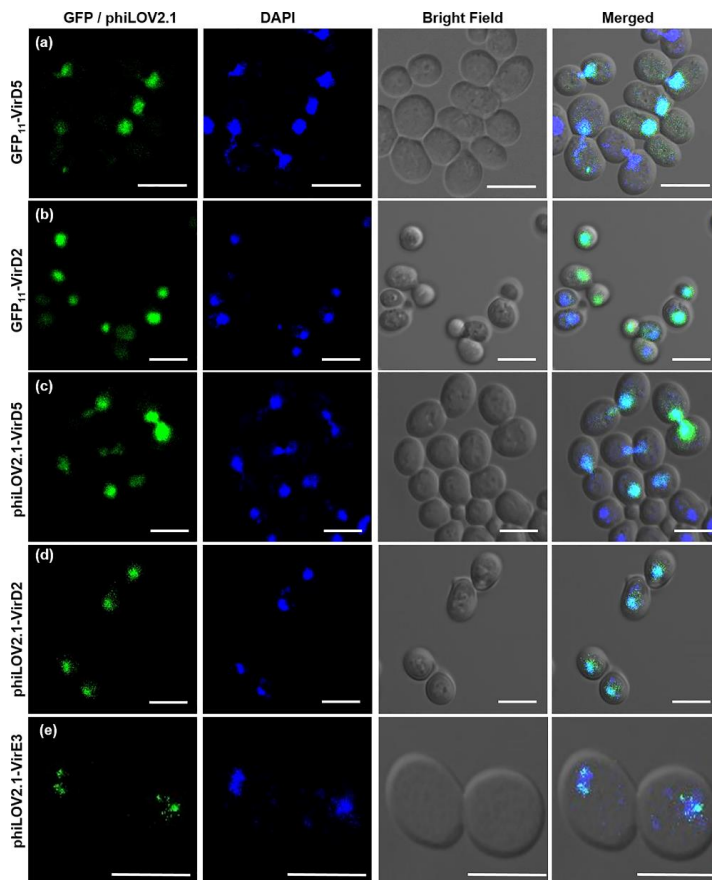


Figure S1. Nuclear localization of ectopically expressed GFP₁₁- and phiLOV2.1-tagged VirD2, VirD5 and VirE3 in yeast. Confocal microscopy of DAPI stained 426::GFP₁₋₁₀ cells transformed with pUG34GFP₁₁[VirD5] (A), or with pUG34GFP₁₁[VirD2] (B) and of BY4741 cells transformed with pUG36-phiLOV2.1-VirD5 (C), with pUG36-phiLOV2.1-VirD2 (D), or with pUG-phiLOV2.1-VirE3 (E). Scale bars: 5 μ m.

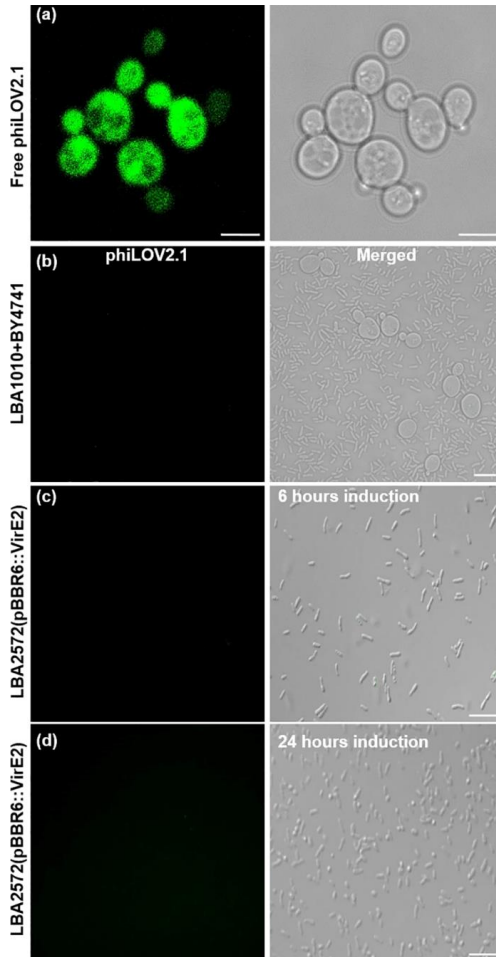


Figure S2. Control microscopy for the detection of phiLOV2.1 in yeast and *Agrobacterium*. A, Confocal microscopy of yeast strain BY4741 containing pUG36phiLOV2.1 expressing free phiLOV2.1. B, confocal microscopy of BY4741 after co-cultivation with *Agrobacterium* strain LBA1010 (lacking phiLOV2.1) for 48 hours. C and D, *Agrobacterium* strain LBA2572 containing pBBR6-VirE2 induced with acetosyringone for 6 and 24 hours, respectively. Scale bars: 5 μ m.



Figure S3. Biological activity assessments. Tumor formation on *N. glauca* plants inoculated with different *A. tumefaciens* strains. A, LBA1010 (positive control); B, LBA1100 (T-DNA deficient, negative control); C, LBA2572 (LBA1010 Δ VirE2); D, LBA2572(pBBR6-phiLOV2.1-VirE2)(N-terminally tagged); E, LBA2572(pBBR6-39phiLOV2.1-VirE2); F, LBA2572(pBBR6-39GFP₁₁-VirE2); G, LBA2569 (LBA1010 Δ VirD2); H, LBA2569(pBBR6-phiLOV2.1-VirD2); I, LBA2566(LBA1010 Δ VirE3 Δ VirF); J, LBA2566(pBBR6-phiLOV2.1-VirF); K, LBA2566(pBBR6-phiLOV2.1-VirE3).

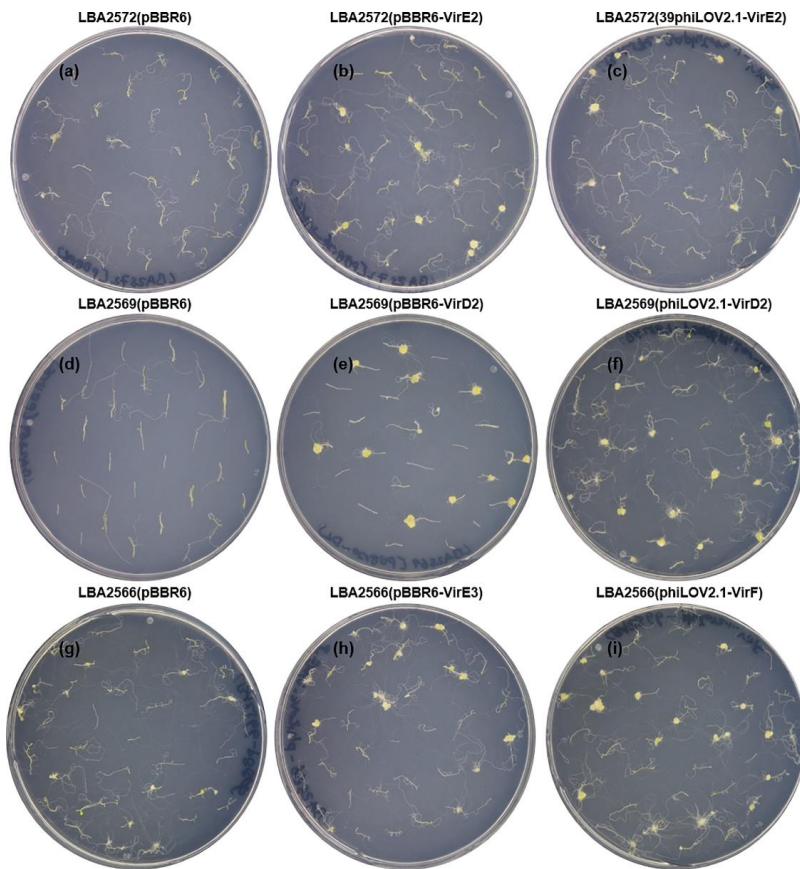


Figure S4. Arabidopsis root transformation assays. *A. thaliana* Col-0 root segments were infected with different *A. tumefaciens* strains. A, LBA2572 (LBA1010 Δ VirE2); B, LBA2572(pSDM3163); C, LBA2572(pBBR6-39phiLOV2.1-VirE2); D, LBA2569 (LBA1010 Δ VirD2); E, LBA2569(pBBR6-VirD2); F, LBA2569(pBBR6-phiLOV2.1-VirD2); G, LBA2566 (LBA1010 Δ VirE3 Δ VirF); H, LBA2566(pBBR6-phiLOV2.1-VirE3); I, LBA2566(pBBR6-phiLOV2.1-VirF). Photographs were taken 4 weeks after infection.

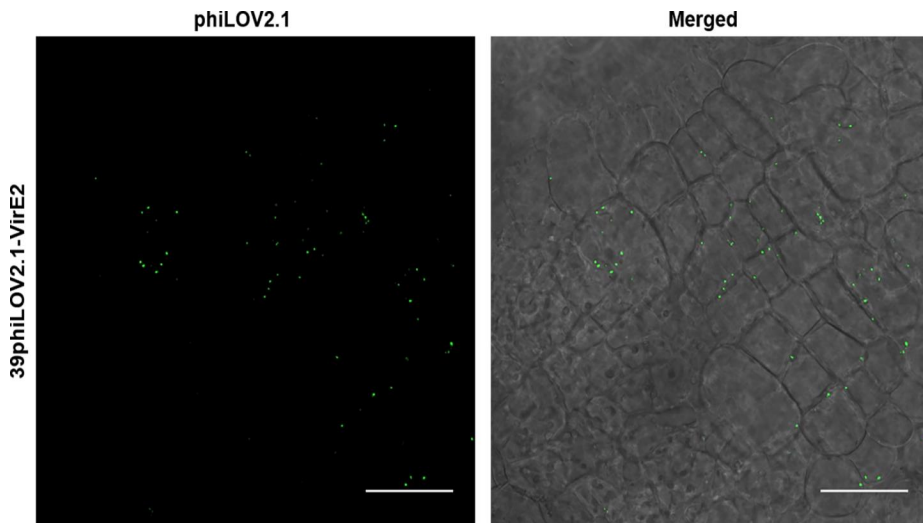


Figure S5. Confocal microscopy of *A. thaliana* root explants co-cultivated for 48 hours with *Agrobacterium* strain LBA2573(pBBR6-39phiLOV2.1-VirE2). Scale bars: 30 μ m.

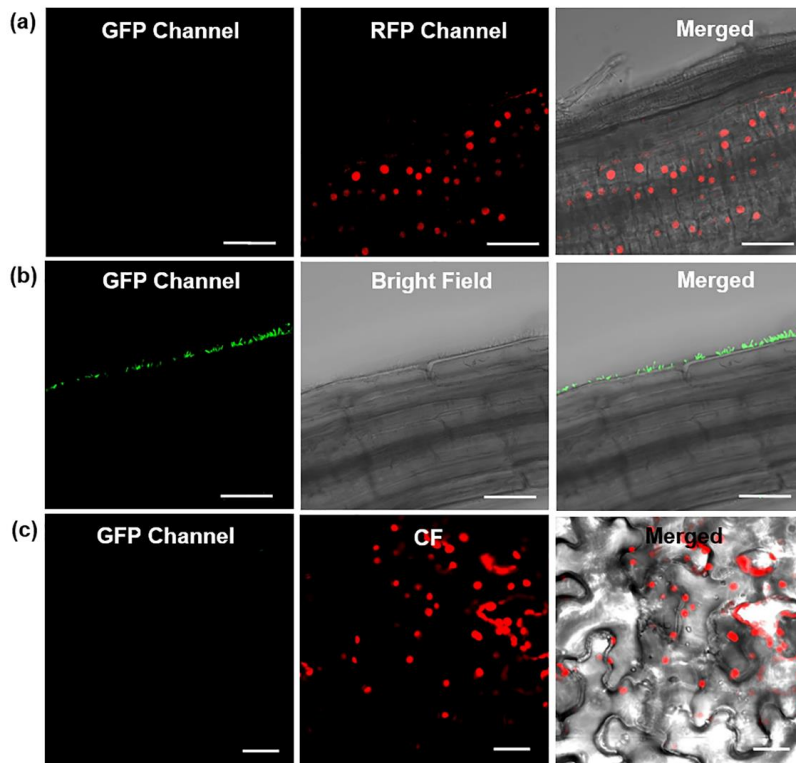


Figure S6. Control microscopy for the detection of phiLOV2.1 in plants. A, *A. thaliana* Col-0 (RFP-NLS) root explants co-cultivated for 20 hours with *Agrobacterium* strain LBA1010 (lacking phiLOV2.1). B, *A. thaliana* Col-0 root explants co-cultivated for 48 hours with LBA3567(*placZ-GFP*) (expressing GFP). C, *N. tabacum* SR1 agroinfiltrated with *Agrobacterium* strain LBA1010; images were taken after 24 hours. Scale bars: 30 μ m. CF, chlorophyll fluorescence.

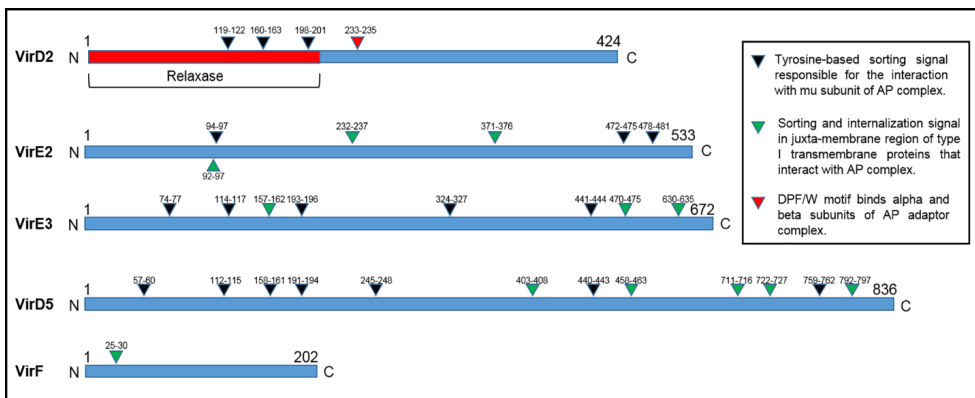


Figure S7. Schematic overview of the putative endocytic motifs. Analysis of the amino acid sequences of *Agrobacterium* VirD2, VirE2, VirE3, VirD5 and VirF effector proteins based on putative endocytic motifs identified by the Eukaryotic Linear Motif resource for functional sites in proteins (www.elm.eu.org).

Chapter 4

Application of *Agrobacterium* – mediated protein translocation to induce mating type switching in the yeast *Saccharomyces cerevisiae*

M.Reza Roushan, Paul J.J. Hooykaas and G. Paul H. van Heusden

Molecular and Developmental Genetics, Institute of Biology, Leiden University, Leiden, The Netherlands.

ABSTRACT

The yeast *Saccharomyces cerevisiae* is an eukaryotic unicellular organism that exists either in haploid or diploid form. Haploid *S. cerevisiae* can have either the a or α mating type determined by the presence of either of two alleles in the mating-type locus, *MATa* or *MAT α* . Homothallic *S. cerevisiae* strains can switch their mating type, a process initiated by a double-strand break in the *MAT* locus by the HO endonuclease. *Agrobacterium tumefaciens* is able to genetically transform plants and fungi by transferring a DNA fragment (T-DNA) into the host cells. During *Agrobacterium* - mediated transformation, in addition to T-DNA, a number of virulence proteins are translocated from the bacterium into the host cells to assist in the transformation process. *Agrobacterium* can be engineered to translocate other proteins as well into the host cells. This property makes *Agrobacterium* an ideal tool to introduce proteins useful for molecular genetic studies, epigenetics or protein therapy into eukaryotic cells. In this study, we showed that the mating type of *S. cerevisiae* cells can be switched after translocation of the HO protein from *Agrobacterium* into yeast yielding an alternative method for mating type switching of yeast cells.

INTRODUCTION

The yeast *Saccharomyces cerevisiae* is an unicellular eukaryote, existing either in haploid form with the a or α mating type or in a diploid form. The mating type of *S. cerevisiae* is determined by the presence of either the *MATa* or *MAT α* allele in the mating-type locus [for review see: (Klar, 1987)(Herskowitz, 1988)(Haber, 1992)(Haber, 2012)]. The proteins encoded by the *MAT α* locus, i.e. *MAT α 1* and *MAT α 2*, activate a set of *MAT α* -specific genes, encoding for instance the Ste2 pheromone receptor and the alpha factor pheromone (Bruhn and Sprague, 1994; Hagen *et al.*, 1993). *Mata2* represses *MATa*-specific genes (Strathern *et al.*, 1988). Likewise, *MATa* consists of two open reading frames, namely *MATa1* and *MATa2* (Tatchell *et al.*, 1981; Goutte and Johnson, 1988). *MATa1* encodes a homeobox-domain protein that, along with *MAT α 2*, represses transcription of haploid-specific genes in diploid cells. The function of *MAT α 2* is still unclear (Jensen *et al.*, 1983; Klar, 1987; Haber 2012). In addition to the active *MATa* or *MAT α* alleles the yeast chromosome contains two silent cryptic copies of mating-type sequences i.e. *HML α* and *HMRa* at a distance of ~ 91kb.

Homothallic *S. cerevisiae* cells can switch their mating type from a to α and *vice versa*. This process is initiated by activation of the *HO* (HOmothallic switching endonuclease) gene (Nasmyth *et al.*, 1987). This gene encodes an endonuclease that can create a double strand break at a specific site in the *MAT* locus during the late G1 phase of haploid cells (Strathern *et al.*, 1982). This double-strand break leads to an intra-chromosomal gene conversion. Hereby either *MATa* or *MAT α* genes present at the silent *HMR* or *HML* loci are copied into the active *MAT* locus by homologous recombination. Thus, once the double-strand break is generated, the break in the *MAT* locus is repaired using either *HMR* or *HML* as template (Figure 1).

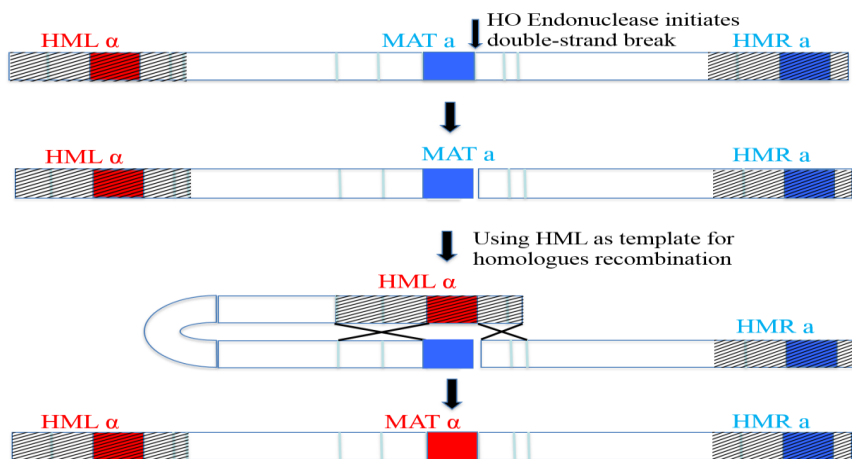


Figure 1. A schematic overview of switching from mating type a to mating type α . Upon induction of *HO*, *HMR* is used as the preferred donor of genetic information to repair the gap in the *MAT* locus by homologous recombination. Hatched blocks illustrate silenced genes.

Agrobacterium tumefaciens is a gram-negative soil-born bacterium which causes crown gall disease in a wide range of dicotyledonous plants (Smith and Townsend 1907; for recent review see Gelvin, 2012). During the infection a piece of single-stranded DNA, called T-DNA, is translocated to the nucleus of host cells where it is integrated into the genome (Hooykaas and Schilperoort, 1992; Tinland *et al.*, 1994). Expression of plant growth hormone genes present on the T-DNA leads to uncontrolled cell proliferation and as a result tumor formation. Simultaneously with T-DNA transfer, several effector proteins (VirD2, VirE2, VirE3, VirD5 and VirF) are translocated into plant cells via the Type IV secretion system (T4SS) of *A. tumefaciens* (Vergunst *et al.*, 2000). Under laboratory conditions, *A. tumefaciens* can also transform yeast (Bundock *et al.*, 1995), algae (Kumar *et al.*, 2004) and fungi (de Groot *et al.*, 1998). *A. tumefaciens* can be engineered to be able to transfer foreign proteins into eukaryotic cells. For example, Cre recombinase can be delivered from *A. tumefaciens* into recipient cells when expressed as an in frame fusion with the C-terminal T4SS targeting signal of the VirE2 or VirF protein (Vergunst *et al.* 2000).

In this study we used *A. tumefaciens* to introduce the HO endonuclease into yeast cells and showed that the translocated endonuclease was able to induce mating type switching. These results further highlight the potential use of *Agrobacterium* in biotechnology and provide an alternative protocol for artificial mating type switching.

MATERIALS AND METHODS

Yeast strains and media. Yeast strains used in this study are listed in Table 1. All yeast strains were grown in YPD medium or selective MY medium supplemented, if required, with histidine, leucine, tryptophan, methionine and/or uracil to the final concentration of 20 mg/L (Zonneveld, 1986). Yeast transformation was performed using the Lithium Acetate method (Gietz *et al.*, 1995). Yeast strains carrying plasmids were obtained by transforming parental strains with the appropriate plasmids followed by selection for uracil and/or histidine prototrophy.

Agrobacterium strains and media. *A. tumefaciens* strains used in this study are listed in Table 2. All *A. tumefaciens* strains were grown in LC medium containing, if required, the appropriate antibiotics at the following concentrations: rifampicin, 20 µg/ml; gentamicin, 40 µg/ml; kanamycin, 100 µg/ml. *A. tumefaciens* carrying plasmids were obtained by electroporation as described by den Dulk-Ras and Hooykaas (1995).

Plasmid constructions. All plasmids used and constructed in this study are listed in Table 3. Cloning steps were performed in *E. coli* strain XL1-Blue. PCR amplifications were done with Phusion™ High-Fidelity DNA Polymerase. Correct construction of plasmids was confirmed by sequencing. Table 4 lists all primers used for PCR amplifications and sequencing.

In order to enable the translocation of the HO endonuclease from *A. tumefaciens* to yeast, plasmid pBBR6[HO] (pSDM3768) was constructed. To this end, a DNA fragment containing the *virD* promoter with *Hind*III and *Eco*RV restriction sites was generated by PCR amplification using *Hind*III-VirD2-Fw and *Eco*RV-VirD2-Rev primers and pSDM3149 as template. After digestion with *Hind*III and *Eco*RV this fragment was cloned into pSDM3264 digested with the same enzymes to give pSDM3774. Next, the HO endonuclease coding sequence (without stop codon) with *Eco*RV and *Xho*I restriction sites was amplified by PCR from yeast BY4741 genomic DNA using the *Eco*RV-HO-Fw and *Xho*I-HO-delTAA-Rev primers. After digestion with *Eco*RV and *Xho*I this fragment was cloned into pSDM3774 digested with the same enzymes to yield pSDM3773. Following digestion with *Xba*I and *Xho*I the pvirD-HO-VirF37C fragment from the latter plasmid was cloned into pBBR6 digested with the same enzymes to construct pBBR6[HO] (pSDM3768). Correct construction

of the plasmid was confirmed by sequencing using the primers Seq-HO-Fw, Seq-HO-Rev, Int-HO-Fw and Int-HO-Rev.

To enable isolation of yeast cells that have switched their mating type, plasmids were constructed allowing mating type-specific expression of *HIS3*. To this end, a DNA fragment with *Bam*HI and *Xba*I restriction sites was generated by PCR amplification on BY4741 genomic DNA of the *HIS3* coding sequences plus additional 200 bp downstream sequences using primers *Bam*HI-*HIS3*[Ter]-Fw and *Xba*I-*HIS3*[Ter]-Rev. After digestion with *Bam*HI and *Xba*I this fragment was cloned into pRS316 digested with the same enzymes. Promoter sequences of *STE2* and *STE3* were amplified by PCR using primer combinations Sall-*STE2*[Promo]-Fw – BamHI-*STE2*[Promo]-Rev and Sall-*STE3*[Promo]-Fw - BamHI-*STE3*[Promo]-Rev, respectively. For the *STE6* promoter, fragments of 440 bp and 862 bp were amplified using primer combinations Sall-*STE6*-Fw1 - BamHI-*STE6*-Rev or Sall-*STE6*-Fw2 - BamHI-*STE6*-Rev, respectively. In this way DNA fragments were obtained with restriction sites for *Sall* and *Bam*HI at the ends. These promoter fragments were inserted upstream of the *HIS3* coding sequence in the plasmid construct described above. In this way, plasmids pRS316[*P*_{STE2}-*HIS3*] (pSDM3769), allowing expression of *HIS3* in *MATa* cells and pRS316[*P*_{STE3}-*HIS3*] (pSDM3770), pRS316[*P*_{STE6(440)}-*HIS3*] (pSDM3771) and pRS316[*P*_{STE6(862)}-*HIS3*] (pSDM3772) allowing expression of *HIS3* in *MATa* cells were obtained. Constructed plasmids were sequenced using primers M13-Fw(-20) and M13-Rev(-24).

Transformation of *A. tumefaciens* by electroporation

Agrobacterium competent cells preparation:

Agrobacterium was grown on LC agar medium for 3 days at 29°C. A loopful of bacteria was transferred into 2 ml of liquid LC medium and incubated at 29°C for 6 hrs with agitation. One hundred µl of this preculture was used to inoculate 100 ml of LC medium and the culture was grown till A₆₆₀=1.0-1.5. Then, cells were collected by centrifugation (4000xg) at 4 °C for 20 minutes. Cells were washed three times with ice-cold HEPES (pH 7.0) followed by washing once with ice-cold 10% glycerol. The cell pellet was re-suspended in 500-750 µl of ice-cold 10% glycerol and this suspension was distributed in 40 µl aliquots, frozen in liquid nitrogen and stored at -80 °C (den Dulk-Ras and Hooykaas, 1995).

Electroporation of *Agrobacterium* :

Competent cells were gently thawed on ice and transferred into a pre-chilled 50*2mm PulseStar electroporation cuvette. The Gene Pulser II Electroporation System (Bio-Rad) was used for electroporation (Capacitance 25 μ F, Voltage 2.5 kV, Pulse controller set to 200 Ω). Immediately after electroporation, 1 ml of SOC-medium was added into the cuvette and the cell suspension was transferred into a culture tube. After cultivation for 1-1.5 hrs at 29 °C, 100 μ l of cells were plated onto LC agar plates with appropriate antibiotics for selection of transformants (den Dulk-Ras and Hooykaas, 1995).

Co-cultivation of *Agrobacterium* and yeast. Co-cultivation of *Agrobacterium* and yeast was performed using an adapted version of the published protocol (Bundock *et al.*, 1995). *Agrobacterium* strains were grown overnight in 15 ml of LC medium with appropriate antibiotics (Table 2). Subsequently, *Agrobacterium* cells were centrifuged and re-suspended in IM medium supplemented with 0.2 mM acetosyringone and grown at 28°C for 6 hrs. After overnight incubation of the yeast strain in 10 ml of YPD medium at 30°C, 100 μ l of cells were inoculated in 20 ml of fresh YPD medium and incubated for an additional 6 hrs at 28°C. Then, 1 ml of yeast culture was washed with 500 μ l of IM medium and re-suspended in 1 ml of IM medium. Sixty microliters of *Agrobacterium* suspension were mixed with 60 μ l of yeast suspension and 100 μ l of the mixture were spotted on cellulose nitrate filters (Sartorius Stedim Biotech). Filters were dried at room temperature and were laid onto IM plates supplemented with appropriate nutrients and incubated at 21°C for 24-48 hrs.

Visualization of yeast mating type switching. To visualize mating type switching the *Eco*RI - *Xho*I fragment from the pHMR::P_{URA3}-GFP-URA3 plasmid was used to transform yeast strain CEN.PK113-3B and transformants were selected for uracil prototrophy yielding strain GG3430. Correct integration at the *HMR* locus was confirmed by PCR analysis with the A1-HMR, A2-HMR, S1-HMR and S2-HMR primers (Table 4). In this way, GFP, under the control of the *URA3* promoter, was integrated at the silent donor locus *HMR*. After *HO* induction *HMR* is used as a template to repair the gap in the *MAT* locus by homologous recombination. This will lead to copying the GFP coding sequence into the active *MAT* locus. Hence, every cell that has switched its mating type from α to a, expresses GFP and can be detected by fluorescence microscopy (Figure 2A). To study mating type switching by translocation of *HO* from *Agrobacterium* into yeast cells, GG3430 was co-cultivated for 24

hrs with LBA1010[HO] or LBA1100[HO]. For microscopy, cells were eluted from the filters by transferring the filters to a 2 ml Eppendorf tube, adding 0.5 ml of MY medium and vigorously vortexing, followed by two more washes of the filter with 0.5 ml MY medium. Cells were centrifuged and re-suspended into 200 μ l of MY medium and an aliquot (5 μ l) was used for confocal microscopy.

Isolation of yeast cells after mating type switching. To enable isolation of mating type switched cells, CEN.PK113-3B (*MAT α*) was transformed with pRS316[P_{STE2}-HIS3], whereas CEN.PK2-1C and BY4741 (*MAT α*) were transformed with pRS316[P_{STE3}-HIS3], pRS316[P_{STE6(440)}-HIS3] or pRS316[P_{STE6(862)}-HIS3]. The resulting strains were co-cultivated with *Agrobacterium* strains LBA1100 or LBA1010 expressing the HO endonuclease (LBA1100[HO] and LBA1010[HO], respectively). After 24 hrs of co-cultivation, filters were transferred to 2ml Eppendorf tubes, 1 ml (MY) was added and the tubes were vortexed vigorously to wash all the cells off the filters. Aliquots of 200 μ l of the cell suspensions were applied on MY plates supplemented with cefotaxime (200 μ g/ml) to select for histidine and uracil prototrophic yeast cells. To induce loss of plasmid pRS316[P_{STE2}-HIS3] yeast cells were streaked on MY plates supplemented with uracil and histidine containing 5-fluoroorotic acid (5-FOA; 1 mg/ml) and incubated for 3 days at 30 °C. Colonies were selected and incubated again in the presence of 5-FOA. One of the colonies was selected for further studies yielding strain GG3431.

Confirmation of mating type switching by PCR. Three oligonucleotide primers were used for determination of the mating type. The M1 oligonucleotide corresponds to a sequence at the right side of and directed towards the *MAT* locus. The M2 oligonucleotide corresponds to a sequence within the *MAT α* and *HML α* loci and the M3 oligonucleotide corresponds to a sequence within the *MAT α* and *HML α* loci. When these three oligo's are used in a single PCR, the *MAT α* locus generates a 404 bp product, whereas the *MAT α* locus generates a 544 bp product. For commonly used laboratory strains, haploid strains yield either the *MAT α* or *MAT α* -specific product corresponding to their mating type, while diploid strains yield both products (adapted from Nasmyth *et al.*, 1980).

Confocal microscopy. For confocal microscopy yeast cells were grown in MY medium supplemented with appropriate nutrients and a 5 μ l aliquot was analyzed using a Zeiss LSM5 Exciter confocal microscope using a 63X magnifying objective. GFP signal was detected

using an argon 488 nm laser and a 505-600 nm band pass emission filter. All images were processed using ImageJ 1.48F software (Abràmoff *et al.*, 2004).

Table 1. Yeast strains used in this study

Yeast strain	Genotype	Source/reference
BY4741	<i>MATa his3Δ1 leu2Δ0 met15Δ0 ura3Δ0</i>	(Brachmann <i>et al.</i> , 1998)
CEN.PK113-3B	<i>MATa ura3-52 his3Δ1</i>	P. Kötter, Göttingen, Germany.
CEN.PK2-1C	<i>MATa ura3-52 leu2-112 trp1-289 his3Δ1</i>	P. Kötter, Göttingen, Germany.
CEN.PK111-32D	<i>MATa leu2-112</i>	P. Kötter, Göttingen, Germany.
GG3430	<i>MATa ura3-52 his3Δ1 ura3-52::pHMR::P_{URA3}-GFP-URA3</i> (CEN.PK113-3B with GFP in silent <i>HMR</i> locus)	This study
GG3431	<i>MATa ura3-52 his3Δ1</i> (CEN.PK113-3B transformant No. 9 after successful mating type switching: with GFP at <i>MAT</i> locus)	This study

Table 2. *Agrobacterium* strains used in this study

<i>Agrobacterium</i> strain	Specifications ^a	Source/reference
LBA1010	C58C9 containing pTiB6, Rif	(Koekman <i>et al.</i> , 1982)
LBA1010[HO]	LBA1010 with pBBR6[HO] encoding the HO endonuclease fused to the virF T4SS-translocation sequence under control of <i>virD</i> promoter, Gm	This study.
LBA1100	C58C9 containing pTiB6Δ (Δ T-DNA, Δ occ, Δ tra), Rif, Spc	Beijersbergen <i>et al.</i> , 1992)
LBA1100 (pRAL7100)	LBA1100 with binary vector pRAL7100, Rif, Km	(Bundock <i>et al.</i> , 1995)
LBA1100[HO]	LBA1100 with pBBR6[HO] encoding the HO endonuclease fused to the VirF T4SS-translocation signal under control of <i>virD</i> promoter, Gm	This study.

a, Rif: rifampicin; Spc: spectinomycin; Km: kanamycin; Gm: gentamicin

Table 3. Plasmids used in this study

Name	Properties	Source/reference
pBBR6	Derivative plasmid of pBBR1-MSC2 vector which is broad host range, nonmobilizable plasmid with Gentamycin resistance marker.	(Kovach <i>et al.</i> , 1995)
(pSDM3768) pBBR6[HO]	pBBR6 with coding sequence of HO endonuclease under control of <i>virD</i> promoter in frame fusion with <i>virF</i> T4SS-translocation sequence.	This study.
pRS316	Yeast centromeric plasmid (<i>URA3</i> , CEN6, ARSH4).	(Sikorski and Hieter, 1989)
pHMR::P _{URA3} -GFP- URA3	pUC19 containing <i>yEGFP</i> under control of <i>URA3</i> promoter and <i>ADHI</i> terminator. <i>URA3</i> marker.	(Laney and Hochstrasser, 2003)
pSDM3149	<i>virD2</i> under control of the <i>virD</i> promoter, located on plasmid pBBR6 (pVD43 was cloned as <i>EcoRV</i> - <i>EcoRI</i> fragment in pIC2OH by Amken den Dulk).	(Vergunst, unpublished)
pSDM3172	pUC18 with <i>cre::virF</i> translocational fusion	(Vergunst, unpublished)
(pSDM3264)	pUC18 with <i>virF</i> promoter-NLS-VirF37C with <i>BglII-XhoI</i> linker inserted between NLS and VirF.	(Vergunst, unpublished)
(pSDM3774) pSDM3172[p <i>virD</i> - VirF37C]	pSDM3264, but <i>virF</i> promoter replaced by <i>virD</i> promoter.	This study.
(pSDM3773) pSDM3172[pVirD-HO- VirF37C]	pSDM3177 with HO endonuclease inserted in frame fused to <i>virF37C</i> .	This study.
(pSDM3769) pRS316[P _{STE2} -HIS3]	pRS316 containing <i>HIS3</i> under control of the <i>STE2</i> promoter and <i>HIS3</i> terminator. <i>URA3</i> marker.	This study.
(pSDM3770) pRS316[P _{STE3} -HIS3]	pRS316 containing <i>HIS3</i> under control of the <i>STE3</i> promoter and <i>HIS3</i> terminator. <i>URA3</i> marker.	This study.
(pSDM3771) pRS316[P _{STE6(440)} -HIS3]	pRS316 containing <i>HIS3</i> under control of the <i>STE6</i> promoter [440bp] and <i>HIS3</i> terminator. <i>URA3</i> marker.	This study.
(pSDM3772) pRS316[P _{STE6(862)} -HIS3]	pRS316 containing <i>HIS3</i> under control of <i>STE6</i> promoter [862bp] and <i>HIS3</i> terminator. <i>URA3</i> marker.	This study.

Table 4. Primers used in this study

Primer name	Sequence (5' → 3'); restriction sites underlined.
A1-HMR	GGACCTAATGCTTCAACTAAC
S1-HMR	CAAGCAAGTG GGGTAACTTAG
A2-HMR	GCGCTTGACAATTCTATATGC
S2-HMR	GCGAGATACCCAGATCATATG
Int-HMR-Fw	GATTTGAATGCGAGATAAACTG
EcoRV-HO-Fw	AAGATATCATGCTTTCTGAAAAC
XhoI-HO-del TAA-Rev	AAA <u>ACTCGAGG</u> CAGATGCGCGCACCTGC
Seq-HO-Fw	TCGTAAGAGAATAAAAGCGGC
Seq-HO-Rev	CGATTCATTAATGCAGCTGGC
Int-HO-Fw	CAGCAACATTACAGTCGTATG
Int-HO-Rev	CCAGTACTCGCAGGAAATG
HindIII- VirD2-Fw	GGG <u>AAGCTT</u> CCATCAAACGGAGTGCATTTG
EcoRV- VirD2-Rev	GGGATATCAGCTTCCTCCAAAAAAGCGG
SalI-STE2[Promo]-Fw	CCCGT <u>CGAC</u> CAAAACGTATTTTGTTAATTGGC
BamHI-STE2[Promo]-Rev	CCCGGATCC ATTCTTGATATGGTTCTTAACG
SalI-STE3[Promo]-Fw	CCCGT <u>CGACT</u> GTTTTCTCCTTCTTTACATG
BamHI-STE3[Promo]-Rev	CCCGGATCCGAAAATTTTGATAGTATTTTGCC
BamHI-HIS3[Ter]-Fw	CCCGGATCCATGACAGAGCAGAAAGCCC
XbaI-HIS3[Ter]-Rev	CC <u>TCTAG</u> TCGAGTTCAAGAGAAAAAAAAAAG
M1	AGTCACATCAAGATCGTTTATGG
M2	GCACGGAATATGGGACTACTTCG
M3	ACTCCACTTCAAGTAAGAGTTTG
SalI-STE6-Fw1	CCCGT <u>CGAC</u> TCCACAGAGGGCATTGA
SalI-STE6-Fw2	CCCGT <u>CGAC</u> CCCTTGCAATATTTCTCTCTCC
BamHI-STE6-Rev	CCCGGATCC GACGTAGCTTGTTCTTTGTTTC
Seq-T4SS-Rev	GATCGAGGTCTGTCCGCCGACATTA
M13-Fw(-20)	GTA AACCGACGGCCAGT
M13-Rev(-24)	AACAGCTATGACCATG

RESULTS

During *Agrobacterium* mediated transformation of eukaryotic organisms, in addition to T-DNA, a number of virulence proteins are translocated from the bacterium into the host cell to assist in the transformation process. This property of *Agrobacterium* can be exploited to deliver proteins into host cells to manipulate these cells. In this chapter we address the possibility to induce mating type switching by translocation of the HO endonuclease from *A. tumefaciens* to yeast cells.

Laney and Hochstrasser (2003) have developed an assay to visualize mating type switching. They introduced the GFP coding sequence into the silent *HMR* locus and upon switching from mating type α to a the GFP sequence is copied into the active *MAT* locus resulting in GFP expression (Figure 2A). In order to study the possibility to induce mating type switching by delivering the HO endonuclease via *Agrobacterium* -mediated protein translocation, we constructed pBBR6[HO] containing a gene encoding the *S. cerevisiae* HO coding sequence fused to sequences required for protein translocation through the T4SS under control of the *Agrobacterium virD* promoter. The plasmid was introduced into *A. tumefaciens* strain LBA1010 (containing T-DNA) and *A. tumefaciens* strain LBA1100 (T-DNA deficient) yielding LBA1010[HO] and LBA1100[HO], respectively. These strains were co-cultivated for 24 hrs with yeast strain GG3430 which has the GFP coding sequence integrated into the silent *HMR* locus of CEN.PK113-3B. As shown in figure 2 a number of cells show GFP expression after co-cultivation either with the *Agrobacterium* strain containing T-DNA (Fig. 2 B and C) or with the strain lacking T-DNA (Fig 2 D and E). Strong GFP expression representing mating type switching could not be detected after co-cultivation of GG3430 with *A. tumefaciens* strain LBA1010 lacking pBBR6[HO] as a negative control (data not shown). To estimate the percentage of mating type switched yeast cells based on GFP expression, several random images were captured by confocal microscopy and the number of highly fluorescent cells was counted. Co-cultivation with *Agrobacterium* LBA1010[HO] or LBA1100[HO] yielded 5.4 and 3.4 percent fluorescent cells, respectively (11 out of 204 and 6 out of 176, respectively). After co-cultivation with the control *A. tumefaciens* strain LBA1010 lacking HO, highly fluorescence cells were not seen. A few cells (4 out of 236) were weakly fluorescent.

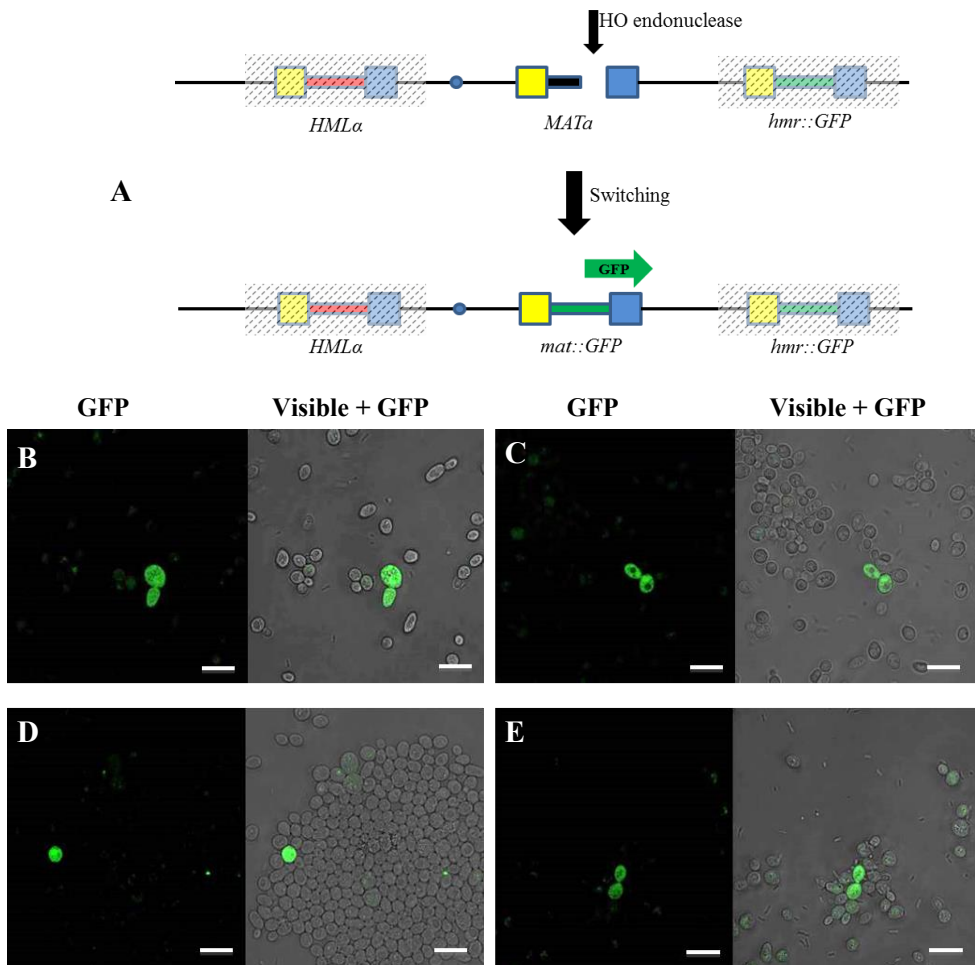


Figure 2. Visualization of yeast mating type switching. (A) Experimental design. GFP was introduced into the silent *HMR* locus (*hmr::GFP*) (Adapted from Laney and Hochstrasser, 2003). When the HO endonuclease induces a break in the *MAT* locus, *hmr::GFP* can be used as a template for repair by homologous recombination leading to expression of GFP. (B and C) Confocal microscopy of GG3430 cells (*MAT α hmr::GFP*) after co-cultivation for 24 hrs with *A. tumefaciens* strain LBA1010 (containing T-DNA) carrying pBBR6[HO]. (D and E) Confocal microscopy of GG3430 cells (*MAT α hmr::GFP*) after co-cultivation for 24 hrs with *A. tumefaciens* strain LBA1100 (lacking T-DNA) carrying pBBR6[HO]. Scale bars: 10 μ m.

To enable isolation of cells that have switched their mating type, we constructed plasmids that allow mating type-specific expression of *HIS3* (Figure 3A). For this purpose we used the *STE2* promoter (Blumer & Thorner 1990) for expression in a cells (pRS316[P_{STE2}-HIS3]) and the *STE3* and *STE6* promoters (Chen and Davis, 2000; Ketchum *et al.*, 2001; Kuchler *et al.*, 1989) for expression in alpha cells (pRS316[P_{STE3}-HIS3] and pRS316[P_{STE6}-HIS3]). CEN.PK113-3B (*MAT α*) cells containing pRS316[P_{STE2}-HIS3] were unable to grow on media lacking histidine, whereas introduction of this plasmid in the *MAT α* strains BY4741 and CEN.PK2 resulted in histidine prototrophy, indicating mating type specific expression of *HIS3* (data not shown). On the other hand, the *STE3* and *STE6* promoters were less mating type specific as both CEN.PK113-3B (*MAT α*) and BY4741 and CEN.PK2 (*MAT α*) cells carrying (pRS316[P_{STE3}-HIS3] or pRS316[P_{STE6}-HIS3]) grew on media lacking histidine (data not shown).

In an initial experiment we co-cultivated *MAT α* strain CEN.PK113-3B carrying pRS316[P_{STE2}-HIS3] for 24 hrs with *Agrobacterium* strain LBA1010 harboring pBBR6[HO]. As shown in Figure 3C histidine prototrophic colonies were selected, indicative of mating type switching. Such colonies were also selected when a T-DNA-deficient *Agrobacterium* strain (LBA1100pBBR6[HO]) was used (Figure 3B). On the other hand, His⁺ transformants were not found when *Agrobacterium* strain LBA1010 lacking HO was used for co-cultivation as a negative control (Fig. 3D). After continued co-cultivation for 48 hrs. a few small His⁺ colonies were found (Figure 3E). To investigate whether the His⁺ yeast cells had indeed successfully switched their mating type we used a PCR based protocol (Nasmyth *et al.*, 1980). Using a mixture of a *MAT α* -specific, a *MAT α* -specific and a mating type independent-PCR primer the mating type can be determined (Figure 4A). Both after co-cultivation with *Agrobacterium* strains containing or lacking T-DNA, 5 out of 14 transformants indeed obtained mating type a (Figures 4B and C, respectively). To investigate mating type switching in a more quantitative way, in two rounds of experiments 105 histidine prototrophic colonies were analyzed. The number of histidine prototrophic transformants with successful mating type switching after co-cultivation with the *A. tumefaciens* strain containing T-DNA was 15 out of 49 (31%) and after co-cultivation with the *A. tumefaciens* strain lacking T-DNA was 24 out of 56 (43%). Co-cultivation with *Agrobacterium* strain LBA1010 (lacking HO) resulted in one His⁺ transformant (out of 19 His⁺ transformants; 5 %) with a *MAT α* PCR fragment. This indicates that the number of mating type switching events

is considerably increased after co-cultivation with *A. tumefaciens* expression the HO endonuclease.

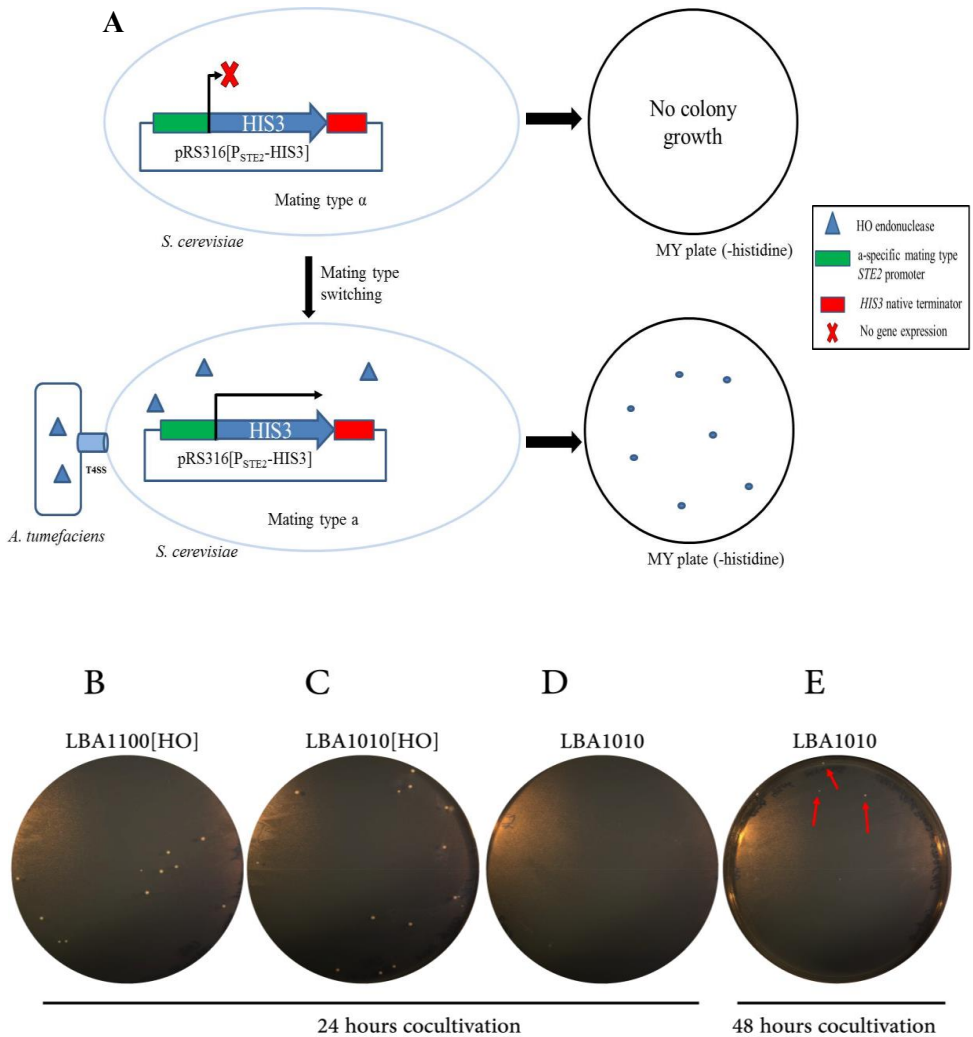


Figure 3. Selection of cells that have potentially switched mating type. A. Experimental setup: pRS316[P_{STE2}-HIS3] allows *MATa* specific expression of *HIS3*. B-E. Selection of histidine prototrophic cells after co-cultivation of CEN.PK113-3B containing pRS316[P_{STE2}-HIS3] with *Agrobacterium* strain LBA1100 carrying pBBR6[HO] (B), LBA1010 carrying pBBR6[HO] (C) or with LBA1010 lacking HO (D) co-cultivated for 24 hrs and/or co-cultivated with LBA1010 lacking HO for 48 hrs (E). Red arrows indicate small His⁺ colonies appeared on negative control plates.

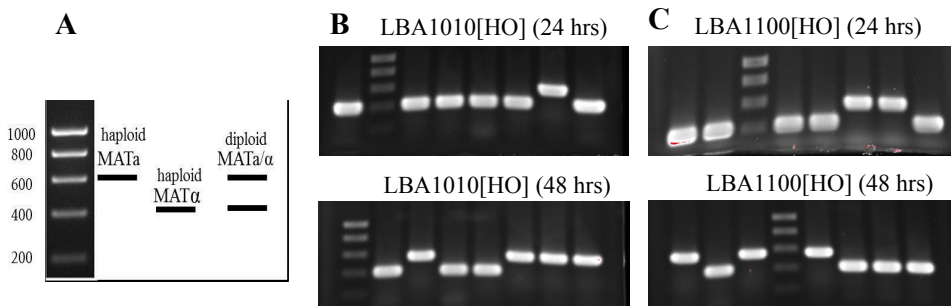


Figure 4. Analysis of mating type switching by PCR. Using a mixture of a *MATa*-specific, a *MATα*-specific and a mating type-independent PCR primer the *MATα* locus generates a 404 bp product whereas the *MATa* locus generates a 544 bp product (Nasmyth *et al.*, 1980) (A). Genomic DNA was extracted from histidine prototrophic transformants of CEN.PK113-3B (*MATα*) containing pRS316[P_{STE2}-HIS3] after co-cultivation with *Agrobacterium* strain LBA1010 (B) or LBA1100 (C) containing pBBR6[HO] and the *MAT* locus was analyzed by PCR. Upper panels represent colonies obtained after 24 hrs co-cultivation, bottom panels after 48 hrs co-cultivation

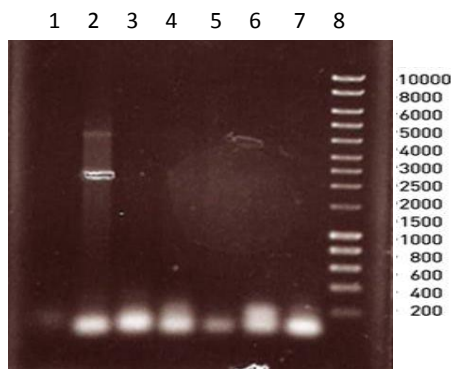


Figure 5. Absence of pBBR6[HO] sequences in DNA isolated from His⁺ transformants. PCR was performed using primers *HindIII*- VirD2-Fw and Seq-T4SS-Rev detecting sequences of the pBBR6[HO] using the indicated DNAs as template. Lane 1, pBBR6[HO] plasmid without Phusion DNA polymerase. Lane 2, pBBR6[HO] plasmid as positive control. Lane 3, DNA of yeast strain CEN.PK11.1C. Lane 4, as one of the unchanged mating type samples. Lane 5-7, transformants with a successful mating type switch. Lane 8, DNA ladder.

In order to exclude the possibility that the pBBR6[HO] plasmid instead of the HO protein was translocated from *Agrobacterium* into the yeast cells via an unknown mechanism, the DNA isolated from the transformants was analyzed for sequences of this plasmid by PCR. As shown in Figure 5, such sequences could not be detected in the analyzed His⁺ transformants.

After a successful mating type switch, the yeast cells still contain plasmid pRS316[P_{STE2}-HIS3]. To induce plasmid loss the strains were grown on plates containing 5-fluoroorotic acid (5-FOA). CEN.PK113-3B yeast strain with *MATa* mating type yielded a number of colonies on this medium indicative of plasmid loss. These colonies were unable to grow on MY medium lacking histidine or uracil (data not shown), in agreement with the absence of the plasmid. These results show that transient introduction of the HO endonuclease protein into *S. cerevisiae* can successfully induce mating type switching. All of the analyzed transformants were able to mate with opposite mating type α (data not shown).

DISCUSSION

It is well known that *A. tumefaciens* has the unique capability to transfer T-DNA into a wide range of plant species through its T4SS which results in T-DNA integration into the host genome (Hooykaas and Schilperoort, 1992; for a recent review see Gelvin, 2012). Under laboratory conditions, *Agrobacterium* is not only able to infect plants, but also other organisms such as yeasts, algae and fungi (Bundock *et al.*, 1995; de Groot *et al.*, 1998; Kumar *et al.*, 2004). Together with T-DNA effector proteins (VirD2, VirE2, VirE3, VirD5 and VirF) are translocated to facilitate the transformation procedure (Vergunst *et al.*, 2000). This property of *Agrobacterium* can be exploited to introduce proteins and enzymes into eukaryotic cells to manipulate them to acquire desired properties. In this study, we successfully used *Agrobacterium* to translocate the HO endonuclease into yeast cells to let them switch from mating type α to a.

As shown in figure 3 upon co-cultivation of yeast cells carrying a plasmid allowing mating type specific expression of *HIS3* with *A. tumefaciens* strains expressing the HO endonuclease we isolated yeast cells that switched from mating type α to a. Unfortunately we could not use the same procedure to obtain the reverse mating type switch as the mating type alpha-specific *STE3* and *STE6* promoters in our selection plasmids were also active in mating type a cells. Addition of 3-amino-1,2,4-triazole, an inhibitor of histidine biosynthesis, to a concentration of up to 100 mM was unable to inhibit growth of CEN.PK113-3B cells containing pRS316[P_{STE3}-HIS3], indicating a substantial leakage of the *STE3* promoter (data not shown). Other promoters, or mutated forms of the *STE3* or *STE6* promoters, may appear useful for selection of mating type alpha cells.

In another study a GAL-HO plasmid was used to induce mating type switching. This plasmid allows expression of the HO endonuclease under control of the *GALI* promoter and upon

cultivation on media with galactose mating type switching was observed (Jensen and Herskowitz, 1984). This protocol is not suitable for mating type switching of yeast strains that grow poorly on media with galactose as sole carbon source. Mating type switching by HO endonuclease translocation from *Agrobacterium* may be a good alternative for those strains. Recently, Xie *et al.* (2018) established a new protocol to induce mating type switching in yeast using CRISPR/Cas9 technology. Although they claimed that using optimal gRNA resulted in less off-target effects, still there is a chance to have double strand breaks anywhere in the yeast genome which could result in unexpected mutations (Zhang *et al.*, 2015, Chapman *et al.*, 2017).

In this study we made use of protein translocation from *Agrobacterium* to yeast cells to induce mating type switching. Also *Agrobacterium* strains lacking T-DNA are able to induce mating type switching (Figure 2-4) indicating that T-DNA translocation is not required. In addition, sequences derived from the pBBR6[HO] plasmid could not be detected in the yeast cells after induction of the mating type switch. Thus, using *Agrobacterium* to induce mating type switching does not require the introduction of foreign DNA into the yeast cells. In our study we still made use of a plasmid (pRS316[P_{STE2}-HIS3]) to facilitate selection. However, using alternative selection procedures like high throughput PCR, isolation of cells in which mating type switching has occurred, will be possible without any genetic manipulation of the yeast cells. Although the yeast strains used in this study were heterothallic and thus lacking expression of *HO*, one His⁺ transformant was found that switched its mating type. This could be due to expression of the silent *HO* gene or due to another unknown recombination event. However the efficiency of mating type switching was much higher after co-cultivation with strains expressing *HO*. This study further highlights the potential of exploiting the ability of *Agrobacterium* to deliver proteins into eukaryotic cells for inducing epigenetic changes, for drug delivery and for protein therapy. In other studies *Agrobacterium* was successfully used to introduce the Cre-recombinase into yeast, fungal and plant cells to allow recombination (Vergunst *et al.*, 2000; Vergunst *et al.*, 2005), to target meganuclease I-SceI into yeast cells to enhance targeted integration (Rolloos *et al.*, 2015) and also into plant cells (van Kregten., 2011).

ACKNOWLEDGEMENTS

We would like to thank Prof. Jeff Laney (University of Arizona) for providing the pHMR::P_{URA3}-GFP-URA3 plasmid.

REFERENCES

- Abràmoff, M.D., Magalhães, P.J. and Ram, S.J.** (2004). Image processing with imageJ. *Biophotonics International*, 11, 36–41.
- Blumer, K.J. and Thorner, J.** (1990). Beta and gamma subunits of a yeast guanine nucleotide-binding protein are not essential for membrane association of the alpha subunit but are required for receptor coupling. *Proc. Natl. Acad. Sci. USA*, 87, 4363–4367.
- Brachmann, C.B., Davies, A., Cost, G.J., Caputo, E., Li J., Hieter, P. and Boeke, J.D.** (1998). Designer deletion strains derived from *Saccharomyces cerevisiae* S288C: A useful set of strains and plasmids for PCR-mediated gene disruption and other applications. *Yeast*, 14, 115–132.
- Bruhn, L. and Sprague, G.F.** (1994). MCM1 point mutants deficient in expression of alpha-specific genes: residues important for interaction with alpha 1. *Mol. Cell. Biol.*, 14, 2534–2544.
- Bundock, P., den Dulk-Ras, A., Beijersbergen, A. and Hooykaas, P.J.J.** (1995). Transkingdom T-DNA transfer from *Agrobacterium tumefaciens* to *Saccharomyces cerevisiae*. *EMBO J.*, 14, 3206–3214.
- Chapman, J. E., Gillum, D. and Kiani.S.** (2017). Approaches to Reduce CRISPR off-target effects for safer genome editing. *J. ABSA. Int.* 22, 7–13.
- Chen, L. and Davis, N.G.** (2000). Recycling of the yeast a-factor receptor. *J. Cell Biol.*, 151, 731–738.
- den Dulk-Ras, A. and Hooykaas, P.J.J.** (1995). Electroporation of *Agrobacterium tumefaciens*. *Methods in molecular biology*, 55, 63–72.
- Gelvin, S.** (2012). Traversing the Cell: *Agrobacterium* T-DNA's Journey to the Host Genome. *Front. Plant Sci.* 3, 1-11.
- Gietz, R.D. Schiestl, R.H., Willems, A.R. and Woods, R.A.** (1995). Studies on the transformation of intact yeast-cells by the LiAc/SS DNA/PEG procedure. *Yeast*, 11, 355–360.
- Goutte, C. and Johnson, A.D.** (1988). A1 protein alters the DNA binding specificity of $\alpha 2$ repressor. *Cell*, 52, 875–882.
- de Groot, M.J., Bundock, P., Hooykaas, P.J.J. and Beijersbergen, A.G.** (1998). *Agrobacterium tumefaciens*-mediated transformation of filamentous fungi. *Nature biotechnology*, 16, 839–842.
- Haber J. E.** (1992). Mating-type gene switching in *Saccharomyces cerevisiae*. *Trends Genet*, 8, 446–452.
- Haber, J.E.** (2012). Mating-type genes and MAT switching. *Genetics*, 191, 33–64.
- Hagen, D.C., Bruhn, L., Westby, C.A. and Sprague, G.F.** (1993). Transcription of α -Specific Genes in *Saccharomyces cerevisiae*: DNA sequence requirements for activity of the coregulator alpha 1. *Am. Soc. Microbiol*, 13, 6866–6875.
- Herskowitz I.** (1988). Life cycle of the budding yeast *Saccharomyces cerevisiae*. *Microbiol. Rev.* 52, 536–553.

- Hooykaas, P.J.J. and Schilperoort, R. A.** (1992). *Agrobacterium* and plant genetic engineering. *Plant molecular biology*, 19, 15–38.
- Jensen, R., Sprague, G.F. and Herskowitz, I.** (1983). Regulation of yeast mating-type interconversion: feedback control of HO gene expression by the mating-type locus. *Proc. Natl. Acad. Sci. USA*, 80, 3035–3039.
- Ketchum, C.J., Schmidt, W.K., Rajendrakumar, G.V., Michaelis, S. and Maloney, P.C.** (2001). The yeast a-factor transporter Ste6p, a member of the ABC superfamily, couples ATP hydrolysis to pheromone export. *J. Biol. Chem.*, 276, 29007–29011.
- Klar A. J.** (1987). Determination of the yeast cell lineage. *Cell*, 49, 433–435.
- Koekman, B.P., Hooykaas, P.J.J. and Schilperoort, R.A.** (1982). A functional map of the replicator region of the octopine Ti plasmid. *Plasmid*, 7, 119–132.
- Kovach, M.E., Elzer, P.H., Phillips, M.E., Robertson, R.W., Peterson, K.M. and Roop, R.M.** (1995). *In vivo* and *in vitro* stability of the broad-host-range cloning Vector pBBR1MCS in six *Brucella* species. *Plasmid*, 33, 51–57.
- Kuchler, K., Sterne, R.E. and Thorner, J.** (1989). *Saccharomyces cerevisiae* STE6 gene product: a novel pathway for protein export in eukaryotic cells. *EMBO J.*, 8, 3973–3984.
- Kumar, S.V. Misquitta, R.W., Reddy, V.S., Rao, B.J. and Rajama, M.V.** (2004). Genetic transformation of the green alga-*Chlamydomonas reinhardtii* by *Agrobacterium tumefaciens*. *Plant Science*, 166, 731–738.
- Laney, J.D. and Hochstrasser, M.** (2003). Ubiquitin-dependent degradation of the yeast Mat(alpha)2 repressor enables a switch in developmental state. *Genes Dev*, 17, 2259–2270.
- Nasmyth, K. A., and Tatchell, K.** (1980). The structure of transposable yeast mating type loci. *Cell*, 19, 753–764.
- Nasmyth, K., Stillman D. and Kipling, D.** (1987). Both positive and negative regulators of HO transcription are required for mother-cell-specific mating-type switching in yeast. *Cell*, 48, 579–587.
- Rolloos, M., Hooykaas, P.J.J. and van der Zaal, B.J.** (2015). Enhanced targeted integration mediated by translocated I-SceI during the *Agrobacterium* mediated transformation of yeast, *Sci Rep*, 5, 8345.
- Rossi, L., Hohn, B. and Tinland, B.** (1993). The VirD2 protein of *Agrobacterium tumefaciens* carries nuclear localization signals important for transfer of T-DNA to plant. *Mol. Gen. Genet*, 239, 345–353.
- Sikorski, R.S. and Hieter, P.** (1989). A system of shuttle vectors and yeast host strains designed for efficient manipulation of DNA in *Saccharomyces cerevisiae*. *Genetics*, 122, 19–27.
- Strathern, J., Shafer, B., Hicks, J. and McGill, C.** (1988). a/Alpha-specific repression by MAT alpha 2. *Genetics*, 120, 75–81.
- Strathern, J. N., Klar, A.J.S., Hicks, J.B., Abraham, J.A., Ivy, J.M., Nasmyth, K.A. and McGill, C.** (1982). Homothallic switching of yeast mating type cassettes is initiated by a double-stranded cut in the MAT locus. *Cell*, 31, 183–192.

- Tatchell, K. Nasmyth, K.A., Hall, B.D., Astell, C. and Smith, M.** (1981). In vitro mutation analysis of the mating-type locus in yeast. *Cell*, 27, 25–35.
- Tinland, B., Hohn, B. and Puchta, H.** (1994). *Agrobacterium tumefaciens* transfers single-stranded transferred DNA (T-DNA) into the plant cell nucleus. *Proc. Natl. Acad. Sci. USA*, 91, 8000–8004.
- Townsend, C.O. and Smith, E.F.** (1907). A Plant-Tumor of Bacterial Origin. *Science*, 25, 671–673.
- van Kregten, M.** (2011). VirD2 of *Agrobacterium tumefaciens* functional domains and biotechnological applications. Ph.D., thesis. Leiden University, Institute of biology of Leiden. Leiden, the Netherlands.
- Vergunst, A.C., van Lier, M.C., den Dulk-Ras, A., Stüve, T.A., Ouwehand, A. and Hooykaas, P.J.J** (2005). Positive charge is an important feature of the C-terminal transport signal of the VirB/D4-translocated proteins of *Agrobacterium*. *Proc. Natl. Acad. Sci. USA*, 102, 832–837.
- Vergunst, A.C. Schrammeijer, B., den Dulk-Ras, A., de Vlaam, C.M., Regensburg-Tuïnk, T.J. and Hooykaas, P.J.J.** (2000). VirB / D4-dependent protein translocation from *Agrobacterium* into plant cells. *Science*, 290, 979–982.
- Xie, Z.X., Mitchell, L.A., Liu, H.M., Li, B.Z., Liu, D., Agmon, N., Wu, Y., Li, X., Zhou, X., Li, B., Xiao, W.H., Ding M.Z., Wang, Y., Yuan, Y.J. and Boeke, J.D.** (2018). Rapid and efficient CRISPR/Cas9-based mating-type switching of *Saccharomyces cerevisiae*. *G3*, 8, 173-183.
- Zhang, X., Tee, L.Y., Wang, X., Huang, Q. and Yang, S.**(2015). Off-target effects in CRISPR/Cas9-mediated genome engineering. *Mol. Ther. Nucleic. Acids*, 4, e264.
- Zonneveld, B.J.M.** (1986). Cheap and simple yeast media. *J Microbiol Methods*, 4, 287–291.

Chapter 5

Targeting *Agrobacterium tumefaciens* virulence proteins into the organelles of plant and yeast cells

M.Reza Roushan, Joyce van der Meer, Sonja van der Wal, G. Paul H. van Heusden and Paul J.J. Hooykaas

Molecular and Developmental Genetics, Institute of Biology, Leiden University, Leiden, The Netherlands.

ABSTRACT

Agrobacterium mediated transformation (AMT) is broadly used as a tool to modify plant nuclear chromosomes. However, for transgenic crops introduction of the transgene into organellar DNA would have advantages over introduction into chromosomal DNA. During AMT, a number of effector proteins i.e. VirD2, VirD5, VirE2, VirE3 and VirF, are translocated from the bacterium into the host cell. Among them, VirE2 and VirD2 play an essential role in the transformation of plant cells and help targeting the T-DNA into the nucleus. In this study we have investigated whether it is possible to redirect the VirD2 and VirE2 effector proteins towards plant chloroplasts or towards yeast mitochondria as a first step to develop AMT systems by which organellar genomes can be modified. To this end, a mitochondrial or chloroplast targeting signal was fused to VirE2 and VirD2 and translocation of these modified virulence proteins was visualized using the fluorescent protein phiLOV2.1 or the split GFP technique. It was found that both proteins can be targeted to mitochondria of the yeast *Saccharomyces cerevisiae*, to chloroplasts of *Arabidopsis thaliana* protoplasts, and, to some extent possibly also to the chloroplasts of cells in *Nicotiana tabacum* leaves. Our results form the basis for future research towards the modification of organellar genomes by AMT.

INTRODUCTION

Agrobacterium tumefaciens, a Gram-negative soil born bacterium, can cause crown gall disease in many plants by transferring a piece of oncogenic DNA, the T-DNA, into its host cells (Smith and Townsend, 1907; Chilton *et al.*, 1977). This DNA is integrated into one of the chromosomes, resulting in expression of genes on the T-DNA responsible for opine synthesis and tumor formation. As foreign genes can be introduced into the T-DNA *Agrobacterium* is widely used for the generation of transgenic plants. Simultaneously with T-DNA transfer, several effector proteins (VirD2, VirE2, VirE3, VirD5 and VirF) are translocated into plant cells via the Type IV secretion system (T4SS) of *A. tumefaciens* (Vergunst *et al.*, 2000). These effector proteins assist in the transformation process and enable targeting of the T-DNA into the nucleus.

Genetic modification of organellar DNA has great potential for biotechnology. One of the advantages of the introduction of transgenes into the chloroplast or mitochondrial genome instead of into the nuclear genome is that these organelles are maternally inherited, which means that no spreading of the transgenic trait occurs via pollen (Bansal and Sharma, 2003; Sharma *et al.*, 2005). Furthermore, organelle transformation allows stable transgene expression by the lack of epigenetic interference and also transgene stacking in operons (Wang *et al.*, 2009) and expression of multiple proteins from polycistronic mRNAs may be possible. High yields of transgenic products may be achieved because of the high number of chloroplast and mitochondrial genomes per cell. Each plant cell contains approximately 100 chloroplasts with up to 50 genome copies per chloroplast, although these numbers vary to some extent depending on cell age and tissue type (Boffey and Leech, 1982; Daniell *et al.*, 2002; Flores-Perez and Jarvis, 2013). Another advantage is that chloroplast and mitochondria have an active homologous recombination system that allows precise targeting into a specific genome area during the transformation (Cerutti *et al.*, 1995; Maliga *et al.*, 1994; Meyers *et al.*, 2010). Besides the introduction of transgenes genetic manipulation of chloroplast DNA can potentially improve the efficiency of photosynthesis in plants (Ort *et al.*, 2015).

The techniques which have been used to transform chloroplasts are particle bombardment (Svab and Maliga, 1993; Hanson *et al.*, 2013; Yu *et al.*, 2017) and polyethylene glycol-mediated (PEG) transformation of protoplasts (Golds *et al.*, 1993). However, these are applicable only in few plant species such as *Nicotiana tabacum* and *Arabidopsis thaliana* and the efficiency of these techniques is low. Using the gold particle bombardment technique is

pricy and requires expensive devices (Daniell *et al.*, 2005; Liu *et al.*, 2013). PEG-mediated transformation requires tedious treatment, precise maintenance and regeneration of protoplasts (Meyers *et al.*, 2010). In an indirect way site-directed mutagenesis of chloroplast DNA was achieved by introduction of a gene encoding the homing endonuclease CreII tagged with a chloroplast targeting signal into nuclear DNA via *Agrobacterium* mediated transformation (AMT) (Avila *et al.*, 2016). Similarly, chloroplast genome interrogation using nuclear encoded artificial transcription factors with zinc fingers as DNA binding domains has been achieved resulting in modulation of photosystem II efficiency in *A. thaliana* (van Tol, 2016).

This study aims to find ways to target the T-DNA into mitochondria or chloroplasts instead of to the nucleus during AMT. As a first step, we investigated whether it is possible to target the *Agrobacterium* effector proteins VirD2 and VirE2 into these organelles. VirD2 and VirE2 are essential mediators of T-DNA transfer and are responsible for directing the T-complex into the nucleus (Yanofsky *et al.*, 1986; Gietl *et al.*, 1987; Christie *et al.*, 1988; Ward and Barnes, 1988; Citovsky *et al.*, 1992; Howard *et al.*, 1992; Atmakuri *et al.*, 2003). In order to direct VirD2 and VirE2 into yeast mitochondria and plant chloroplasts, they were N-terminally tagged with the mitochondrial targeting sequence of yeast citrate synthase 1 (MTS) (Okamoto *et al.*, 2001) or the chloroplast targeting sequence (CTS) of the *FedA* gene including the first 8 amino acids of mature *FedA* (Smeekens *et al.*, 1987; Jin *et al.*, 2003), respectively. To visualize the translocation and localization of the tagged proteins we used the fluorescent protein phiLOV2.1 (Gawthorne *et al.*, 2016; McIntosh *et al.*, 2017; Roushan *et al.*, 2018) and the split GFP technique (Van Engelenburg and Palmer, 2010; Sakalis *et al.*, 2014, Li and Pan, 2014,; Kamiyama *et al.*, 2016; Roushan *et al.*, 2018). With this approach we were able target both VirE2 and VirD2 to mitochondria of the yeast *Saccharomyces cerevisiae* and to the chloroplasts of *Nicotiana tabacum* leaves and *Arabidopsis thaliana* protoplasts.

MATERIALS AND METHODS

Yeast strains and media. Yeast strains used in this study are listed in Table 1. All yeast strains were grown in YPD medium or selective MY medium supplemented, if required, with histidine, tryptophan, methionine and/or uracil to the final concentration of 20 mg/ml (Zonneveld, 1986). Yeast transformation was performed using the Lithium Acetate method (Gietz *et al.*, 1995). Yeast strains carrying plasmids were obtained by transforming parental strains with the appropriate plasmids followed by selection for histidine, leucine and/or uracil prototrophy.

***Agrobacterium* strains and media.** The *Agrobacterium* strains used are listed in Table 2. *Agrobacterium* was grown in LC supplemented with the appropriate antibiotics (40 µg/ml gentamicin, 20 µg/ml rifampicin) at 28°C and 175 rpm. *Agrobacterium* strains carrying plasmids were obtained by electroporation as described by den Dulk-Ras and Hooykaas, (1995).

Plasmid constructions. All plasmids used and constructed in this study are listed in Table 3. *E. coli* strain XL1-Blue was used for cloning of the plasmids and the cultures were grown in LC medium containing 10 µg/ml gentamycin or 100 µg/ml carbenicillin while shaking 175 rpm at 37°C. PCR amplifications were done with Phusion™ High-Fidelity DNA Polymerase. Table 4 lists all primers used for PCR amplification and sequencing.

To target VirE2 and VirD2 into yeast mitochondria the following plasmids were made: pRS305[MTS-GFP₁₋₁₀], pUG36[MTS-39GFP₁₁-VirE2], pBBR6[MTS-39GFP₁₁-VirE2], pUG36[GFP₁₁-VirD2(mod)] and pUG36[MTS-GFP₁₁-VirD2(mod)]. In these plasmids, we inserted the N-terminal mitochondrial targeting sequence (MTS) of the *S. cerevisiae* Citrate synthase 1 (*CIT1*) which is able to target GFP into yeast mitochondria (Okamoto *et al.*, 2001). To generate the MTS, a DNA fragment was amplified from yeast strain BY4741 genomic DNA with *Xba*I restriction sites at the ends using *Xba*I-MTS-Fw and *Xba*I-MTS-Rev primers and ligated into vector pJET1.2 plasmid yielding pJET1.2[*Xba*I-MTS-*Xba*I]:

5'TCTAGAATGTTCAGCGATATTATCAACAACACTAGCAAAAAGTTTCTTATCAAGGGG
CTCCACAAGACAATGTCAAAATATGCAAAAAGGCTCTTTTTGCACTATTGAATGCT
CGCCACTATAGTAGCGCTCCGAACAAACGTTGAAGGAGAGATTTGCTGAAATT
TCTAGA3'.

Subsequently, the *XbaI*-MTS-*XbaI* DNA fragment was ligated into pRS305-GFP₁₋₁₀ and pUG36 after digestion with *XbaI* and dephosphorylation, to create pRS305[MTS-GFP₁₋₁₀] and pUG36[MTS], respectively. The integrative plasmid pRS305[MTS-GFP₁₋₁₀] was used to transform strain CEN.PK2-1C followed by selection for leucine prototrophy. To confirm correct integration, isolated genomic DNA was analysed by PCR using combination of Leu2 1A & Leu2 1S and Leu2 2A & Leu2 2S primers that generated DNA fragments of 2399 bp and 2724 bp, respectively. To obtain pUG36[MTS-39GFP₁₁-VirE2], pBBR6[39GFP₁₁-VirE2] (Roushan *et al.*, 2018) was digested with *NdeI* and *XbaI* and the *NdeI*-39GFP₁₁-VirE2-*XbaI* DNA fragment was ligated into pUG36[MTS] digested by *NdeI* and *XbaI* restriction enzymes. Plasmid pBBR6[MTS-39GFP₁₁-VirE2] was constructed by insertion of a *NdeI*-MTS-*NdeI* DNA fragment amplified from pRS305[MTS-GFP₁₋₁₀] as a template with primers *NdeI*-MTS-Fw and *NdeI*-MTS-Rev into pBBR6[39GFP₁₁-VirE2] (Roushan *et al.*, 2018) after digestion with *NdeI* and dephosphorylation of the vector.

A DNA fragment with *virD2*(mod), i.e. the *virD2* relaxase part of *virD2* containing the *virF* type four secretion translocation signal (van Kregten *et al.*, 2009), was obtained by PCR using pBBF[flag-D2-204-F] as template using *BamHI*-VirD2mod-Fw and *ClaI*-VirD2mod-Rev primers. pUG36[GFP₁₁] was constructed by replacement of the GFP coding sequence of pUG36 by a DNA fragment with the 48 bp coding sequences of GFP₁₁ linked to a 27 bp linker sequence (Kaddoum *et al.*, 2010), which was generated by annealing phosphorylated oligonucleotides *XbaI*-GFP₁₁-Fw and *SpeI*-GFP₁₁-Rev. To this end, the oligonucleotides were mixed, boiled for 5 min and incubated at room temperature for 3 hours. This fragment, which is flanked by *XbaI* and *SpeI* compatible overhangs, was inserted into digested pUG36 with *XbaI* and *SpeI*.

To target and visualize VirD2(mod) into yeast mitochondria, pUG36[GFP₁₁-VirD2(mod)] and pUG36[MTS-GFP₁₁-VirD2(mod)] were constructed. pART7[phiLOV2.1-VirD2(mod)] (see below) was digested with *BamHI* and *ClaI* restriction enzymes to obtain the *BamHI*-VirD2(mod)-*ClaI* DNA fragment. Subsequently, this fragment was ligated into pUG36[GFP₁₁] digested with *BamHI* and *ClaI* resulting in pUG36[GFP₁₁-VirD2(mod)]. Finally, the *XbaI*-MTS-*XbaI* DNA fragment was digested from pJET1.2[*XbaI*-MTS-*XbaI*] and ligated into digested (*XbaI*) and dephosphorylated pUG36[GFP₁₁-VirD2(mod)] to produce pUG36[MTS-GFP₁₁-VirD2(mod)].

To produce pBBR6[*pvirE*], the *EcoRI-pvirE-PstI* fragment was obtained by PCR with *EcoRI-pvirE-Fw* and *PstI-pvirE-Rev* primers using pSDM3756 (Sakalis *et al.*, 2014) as a template, and the PCR fragment was ligated into pBBR6 digested with *EcoRI* and *PstI*. To construct pBBR6[*pvirF*] plasmid, the *virF* promoter was amplified from pSDM3760. The *EcoRI-pvirF-PstI* PCR fragment, amplified with *EcoRI-pvirF-Fw* and *PstI-pvirF-Rev* primers, was cloned into pBBR6 digested with *EcoRI* and *PstI* yielding pBBR6[*pvirF*]. The N-terminal chloroplast targeting sequence (CTS) of the *A. thaliana FedA* gene was amplified from pCTP-Linker plasmid (van Tol, 2016). A *PstI-CTS-XmaI* PCR fragment, amplified using the primer pair *PstI-CTS-Fw* and *XmaI -CTS-Rev*, was cloned into the pBBR6[*pvirE*] and pBBR6[*pvirF*] constructing pBBR6[*pvirE-CTS^{XmaI}*] and pBBR6[*pvirF-CTS^{XmaI}*], respectively. To generate pBBR6[*pvirE-phiLOV2.1^{BamHI}*], pBBR6[*pvirF-phiLOV2.1^{BamHI}*], pBBR6[*pvirE-CTS-phiLOV2.1^{BamHI}*] and pBBR6[*pvirF-CTS-phiLOV2.1^{BamHI}*], DNA sequence coding for phiLOV2.1ΔTAA was amplified from pSDM3784 (Roushan *et al.*, 2018). A *XmaI-phiLOV2.1ΔTAA-BamHI* PCR fragment, amplified with the *XmaI-phiLOV2.1-Fw* and *BamHI-phiLOV2.1ΔTAA-Rev* primers, was cloned into the pBBR6[*pvirE*], pBBR6[*pvirF*], pBBR6[*pvirE-CTS*] and pBBR6[*pvirF-CTS*].

A *BamHI-VirE2-XbaI* PCR fragment was produced by PCR using *BamHI-VirE2-Fw* and *XbaI-VirE2-Rev* primers and pJET1.2[VirE2] (Sakalis *et al.*, 2014) as template and was ligated into digested (with *BamHI* and *XbaI*) pBBR6[pVirE], pBBR6[*pvirE-CTS^{BamHI}*], pBBR6[*pvirE-phiLOV2.1*] and pBBR6[*pvirE-CTS-phiLOV2.1*] to obtain pBBR6[*pvirE-VirE2*], pBBR6[*pvirE-CTS-VirE2*], pBBR6[*pvirE-phiLOV2.1-VirE2*] and pBBR6[*pvirE-CTS-phiLOV2.1-VirE2*], respectively.

To produce pBBR6[*pvirF-phiLOV2.1-VirD2*], the *SpeI-VirD2-XbaI* DNA fragment amplified by PCR using the *SpeI-VirD2-Fw* and *XbaI-VirD2-Rev* primers and pSDM3149 as a template, was inserted into *SpeI* and *XbaI* digested pBBR6[*pvirF-phiLOV2.1*]. The *BamHI-VirD2mod-XbaI* PCR fragment, amplified with *BamHI-VirD2mod-Fw* and *XbaI-VirD2mod-Rev* primers, was cloned into pBBR6[*pvirF*], pBBR6[*pvirF-phiLOV2.1*], pBBR6[*pvirF-CTS^{BamHI}*] and pBBR6[*pvirF-CTS-phiLOV2.1*] digested with *BamHI* and *XbaI* to produce pBBR6[*pvirF-VirD2(mod)*], pBBR6[*pvirF-PhiLOV2.1-VirD2(mod)*], pBBR6[*pvirF-CTS-VirD2(mod)*] and pBBR6[*pvirF-CTS-phiLOV2.1-VirD2(mod)*], respectively.

A *Pst*I-CTS-*Sph*I-*Spe*I PCR fragment, amplified using the primers *Pst*I-CTS-Fw and *Sph*I*Spe*I-CTS-Rev and pCTP-Linker plasmid as template, was cloned into the pBBR6[*pvirF*] creating pBBR6[*pvirF*-CTS^{*Sph*I*Spe*I}]. Next, the sequence coding for the phiLOV2.1ΔTAA, amplified by using *Sph*I-phiLOV2.1-Fw and *Spe*I-phiLOV2.1ΔTAA-Rev as primers and pUG36[phiLOV2.1ΔTAA] (Roushan *et al.*, 2018) as PCR template, was inserted into pBBR6[*pvirF*-CTS^{*Sph*I*Spe*I}] after digestion with *Sph*I and *Spe*I, generating pBBR6[*pvirF*-CTS-PhiLOV2.1^{*Spe*I}]. A *Spe*I-*VirD2*-*Xba*I PCR fragment was obtained by PCR using pSDM3149 as template and the primers *Spe*I-*VirD2*-Fw and *Xba*I-*VirD2*-Rev. This PCR fragment was cloned into pBBR6[*pvirF*], pBBR6[*pvirF*-phiLOV2.1], pBBR6[*pvirF*-CTS^{*Spe*I}] and pBBR6[*pvirF*-CTS-phiLOV2.1] digested by *Spe*I and *Xba*I, generating pBBR6[*pvirF*-*VirD2*], pBBR6[*pvirF*-phiLOV2.-*VirD2*], pBBR6[*pvirF*-CTS-*VirD2*] and pBBR6[*pvirF*-CTS-phiLOV2.1-*VirD2*], respectively.

All plasmids with pBBR6 backbone were sequenced with pBBR6-80bpseq-FW and pBBR6-80bpseq-Rev primers. The pBBR6[*pvirF*-CTS-*VirD2*(mod)], pBBR6[*pvirF*-phiLOV-*VirD2*(mod)], pBBR6[*pvirE*-CTS-*VirE2*], pBBR6[*pvirE*-phiLOV-*VirE2*], pBBR6[*pvirE*-CTS-phiLOV-*VirE2*], pBBR6[*pvirF*-CTS-*VirD2*], pBBR6[*pvirF*-phiLOV-*VirD2*] and pBBR6[*pvirF*-CTS-phiLOV-*VirD2*] were additionally sequenced with the use of sequencing primers Seq-*pvirF*-*VirD2*mod-Fw and Seq-*pvirF*-*VirD2*mod-Rev, Seq-*pvirE*-*VirE2*-Fw and Seq-*pvirE*-*VirE2*-Rev, Seq-int-CTS and Seq-int-*VirD2*wt, respectively.

To express phiLOV2.1-tagged *VirE2*, *VirD2* and *VirD2*(mod) with or without CTS in protoplasts under control of 35S promoter, the *Xho*I-CTS-phiLOV2.1-*VirE2*-*Xba*I, *Cla*I-CTS-phiLOV2.1-*VirD2*-*Xba*I and *Cla*I-CTS-phiLOV2.1-*VirD2*(mod)-*Xba*I PCR fragments were generated using the primer pairs of *Xho*I-CTS-*VirE2*-Fw & *Xba*I-*VirE2*-Rev, *Cla*I-CTS-*VirD2*-Fw & *Xba*I-*VirD2*-Rev or *Cla*I-CTS-*VirD2*(mod)-Fw & *Xba*I-*VirD2*-Rev and pBBR6[CTS-phiLOV2.1-*VirE2*], pBBR6[CTS-phiLOV2.1-*VirD2*] and pBBR6[CTS-phiLOV2.1-*VirD2*(mod)], respectively, as templates. These PCR fragments were cloned into pART7 digested via either *Xho*I and *Xba*I (*VirE2*) or *Cla*I and *Xba*I (*VirD2* and *VirD2*(mod)), to obtain pART7[CTS-phiLOV2.1-*VirE2*], pART7[CTS-phiLOV2.1-*VirD2*] and pART7[CTS-phiLOV2.1-*VirD*(mod)]. To generate, pART7[39phiLOV2.1-*VirE2*], first phiLOV2.1-tagged *virE2*, was amplified by PCR on pBBR6[39phiLOV2.1-*VirE2*] using the primers *Kpn*I-39phiLOV2.1-Fw and *Xba*I-39phiLOV2.1-Rev. Then, pART7[39phiLOV2.1-*VirE2*] was created by ligation of this 39phiLOV2.1-*VirE2* fragment into pART7 after

digestion with *XbaI* and *KpnI*. An *XhoI*-phiLOV2.1-VirD2-*XbaI* PCR fragment was obtained using the *XhoI*-phiLOV2.1-Fw and *XbaI*-VirD2-Rev primers and pBBR6[phiLOV2.1-VirD2] as template. This PCR fragment was ligated into pART7 after digestion with *XhoI* and *XbaI* to obtain pART7[phiLOV2.1-VirD2]. Plasmid pART7[CTS-phiLOV2.1-VirD2(mod)] was digested with *SmaI* and *XbaI* to obtain *smaI*-phiLOV2.1-VirD2(mod)-*XbaI* and this fragment was ligated into the pART7 after digestion with *SmaI* and *XbaI* to generate pART7[phiLOV2.1-VirD2(mod)].

Plant lines. The plant lines used in this study were: *Nicotiana tabacum* (SR1), *Arabidopsis thaliana* Col-0, *A.thaliana efr-1* (SALK_044334) and *Nicotiana glauca*.

Co-cultivation of *Agrobacterium* and yeast. Cocultivation of *Agrobacterium* and yeast was performed using an adapted version of the published protocol (Bundock *et al.*, 1995). *Agrobacterium* strains were grown overnight in 15 ml of LC medium with appropriate antibiotics (Table 2) at 28°C. Subsequently, *Agrobacterium* cells were centrifuged and re-suspended in IM supplemented with 0.2 mM acetosyringone and grown at 28°C for 6 hours. After overnight incubation of yeast strains in 10 ml of YPD medium at 30°C, 100 µl of the culture was inoculated in 20 ml of fresh YPD medium and incubated for 6 hours at 28°C. Then, 1 ml of yeast culture was washed with 500 µl of IM and re-suspended in 1 ml of IM. Sixty microliters of *Agrobacterium* suspension were mixed with 60 µl of yeast suspension and 100 µl of the mixture were spotted on cellulose nitrate filters (Sartorius). Filters were dried at room temperature and were laid onto IM plates supplemented with histidine (2 mg/ml), uracil (2 mg/ml), tryptophan (2 mg/ml) and incubated at 21°C. For microscopy, cells were eluted from the filters by transferring the filters to an 2 ml Eppendorf tube, adding 0.5 ml of MY medium and vigorously vortexing, followed by two more washes with 0.5 ml MY medium. Cells were centrifuged and were re-suspended into 200 µl of MY medium and an aliquot (5µl) was used for microscopy.

Agroinfiltration of plants. After overnight growth of *A. tumefaciens* strains at 28°C in LC medium, cultures were diluted to the OD₆₀₀≈0.8 in 10 ml of induction medium with 200 µM acetosyringone (AS) and incubated for three hours at 28°C. A blunt-tipped 10 ml plastic syringe (Nissho NIPRO Europe N.V) was used to inject smoothly and with gentle pressure into the lower surface of the leaves of *N. tabacum* SR1. After approximately 24 hours, the lower side of injected leaves was used for confocal microscopy (Wroblewski *et al.*, 2005).

Tumor formation assay. *A. tumefaciens* was grown overnight at 28°C in LC medium with the appropriate antibiotics. Then, cells were washed three times with a 0.9% (w/v) NaCl solution and diluted to OD₆₆₀ ≈ 1.0 in 0.9% (w/v) NaCl. One month old *N. glauca* plants were wounded at three sites on the stem with a sterile toothpick. Subsequently, 20 µl of *A. tumefaciens* suspension was inoculated at each wounded site. Tumors were photographed one month after inoculation.

AGROBEST infection and GUS assay. The AGROBEST infection procedure was performed as described by Wu *et al.*, 2014 with some minor modifications. *A. thaliana efr-1* seeds were sterilized and grown on 6-wells plates containing MA medium. Seeds were grown for 4 days before AGROBEST infection. *A. tumefaciens* was freshly streaked from -80°C glycerol stock onto a LC agar plate containing appropriate antibiotics and incubated for 2 days at 28°C. A fresh single colony from the plate was used to inoculate 5 ml of LC liquid medium containing appropriate antibiotics and the culture was incubated at 28°C overnight with shaking. For pre-induction of *A. tumefaciens vir* gene expression, *A. tumefaciens* cells were pelleted and re-suspended to OD₆₀₀ 0.2 in 3ml of IM with 200 µM Acetosyringone with appropriate antibiotics and incubated at 20°C overnight. Before co-cultivation, *A. tumefaciens* cells were pelleted and re-suspended in IM to OD₆₀₀ 0.02. The 4 days grown *efr-1* seedlings were transferred into plates containing MA with 200 µM Acetosyringone and 200 µl *A. tumefaciens* cells freshly prepared was added to the 6-wells plates and incubated in a growth chamber (16hr light/8hr darkness) at 21°C for 4 days before GUS staining (Wu *et al.*, 2014).

For GUS staining, seedlings were stained with 5-bromo-4-chloro-3-indolyl glucuronide (X-Gluc) at 37°C for 24 hours in dark with gentle shaking. After staining, seedlings were destained with 70% ethanol for 24 hours. Then, pictures were taken with a Leica MZ16 FA fluorescence stereomicroscope using zoom drive of 7.17X (exposure: 1.1 s, gain: 1.0, saturation: 1.0, gamma: 1.21).

Protoplast transformation. Protoplasts were derived from a five days old *A. thaliana* Col-0 cell suspension as described by Schirawski *et al.* (2000) and were transformed with 10 µg of plasmid DNA per 10⁶ protoplasts using Polyethyleneglycol (PEG) (Schirawski *et al.*, 2000). The transformed protoplasts were incubated at 27°C in the dark for 24 hours before treatments and microscopy.

Confocal microscopy. To observe leaf epidermis, agro-infiltrated leaf tissues were detached from *N. tabacum* SR1 plants and put in 1.5% low-melting agarose gel on a glass slide with a coverslip. For yeast images, the cells were grown in MY medium supplemented with appropriate nutrients and then put on a slide with a coverslip. Plant and yeast cells were analyzed using a Zeiss LSM5 Exciter confocal microscope using a 20X and 63X magnifying objective, respectively. GFP and phiLOV2.1 signal were detected using an argon 488 nm laser and a 505-600 nm band pass emission filter. Yeast cells were visualized directly or after staining with MitoTracker (MitoTracker Red FM) according to the standard protocol from Molecular Probes (Invitrogen). MitoTracker and RFP were excited at 543 nm and emitted light collected at 580-640 nm. Chlorophyll fluorescence was determined using a long pass 650 nm emission filter after excitation at 488 nm. All images were processed using ImageJ 1.48F software (Abràmoff *et al.*, 2004).

Table 1: Yeast strains used in this study

Yeast strain	Genotype	Source/reference
CEN.PK2-1C	<i>MATa ura3-52 leu2-112 trp1-289 his3-Δ1</i>	P. Kötter, Göttingen, Germany.
426::GFP ₁₋₁₀ (GG3388)	CEN.PK2-1C <i>leu2::pRS306[P_{MET25}-GFP₁₋₁₀-T_{CYC1}] (LEU2)</i>	(Sakalis <i>et al.</i> , 2014)
MTS-GFP ₁₋₁₀ (GG3458)	CEN.PK2-1C <i>leu2::pRS305[P_{MET25}-MTS-GFP₁₋₁₀-T_{CYC1}] (LEU2)</i>	This study.
MTS-GFP ₁₋₁₀ - 34GFP ₁₁ [VirD2] (GG3459)	CEN.PK2-1C <i>leu2::pRS305[P_{MET25}-MTS-GFP₁₋₁₀-T_{CYC1}] (LEU2)</i> <i>pUG34[P_{MET25}-GFP₁₁-VirD2-T_{CYC1}] (HIS3)</i>	This study.
MTS-GFP ₁₋₁₀ - 36::39GFP ₁₁ [VirE2] (GG3440)	CEN.PK2-1C <i>leu2::pRS305[P_{MET25}-MTS-GFP₁₋₁₀-T_{CYC1}] (LEU2)</i> <i>pUG36[P_{MET25}-39GFP₁₁-VirE2-T_{CYC1}] (URA3)</i>	This study.
426::GFP ₁₋₁₀ - 34GFP ₁₁ [VirD2] (GG3392)	CEN.PK2-1C <i>leu2::pRS305[P_{MET25}-GFP₁₋₁₀-T_{CYC1}] (LEU2)</i> <i>pUG34[P_{MET25}-GFP₁₁-VirD2-T_{CYC1}] (HIS3)</i>	(Sakalis, 2013)
426::GFP ₁₋₁₀ - 36GFP ₁₁ [VirD2(mod)] (GG3441)	CEN.PK2-1C <i>leu2::pRS305[P_{MET25}-GFP₁₋₁₀-T_{CYC1}] (LEU2)</i> <i>pUG36[P_{MET25}-GFP₁₁-VirD2(mod)-T_{CYC1}] (URA3)</i>	This study.
426::GFP ₁₋₁₀ - 36GFP ₁₁ [MTS- VirD2(mod)] (GG3442)	CEN.PK2-1C <i>leu2::pRS305[P_{MET25}-GFP₁₋₁₀-T_{CYC1}] (LEU2)</i> <i>pUG36[P_{MET25}-MTS-GFP₁₁-VirD2(mod)-T_{CYC1}] (URA3)</i>	This study.
MTS-GFP ₁₋₁₀ - 36GFP ₁₁ [VirD2(mod)] (GG3443)	CEN.PK2-1C <i>leu2::pRS306[P_{MET25}-MTS-GFP₁₋₁₀-T_{CYC1}] (LEU2)</i> <i>pUG36[P_{MET25}-GFP₁₁-VirD2(mod)-T_{CYC1}] (URA)</i>	This study.
MTS-GFP ₁₋₁₀ - 36GFP ₁₁ [MTS- VirD2(mod)] (GG3444)	CEN.PK2-1C <i>leu2::pRS306[P_{MET25}-MTS-GFP₁₋₁₀-T_{CYC1}] (LEU2)</i> <i>pUG36[P_{MET25}-MTS-GFP₁₁-VirD2(mod)-T_{CYC1}] (URA)</i>	This study.

Table 2: *Agrobacterium* strains used in this study

<i>Agrobacterium</i> strain	Specifications	Source/reference
LBA1010	C58 containing pTiB6, Rif	(Koekman <i>et al.</i> , 1982)
LBA1100	C58 containing pTiB6Δ (ΔT-DNA, Δocc, Δtra), Rif, Spc [†]	(Beijersbergen <i>et al.</i> , 1992)
LBA1100 (pRAL7100)	LBA1100 with binary vector pRAL7100, Rif, Km [†]	(Bundock <i>et al.</i> , 1995)
LBA2572 (LBA1010ΔE2)	<i>virE2</i> deletion in LBA1010, Rif	den Dulk-Ras, unpublished
LBA2573 (LBA1100 ΔE2)	<i>virE2</i> deletion in LBA1100, Rif, Spc	(Hodges <i>et al.</i> , 2006)
LBA2556 (LBA1100ΔD2)	<i>virD2</i> deletion in LBA1100, Rif, Spc	Jurado-Jácome, den Dulk-Ras, Vergunst, and Hooykaas, unpublished
LBA2569 (LBA1010ΔD2)	<i>virD2</i> deletion in LBA1010, Rif	Vergunst, den Dulk-Ras and Hooykaas, unpublished
LBA1010(pBBR6)	LBA1010 with pBBR6. Rif, Gm	This study.
LBA1100(pBBR6)	LBA1100 with pBBR6. Rif, Spc, Gm	This study.
LBA2572(pBBR6)	LBA2572 with pBBR6. Rif, Gm	This study.
LBA2569(pBBR6)	LBA2569 with pBBR6. Rif, Gm	This study.
LBA2573 (pBBR6-phiLOV2.1-VirE2)	LBA2573 with pBBR6[phiLOV2.1-VirE2]. Expression of the internal-tagged phiLOV2.1-VirE2 fusion protein under control of the <i>virE</i> promoter, Rif, Spc, Gm	This study.
LBA2572 (pBBR6-phiLOV2.1-VirE2)	LBA2572 with pBBR6[phiLOV2.1-VirE2]. Expression of the internal-tagged phiLOV2.1-VirE2 fusion protein under control of the <i>virE</i> promoter, Rif, Spc, Gm	This study.
LBA2572 (pBBR6-VirE2)	LBA2572 with pBBR6-VirE2. Expression of the VirE2 protein under control of the <i>virE</i> promoter, Rif, Spc, Gm	This study.

LBA2573 (pBBR6-CTS- phiLOV2.1-VirE2)	LBA2573 with pBBR6[CTS-phiLOV2.1- VirE2]. Expression of the N-terminally-tagged phiLOV2.1-VirE2 fusion protein under control of the <i>virE</i> promoter, Rif, Spc, Gm	This study.
LBA2572 (pBBR6-CTS- phiLOV2.1-VirE2)	LBA2572 with pBBR6[CTS-phiLOV2.1- VirE2]. Expression of the N-terminally-tagged phiLOV2.1-VirE2 fusion protein under control of the <i>virE</i> promoter, Rif, Spc, Gm	This study.
LBA2556 (pBBR6-phiLOV2.1- VirD2)	LBA2556 with pBBR6[phiLOV2.1-VirD2]. Expression of the N-terminally-tagged phiLOV2.1-VirD2 fusion protein under control of the <i>virD</i> promoter, Rif, Spc, Gm	This study.
LBA2569 (pBBR6-VirD2)	LBA2569 with pBBR6 [VirD2]. Expression of VirD2 protein under control of the <i>virD</i> promoter, Rif, Gm	This study.
LBA2569 (pBBR6-phiLOV2.1- VirD2)	LBA2569 with pBBR6 [phiLOV2.1-VirD2]. Expression of the N-terminally-tagged phiLOV2.1-VirD2 fusion protein under control of the <i>virD</i> promoter, Rif, Gm	This study.
LBA2556 (pBBR6-CTS- phiLOV2.1-VirD2)	LBA2556 with pBBR6[CTS-phiLOV2.1- VirD2]. Expression of the N-terminally-tagged phiLOV2.1-VirD2 fusion protein under control of the <i>virD</i> promoter, Rif, Spc, Gm	This study.
LBA2569 (pBBR6-CTS- phiLOV2.1-VirD2)	LBA2569 with pBBR6 [CTS-phiLOV2.1- VirD2]. Expression of the N-terminally-tagged phiLOV2.1-VirD2 fusion protein under control of the <i>virD</i> promoter, Rif, Gm	This study.
LBA2556 (pBBR6-VirD2(mod))	LBA2556 with pBBR6[VirD2(mod)]. Expression of the VirD2(mod) protein under control of the <i>virD</i> promoter, Rif, Spc, Gm	This study.
LBA2556 (pBBR6-phiLOV2.1- VirD2(mod))	LBA2556 with pBBR6[phiLOV2.1- VirD2(mod)]. Expression of the N-terminally-tagged phiLOV2.1-VirD2 fusion protein under control of the <i>virD</i> promoter, Rif, Spc, Gm	This study.

LBA2569 (pBBR6-phiLOV2.1- VirD2(mod))	LBA2569 with pBBR6 [phiLOV2.1- VirD2(mod)]. Expression of the N-terminally-tagged phiLOV2.1-VirD2 fusion protein under control of the <i>virD</i> promoter, Rif, Gm	This study.
LBA2556 (pBBR6-CTS- phiLOV2.1- VirD2(mod))	LBA2556 with pBBR6[CTS-phiLOV2.1- VirD2(mod)]. Expression of the N-terminally-tagged phiLOV2.1-VirD2 fusion protein under control of the <i>virD</i> promoter, Rif, Spc, Gm	This study.
LBA2569 (pBBR6-CTS- phiLOV2.1- VirD2(mod))	LBA2569 with pBBR6 [CTS-phiLOV2.1- VirD2(mod)]. Expression of the N-terminally-tagged phiLOV2.1-VirD2 fusion protein under control of the <i>virD</i> promoter, Rif, Gm	This study.

Table 3: Plasmids used in this study

Name	Properties	Source/reference
chloroplast-mCherry (CD3- 1000)	pFGC plasmid with targeting sequence (first 79 amino acids) of the small subunit of tobacco rubisco fused with mCherry under control of <i>35S</i> promoter. Glufosinate selection.	Nelson <i>et al.</i> , 2007).
pART7	Plant cloning vector containing <i>35S</i> promoter, octopine synthase (<i>OCS</i>) terminator and ampicillin resistance marker.	(Gleave, 1999)
pART7[39phiLOV2.1-VirE2] (pSDM3774)	pART7 based vector containing internally- tagged phiLOV2.1- <i>virE2</i> under control of <i>35S</i> promoter and octopine synthase (<i>OCS</i>) terminator.	(Roushan <i>et al.</i> , 2018).
pART7[CTS-39phiLOV2.1- VirE2] (pSDM4124)	pART7 based vector containing chloroplast targeting sequence (CTS) of <i>FedA</i> gene fused to 39phiLOV2.1- <i>virE2</i> under control of <i>35S</i> promoter and octopine synthase (<i>OCS</i>) terminator.	This study.
pART7[phiLOV2.1-VirD2] (pSDM4125)	pART7 based vector containing phiLOV2.1- <i>virD2</i> under control of <i>35S</i> promoter and octopine synthase (<i>OCS</i>) terminator.	This study.

pART7[CTS-phiLOV2.1-VirD2] (pSDM4126)	pART7 based vector containing chloroplast targeting sequence (CTS) of <i>FedA</i> gene fused to phiLOV2.1- <i>virD2</i> under control of 35S promoter and octopine synthase (<i>OCS</i>) terminator.	This study.
pART7[phiLOV2.1-VirD2(mod)] (pSDM4127)	pART7 based vector containing phiLOV2.1- <i>virD2</i> (mod) under control of 35S promoter and octopine synthase (<i>OCS</i>) terminator.	This study.
pART7[CTS-phiLOV2.1-VirD2(mod)] (pSDM4128)	pART7 based vector containing chloroplast targeting sequence (CTS) of <i>FedA</i> gene fused to phiLOV2.1- <i>virD2</i> (mod) under control of 35S promoter and octopine synthase (<i>OCS</i>) terminator.	This study.
pBBF[flag-D2-204-F]	pBBF containing the relaxase domain of VirD2 with a flag tag and the terminator/T4SS translocation signal of VirF	(van Kregten <i>et al.</i> , 2009)
pBBR6	Broad host range, non-mobilizable plasmid with Gentamycin resistance marker derived from pBBR1-MS2.	(Kovach <i>et al.</i> , 1994)
pBBR6[p <i>virE</i>] (pSDM4129)	pBBR6 backbone containing <i>virE</i> promoter.	This study.
pBBR6[p <i>VirF</i>] (pSDM4130)	pBBR6 backbone with <i>virF</i> promoter.	This study.
pBBR6[39GFP ₁₁ - <i>VirE2</i>] (pSDM4131)	pBBR6 backbone containing 39GFP ₁₁ - <i>virE2</i> under control of the <i>virE</i> promoter.	This study.
pBBR6[p <i>VirE</i> -CTS ^{XmaI}] (pSDM4132)	pBBR6 backbone containing chloroplast targeting sequence (CTS) of <i>FedA</i> under control of the <i>virE</i> promoter.	This study.
pBBR6[p <i>VirF</i> -CTS ^{XmaI}] (pSDM4133)	pBBR6 backbone containing chloroplast targeting sequence (CTS) of <i>FedA</i> under control of the <i>virF</i> promoter.	This study.
pBBR6[p <i>VirF</i> -CTS ^{SphI/SpeI}] (pSDM4134)	pBBR6 backbone containing chloroplast targeting sequence (CTS) of <i>FedA</i> under control of the <i>virF</i> promoter.	This study.

pBBR6[pVirE- phiLOV2.1 ^{BamHI}] (pSDM4135)	pBBR6 backbone containing phiLOV2.1 under control of the <i>virE</i> promoter.	This study.
pBBR6[pVirF- phiLOV2.1 ^{BamHI}] (pSDM4136)	pBBR6 backbone containing phiLOV2.1 under control of the <i>virF</i> promoter.	This study.
pBBR6[MTS-39GFP ₁₁ -VirE2] (pSDM4137)	pBBR6 backbone containing mitochondrial targeting sequence (MTS) of citrate synthase I fused to 39GFP ₁₁ . <i>virE2</i> under control of the <i>virE</i> promoter.	This study.
pBBR6[pVirF-CTS- phiLOV2.1 ^{SpeI}] (pSDM4138)	pBBR6 backbone containing chloroplast targeting sequence (CTS) of <i>FedA</i> fused to phiLOV2.1 under control of the <i>virF</i> promoter.	This study.
pBBR6[pVirE-VirE2] (pSDM4139)	pBBR6 backbone containing the <i>virE2</i> gene under control of the <i>virE</i> promoter.	This study.
pBBR6[pVirE-CTS-VirE2] (pSDM4140)	pBBR6 backbone with chloroplast targeting sequence (CTS) of <i>FedA</i> fused to <i>virE2</i> under control of the <i>virF</i> promoter.	This study.
pBBR6[pVirE-phiLOV2.1- VirE2] (pSDM4141)	pBBR6 backbone containing phiLOV2.1- <i>virE2</i> under control of the <i>virE</i> promoter.	This study.
pBBR6[pVirE-CTS- phiLOV2.1] (pSDM4142)	pBBR6 containing chloroplast targeting sequence (CTS) of <i>FedA</i> fused to phiLOV2.1 under control of the <i>VirE</i> promoter.	This study.
pBBR6[pVirE-CTS- phiLOV2.1-VirE2] (pSDM4143)	pBBR6 containing the CTS of <i>FedA</i> fused to phiLOV2.1 under control of the <i>VirE</i> promoter.	This study.
pBBR6[pVirF-VirD2] (pSDM4144)	pBBR6 containing <i>virD2</i> under control of the <i>VirF</i> promoter.	This study.

pBBR6[pVirF-CTS-VirD2] (pSDM4145)	pBBR6 containing CTS of <i>FedA</i> tagged to <i>virD2</i> under control of the <i>virF</i> promoter.	This study.
pBBR6[pVirF-phiLOV2.1-VirD2] (pSDM4146)	pBBR6 containing phiLOV2.1 tagged to <i>virD2</i> under control of the <i>virF</i> promoter.	This study.
pBBR6[pVirF-CTS-phiLOV2.1] (pSDM4147)	pBBR6 containing phiLOV2.1 tagged with the CTS of <i>FedA</i> under control of the promoter VirF.	This study.
pBBR6[pVirF-CTS-phiLOV2.1-VirD2] (pSDM4148)	pBBR6 containing the CTS of <i>FedA</i> tagged to phiLOV2.1- <i>virD2</i> under control of the promoter VirF.	This study.
pBBR6[pVirF-VirD2(mod)] (pSDM4149)	pBBR6 containing the relaxase domain of VirD2 under control of the <i>VirF</i> promoter.	This study.
pBBR6[pVirF-CTS-VirD2(mod)] (pSDM4150)	pBBR6 containing the CTS of <i>FedA</i> tagged to relaxase domain of VirD2 under control of the <i>VirF</i> promoter.	This study.
pBBR6[pVirF-phiLOV2.1-VirD2(mod)] (pSDM4151)	pBBR6 containing the phiLOV2.1 tagged to relaxase domain of VirD2 under control of the <i>VirF</i> promoter.	This study.
pBBR6[pVirF-CTS-phiLOV2.1-VirD2(mod)] (pSDM4152)	pBBR6 containing the CTS of <i>FedA</i> tagged to phiLOV2.1-VirD2(mod) under control of the <i>VirF</i> promoter.	This study.
pCTP-Linker	Plasmid containing the chloroplasts transit peptide of <i>A. thaliana FedA</i> and the first 8 amino acids of the <i>FedA</i> protein with a linker.	(van Tol, 2016)
pJET1.2[<i>XbaI</i> -MTS- <i>XbaI</i>]	Clonejet™ PCR cloning pUC19 based vector for blunt cloning with MTS flanked by <i>XbaI</i> and <i>XbaI</i> restriction sites.	This study.
pJET1.2[VirE2]	Clonejet™ PCR cloning pUC19 based vector for blunt cloning containing VirE2.	(Sakalis <i>et al.</i> , 2014)

pRS305[MTS-GFP ₁₋₁₀] (pSDM4153)	Yeast integrative vector with MTS-GFP ₁₋₁₀ under control of the <i>MET25</i> promoter and terminator. <i>LEU2</i> marker.	This study.
pSDM3149	<i>virD2</i> gene (wildtype) behind <i>virD</i> promoter, located on plasmid pBBR6 (pVD43 was cloned as EcoRV/EcoRI fragment in pIC2OH by Amke den Dulk).	(Vergunst, unpublished)
pSDM3163[GFP ₁₁ -VirF] (pSDM3760)	pSDM3163 backbone with coding sequence of GFP ₁₁ - <i>virF</i> under control of the <i>virF</i> promoter	(Sakalis, 2013)
pUG36[phiLOV2.1ΔTAA] (pSDM3784)	pUG36 centromeric plasmid containing phiLOV2.1 without stop codon under control of <i>MET25</i> promoter and <i>CYC1</i> terminator. <i>URA3</i> marker.	(Roushan <i>et al.</i> , 2018)(Chapter 3)
pUG34[GFP ₁₁ -VirD2] (pRUL1280)	Centromeric plasmid with <i>GFP 11-virD2</i> under control of the <i>MET25</i> promoter and <i>CYC1</i> terminator. <i>HIS3</i> marker.	(Sakalis, 2013)
pUG36[phiLOV2.1ΔTAA] (pSDM3784)	Centromeric plasmid containing phiLOV2.1 without stop codon under control of <i>MET25</i> promoter and <i>CYC1</i> terminator. <i>URA3</i> marker.	(Roushan <i>et al.</i> , 2018)
pUG36[GFP ₁₁] (pSDM4154)	Centromeric plasmid containing GFP ₁₁ under control of <i>MET25</i> promoter and <i>CYC1</i> terminator. <i>URA3</i> marker.	This study.
pUG36[GFP ₁₁ -VirD2(mod)] (pSDM4155)	Centromeric plasmid for expression of GFP ₁₁ -VirD2(mod) under control of <i>MET25</i> promoter and <i>CYC1</i> terminator. <i>URA3</i> marker.	This study.
pUG36[MTS-GFP ₁₁ -VirD2(mod)] (pSDM4156)	Centromeric plasmid for expression of mitochondrial targeting sequence (MTS) of citrate synthase I fused to GFP ₁₁ -VirD2(mod) under control of <i>MET25</i> promoter and <i>CYC1</i> terminator. <i>URA3</i> marker.	This study.

pUG36[MTS] (pSDM4157)	Centromeric plasmid containing mitochondrial targeting sequence (MTS) of citrate synthase I under control of <i>MET25</i> promoter and <i>CYC1</i> terminator. <i>URA3</i> marker.	This study.
pUG36[MTS-39GFP ₁₁ -VirE2] (pSDM4158)	Centromeric plasmid for expression of mitochondrial targeting sequence (MTS) of citrate synthase I gene fused to 39GFP ₁₁ -VirE2 under control of <i>MET25</i> promoter and <i>CYC1</i> terminator. <i>URA3</i> marker.	This study.

Table 4: Primers used in this study

Primer name	Sequence (5' → 3') ^{a,b}
<i>Xba</i> I-MTS-Fw	AATCTAGAAATGTCAGCGATATTATCAACAAC
<i>Xba</i> I-MTS-Rev	AATCTAGAAATTTTCAGCAAATCTCTCCTTC
<i>Nde</i> I-MTS-Fw	AACATATGTCAGCGATATTATCAACAAC
<i>Nde</i> I-MTS-Rev	AACATATGAATTTTCAGCAAATCTCTCCTTC
<i>Xba</i> I- GFP ₁₁ -Fw	CTAGA CGGGACCACATGGTGCTGCACGAGTACGTGAACGCCGC CGGCATCACA ggcgacggcggcagcggcggcggcgcgcg <u>A</u>
<i>Spe</i> I-GFP ₁₁ -Rev	CTAGT gctgccgcgcgcgtgccgccgtgcc TGTGATGCCGGCGCGTTCACGTACTCGTGCAGCACCAT GTGGTCCCG <u>T</u>
Leu2 1A	CAAGGATCTTACCGCTGTTG
Leu2 1S	AGAGGTCGCCTGACGCATAT
Leu2 2A	ACAACGACCAAGCTCACATC
Leu2 2S	ACTGGAACAACACTCAACCCTA
<i>Eco</i> RI-pVirE-Fw	GGGGAATTCGGCTGCTCGTCACCAAC
<i>Pst</i> I-pVirE-Rev	GGGCTGCAGTGTCTCTCTCTGCAAAATTGCG
<i>Eco</i> RI-pVirF-Fw	GGGGAATTCACCGAGCTCCTATGATAGTCG
<i>Pst</i> I-pVirF-Rev	GGGCTGCAGGCTCCTGTGCTTTTGAAAGG
<i>Pst</i> I-CTS-Fw	GGCTGCAGATGGCTTCCACTGCTCTCTC

<i>Xma</i> I-CTS-Rev	GG <u>CCCGGG</u> GATGAACTTGACCTTGTATGTAGC
<i>Bam</i> HI-CTS-Rev	GGGGGATCCGATGAACTTGACCTTGTATGTAGC
<i>Spe</i> I-CTS-Rev	GG <u>ACTAGT</u> GATGAACTTGACCTTGTATGTAGC
<i>Sph</i> I <i>Spe</i> I-CTS- Rev	GG <u>ACTAGTGCATGCG</u> ATGAACTTGACCTTGTATGTAGC
<i>Xma</i> I-phiLOV-Fw	GGCCCGGGATGATAGAGAAGAGTTTC
<i>Bam</i> HI-phiLOV(Δ TAA)-Rev	AAAGGATCC <u>TACATGATCACTTCCA</u> ACGAG
<i>Spe</i> I-phiLOV(Δ TAA)-Rev	GG <u>ACTAGT</u> TACATGATCACTTCCAAC
<i>Sph</i> I-phiLOV-Fw	GGGGC <u>ATGCATGATAGAGA</u> AAGAGTTTC
<i>Bam</i> HI-VirD2mod-Fw	AAAGGATCCATGGCCGACTACAAGGACG
<i>Clal</i> -VirD2mod-Rev	GGGG <u>ATCGAT</u> GGATTAGACCGCGCGTTGATC
<i>Xba</i> I-VirD2mod-Rev	GGTCTAGATCATAGACCGCGCGTTG
<i>Bam</i> HI-VirE2-Fw	GGGGGATCCATGGATCTTTCTGGCAATG
<i>Xba</i> I-VirE2-Rev	GGTCTAGATCAAAAAGCTGTTGACGCTTTG
<i>Spe</i> I-VirD2-Fw	GG <u>ACTAGT</u> ATGCCCGATCGCG
<i>Xba</i> I-VirD2-Rev	GGTCTAGACTAGGTCCCCCGC
pBPR6-80bpseq-Fw	CAGGGTTTTCCAGTCACGAC
pBPR6-80bpseq-Rev	GACCATGATTACGCCAAGCGCG
Seq-pVirF-VirD2mod-Fw	GCCTATCATCGTCTGACTGAC
Seq-pVirF-VirD2mod-Rev	ACTTCTATGCCACCGATC
Seq-pVirE-VirE2-Fw	GCGCTTGACGGTGTGTTCAA
Seq-pVirE-VirE2-Rev	GACAGAGTATTCGCGCGAGG
Seq-int-CTS-Fw	GCTCCAATCAGTCTCCGTTCC
Seq-int-VirD2wt	CGTGGTAGGCTGTCAGATAG
<i>Xho</i> I-CTS-VirE2-Fw	AAA <u>ACTCGAGT</u> GGCTTCCACTGCTCTCTC
<i>Clal</i> -CTS-VirD2-Fw	GGGG <u>ATCGAT</u> ATGGCTTCCACTGCTCTCTC
<i>Xba</i> I-VirD2-Rev	AATCTAGACTAGGTCCCCCGCG
<i>Clal</i> -CTS-VirD2mod-Fw	GGGG <u>ATCGAT</u> ATGGCTTCCACTGCTCTCTC
<i>Xba</i> I-VirD2mod-Rev	AATCTAGATAGACCGCGCGTTGATC

<i>Xho</i> I-phiLOV2.1-Fw	GGGGCTCGAGATGATAGAGAAGAGTTTCGTC
<i>Kpn</i> I-39phiLOVE2-Fw	CCC <u>GGTACCA</u> TGGATCTTTCTGGCAATGAG
<i>Xba</i> I-39phiLOVE2-Rev	GGT <u>CTAGAT</u> CAAAAGCTGTTGACGC
pART7-Seq-Fw	GCGATAAAGGAAAGGCTATC
pART7-Seq-Rev	GTACAATCAGTAAATTGAACGG
<i>Bam</i> HI-phiLOV(Δ TAA)-Rev	AA <u>AGGATCCT</u> TACATGATCACTTCCAACGAG

a, (partial) restriction sites are underline.

b, linker sequences are annotated in lowercase.

RESULTS

Targeting VirD2 and VirE2 into yeast mitochondria

The effector protein VirD2 contains NLSs and as shown in Chapters 2 and 3 it is targeted into the nucleus both after ectopic expression in yeast as well as after AMT of plants and yeast. In this way, VirD2 may guide the T-DNA into the nucleus. In order to guide VirD2 into organelles we made use of VirD2(mod) which is the relaxase part of VirD2 lacking the NLSs and to which the VirF T4SS signal was added at the C-terminus. It has been shown that VirD2(mod) can replace wild type VirD2 during AMT (van Kregten *et al.*, 2009). To target VirD2(mod) and VirE2 into yeast mitochondria these proteins were tagged with the mitochondrial targeting sequence (MTS) of citrate synthase 1 (*CIT1*) consisting of the first 52 amino acids of Cit1 (Okamoto *et al.*, 2001).

To visualize the localization of MTS-VirD2 and MTS-VirD2(mod), the split-GFP technique was used. To this end, MTS-VirD2 and MTS-VirD2(mod) were tagged with GFP₁₁. The remaining part of GFP, GFP₁₋₁₀, was expressed in yeast. As GFP₁₋₁₀ may not enter the mitochondria, we also constructed yeast strains expressing GFP₁₋₁₀ tagged with the MTS (MTS-GFP₁₋₁₀). To study the localization of those newly constructed proteins yeast strain CEN.PK2-1C expressing GFP₁₋₁₀ was transformed with pUG34[GFP₁₁-VirD2], with pUG36[GFP₁₁-VirD2(mod)] and with pUG36[MTS-GFP₁₁-VirD2(mod)] and yeast strain CEN.PK2-1C expressing MTS-GFP₁₋₁₀ likewise was transformed with pUG34[GFP₁₁-VirD2], with pUG36[GFP₁₁-VirD2(mod)] and with pUG36[MTS-GFP₁₁-VirD2(mod)].

A nuclear localization of GFP₁₁-VirD2 (wild type) was observed in most cells of yeast strain CEN.PK2-1C expressing GFP₁₋₁₀ (Figure 1A-C) similarly as we reported previously (Sakalis *et al.*, 2014; Chapters 2 and 3). In contrast, no reconstituted GFP signal was found in yeast strain CEN.PK2-1C expressing GFP₁₋₁₀ and GFP₁₁-VirD2(mod) (Figure 1G-I), suggesting that VirD2(mod) is degraded when not entering the nucleus. Tagging GFP₁₁-VirD2(mod) with the MTS did not give a reconstituted GFP signal in the yeast strain expressing GFP₁₋₁₀ (Figure 1J-L). However, MTS- GFP₁₁-VirD2(mod) gave a very clear signal in the yeast strain expressing MTS-GFP₁₋₁₀ (Figure 1 P-R). This signal was not observed in strains expressing MTS-GFP₁₋₁₀ and GFP₁₁-VirD2(mod) (Figure 1M-O) nor in strains expressing MTS-GFP₁₋₁₀ and GFP₁₁-VirD2 (wild type) (Figure 1D-F). These results show that only when GFP₁₋₁₀ and GFP₁₁-VirD2(mod) are both tagged with the MTS a clear fluorescent signal is found in the transformed cells. To confirm that the signal is indeed localized in the mitochondria, we visualized the mitochondria by using the MitoTracker fluorescent dye. As shown in figure 2

the reconstituted GFP signal co-localized with the Mito Tracker signal, indicating that MTS-GFP₁₁-VirD2(mod) was successfully targeted to the mitochondria. In a similar way we investigated whether VirE2 can be targeted into mitochondria. To this end, we ectopically expressed MTS-39GFP₁₁-VirE2 in yeast strain CEN.PK2-1C expressing MTS-GFP₁₋₁₀. As shown in Figure 3 (D-F) a clear GFP signal was found, similar as for MTS-GFP₁₁-VirD2(mod) (Figure 2). Staining with the MitoTracker fluorescent dye confirmed the mitochondrial localization of the GFP signal (Figure 3 D-F). The GFP signal was not found in a yeast strain expressing MTS-GFP₁₋₁₀ but lacking MTS-39GFP₁₁-VirE2 (Figure 3A-C).

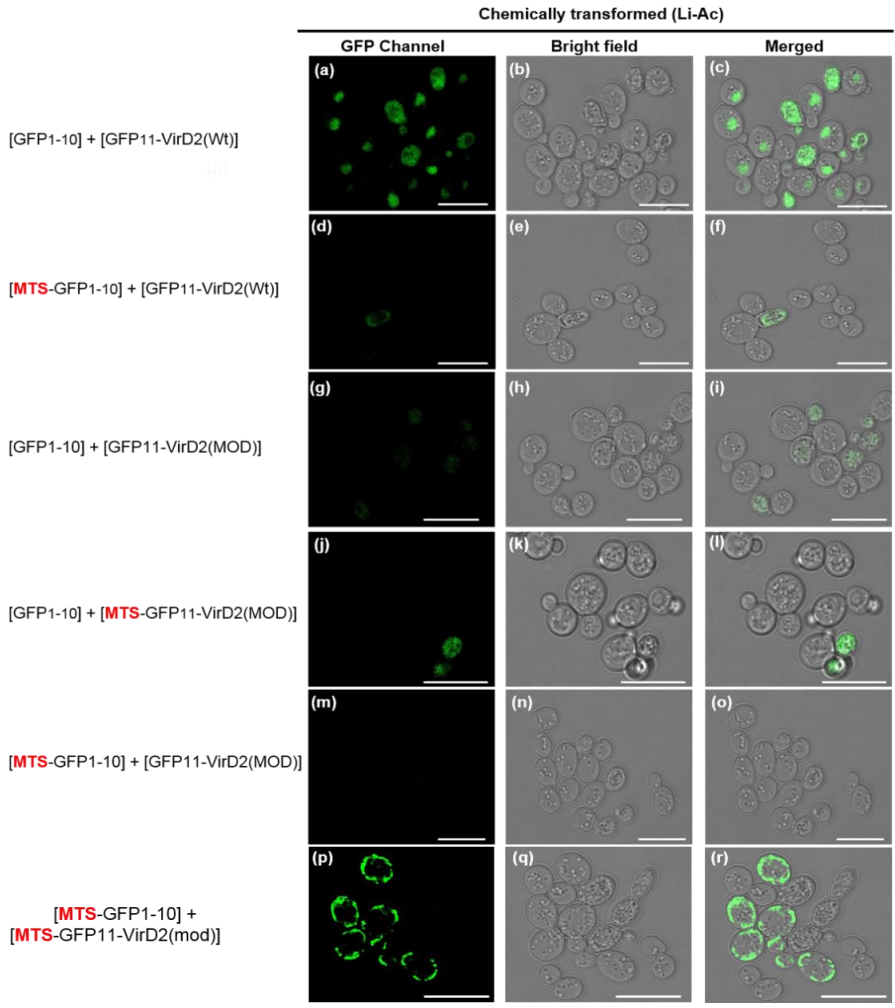


Figure 1. Microscopy of different MTS-tagged VirD2 and VirD2(mod) variants in yeast. Confocal microscopy of yeast strain CEN.PK2-1C expressing GFP₁₋₁₀ chemically transformed with pUG34[GFP₁₁-VirD2] (a-c), with pUG36[GFP₁₁-VirD2(mod)] (g-i) or with pUG36[MTS-GFP₁₁-VirD2(mod)] (j-l) and of yeast strain CEN.PK2-1C expressing MTS-GFP₁₋₁₀ transformed with pUG34[GFP₁₁-VirD2] (d-f), with pUG36[GFP₁₁-VirD2(mod)] (m-o) or with pUG36[MTS-GFP₁₁-VirD2(mod)] (p-r). Scale bars: 5 μm.

To study whether MTS-39GFP₁₁-VirE2 that is translocated from *Agrobacterium* into yeast cells can also be targeted into the mitochondria, we cocultivated yeast strain CEN.PK2-1C expressing MTS-GFP₁₋₁₀ with *Agrobacterium* strain LBA2572 harboring pBBR6[MTS-39GFP₁₁-VirE2] for 24 hours. As shown in Figure 3 G-I, the GFP signal partly colocalized with the MitoTracker signal, indicating that a significant part of the translocated MTS-39GFP₁₁-VirE2 is targeted into the mitochondria.

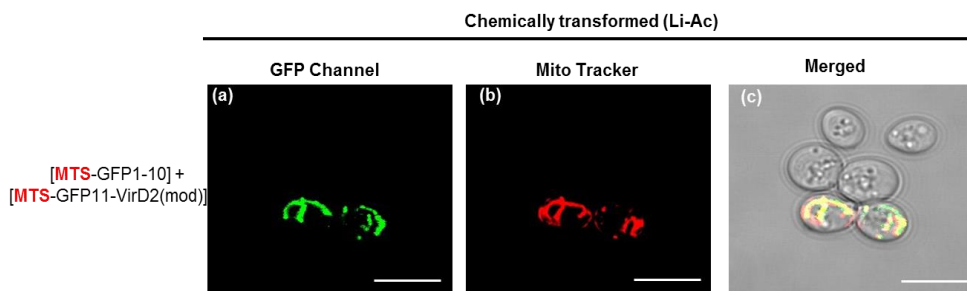


Figure 2. Localization of ectopically expressed MTS-tagged VirD2(mod) in yeast mitochondria. Confocal microscopy of yeast strain CEN.PK2-1C expressing MTS-GFP₁₋₁₀ transformed with pUG36[MTS-GFP₁₁-VirD2(mod)] stained with the MitoTracker dye. A, GFP fluorescence; B, MitoTracker signal; C, merged with the bright field signal. Scale bars: 5 μ m.

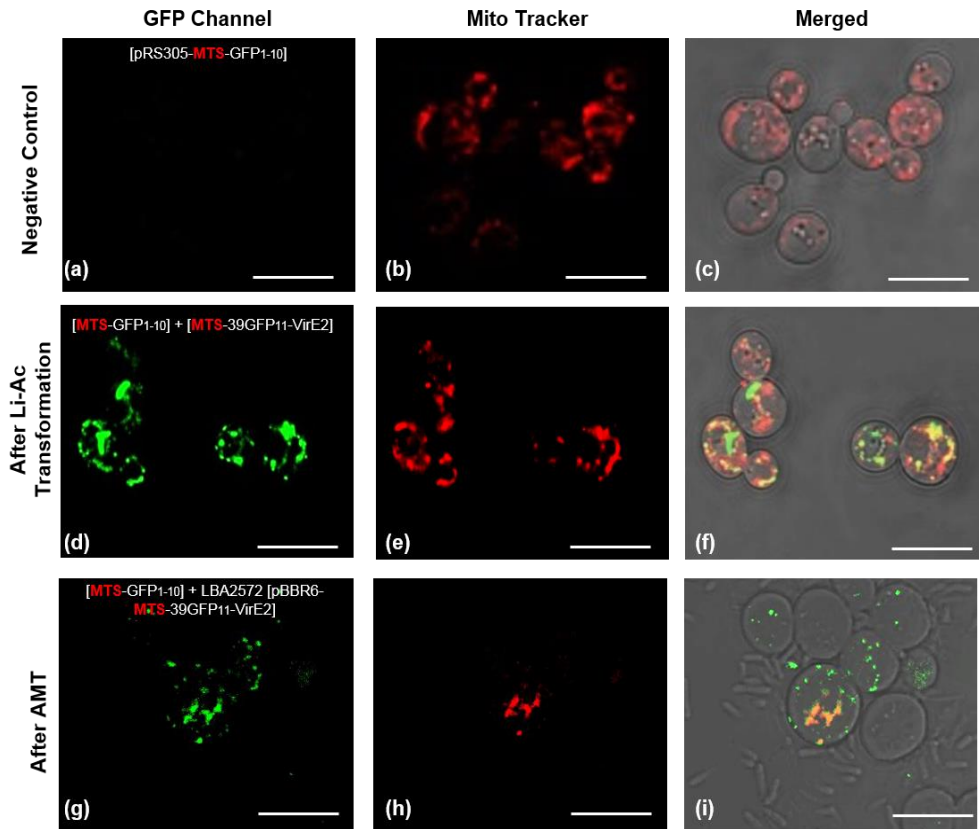


Figure 3. Localization of ectopically expressed and translocated MTS-tagged VirE2 in yeast mitochondria. Confocal microscopy of yeast strain CEN.PK2-1C expressing MTS-GFP₁₋₁₀ (a-c), of CEN.PK2-1C expressing MTS-GFP₁₋₁₀ transformed with pUG36[MTS-39GFP₁₁-VirE2] (d-f) and of CEN.PK2-1C expressing MTS-GFP₁₋₁₀ after cocultivation for 24 hours with *Agrobacterium* strain LBA2572 harboring pBBR6[MTS-39GFP₁₁-VirE2] (g-i). Mitochondria were stained with MitoTracker.

Targeting VirD2 and VirE2 into chloroplasts in *A. thaliana* protoplasts

To target VirD2 and VirE2 into chloroplasts we made use of the CTS of the Arabidopsis FedA protein including the first 8 amino acids of mature FedA and for visualization of the CTS-tagged proteins we made use of the phiLOV2.1 fluorescent protein (Gawthorne *et al.*, 2016; McIntosh *et al.*, 2017; Chapter 3). To investigate the localization of the tagged virulence proteins we expressed them in *A. thaliana* Col-0 cell suspension protoplasts together with a chloroplast mCherry marker. As shown in Figure 4 (a-d) phiLOV2.1-VirD2

(wild type) is localized, as expected, in a structure resembling the nucleus. However, tagging phiLOV2.1-VirD2 (wild type) with the CTS resulted in colocalization of the phiLOV2.1 fluorescence with that of the chloroplast mCherry marker (Figure 4 e-h). This indicates that CTS-phiLOV2.1-VirD2 is targeted into the chloroplasts, despite the presence of NLSs in the wild type VirD2 protein. The localization of phiLOV2.1-VirD2 (mod) which lacks the NLSs is different from that of phiLOV2.1-VirD2 (wild type), which contains the NLSs (Figure 4 i-l). After tagging phiLOV2.1-VirD2 (mod) with the CTS, fluorescence was found in structures containing the chloroplast mCherry marker, indicating that the protein was successfully targeted into the chloroplasts (Figure 4 m-p). The phiLOV2.1-VirE2 protein is localized in structures not containing the chloroplast mCherry marker when the CTS tag is lacking (Figure 4 q-t). However, after tagging with the CTS also VirE2 was successfully targeted to the chloroplasts (Figure 4 u-x).

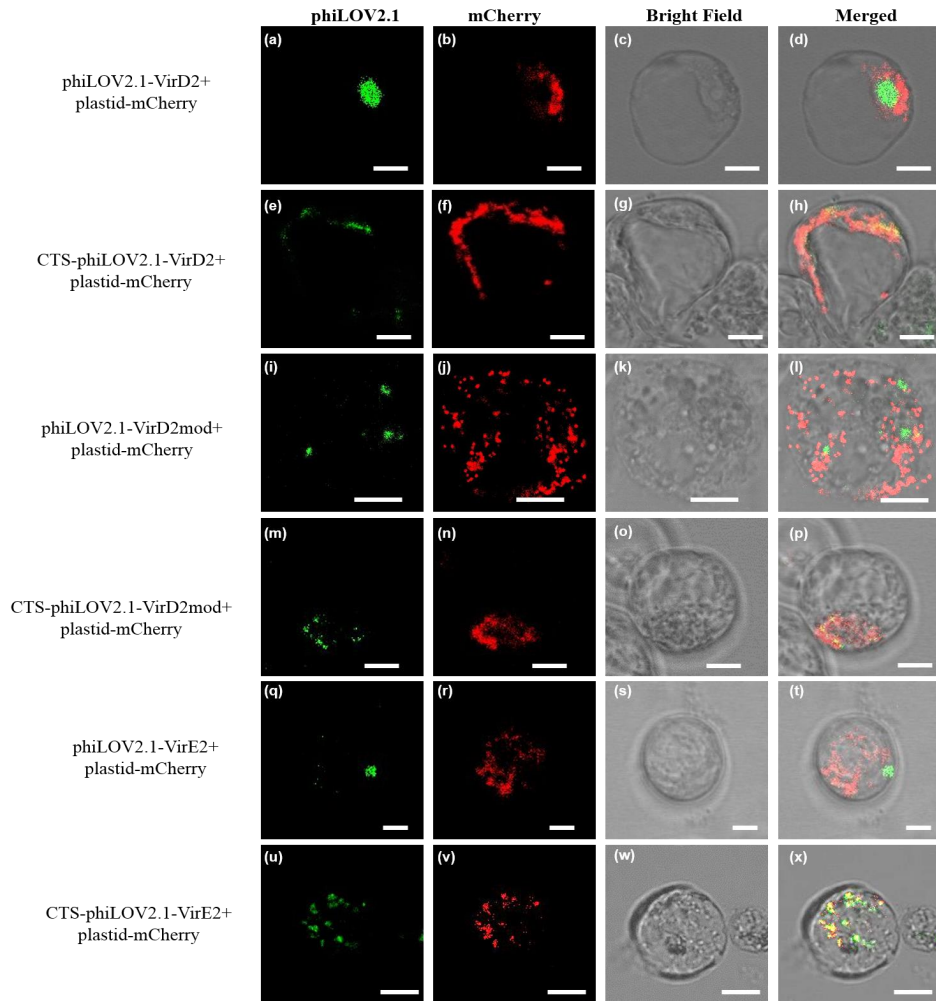


Figure 4. Retargeting of VirE2, VirD2 and VirD2(mod) after chloroplast transit peptide fusion into chloroplasts of *A. thaliana* Col-0 cell suspension protoplasts. Protoplasts of *A. thaliana* Col-0 were co-transformed with chloroplast-mCherry (CD3-1000) and plasmids pART7(phiLOV2.1-VirD2) (A-D), with pART7(CTS-phiLOV2.1-VirD2) (E-H), with pART7(phiLOV2.1-VirD2(mod)) (I-L), with pART7(CTS-phiLOV2.1-VirD2(mod)) (M-P), with pART7(39phiLOV2.1-VirE2) (Q-T) and with pART7(CTS-39phiLOV2.1-VirE2) (U-X). Images were captured 24 hours after PEG transformation. Scale bars: 15µm.

Biological activity of CTS -tagged VirE2 and VirD2

To investigate whether virulence proteins have retained their biological activity after tagging with the CTS and phiLOV2.1, tumor formation assays were performed on *N. glauca* shoots. To this end, *N. glauca* shoots were injected with the different *Agrobacterium* strains and after 4 weeks tumor formation was scored. Tumors were clearly visible after injection of the positive control strains LBA1010 and LBA1010(pBBR6), and tumors were not formed after injection of the negative control strains lacking T-DNA (LBA1100) and LBA1100(pBBR6) (Figure 5 A-D). The tumors of LBA1010 and LBA1010(pBBR6) were comparable in size suggesting that the presence of pBBR6 did not interfere with tumor formation (Figure 5A and C). *N. glauca* shoots which were infected with *Agrobacterium* strain LBA2572(pBBR6) which lacks *virE2*, did not develop tumors, in line with the essential role of *virE2* in AMT (Figure 5F). *Agrobacterium* strains LBA2572(pBBR6-CTS-VirE2), LBA2572(pBBR6-phiLOV2.1-VirE2) and LBA2572(pBBR6-CTS-phiLOV2.1-VirE2) did not induce tumor growth (Figure 5 H, I and J, respectively) as expected because of the negative effect of N-terminally tagging of VirE2. Unexpectedly, no tumor formation was observed after injection of LBA2572 (pBBR6-VirE2) expressing untagged VirE2 (Figure 5G). This may be caused by an imbalance between the expression of VirE1 and VirE2 (Zhou *et al.*, 1999). *Agrobacterium* strain LBA2569(pBBR6) which lacks *virD2*, did not induce tumor formation (Figure 5K), in line with the essential role of *virD2* in AMT. This *virD2* deficiency can be complemented by expression of untagged VirD2, CTS-VirD2, phiLOV2.1-VirD2 and CTS-phiLOV2.1-VirD2 (Figure 5 l-o), indicating that intact, CTS-, phiLOV2.1 and CTS-phiLOV2.1- tagged VirD2 had retained at least some biological activity. To check whether the biological activity of VirD2(mod) was affected by tagging with CTS, phiLOV2.1 or CTS-phiLOV2.1 *N. glauca* shoots were infected by *virD2* deficient *Agrobacterium* strains expressing VirD2(mod), CTS-VirD2(mod), phiLOV2.1-VirD2(mod)) and CTS-phiLOV2.1-VirD2(mod). As shown in Figures 5 p-s all these strains could induce tumors.

To further investigate to what extent CTS tagging affects the biological activity of the effector proteins, we co-cultivated *A. thaliana* seedlings with various *Agrobacterium* strains expressing the tagged virulence proteins and harboring the pCAMBIA3310 plasmid. This plasmid contains the β -glucuronidase (GUS) marker gene on its T-DNA. When the T-DNA is successfully transferred and the *gusA* gene is (transiently) expressed, transformed cells in the seedlings are able to process 5-bromo-4-chloro-3-indolyl glucuronide (X-Gluc) and blue spots will be detectable in the seedlings (Jefferson *et al.*, 1987). Co-cultivation with

Agrobacterium control strains lacking *virD2* or *virE2* did not generate blue spots (Figure 6 A and B). On the other hand, clear blue spots were visible upon co-cultivation with *Agrobacterium* strains expressing CTS-VirD2, CTS-VirD2(mod) or CTS-VirE2 (Figure 6 C-E). These results indicate that the CTS tagging approach did not destroy the biological activity of the tested effector proteins in the transient gene expression assay. Remarkably, while no biological activity was detected in the tumor assay, at least some biological activity of CTS-VirE2 was seen in the Gus assay.

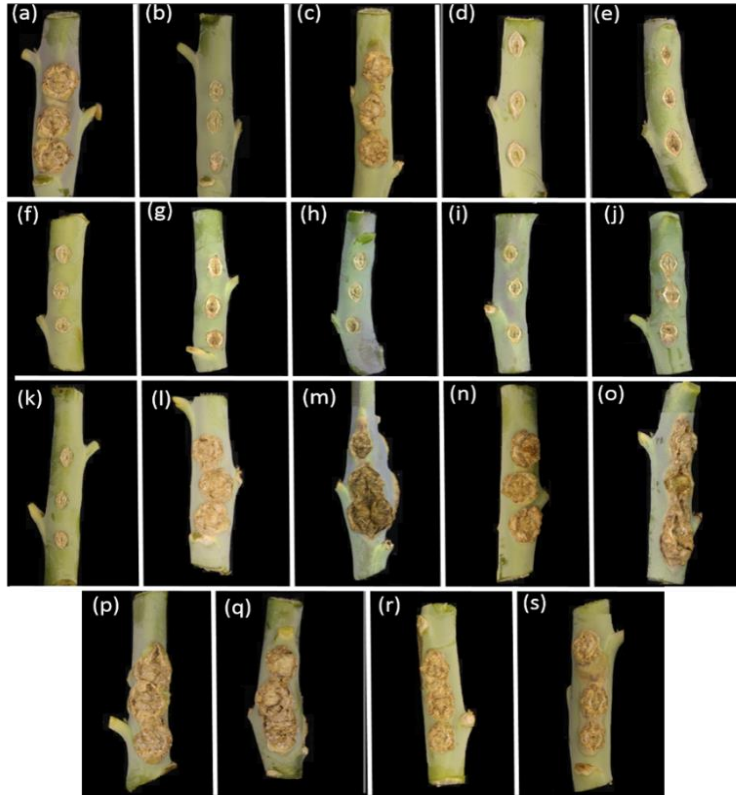


Figure 5. Tumor formation on *N. glauca* plants inoculated with *A. tumefaciens* strains expressing CTS-tagged VirE2 and VirD2. *N. glauca* stems were infected with different *Agrobacterium* strains and after 4 weeks tumor formation was scored. A, LBA1010 (positive control); B, LBA1100 (T-DNA deficient, negative control); C, LBA1010(pBBR6); D, LBA1100(pBBR6); E, LBA2573(pBBR6-VirE2); F, LBA2572(pBBR6); G, LBA2572(pBBR6-VirE2); H, LBA2572(pBBR6-CTS-VirE2); I, LBA2572(pBBR6-phiLOV2.1-VirE2); J, LBA2572(pBBR6-CTS-phiLOV2.1-VirE2); K, LBA2569(pBBR6); L, LBA2569(pBBR6-VirD2); M, LBA2569(pBBR6-CTS-VirD2); N, LBA2569(pBBR6-phiLOV2.1-VirD2); O, LBA2569(pBBR6-CTS-phiLOV2.1-VirD2); P, LBA2569(pBBR6-VirD2(mod)); Q, LBA2569(pBBR6-CTS-VirD2(mod)); R, LBA2569(pBBR6-phiLOV2.1-VirD2(mod)) and S, LBA2569(pBBR6-CTS-phiLOV2.1-VirD2(mod)).

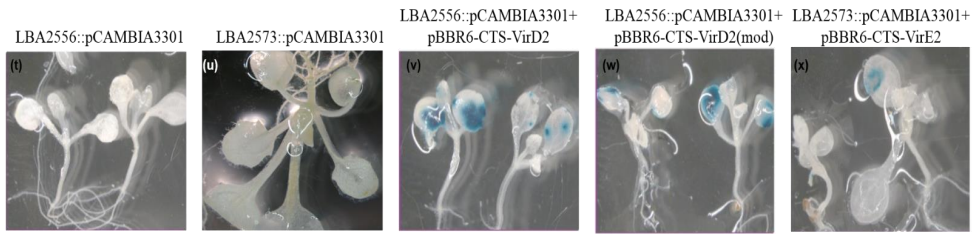


Figure 6. Transient expression of the T-DNA derived β -glucuronidase (GUS) after co-cultivation with *A. tumefaciens* strains expressing CTS-tagged VirE2 and VirD2. *A. thaliana efr-1* mutant seedlings were transfected with the *A. tumefaciens* strains containing pCAMBIA3301, i.e. LBA2556 (LBA1100 Δ VirD2) (A), LBA2573 (LBA1100 Δ VirE2) (B), LBA2556 (pBBR6::CTS-VirD2) (C), LBA2556 (pBBR6::CTS-VirD2(mod))(D) or LBA2573(pBBR6-CTS-VirE2)(E), and the GUS activity was determined.

Targeting VirD2 and VirE2 into chloroplasts after AMT in *N. tabacum* leaves

To investigate whether the virulence proteins can also be targeted into the chloroplasts after AMT, *N. tabacum* leaves were infiltrated with *Agrobacterium* strains harbouring wild type or CTS-tagged 39phiLOV2.1-VirE2, phiLOV2.1-VirD2 (wild type) or phiLOV2.1-VirD2(mod). As shown in Figure 7 A-F untagged 39phiLOV2.1-VirE2 was translocated into the leaf cells and was localized close to the cell membrane and in the cytoplasm, similar as described in Chapter 3. The localization was not influenced by the presence of T-DNA. Localization of VirE2 in chloroplasts was not found in case of untagged VirE2 (Figure 7 A-F) (0 out of counted 150). After tagging VirE2 with the CTS, the protein was found colocalizing in 6 out of 158 counted chloroplasts in cells in which fluorescent signals were seen (Figure 7 G-L). Co-localization with the chloroplasts was observed both in the absence as in the presence of T-DNA. It was also found near the cell membrane and in the cytoplasm, indicating that the CTS only partly guides VirE2 to the chloroplasts. Although CTS-39phiLOV2.1-VirE2 colocalized with the chloroplasts, it is still unclear whether the protein is really present inside the chloroplasts. Hanson and Sattarzadeh (2008) visualized chloroplast stromules in *N. tabacum* (Figure 8D-F) and we interestingly found a pattern for the CTS-phiLOV2.1-VirE2 localization strongly resembling that of stromules (Figure 8A). To visualise the effect of the CTS-tag on the localization of phiLOV2.1-VirD2 *N. tabacum* leaves were infiltrated with *Agrobacterium* strains LBA2556 (T-DNA deficient) and LBA2569 (T-DNA containing) carrying pBBR6[phiLOV2.1-VirD2] or pBBR6[CTS-phiLOV2.1-VirD2]. As shown in figure 9, phiLOV2.1-VirD2 was found in structures resembling the nucleus (Figure 9B-C, insert) and in the cytoplasm (Figure 9D-F)

approximately 24 hours after agroinfiltration. We saw overlap in 2 out of 260 green fluorescent signals with chloroplasts present in the cells. CTS-phiLOV2.1-VirD2 was found colocalizing with the chloroplasts in 3 out of 148 chloroplasts present in cells in which fluorescent signals were detected (Figure 9 G-I). This low number not significantly different from that are without CTS which is probably due to the dominant effect of the NLSs over the CTS. Indeed, CTS-phiLOV2.1-VirD2(mod) colocalized more frequently with the chloroplasts (in 20 out of 360 chloroplasts present in cells in which fluorescent signals were detected) (Figure 10 I-P). Untagged phiLOV2.1-VirD2(mod) was not detectable after agroinfiltration with LBA2556(pBBR6-phiLOV2.1-VirD2(mod)) (lacking T-DNA) or with LBA2569(pBBR6-phiLOV2.1-VirD2(mod)) (containing T-DNA) (Figure 10 A-F), which might be due to low levels of VirD2(mod) as it possibly spread all over the cell or is degraded when not targeted to the nucleus or chloroplasts. Like CTS-VirE2, also translocated CTS-VirD2 and CTS-VirD2(mod) may be located in the stromules (Figure 8B and C, respectively).

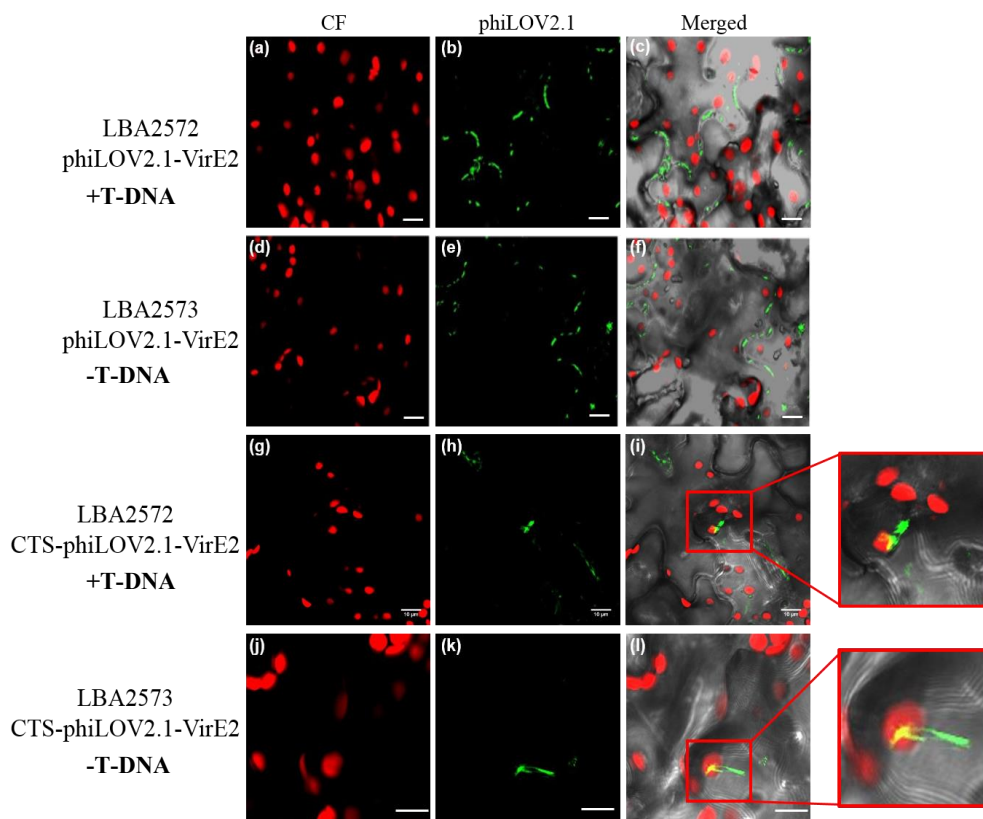


Figure 7. Localization of (CTS)-phiLOV2.1-VirE2 in *N. tabacum* leaf cells after AMT. Leaves of *N. tabacum* SR1 plants were agroinfiltrated with LBA2572(pBBR6-39phiLOV2.1-VirE2) (containing T-DNA)(a-c); with LBA2573(pBBR6-phiLOV2.1-VirE2) (lacking T-DNA)(d-f); with LBA2572(pBBR6-CTS-phiLOV2.1-VirE2) (g-i) and with LBA2573(pBBR6-CTS-phiLOV2.1-VirE2) (j-l). Images were captured between 19 and 29 hours after agroinfiltration. Both cytoplasmic localizations and membrane localizations of translocated phiLOV2.1-VirE2 were observed (a-f). Partially chloroplast colocalization of

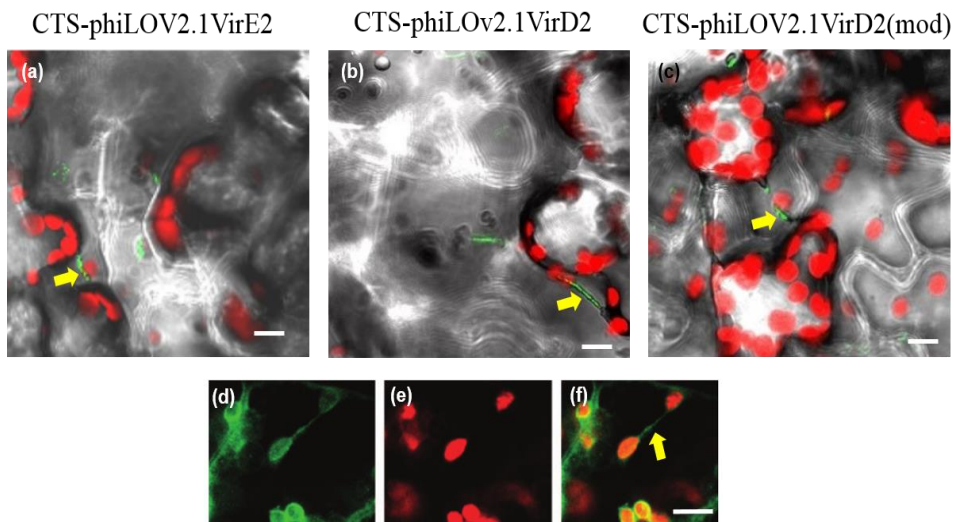


Figure 8. Possible localization of CTS-39-phiLOV2.1-VirE2, CTS-phiLOV2.1-VirD2 and CTS-phiLOV2.1-VirD2(mod) in chloroplast stromules after translocation from *Agrobacterium* to *N. tabacum* leaves. Leaves of *N. tabacum* SR1 wild type plants were agroinfiltrated with LBA2573(pBBR6-CTS-39phiLOV2.1-VirE2) (a); with LBA2569(pBBR6-CTS-phiLOV2.1-VirD2) and with LBA2569(pBBR6-CTS-phiLOV2.1-VirD2(mod)). Images were captured between 19 and 29 hours after agroinfiltration. (A-C) suggesting the accumulation of virulence proteins targeted into stromules localized between chloroplasts (yellow arrows). CF, chlorophyll fluorescence. Scale bars: 10 μ m. For comparison: d – f: Laser scanning confocal microscopy images of chloroplasts and stromules in *N. tabacum* expressing chloroplast marker TOC34–GFP, taken from Hanson and Sattarzadeh, (2008). (d), GFP fluorescence, (e) chlorophyll fluorescence, and (f) merged image of (d) and (e); scale bar: 7.5 μ m.

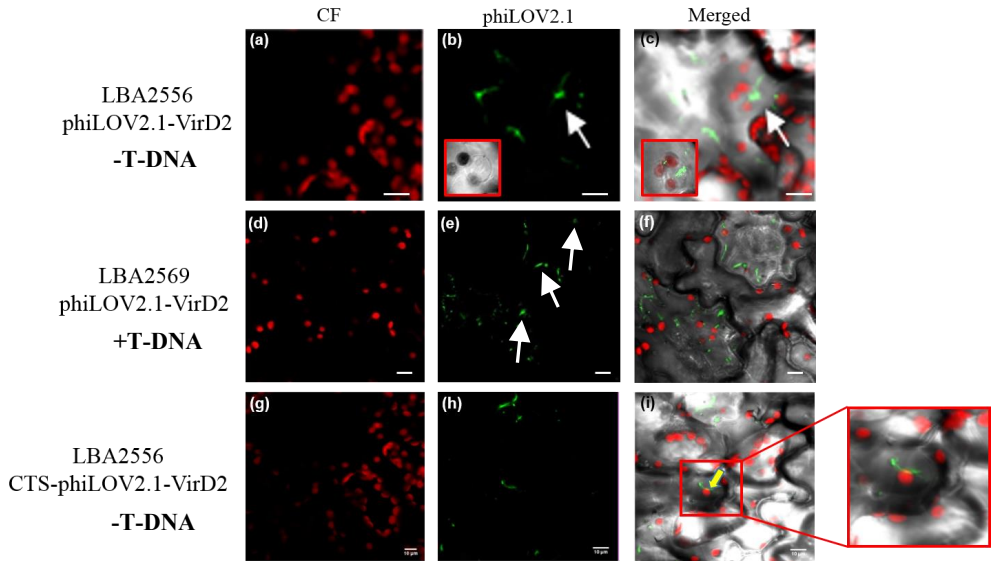


Figure 9. Analysis of the effect of the CTS-tag on phiLOV2.1-VirD2 localization in *N. tabacum* leaves after AMT. Leaves of *N. tabacum* SR1 plants were agroinfiltrated with LBA2556(pBBR6-phiLOV2.1-VirD2) (lacking T-DNA) (a-c); with LBA2569(pBBR6-phiLOV2.1-VirD2) (containing T-DNA) (d-f); or with LBA2556(pBBR6-CTS-phiLOV2.1-VirD2) (g-i). Images were captured between approximately 24 hours after agroinfiltration. Both nuclear (insert) (a-c) and cytoplasmic (d-f) (white arrows) localizations of translocated phiLOV2.1-VirD2 were observed. Translocated CTS-phiLOV2.1-VirD2 partially colocalized with chloroplasts (g-i) (yellow arrow). CF, chlorophyll fluorescence. Scale bars: 10µm.

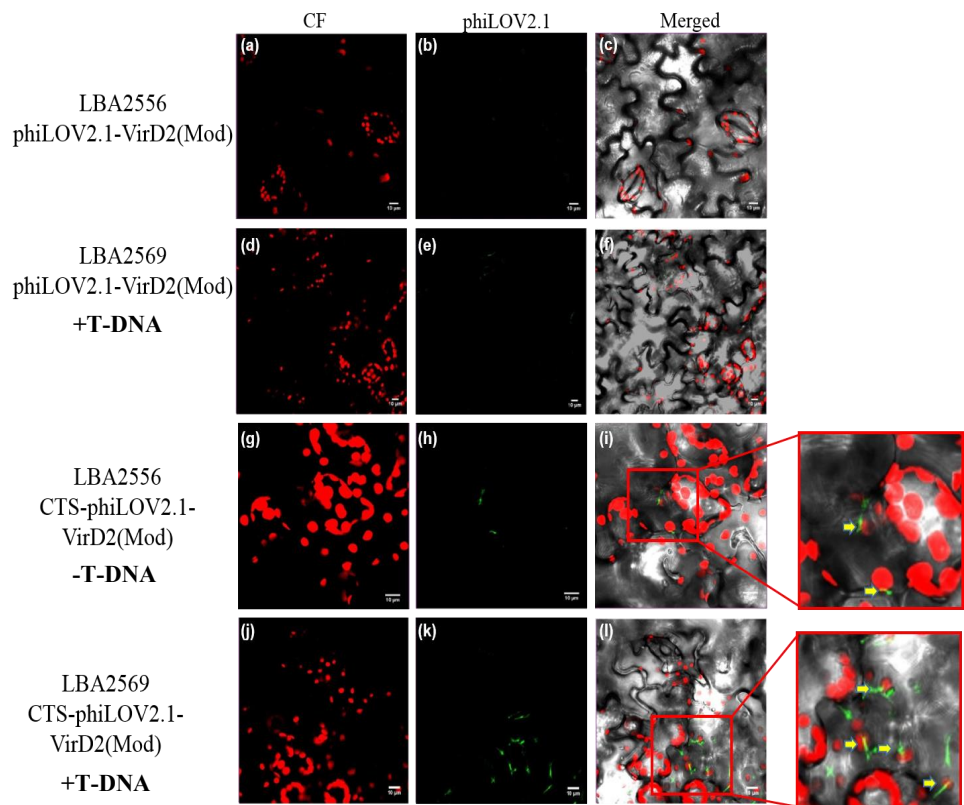


Figure 10. Analysis of the effect of the CTS-tag on phiLOV2.1-VirD2(mod) localization in *N. tabacum* leaves. Leaves of *N. tabacum* SR1 plants were agroinfiltrated with LBA2556(pBBR6-phiLOV2.1-VirD2(mod)) (lacking T-DNA) (a-c); with LBA2569(pBBR6-phiLOV2.1-VirD2(mod)) (containing T-DNA) (d-f); with LBA2556(pBBR6-CTS-phiLOV2.1-VirD2(mod)) (g-i); or with LBA2569(pBBR6-CTS-phiLOV2.1-VirD2(mod)) (j-l). Images were captured approximately 24 hours after agroinfiltration. No phiLOV2.1 signal was observed after phiLOV2.1-VirD2(mod) translocation (a-f). A partial colocalization of translocated CTS-phiLOV2.1-VirD2(mod) with chloroplasts was observed (g-l). CF, chlorophyll fluorescence. Scale bars: 10µm.

DISCUSSION

Agrobacterium is an excellent tool to modify the plant nuclear genome by transferring a T-DNA with the genes of interest into plant cells. During transformation several *Agrobacterium* effector proteins (VirD2, VirD5, VirE2, VirE3 and VirF) are translocated from *Agrobacterium* into the recipient cells. While strains lacking VirD5, VirE3 and VirF are almost as good as wild type in plant transformation under the lab conditions, strains lacking VirD2 or VirE2 are no longer able to do so. The proteins VirD2 and VirE2 play an important role in nuclear targeting and delivery, and in protection of the T-complex against host cell endonucleases (for a recent review see Gelvin, 2012). *Agrobacterium* can therefore not only be exploited to introduce foreign DNA into cells (AMT), but also to introduce foreign proteins into eukaryotic cells (AMPT) to manipulate them to acquire desired properties.

Genetic modification of organellar DNA has great potential for biotechnology. For example, chloroplast genome engineering can be considered as an option for improving photosynthesis (Ort *et al.*, 2015). However, few protocols are available for transformation of organellar DNA, namely PEG-mediated transformation (Svab and Maliga, 1993; Hanson *et al.*, 2013; Yu *et al.*, 2017) and particle bombardment (Golds *et al.*, 1993). Cells contain many plastids and therefore in extensive selection procedure is needed to obtain a homoplasmic plant. Yu *et al.* (2017) established a protocol to transform *A. thaliana* leaves by gold particle bombardment resulting in 100 fold increase in chloroplast transformation efficiency compared to transformation of *N. tabacum*. However, despite this improvement the transformation efficiency of this techniques is still low. Moreover, the biolistic technique requires an expensive device and it is costly because of using gold particles (Daniell *et al.*, 2005; Liu *et al.*, 2013). The disadvantages of PEG-mediated transformation of protoplasts relate to the tedious treatment, maintenance and regeneration of protoplasts (Meyers *et al.*, 2010). Although *Agrobacterium*-mediated chloroplast transformation was reported by DeBlock *et al.* (1985), this result has never been repeated and therefore may reflect a rare, exceptional event. To facilitate AMT of organellar DNA, in theory, the first step that needs to be done is to modify VirD2 and VirE2, so that they are targeted into the desired cell organelles instead of the nucleus. To this end, nuclear localization sequences (NLS) need to be removed as much as possible and a mitochondrial or chloroplast-targeting signal needed to be added to these proteins. Targeting of virD2 and VirE2 to the organelles may also direct the complete T-complex to the mitochondria or chloroplasts, respectively. Of course the T-DNA

itself needs to be modified so that it can integrate in the organellar genome by homologous recombination and selection of transformants is possible. As a first step we investigated whether it is possible to target VirD2 and VirE2 into yeast mitochondria. Previously, we showed that ectopically expressed GFP/YFP/CFP-tagged VirE2 formed filamentous structures associated with the microtubules in both yeast and *A. thaliana* protoplasts (Sakalis, 2013; Sakalis *et al.*, 2014). Similar localization was found for GFP₁₁-tagged VirE2 in yeast cells expressing GFP₁₋₁₀ (Sakalis *et al.*, 2014; Chapter 2). As shown in Figure 3 addition of the MTS to GFP₁₁-VirE2 indeed targeted most of the protein to the mitochondria. Also MTS-GFP₁₁-VirE2 translocated from *Agrobacterium* after AMT, was partly localized in the mitochondria (Figure 3 G-I). VirD2 contains nuclear localization signals (NLS) that facilitate nuclear uptake of the T-complex into the nucleus of the host cell (Ziemienowicz *et al.*, 2001). Ectopically expressed GFP-VirD2 has a nuclear localization in both yeast and plant cells (Citovsky *et al.*, 1994; Wolterink-van Loo *et al.*, 2015). A nuclear localization was also found for GFP₁₁-VirD2 in yeast cells expressing GFP₁₋₁₀ (Figure 1 A-C)(Chapter 3; Roushan *et al.*, 2018). Removal of the C-terminal part of VirD2 containing the NLSs (VirD2(mod)) abolished this nuclear localization (Figure 1G-I). Addition of the MTS to GFP₁₁-VirD2(mod) successfully targeted most of the protein to the mitochondria (Figure 1 P-R; Figure 2). The successful targeting of both VirE2 and VirD2 into the yeast mitochondria opens ways for new studies to target T-DNA into the yeast mitochondria and to modify the mitochondrial genome.

To investigate targeting of VirE2 and VirD2 into chloroplasts we made use of *A. thaliana* protoplasts as well as *N. tabacum* leaves. In protoplasts ectopically expressed 39phiLOV2.1-VirE2 was found in dot-shaped structures associated with tubulins (Figure 4Q-T) (Roushan *et al.*, 2018). These structures were not overlapping with chloroplasts (Figure 4Q-T). However, after tagging with a CTS, the protein (CTS-phiLOV2.1-VirE2) colocalized to some extent with the chloroplast marker protein (Figure 4 U-X). Ectopically expressed GFP-VirD2 has a nuclear localization in both yeast and plant cells (Citovsky *et al.*, 1992; Wolterink-van Loo *et al.*, 2015). We found a similar nuclear localization for phiLOV2.1-VirD2 in both yeast and *A. thaliana* root cells (Chapter 3)(Roushan *et al.* (2018). As expected, phiLOV2.1-VirD2 was localized in a structure resembling the nucleus in *A. thaliana* protoplasts (Figure 4 A-D). The nuclear localization of VirD2 vanished and phiLOV2.1 signals overlapped with the mCherry chloroplast marker upon tagging with CTS (Figure 4 E-H). The first 228 amino acids of

VirD2, containing the relaxase domain, is required for the endonuclease activity of VirD2 (Steck *et al.*, 1990). The relaxase domain was further minimized to 204 amino acids based on sequence comparison between different relaxases (van Kregten *et al.*, 2009). Because of the removal of the C-terminal NLSs, we hypothesized that the VirD2 relaxase domain by itself would no longer be targeted to the nucleus. Indeed, we found that after transfection of *A. thaliana* protoplasts with pART7[phiLOV2.1-VirD2(mod)], there was no longer a condense nuclear localization, but dot-shape accumulations of VirD2(mod) with subcellular localization that did not overlap with chloroplasts were seen (Figure 4 I-L). The CTS-tagged VirD2(mod) protein was shown to be localized in chloroplasts (Figure 4 M-P). Thus, ectopically expressed phiLOV2.1-VirE2 and phiLOV2.1-VirD2 can indeed be targeted into the chloroplasts by tagging these proteins with a CTS.

To investigate whether VirE2 and VirD2 originating from *Agrobacterium* during AMT can be targeted into the chloroplasts, we made use of agroinfiltration of *N. tabacum* leaves. Li and Pan (2017) presented data which may suggest that in *N. benthamiana* leaf cells *Agrobacterium* -delivered GFP₁₁-VirE2 initially accumulated on plant plasma membranes, but was subsequently internalized through clathrin-mediated endocytosis resulting in accumulation of GFP₁₁-VirE2 in the endomembrane compartments. Fluorescent signals in the cytoplasm and near the plasma membrane were detected by us after *N. tabacum* leaf agroinfiltration with the *Agrobacterium* strains LBA2572 or LBA2573 harboring pBRR6-phiLOV2.1-VirE2 (Figure 7A-C and D-F, respectively) as we showed previously (Chapter 3). To investigate the effect of the CTS on the localization of phiLOV2.1-VirE2 in tobacco cells, four weeks old *N. tabacum* SR1 leaves were infiltrated with *Agrobacterium* strains LBA2572 (containing T-DNA) or LBA2573 (lacking T-DNA) harboring pBRR6-CTS-phiLOV2.1-VirE2. After approximately 24 hours filamentous and dot-like structures of VirE2 were found partially colocalizing with the chloroplasts of leaf epidermal cells (Figure 7 G-I and J-L, respectively). After infiltration of *N. tabacum* leaves with *Agrobacterium* strains LBA2556 (pBRR6-phiLOV2.1-VirD2) and LBA2569 (pBRR6-phiLOV2.1-VirD2), fluorescent signals were seen in the nucleus (Figure 9 A-C, insert), cytoplasm and near the plasma membrane (Figure 9 D-F). These signals did not overlap with chlorophyll fluorescence. After tagging with a CTS hardly any phiLOV2.1 fluorescence was found in the chloroplasts (9 G-I). Agroinfiltration of *N. tabacum* SR1 leaves with the *Agrobacterium* strains LBA2556 and LBA2569 harboring pBRR6-phiLOV2.1-VirD2(mod) did not yield

any phiLOV2.1 fluorescent signals inside the plant cells probably due to the low fraction of VirD2(mod) concentrated inside a specific cell compartment or it might be due to rapid degradation of phiLOV2.1-VirD2(mod) in plant cells. Upon infiltration of *N. tabacum* SR1 leaves with *Agrobacterium* strains LBA2556 and LBA2569 harboring pBBR6-CTS-phiLOV2.1-VirD2(mod), however a clear signal was obtained, which overlapped to some extent with the chlorophyll fluorescence signals (Fig.10 G-I and J-L, respectively), indicating that the CTS of FedA allowed for translocation of some CTS-phiLOV2.1-VirD2(mod) into the chloroplasts of the plant cells.

In summary, we can conclude from this study that the crucial effector proteins of the AMT process VirE2 and VirD2(mod), were successfully modified so that they are now targeted from *Agrobacterium* to mitochondria (of yeast) and chloroplasts (of plant cells). However, the protein translocation frequencies are quite low and the proteins are only partially targeted into the organelles. On the other hand our results make it very worthwhile to further investigate strategies to use AMT to manipulate mitochondrial or chloroplast genomes using organelle targeting of the VirE2 and VirD2 virulence proteins.

ACKNOWLEDGEMENTS

We would like to thank Dr. Niels van Tol (our institute) for providing the chloroplast targeting sequence (CTS) of the *FedA* gene and Gerda Lamers (our institute) for her help with microscopy. We acknowledge Dr. Bert van der Zaal and Dr. Maartje van Kregten for construction of plasmid pBBF[flag-D2-204-F] encoding *virD2(mod)* we used in this study. This study was partly supported by a grant from the Royal Academy of Sciences of The Netherlands to PJJH associated with his appointed as academy professor.

REFERENCES

- Abràmoff, M. D., Magalhães, P. J. and Ram, S. J.** (2004). Image processing with imageJ. *Biophotonics Int.* 11, 36–41.
- Atmakuri, K., Ding, Z. and Christie, P.J.** (2003). VirE2, a type IV secretion substrate, interacts with the VirD4 transfer protein at cell poles of *Agrobacterium tumefaciens*. *Mol. Microbiol.* 49,1699– 1713.
- Avila, E.M., Gisby, M.F. and Day, A.** (2016). Seamless editing of the chloroplast genome in plants. *BMC Plant Biol.* 16, 168.
- Bansal, K. C. and Sharma, R. K.** (2003). Chloroplast transformation as a tool for prevention of gene flow from GM crops to weedy or wild relatives. *Current Science*, 84, 1286-1287.
- Beijersbergen, A., den Dulk-Ras, A., Schilperoort, R.A. and Hooykaas, P.J.J.** (1992). Conjugative Transfer by the Virulence System of *Agrobacterium tumefaciens*. *Science*, 256, 1324–1327.
- Boffey, S. A. and Leech, R. M.** (1982). Chloroplast DNA levels and the control of chloroplast division in light-grown wheat leaves. *Plant Physiol.* 69, 1387- 91.
- Bundock P, den DRA, Beijersbergen A, Hooykaas PJ.** (1995). Trans-kingdom T-DNA transfer from *Agrobacterium tumefaciens*. *EMBO J*, 14, 3206–14.
- Cerutti, H., Johnson, A.M., Boynton, J.E. and Gilham, N.W.** (1995) Inhibition of chloroplast DNA recombination and repair by dominant negative mutants of *Escherichia coli* RecA. *Mol Cell Biol*, 15, 3003-3011.
- Chilton, M.-D., Drummond, M. H., Merlo, D. J., Sciaky, D., Montoya, A. L., Gordon, M. P. and Nester, E. W.** (1977). Stable incorporation of plasmid DNA into higher plant cells: the molecular basis of crown gall tumorigenesis. *Cell*, 11, 263–271.
- Christie, P.J., Ward, J.E., Winans, S.C. and Nester, E.W.** (1988). The *Agrobacterium tumefaciens virE2* gene product is a single-stranded-DNA-binding protein that associates with T-DNA. *J. Bacteriol*, 170, 2659–2667.
- Citovsky, V., Zupan, J., Warnick, D. and Zambryski, P.** (1992). Nuclear localization of *Agrobacterium* VirE2 protein in plant cells. *Science*, 256, 1802–1805.
- Daniell, H., Khan, M. S. & Allison, L.** (2002) Milestones in chloroplast genetic engineering: an environmentally friendly era in biotechnology. *Trends Plant Sci.* 7, 84–91.
- Daniell, H., Kumar, S., and Dufourmantel, N.** (2005). Breakthrough in chloroplast genetic engineering of agronomically important crops. *Trends Biotechnol*, 23, 238-245.

- DeBlock, M., J. Schell, and M. Van Montagu.** (1985). Chloroplast transformation by *Agrobacterium tumefaciens*. *EMBO J.*, 4, 1367–1372
- den Dulk-Ras, A. and Hooykaas, P.J.J.** (1995). Electroporation of *Agrobacterium tumefaciens*. *Methods Mol. Biol.* 55, 63–72.
- Flores-Perez., U. and Jarvis, P.** (2013). Molecular chaperone involvement in chloroplast protein import. *BBA Mol Cell Res*, 2, 332-340.
- Gietl, C., Koukolfkova-Nicola, Z. and Hohn, B.** (1987). Mobilization of T-DNA from *Agrobacterium* to plant cells involves a protein that binds single-stranded DNA. *Cell Biol.* 84, 9006–9010.
- Gietz, R. D., Schiestl, R. H., Willems, A. R. and Woods, R. A.** (1995). Studies on the transformation of intact yeast-cells by the LiAc/ssDNA/PEG procedure . *Yeast*, 11, 355–360.
- Gleave, A.P.** (1992) A versatile binary vector system with a T-DNA organizational structure conducive to efficient integration of cloned DNA into the plant genome. *Plant Mol. Biol.*, 20, 1203–1207.
- Golds T, Maliga P, Koop H-U.** (1993). Stable chloroplast transformation in PEG-treated protoplasts of *Nicotiana tabacum*. *Nature Biotechnol.*, 11, 95–97.
- Hanson, M.R. and Sattarzadeh A.** (2008). Dynamic morphology of chloroplasts and stromules in angiosperm plants. *Plant, Cell & Environment*, 31, 646–657.
- Hanson, M.R., Gray, B.N. and Ahner, B.A.** (2013). Chloroplast transformation for engineering of photosynthesis. *J. Exp. Bot.*, 64, 731–742.
- Hodges, L.D., Vergunst, A.C., Neal-McKinney, J., den Dulk-Ras, A., Moyer, D.M., Hooykaas, P.J.J. and Ream, W.** (2006). *Agrobacterium rhizogenes* GALLS protein contains domains for ATP binding, nuclear localization, and type IV secretion. *J. Bacteriol.*, 188, 8222–8230.
- Howard, E.A., Zupan, J.R., Citovsky, V. and Zambryski, P.C.** (1992). The VirD2 protein of *A. tumefaciens* contains a C-terminal bipartite nuclear localization signal: Implications for nuclear uptake of DNA in plant cells. *Cell*, 68, 109–118.
- Jefferson, R. A., Kavanagh, T. A. and Bevan, M. W.** (1987). GUS fusions: Beta-glucuronidase as a sensitive and versatile gene fusion marker in higher plants. *The EMBO Journal*. 6, 3901–7.
- Jin, R., Richter, S., Zhong, R. and Lamppa, G.K.** (2003) Expression and import of an active cellulase from a thermophilic bacterium into the chloroplast both in vitro and in vivo. *Plant Mol. Biol.*, 51, 493–507.
- Kaddoum, L., Magdeleine, E., Waldo, G.S., Joly, E. and Cabantous, S.** (2010). One-step split GFP staining for sensitive protein detection and localization in mammalian cells. *BioTechniques*, 49, 727–736.

Kamiyama, D., Sekine, S., Barsi-Rhyne, B., Hu, J., Chen, B., Gilbert, L. A., Ishikawa, H., Leonetti, M.D., Marshall, W.F. and Weissman, J.S. (2016). Versatile protein tagging in cells with split fluorescent protein. *Nat. Commun.*, 7, 11046. doi: 10.1038/ncomms11046.

Koekman, B.P., Hooykaas, P.J.J. and Schilperoort, R.A. (1982). A functional map of the replicator region of the octopine Ti plasmid. *Plasmid.*, 7, 119–132.

Kovach, M. E., Elzer, P. H., Hill, D. S., Robertson, G. T., Farris, M. A., Roop, R. M, and Peterson, K. M. (1995). Four new derivatives of the broad-host-range cloning vector pBBR1MCS carrying different antibiotic-resistance cassettes. *Gene* 166, 175-176.

Li, X. and Pan, S.Q. (2017). *Agrobacterium* delivers VirE2 protein into host cells via clathrin-mediated endocytosis. *Sci. Adv.* 3, e1601528.

Lin, Yi-Han., Gao, R., Binns A.N. and Lynn, D.G. (2008) Capturing the VirA/VirG TCS of *Agrobacterium tumefaciens*. *Adv Exp Med Biol*, 631, 161-177.

Liu, W.S., Yuan, J.S. and Stewart, C.N. (2013). Advanced genetic tools for plant biotechnology. *Nat Rev Genet.* 14, 781-793.

Maliga, P., Staub, J., Carrer, H., Kanevski, I. and Svab, Z. (1994). Homologous recombination and integration of foreign DNA in chloroplasts of higher plants. Homologous Recombination and Gene Silencing in Plants, Kluwer Academic Publishers, the Netherlands, pp. 83–93.

Meyers, B., Zaltsman, A., Lacroix, B., Kozlovsky, S.V. and Krichevsky, A. (2010). Nuclear and chloroplast genetic engineering of plants: comparison of opportunities and challenges. *Biotechnol Adv*, 28, 747–756.

Okamoto, K., Perlman, P.S. and Butow, R.A. (2001). Targeting of green fluorescent protein to mitochondria. *Methods Cell Biol*, 65, 277–283.

Ort, D.R., Merchant, S.S., Alric, J., Barkan, A., Blankenship, R.E., Bock, R., Croce, R., Hanson, M.R., Hibberd, J.M., Long, S.P., Moore, T.A., Moroney, J., Niyogi, K.K., Parry, A.M.J., Peralta-Yahya, P.P., Prince, R.C., Redding, K.E., Spalding, M.H., van Wijk, K.J., Vermaas, W.F.J., von Sharma, von Caemmerer, S., Weber, A.P., Yeates, T.O., Yuan, J.S. and Zhu, X.G. (2015). Redesigning photosynthesis to sustainably meet global food and bioenergy demand. *Proc. Natl. Acad. Sci. U. S. A.*, 112, 8529-8536.

Roushan, M. R., de Zeeuw, M. A., Hooykaas, P. J. J. and van Heusden, G. P. H. (2018), Application of phiLOV2.1 as a fluorescent marker for visualization of *Agrobacterium* effector protein translocation. *Plant J.* Accepted Author Manuscript. doi:[10.1111/tbj.14060](https://doi.org/10.1111/tbj.14060).

Sakalis, P.A., van Heusden, G.P.H. and Hooykaas, P.J.J. (2014). Visualization of VirE2 protein translocation by the *Agrobacterium* type IV secretion system into host cells. *MicrobiologyOpen*, 3, 104–117.

Schirawski, J., Planchais, S. and Haenni, A.L. (2000) An improved protocol for the preparation of protoplasts from an established *Arabidopsis thaliana* cell suspension culture and infection with RNA of turnip yellow mosaic tymovirus: a simple and reliable method. *J. Virol. Methods*, 86, 85–94.

Sharma, K.K., Bhatnagar-Mathur, P. and Thorpe, T.A. (2005). Genetic transformation technology: status and problems. *In Vitro Cell Dev Biol Plant*, 41, 102–112.

Smeekens, S., van Steeg, H., Bauerle, C., Bettenbroek, H., Keegstra, K., and Weisbeek, P. (1987). Import into chloroplasts of a yeast mitochondrial protein directed by ferredoxin and plastocyanin transit peptides. *Plant Mol Biol.*, 9, 377-388.

Smith, E.F. and Townsend, C.O. (1907). A plant-tumor of bacterial origin. *Science*, 25, 671–673.

Steck, T.R., Lin, T.S. and Kado, C.I. (1990). *VirD2* gene product from the nopaline plasmid pTiC58 has at least 2 activities required for virulence. *Nucleic Acids Res*, 18, 6953-6958.

Svab, Z. and Maliga, P. (1993). High-frequency chloroplast transformation in tobacco by selection for a chimeric *aadA* gene. *Proc. Nat. Acad. Sci. U. S. A.*, 90, 913–917.

van Kregten, M., Lindhout, B.I., Hooykaas P.J.J. and van der Zaal, B.J. (2009) *Agrobacterium* -mediated T-DNA transfer and integration by minimal *VirD2* consisting of the relaxase domain and a type IV secretion system translocation signal. *Mol Plant-Microbe Inter*, 22,1356–1365.

van Engelenburg, S. B. and Palmer, A. E. (2010). Imaging type-III secretion reveals dynamics and spatial segregation of *Salmonella* effectors. *Nat. Methods*, 7, 325–330.

van Slogteren, G. M. S., Hooykaas, P. J. J. and Schilperoort, R. A. (1984). Silent T-DNA genes in plant lines transformed by *Agrobacterium tumefaciens* are activated by grafting and by 5-azacytidine treatment. *Plant Mol. Biol*, 3, 333–336.

van Tol, N. (2016). Phenotypic engineering of photosynthesis related traits in *Arabidopsis thaliana* using genome interrogation. Leiden University, Institute of biology of Leiden. Leiden, the Netherlands.

Vergunst, B., den Dulk-Ras, A., Vlaam, C.M.T., Regensburg-Tuink, T.J.G. and Hooykaas, P.J.J., (2000). *VirB/D4* dependent protein translocation from *Agrobacterium* into plant cells. *Science*, 290, 979–981.

Wang, H.-H., Yin, W.-B. and Hu, Z. M. (2009). Advances in chloroplast engineering. *Genet. Genomics*, 36, 387–398.

Ward, E. and Barnes, W. (1988) *VirD2* protein of *Agrobacterium tumefaciens* very tightly linked to the 5' end of T-strand DNA. *Science*, 242, 927–930.

Wroblewski, T., Tomczal, A. and Michelmore, R.W. (2005). Optimization of *Agrobacterium* -mediated transient assays of gene expression in lettuce, tomato and Arabidopsis. *Plant Biotechnol. J.* 3, 259–273.

Wu, H.-Y., Liu, K.-H., Wang, Y.-C., Wu, J.-F., Chiu, W.-L., Chen, C.-Y., Wu, S.-H., Sheen, J. and Lai, E.-M. (2014). AGROBEST: an efficient *Agrobacterium* -mediated transient expression method for versatile gene function analyses in *Arabidopsis* seedlings. *Plant Methods*, 10, 1–16.

Yanofsky, M. F., Porter, S. G., Young, C., Albright, L. M., Gordon, M. P., and Nester, E. W. (1986). The *virD* operon of *Agrobacterium tumefaciens* encodes a site-specific endonuclease. *Cell*, 47, 471-477.

Yu, Q., Lutz, K.A. and Maliga, P. (2017) Efficient Chloroplast Transformation in Arabidopsis. *Plant Physiol* 175: 186-193.

Zhou, X. R. and P. J. Christie. (1999). Mutagenesis of the *Agrobacterium* VirE2 single-stranded DNA-binding protein identifies regions required for self-association and interaction with VirE1 and a permissive site for hybrid protein construction. *J. Bacteriol.* 181, 4342–4352.

Ziemienowicz, a, Merkle, T., Schoumacher, F., Hohn, B. and Rossi, L. (2001). Import of *Agrobacterium* T-DNA into plant nuclei: two distinct functions of VirD2 and VirE2 proteins. *Plant Cell*, 13, 369–383.

Zonneveld, B.J.M. (1986). Cheap and simple yeast media. *J Microbiol Methods*, 4, 287–291.

Chapter 6

Summary

Summary

The soil-borne bacterium *Agrobacterium tumefaciens* has a unique interkingdom gene transfer capability and is known as natural genetic engineer. *A. tumefaciens* transfers part of its DNA (T-DNA) located on a tumor-inducing plasmid (Ti-Plasmid) into host cells resulting in tumor formation on plants, the crown gall disease. *Agrobacterium* can transfer T-DNA not only into plants, but also into yeast, fungi, algae, sea urchin embryos and possibly even human cells under laboratory conditions. Therefore, *A. tumefaciens* can be used as a genetic tool to modify eukaryotic organisms for molecular biology and biotechnology purposes. During *Agrobacterium*-mediated transformation (AMT), simultaneously with T-DNA transfer, effector proteins such as VirD2, VirE2, VirF, VirE3 and VirD5 are translocated into the host cells which play important roles in transformation (for reviews see: Tzfira and Citovsky, 2006; Gelvin, 2010). Many aspects about the exact functions of these proteins, the mechanisms of their translocation and their trafficking inside the host cell are unknown. To further investigate about *Agrobacterium* effector protein translocation, localization and trafficking we have developed two different visualization approaches which are described specifically in **Chapter 2** and **Chapter 3**. Furthermore, as *A. tumefaciens* can be engineered to be able to transfer foreign proteins into eukaryotic cells, in **Chapter 4**, we took advantage of its protein translocation capability to change the yeast mating type by *Agrobacterium*-mediated protein translocation (AMPT) of the HO-endonuclease. Subsequently, in **Chapter 5** we studied whether we could modify the essential two T-DNA nuclear uptake mediators VirE2 and VirD2 in such a way that they would be targeted to the mitochondria or chloroplasts instead of the nucleus. This as a first step towards the development of a system of *Agrobacterium* mediated organelle transformation using AMPT.

In **Chapter 2**, we have used the split-GFP system to visualize translocation and localization of VirE2, VirD2, VirF and VirE3 in plant and yeast cells. This system makes use of the observation that GFP can be split into two non-fluorescent fragments: GFP₁₋₁₀ and GFP₁₁ (Cabantous *et al.*, 2005). To visualize protein translocation, genetically modified recipient cells are needed to express GFP₁₋₁₀. Following translocation of the GFP₁₁-tagged effector protein, GFP fluorescence is restored and can be detected under confocal or fluorescent microscopes (Henry *et al.*, 2017; Li *et al.*, 2014; Sakalis *et al.*, 2014). In this chapter, we tagged the VirE2 protein with GFP₁₁ internally instead of N-terminally and the quality of signal observation, biological activities and expression timing were greatly improved compared to those obtained with N-terminally tagged VirE2. Besides, we were able to

capture the movement of internally tagged VirE2 which was impossible using N-terminally tagged GFP₁₁-VirE2. Despite all of these improvements the system still has clear limitations. The most important being that GFP₁₋₁₀ expressing transgenic plant and yeast cell lines are required. Also we were unsuccessful in detecting translocation of the virulence proteins VirF and VirE3 by the split-GFP system, possibly due to conformational restraints allowing GFP reconstitution. This encouraged us to test another fluorescent protein with possible advantages over split GFP. Hence, we have used the LOV fluorescent protein to study *Agrobacterium* protein translocation which is described in **Chapter 3**.

In **Chapter 3**, we made use of the phiLOV2.1 fluorescent protein to directly visualize effector protein translocation the host cells (Christie, 2007; Huala *et al.*, 1997; Buckley *et al.*, 2015; Chapman *et al.*, 2008; Gawthorne *et al.*, 2016; McIntosh *et al.*, 2017). In contrast to previous GFP based methodologies, the new method does not rely on special transgenic host cells and we successfully visualized VirE2, VirD2, VirE3, VirF and VirD5 effector protein translocation into *Arabidopsis thaliana* root, tobacco leaf and yeast cells. Clear signals were obtained that are easily distinguishable from the background, even in cases of VirE3 and VirF where the split GFP system did not generate signals in plant and yeast cells. Regardless of these advantages, weaker fluorescence signals were seen than with the split-GFP system; also photobleaching of phiLOV2.1 fluorescent protein and the more often observation of dot-shaped and filamentous structures of effector proteins are concerning. Therefore, combination of different techniques and fluorescent proteins is more efficient and reliable.

Inside *Agrobacterium* internally tagged phiLOV2.1-VirE2 was localized at the bacterial membrane as revealed by horseshoe-like structures. This is in line with the detection of VirE2 in the membrane fraction of *Agrobacterium* (Christie *et al.*, 1988; Dumas *et al.*, 2001) and with the observation that VirE2 may act as a channel to transfer ss-DNA *in vitro* (Christie *et al.*, 1988; Dumas *et al.*, 2001; Duckely and Hohn, 2003). Recently, Li and Pan (2017) proposed that VirE2 enters the host cell by hijacking the clathrin-mediated endocytosis pathway, but first is localized at the plant cell membrane. We also observed the (near) plasma membrane localization of not only VirE2, but also VirD2, VirF, VirD5 and VirE3 effector proteins which would suggest a similar pathway for the other effector proteins to penetrate into the host cells. Previously, we showed that 39phiLOV2.1-VirE2 formed filamentous and dot-like structures in yeast cells and plant cells that were strongly affected by

treatments disrupting microtubules. This is suggesting the existence of another pathway for effector protein trafficking inside the host cells. Further investigations are clearly needed.

In **Chapter 4**, we used *A. tumefaciens* to introduce the HO endonuclease into yeast cells and showed that the translocated endonuclease was able to induce mating type switching. Recently a research group established a new protocol to induce mating type switching in yeast using CRISPR/Cas9 technology (Xie *et al.*, 2018). This chapter further emphasize the potential of exploiting the ability of *Agrobacterium* to deliver proteins into eukaryotic cells. Translocation of proteins may result in altered properties of the target cells without genetic transformation. In other studies *Agrobacterium* was successfully engineered to introduce the Cre-recombinase into yeast, fungal and plant cells to allow recombination (Vergunst *et al.*, 2000; Vergunst *et al.*, 2005), to target meganuclease I-SceI into yeast and plant cells to enhance targeted integration (Rolloos *et al.*, 2005; van Kregten *et al.*, 2011). Recently the ability of *Agrobacterium* to transfer protein into plant cells has been exploited to enhance the regeneration of recalcitrant plants such as tulip and sweet pepper via transferring the BABY BOOM developmental regulator (Khan, 2017). Also Schmitz (2018) showed that targeted mutagenesis the *Nicotiana benthamiana* is achievable by translocating the Cas9 protein translocation from *Agrobacterium* (Schmitz, 2018). Furthermore, a novel approach is described to transfer isopentenyl transferase (IPT) for selection of transformed plants in *Arabidopsis* using *Agrobacterium* mediated protein translocation (Schmitz, 2018).

Engineering of organellar DNA is of great interest for biotechnology. One of the advantages of introducing transgenes into the chloroplast or mitochondrial genome instead of into the nuclear genome is that these organelles are maternally inherited, (Bansal and Sharma, 2003; Sharma *et al.*, 2005), organelle transformation allows stable transgene expression by the lack of epigenetic interference, and transgene stacking in operons (Wang *et al.*, 2009) and expression of multiple proteins from polycistronic mRNAs may be possible. High yields of transgenic products may be achieved because of the high number of chloroplast or mitochondrial genomes per cell. We assumed that *Agrobacterium* with an unique ability of transferring T-DNA facilitated by VirE2 and VirD2 virulence proteins into the host cell nucleus might be a good candidate to develop into an organelle vector. To end this, we aimed first to modify VirE2 and VirD2 in such a way that they would be targeted into the mitochondria and chloroplasts. In **Chapter 5**, we showed that modified VirE2 and VirD2 tagged with mitochondrial and chloroplast targeting sequence can be directed into the

mitochondria and chloroplasts of yeast and plant cells, respectively. However, while targeting to yeast mitochondria seemed efficient targeting to the chloroplasts was inefficient. Nevertheless, our results make it very worthwhile to invest in further optimization and to test whether T-DNA transfer into the organelles becomes possible with these modified effector proteins.

References

- Bansal, K. C. and Sharma, R. K.** (2003). Chloroplast transformation as a tool for prevention of gene flow from GM crops to weedy or wild relatives. *Current Science*, 84, 1286-1287.
- Cabantous, S., Terwilliger, T. C. and Waldo, G. S.** (2005). Protein tagging and detection with engineered self-assembling fragments of green fluorescent protein. *Nat. Biotechnol.*, 23, 102–107.
- Chapman, J. E., Gillum, D. and Kiani, S.** (2017). Approaches to Reduce CRISPR off-target effects for safer genome editing. *J. ABSA. Int.* 22, 7–13.
- Chapman, S., Faulkner, C., Kaiserli, E., Garcia-Mata, C., Savenkov, E.I., Roberts, A.G., Oparka, K.J. and Christie, J.M.** (2008). The photoreversible fluorescent protein iLOV outperforms GFP as a reporter of plant virus infection. *Proc. Natl. Acad. Sci. USA*, 105, 20038–20043.
- Christie, P.J., Ward, J.E., Winans, S.C. and Nester, E.W.** (1988). The *Agrobacterium tumefaciens virE2* gene product is a single-stranded-DNA-binding protein that associates with T-DNA. *J. Bacteriol.*, 170, 2659–2667.
- Christie, J.M., Corchnoy, S.B., Swartz, T.E., Hokensn, M., Han, I.S., Briggs, W.R. and Bogomolni, R.A.** (2007). Steric interactions stabilize the signaling state of the LOV2 domain of phototropin 1. *Biochem.* 46, 9310–19.
- Duckely., M. and Hohn., B.** (2003) The VirE2 protein of *Agrobacterium tumefaciens*: the Yin and Yang of T-DNA transfer. *FEMS Microbiol Lett*, 223, 1–6.
- Dumas, F., Duckely, M., Pelczar, P., Van Gelder, P. and Hohn, B.** (2001). An *Agrobacterium* VirE2 channel for transferred-DNA transport into plant cells. *Proc. Natl. Acad. Sci. USA.*, 98, 485–490.
- Gawthorne, J.A., Audry, L., McQuitty, C., Dean, P., Christie, J.M., Enninga, J. and Roe, A.J.** (2016). Visualizing the translocation and localization of bacterial type III effector proteins by using a genetically encoded reporter system. *Appl. Environ. Microbiol.* 82, 2700–2708.
- Gelvin, S.B.** (2010). Plant proteins involved in *Agrobacterium* -mediated genetic transformation. *Annu. Rev. Phytopathol.* 48, 45-68.
- Huala, E., Oeller, P.W., Liscum, E., Han, I.S., Larsen, E. and Briggs, W.R.** (1997). *Arabidopsis* NPH1: a protein kinase with a putative redox-sensing domain. *Science*, 278, 2120–2123.
- Henry, E., Toruño, T.Y., Jauneau, A., Deslandes, L. and Coaker, G.L.** (2017) Direct and indirect visualization of bacterial effector delivery into diverse plant cell types during infection. *Plant Cell*, 29, 1555-1570.

- Khan, M.** (2017). Molecular engineering of plant development using *Agrobacterium* - mediated protein translocation. PhD thesis, Leiden University, Leiden, the Netherlands.
- Li, X., Yang, Q., Tu, H., Lim, Z. and Pan, S. Q.** (2014). Direct visualization of *Agrobacterium*-delivered VirE2 in recipient cells. *Plant J.* 77(3), 487–495.
- Li, X. and Pan, S.Q.** (2017). *Agrobacterium* delivers VirE2 protein into host cells via clathrin-mediated endocytosis. *Sci. Adv.* 3. e1601528.
- McIntosh, A., Meikle, L. M., Ormsby, M. J., McCormick, B. A., Christie, J. M., Brewer, J. M., Roberts, M. and Wall, D. M.** (2017). SipA activation of caspase-3 is a decisive mediator of host cell survival at early stages of *Salmonella enterica* serovar typhimurium infection. *Infect. Immun.* 85. e00393-17.
- Rolloos ,M., Hooykaas, P.J.J. and van der Zaal, B.J.** (2015). Enhanced targeted integration mediated by translocated I-SceI during the *Agrobacterium* mediated transformation of yeast. *Sci. Rep.* 5, 8345.
- Sakalis, P.A., van Heusden, G.P.H. and Hooykaas, P.J.J.** (2014). Visualization of VirE2 protein translocation by the *Agrobacterium* type IV secretion system into host cells. *MicrobiologyOpen*, 3, 104–117.
- Schmitz, D.** (2018). CRISPR/Cas-induced targeted mutagenesis with *Agrobacterium* mediated protein delivery. PhD thesis, Leiden University, Leiden, the Netherlands.
- Sharma, K.K., Bhatnagar-Mathur, P. and Thorpe, T.A.** (2005). Genetic transformation technology: status and problems. *In Vitro Cell Dev Biol Plant*, 41, 102–112.
- Tzfira, T. and Citovsky, V.** (2006). *Agrobacterium*-mediated genetic transformation of plants: biology and biotechnology. *Curr. Opin. Biotechnol.* 17, 147–54.
- van Kregten, M.** (2011). *Agrobacterium*-mediated delivery of a meganuclease into target plant cells. PhD thesis, Leiden University, Institute of biology of Leiden. Leiden, the Netherlands.
- Vergunst, A. C., Schrammeijer, B., den Dulk-Ras, A., de Vlaam, C. M. T. , Regensburg-Tuink, T. J. G. and Hooykaas, P. J. J.** (2000). VirB/D4-dependent protein translocation from *Agrobacterium* into plant cells. *Science*, 290, 979–982.
- Vergunst, A.C., van Lier, M.C., den Dulk-Ras, A., Grosse Stuve, T.A., Ouwehand, A. and Hooykaas, P.J.J.** (2005). Positive charge is an important feature of the C-terminal transport signal of the VirB/D4-translocated proteins of *Agrobacterium* . *Proc. Natl. Acad. Sci. USA*, 102,832–837.
- Wang, H.-H., Yin, W.-B. and Hu, Z. M.** (2009). Advances in chloroplast engineering. *Genet. Genomics*, 36, 387–398.

Xie, Z.X., Mitchell, L.A., Liu, H.M., Li, B.Z., Liu, D., Agmon, N., Wu, Y., Li, X., Zhou, X., Li, B., Xiao, W.H., Ding M.Z., Wang, Y., Yuan, Y.J. and Boeke, J.D. (2018). Rapid and efficient CRISPR/Cas9-based mating-type switching of *Saccharomyces cerevisiae*. *G3*, 8, 173-183.

Zhang, X., Tee, L.Y., Wang, X., Huang, Q. and Yang, S.(2015). Off-target effects in CRISPR/Cas9-mediated genome engineering. *Mol. Ther. Nucleic. Acids*, 4, e264.

Samenvatting

Samenvatting

De bodembacterie *Agrobacterium tumefaciens* heeft het unieke vermogen om genetisch materiaal over te dragen naar organismen behorend tot andere fylogenetische koninkrijken, met name planten, en staat daarom bekend als een natuurlijke genetische ingenieur. *Agrobacterium* draagt een deel van zijn DNA (T-DNA), dat zich op een tumor-inducerend plasmide (Ti-plasmide) bevindt, over naar gastheercellen. Dit resulteert in de vorming van tumoren op planten, een fenomeen dat bekend staat als wortelhalsknobbel of kroongalziekte. *Agrobacterium* kan T-DNA niet alleen overbrengen naar planten, maar ook naar gist, schimmels, algen, zee-egelembryo's en mogelijk zelfs naar menselijke cellen onder laboratoriumomstandigheden. Daarom kan *Agrobacterium* worden gebruikt als een hulpmiddel om eukaryote organismen genetisch te modificeren voor moleculair biologische en biotechnologische doeleinden. Tijdens *Agrobacterium*-gemediëerde transformatie (AMT) worden naast het T-DNA ook effectoreiwitten (VirD2, VirE2, VirF, VirE3 en VirD5) overgedragen naar de gastheercellen. Ook deze effectoreiwitten spelen een belangrijke rol bij het proces van transformatie (voor overzichtsartikelen zie: Tzfira en Citovsky, 2006; Gelvin, 2010). Veel aspecten van de functies van deze eiwitten, de mechanismen van hun translocatie en hun transport binnen de gastheercel zijn onbekend. Om verder onderzoek te doen naar translocatie, lokalisatie en intracellulair transport van de *Agrobacterium* effectoreiwitten heb ik twee verschillende visualisatiebenaderingen ontwikkeld die specifiek in **Hoofdstuk 2** en **Hoofdstuk 3** van dit proefschrift worden beschreven. In **Hoofdstuk 4** heb ik gebruik gemaakt van het feit dat *Agrobacterium* ook kan worden gemanipuleerd om andersoortige eiwitten over te brengen naar eukaryote cellen, door via *Agrobacterium*-gemediëerde eiwittranslocatie (AMPT) van het HO-endonuclease het paringstype van bakkersgist te veranderen. Vervolgens heb ik in **Hoofdstuk 5** onderzocht of we de twee effectoreiwitten die essentieel zijn voor de opname van het T-DNA in de celkern van de gastheercellen, VirE2 en VirD2, zodanig gemodificeerd konden worden dat ze getransporteerd zouden worden naar de mitochondriën of chloroplasten in plaats van de celkern. Dit is een eerste stap naar de ontwikkeling van een systeem van *Agrobacterium*-gemediëerde transformatie van celorganellen.

In **Hoofdstuk 2** hebben we het zogenaamde “split-GFP” systeem gebruikt om de translocatie en lokalisatie van de effectoreiwitten VirE2, VirD2, VirF en VirE3 in planten- en gistcellen te visualiseren. Dit systeem maakt gebruik van het feit dat GFP kan worden opgesplitst in

twee niet-fluorescerende fragmenten: GFP1-10 en GFP11 (Cabantous *et al.*, 2005). Om de translocatie van eiwitten via deze methode te visualiseren, zijn genetisch gemodificeerde gastheercellen nodig die GFP1-10 tot expressie te brengen. Na translocatie van een effectoreiwit dat gekoppeld is aan GFP-11 wordt de fluorescentie van GFP hersteld en kan dan worden gedetecteerd met behulp van confocale of fluorescentiemicroscopen (Henry *et al.*, 2017; Li *et al.*, 2014; Sakalis *et al.*, 2014). In dit hoofdstuk hebben we het effectoreiwit VirE2 intern gelabeld met GFP₁₁ in plaats van aan de N-terminus, waardoor de kwaliteit van het fluorescentiesignaal, de biologische activiteit en de timing van de expressie sterk verbeterden in vergelijking tot die verkregen met N-terminaal gelabeld VirE2. Bovendien konden we de beweging van intern gelabeld VirE2 vastleggen, wat onmogelijk was met behulp van N-terminaal gelabeld GFP₁₁-VirE2. Ondanks al deze verbeteringen heeft het systeem nog steeds duidelijke beperkingen. De belangrijkste beperking is dat transgene planten en gistcellen nodig zijn die GFP₁₋₁₀ tot expressie brengen. Ook was het niet mogelijk om de translocatie van de effectoreiwitten VirF en VirE3 met het split-GFP-systeem te detecteren, mogelijk als gevolg van conformationele beperkingen die GFP-restitutie onmogelijk maken. Dit moedigde mij aan om een ander fluorescerend eiwit te testen met mogelijke voordelen ten opzichte van het split-GFP systeem. Daartoe hebben we het fluorescerende eiwit LOV in huis gehaald om de translocatie van *Agrobacterium*-eiwitten te bestuderen, een aanpak die in **Hoofdstuk 3** wordt beschreven.

In **Hoofdstuk 3** hebben we gebruik gemaakt van het fluorescerende eiwit phiLOV2.1 om translocatie van effectoreiwitten naar gastheercellen direct te kunnen visualiseren (Christie, 2007; Huala *et al.*, 1997; Buckley *et al.*, 2015; Chapman *et al.*, 2008; Gawthorne *et al.*, 2016; McIntosh *et al.*, 2017). In tegenstelling tot eerdere, op GFP gebaseerde methodologieën, is deze nieuwe methode niet afhankelijk van speciale transgene gastheercellen. Via deze aanpak hebben we met succes translocatie van VirE2, VirD2, VirE3, VirF en VirD5 naar cellen van wortels van *Arabidopsis thaliana*, tabaksbladeren en bakkersgist gevisualiseerd. Er werden duidelijke signalen verkregen die gemakkelijk te onderscheiden waren van het achtergrondsignaal, zelfs in de gevallen van VirE3 en VirF, waarvoor met het split-GFP-systeem geen signalen in planten- en gistcellen konden worden verkregen. Er werden echter zwakkere fluorescentiesignalen waargenomen dan met het split-GFP-systeem. Ook 'photobleaching' van phiLOV2.1 en de vaker voorkomende observatie van puntvormige en filamenteuze structuren van de effectoreiwitten vormen mogelijke nadelen. Daarom lijkt een

combinatie van het gebruik van verschillende technieken en fluorescerende eiwitten efficiënter en betrouwbaarder. Binnen *Agrobacterium* cellen was intern gelabeld phiLOV2.1-VirE2 gelocaliseerd bij de celmembraan in zichtbare, hoefijzervormige structuren. Dit is in overeenstemming met de detectie van VirE2 in de membraanfractie van *Agrobacterium* (Christie *et al.*, 1988; Dumas *et al.*, 2001) en met de waarneming dat VirE2 kan fungeren als een kanaal om enkelstrengs DNA *in vitro* over te brengen (Christie *et al.*, 1988; Dumas *et al.*, 2001; Duckely and Hohn, 2003). Onlangs hebben Li en Pan (2017) voorgesteld dat VirE2 de gastheercel binnentreedt door de clathrine-gemedieerde endocytose-route te kapen, maar eerst gelokaliseerd is bij de membraan van de plantencel. Wij observeerden ook de (bijna) plasmamembraanlokalisatie van de effectoreiwitten VirD2, VirF, VirD5 en VirE3, daarmee een vergelijkbare route suggererend waarmee de andere effectoreiwitten de gastheercel binnen komen. Eerder hebben we echter aangetoond dat het 39phiLOV2.1-VirE2 eiwit filament-achtige en punt-achtige structuren vormt in gist- en plantencellen die sterk beïnvloed werden door behandelingen die microtubuli verstoorden. Of dit het een andere route voor het transport van effectoreiwitten in de gastheercellen indiceert, zal verder onderzoek moeten uitwijzen.

In **Hoofdstuk 4** hebben we *Agrobacterium* gebruikt om het HO-endonuclease te introduceren in gistcellen en aangetoond dat het overgedragen eiwit het wisselen van het paringstype van de gistcellen kon induceren. Dit hoofdstuk benadrukt verder het potentieel van het benutten van AMPT naar eukaryote cellen. Translocatie van eiwitten kan resulteren in veranderde eigenschappen van de doelcellen zonder genetische transformatie. In eerdere studies is *Agrobacterium* met succes gemanipuleerd om het Cre-recombinase te introduceren in gist-, schimmel- en plantencellen om DNA-recombinatie te bewerkstelligen (Vergunst *et al.*, 2000; Vergunst *et al.*, 2005), en om het meganuclease I-SceI naar gist- en plantencellen over te dragen om gerichte integratie van DNA te verbeteren (Rolloos *et al.*, 2005; van Kregten *et al.*, 2011). Daarnaast is onlangs AMPT naar plantencellen ingezet om de regeneratie van recalcitrante plantensoorten zoals tulp en paprika te verbeteren via de overdracht van de ontwikkelingsregulator BABYBOOM (Khan, 2017). Schmitz (2018) toonde aan dat gerichte mutagenese van *Nicotiana benthamiana* haalbaar is door translocatie van het Cas9 eiwit via AMPT. Verder wordt in deze studie een nieuwe benadering beschreven om isopentenyltransferase (IPT) over te dragen voor selectie van getransformeerde Arabidopsis planten met behulp van AMPT (Schmitz, 2018).

De manipulatie van het DNA van celorganellen is van groot belang voor de biotechnologie. Een van de voordelen van het introduceren van transgenen in het chloroplast of mitochondriaal genoom in plaats van in het nucleaire genoom is dat deze organellen alleen maternaal worden overgeërfd (Bansal and Sharma, 2003; Sharma *et al.*, 2005). Transformatie van organellen maakt ook stabiele expressie van transgenen zonder epigenetische interferentie mogelijk en faciliteert de introductie van meerdere transgenen tegelijkertijd in een operonstructuur (Wang *et al.*, 2009), leidend tot gelijktijdige expressie van meerdere eiwitten via polycistronische mRNAs. Daarnaast kunnen hoge opbrengsten van transgenproducten worden bereikt door het grote aantal kopieën van de chloroplast- of mitochondriale genomen per cel. *Agrobacterium* zou, door zijn unieke vermogen om T-DNA efficiënt over te dragen in gastheercellen, een ideale kandidaat zijn om te ontwikkelen tot een organelvector. Om dit te bewerkstelligen, moesten VirE2 en VirD2, de belangrijke effectoreiwitten die transformatie via AMT faciliteren, zodanig gemodificeerd worden dat ze getransporteerd worden naar de mitochondriën en chloroplasten. In **Hoofdstuk 5** heb ik aangetoond dat VirE2 en VirD2, voorzien van mitochondriale en chloroplast overdrachtpeptides, kunnen worden overgedragen naar respectievelijk de mitochondriën en chloroplasten van gist en plantencellen. Hoewel translocatie naar de mitochondriën van gist efficiënt was, was overdracht naar chloroplasten van cellen van *Arabidopsis* dat niet. Desondanks maken onze resultaten het zeer de moeite waard om te investeren in verdere optimalisatie van deze aanpak en om te testen of de overdracht van T-DNA naar de organellen mogelijk wordt met deze gemodificeerde effectoreiwitten.

Referenties

Bansal, K. C. and Sharma, R. K. (2003). Chloroplast transformation as a tool for prevention of gene flow from GM crops to weedy or wild relatives. *Current Science*, 84, 1286-1287.

Cabantous, S., Terwilliger, T. C. and Waldo, G. S. (2005). Protein tagging and detection with engineered self-assembling fragments of green fluorescent protein. *Nat. Biotechnol.*, 23, 102–107.

Chapman, J. E., Gillum, D. and Kiani, S. (2017). Approaches to Reduce CRISPR off-target effects for safer genome editing. *J. ABSA. Int.* 22, 7–13.

Chapman, S., Faulkner, C., Kaiserli, E., Garcia-Mata, C., Savenkov, E.I., Roberts, A.G., Oparka, K.J. and Christie, J.M. (2008). The photoreversible fluorescent protein iLOV outperforms GFP as a reporter of plant virus infection. *Proc. Natl. Acad. Sci. USA*, 105, 20038–20043.

Christie, P.J., Ward, J.E., Winans, S.C. and Nester, E.W. (1988). The *Agrobacterium tumefaciens virE2* gene product is a single-stranded-DNA-binding protein that associates with T-DNA. *J. Bacteriol.*, 170, 2659–2667.

Christie, J.M., Corchnoy, S.B., Swartz, T.E., Hokensn, M., Han, I.S., Briggs, W.R. and Bogomolni, R.A. (2007). Steric interactions stabilize the signaling state of the LOV2 domain of phototropin 1. *Biochem.* 46, 9310–19.

Duckely., M. and Hohn., B. (2003) The VirE2 protein of *Agrobacterium tumefaciens*: the Yin and Yang of T-DNA transfer. *FEMS Microbiol Lett*, 223, 1–6.

Dumas, F., Duckely, M., Pelczar, P., Van Gelder, P. and Hohn, B. (2001). An *Agrobacterium* VirE2 channel for transferred-DNA transport into plant cells. *Proc. Natl. Acad. Sci. USA.*, 98, 485–490.

Gawthorne, J.A., Audry, L., McQuitty, C., Dean, P., Christie, J.M., Enninga, J. and Roe, A.J. (2016). Visualizing the translocation and localization of bacterial type III effector proteins by using a genetically encoded reporter system. *Appl. Environ. Microbiol.* 82, 2700–2708.

Gelvin, S.B. (2010). Plant proteins involved in *Agrobacterium* -mediated genetic transformation. *Annu. Rev. Phytopathol.* 48, 45-68.

Huala, E., Oeller, P.W., Liscum, E., Han, I.S., Larsen, E. and Briggs, W.R. (1997). *Arabidopsis* NPH1: a protein kinase with a putative redox-sensing domain. *Science*, 278, 2120–2123.

Henry, E., Toruño, T.Y., Jauneau, A., Deslandes, L. and Coaker, G.L. (2017) Direct and indirect visualization of bacterial effector delivery into diverse plant cell types during infection. *Plant Cell*, 29, 1555-1570.

- Khan, M.** (2017). Molecular engineering of plant development using *Agrobacterium* -mediated protein translocation. PhD thesis, Leiden University, Leiden, the Netherlands.
- Li, X., Yang, Q., Tu, H., Lim, Z. and Pan, S. Q.** (2014). Direct visualization of *Agrobacterium* -delivered VirE2 in recipient cells. *Plant J.* 77(3), 487–495.
- Li, X. and Pan, S.Q.** (2017). *Agrobacterium* delivers VirE2 protein into host cells via clathrin-mediated endocytosis. *Sci. Adv.* 3. e1601528.
- McIntosh, A., Meikle, L. M., Ormsby, M. J., McCormick, B. A., Christie, J. M., Brewer, J. M., Roberts, M. and Wall, D. M.** (2017). SipA activation of caspase-3 is a decisive mediator of host cell survival at early stages of *Salmonella enterica* serovar typhimurium infection. *Infect. Immun.* 85. e00393-17.
- Rolloos ,M., Hooykaas, P.J.J. and van der Zaal, B.J.** (2015). Enhanced targeted integration mediated by translocated I-SceI during the *Agrobacterium* mediated transformation of yeast. *Sci. Rep.* 5, 8345.
- Sakalis, P.A., van Heusden, G.P.H. and Hooykaas, P.J.J.** (2014). Visualization of VirE2 protein translocation by the *Agrobacterium* type IV secretion system into host cells. *MicrobiologyOpen*, 3, 104–117.
- Schmitz, D.** (2018). CRISPR/Cas-induced targeted mutagenesis with *Agrobacterium* mediated protein delivery. PhD thesis, Leiden University, Leiden, the Netherlands.
- Sharma, K.K., Bhatnagar-Mathur, P. and Thorpe, T.A.** (2005). Genetic transformation technology: status and problems. *In Vitro Cell Dev Biol Plant*, 41, 102–112.
- Tzfira, T. and Citovsky, V.** (2006). *Agrobacterium*-mediated genetic transformation of plants: biology and biotechnology. *Curr. Opin. Biotechnol.* 17, 147–54.
- van Kregten, M.** (2011). *Agrobacterium*-mediated delivery of a meganuclease into target plant cells. PhD thesis, Leiden University, Institute of biology of Leiden. Leiden, the Netherlands.
- Vergunst, A. C., Schrammeijer, B., den Dulk-Ras, A., de Vlaam, C. M. T. , Regensburg-Tuink, T. J. G. and Hooykaas, P. J. J.** (2000). VirB/D4-dependent protein translocation from *Agrobacterium* into plant cells. *Science*, 290, 979–982.
- Vergunst, A.C., van Lier, M.C., den Dulk-Ras, A., Grosse Stuve, T.A., Ouweland, A. and Hooykaas, P.J.J.** (2005). Positive charge is an important feature of the C-terminal transport signal of the VirB/D4-translocated proteins of *Agrobacterium* . *Proc. Natl. Acad. Sci. USA*, 102,832–837.
- Wang, H.-H., Yin, W.-B. and Hu, Z. M.** (2009). Advances in chloroplast engineering. *Genet. Genomics*, 36, 387–398.

Xie, Z.X., Mitchell, L.A., Liu, H.M., Li, B.Z., Liu, D., Agmon, N., Wu, Y., Li, X., Zhou, X., Li, B., Xiao, W.H., Ding M.Z., Wang, Y., Yuan, Y.J. and Boeke, J.D. (2018). Rapid and efficient CRISPR/Cas9-based mating-type switching of *Saccharomyces cerevisiae*. *G3*, 8, 173-183.

Zhang, X., Tee, L.Y., Wang, X., Huang, Q. and Yang, S.(2015). Off-target effects in CRISPR/Cas9-mediated genome engineering. *Mol. Ther. Nucleic. Acids*, 4, e264.

Chapter 8

Curriculum vitae

Curriculum vitae

Mohammad Reza Roushan was born on March 24th 1983 in Tehran, Iran. In September 2004, he started his BSc studies of Cellular and Molecular Biology- Microbiology at Azad University in Tonekabon, Iran, receiving his BSc degree in September 2008. In 2010, he moved to Malaysia to continue his scientific education by enrolling at the International Malaysian English Center (IMEC). He obtained his advance-level English diploma within three months, and then started his Master's studies in the field of biotechnology at the University of Malaya, Kuala Lumpur, Malaysia. During the second year of his Master's program, he completed his thesis on the 'Antioxidant properties and geno-protective effect of selected *Pleurotus* spp. on raw cells' in the laboratory of Prof. Uma Kuppusamy. In the last year of his studies, he was appointed as research assistant in the research group of Dr. Tan Yee Shi's, who was working on the molecular mechanism(s) of the geno-protective effect of *Pleurotus* spp. mushrooms. In August 2013, he obtained his Master's degree in General Biotechnology. On the 1st of September 2014, he started his PhD research in the department of Molecular and Developmental Genetics of the Institute of Biology Leiden, under the daily supervision of Dr. Paul van Heusden and promoter Prof. Paul Hooykaas. His PhD research was mainly focused on visualization of *Agrobacterium* protein translocation into yeast and plant cells, the results of which are described in this thesis.